

ScP-01-A

Topical Report
γ-RADCAL GAMMA THERMOMETERS
February 1982
Rev. 4

8210040319 820929
PDR TOPRP EECSCAP
B PDR

TOPICAL REPORT

RADCAL Gamma Thermometers
as Local Fuel Power Measuring Devices
for use in the Cores of Pressurized Water Reactors

ScP-01 -A

Submitted to NRC by Scandpower for review on behalf of several U.S. nuclear power suppliers (utilities) who are participants in a group* of nuclear organizations intending to develop, license, and employ full scale systems of gamma thermometers.

Submitted: February, 1982

Scandpower, Inc.
Triangle Towers
4853 Cordell Ave.
Bethesda, Maryland 20814
Attn: Robert D. Smith

* Gamma Thermometer Investigation Group (GTIG)

<u>U.S. Power Suppliers:</u>	<u>Foreign Power Suppliers:</u>	<u>Other:</u>
DUKE Power	Electricite de France	Exxon Nuclear
Tennessee Valley Authority	Rheinisch-Westfalisches	Scandpower
Public Service Electric	Elektrizitatswerk	
and Gas	Swedish State Power Board	
	Kansai Electric Power	



UNITED STATES
NUCLEAR REGULATORY COMMISSION
WASHINGTON, D. C. 20555

AUG 03 1982

Mr. Peter A. Morris, Executive Vice President
Scandpower, Inc.
4853 Cordell Avenue
Bethesda, Maryland 20014

Dear Mr. Morris:

Subject: Acceptance for Referencing of Licensing Topical Report ScP-01

The Nuclear Regulatory Commission has completed its review of the Scandpower, Inc. licensing topical report ScP-01 entitled "RADCAL GAMMA THERMOMETERS, Revision 4" dated February 1982. Scandpower, Inc. submitted this report on behalf of several U.S. utilities who are participants in a group of nuclear organizations intending to develop, license and employ full scale systems of gamma thermometers. The ScP-01 report provides a detailed description of the gamma thermometer construction, operation, and expected performance as a local power measuring device for use in the cores of pressurized water reactors. A copy of our safety evaluation is enclosed.

Based on our review we conclude that the principle of the instrument, the feasibility of the design, the experimental verification and the theoretical analysis are adequately documented and acceptable.

As a result of our review we find that the Scandpower, Inc. licensing topical report ScP-01 entitled "RADCAL GAMMA THERMOMETERS, Revision 4" dated February 1982 to be acceptable for referencing in license applications to the extent specified and under limitations stipulated in the submitted document and the enclosed safety evaluation.

We do not intend to repeat the review of the safety features described in the topical report and found acceptable in the enclosure when it appears as a reference in a particular license application. However, we will assure that the material presented in the report is applicable to the specific plant involved and will review the use of the instruments as local power-measuring devices on a plant specific basis. Our acceptance applies only to the features described in the topical report.

In accordance with established procedures (NUREG 390), it is requested that Scandpower, Inc. publish an accepted version of the report within three months of receipt of this letter. The revision is to incorporate this letter and the enclosed evaluation following the title page and thus just in front of the abstract. The report identification symbol of the accepted report is to include a - A suffix.

AUG 03 1982

Mr. Peter A. Morris

-2-

Should Nuclear Regulatory Commission criteria or regulations change such that our conclusions as to the acceptability of the report are invalidated, Scand-power, Inc. and/or the applicants referencing the topical report will be expected to revise and resubmit their respective documentation or submit justification for the continued effective applicability of the topical report without revisions of their respective documentation.

Sincerely,

Robert E. Learter

for Harold Bernard, Acting Branch Chief
Standardization & Special
Projects Branch
Division of Licensing

Enclosure:
As stated

JUN 23 1982

Evaluation of a SCANDPOWER, Inc. Licensing Topical Report

Report Number: ScP-01, Rev. 4
Report Title: γ -RADCAL Gamma Thermometers
Report Date: February 1982
Originating Organization: SCANDPOWER, Inc.,
Reviewed by: Reactor Physics Section,
Core Performance Branch,
Division of Systems Integration
Date of Evaluation: June 1982

The SCANDPOWER Company has submitted the Topical Report ScP-01, Rev. 4 entitled, " γ -RADCAL Gamma Thermometers" for our review. SCANDPOWER, Inc. is acting on behalf of a number of utilities. This report provides a detailed description of the gamma thermometer construction, operation and expected performance as local power-measuring device for use in the cores of pressurized water reactors. Our evaluation of this report follows.

1. SUMMARY OF REPORT

The purpose of this report is to describe gamma thermometers and show that they are adequate for use as a basic local power-measuring in-core instrument for pressurized water reactors. This report provides a description of principle, construction, operation and performance of the instrument for use in future licensing submittals by several licensees.

The report includes sections on: (1) the principles of gamma thermometry, (2) the design of the RADCAL Gamma Thermometer (RGT) for PWRs, (3) discussion of the RGT sensitivity by computation and measurement, and (4) discussion

of the components of the uncertainty of gamma ray heating and local power. The information has, to a great extent, been derived from heavy water reactor experience (the Savannah River reactor and the Halden BWR). Some pressurized water reactor experience has been cited from French reactors. An ongoing program for extensive measurements and calculations to determine the uncertainties is described.

The report is generally responsive to our comments for a revision of the previous submittal by deleting irrelevant material and including additional experimental results.

2. SUMMARY OF EVALUATION

Our review is based on the applicant's submittal ScP-01, Rev. 4, but additional information was also obtained in (a) a presentation to the staff made by the applicant, with French and other participants, and (b) a meeting held in Bethesda in SCANDPOWER's headquarters, where a discussion was held and a presentation was made on RGTs.

Relative Merits of Power Measurement Principle with Gamma Thermometry

Gamma thermometers measure the temperature drop along a heat path which is provided to dissipate the heat generated by gamma rays and fast neutrons in a metal block. The volumetric heat generation rate in the metal is proportional to the gamma ray and fast neutron field in that location and correspondingly to the power of the adjacent and nearby fuel rods. Power measurement in this manner does not depend on thermal neutron flux, hence,

no correction is made for fuel burnup. The heat generation rate provides a strong signal which can be directly interpreted as proportional to the local power. The temperature drop can be varied by varying the cross sectional area of the heat path and/or the volume of the metal block where most of the heat is generated. The gamma thermometer is affected little, if at all, by the thermal flux. Therefore, when such an instrument is near a control rod, which severely suppresses the thermal flux and the local power, the corresponding response will not be proportional to that thermal flux decrease because the fast neutron and the gamma ray mean free paths are much longer than the thermal neutron mean free path.

Gamma Thermometer Design

The design proposed by SCANDPOWER, Inc., and which has been investigated, consists of a cylindrical aluminum housing about two inches long, containing argon gas in the cavity and the stainless steel mass where the heat is generated, the heat path, two thermocouples to measure the temperature difference and ceramic insulated thermocouple leads. Seven to nine such sensors mounted at equal distances along a 7.5 mm diameter tube of the necessary length and a seal flange, constitute a gamma thermometer assembly. Such an assembly would measure local power at 7-9 axial locations simultaneously. The nature of this design gives this instrument significant durability, reproducibility of the signal and small variations with radiation exposure. The weakest point of the design seems to be the possibility of breakage of the leads. The proposed design offers the possibility of performing electrical heating calibration without taking the instrument out of the reactor. The proposed design is intended to be a steady state instrument and can be fitted into the instrument tubes of existing PWRs.

Uncertainties of Gamma Thermometer Used as Local Power Measurement Instruments

Numerical values have been established for the gamma thermometer sensitivity and the fuel power to sensor heating. However, the spatial extrapolation uncertainty and the non-steady state uncertainty are not quantified.

The gamma thermometer sensitivity refers to the indicated ΔT per Watt/g of mass of the heated stainless steel. (A real and indicated sensitivity can be distinguished). Based on the existing data for a well calibrated gamma thermometer at the beginning of life, the sensitivity is $\pm 1.9\%$ and is expected to be $\pm 5\%$ at the end of life of the instrument.

The sensor heating to the local power uncertainty is given as $\pm 6.5\%$. It is reported that programs have been initiated to reduce this value.

The spatial extrapolation uncertainty depends on the system geometry, material composition, unfolding program, heating block material, the mean free paths of the absorbed gammas and neutrons and the proportion of the delayed fission product decay gammas. This quantity is plant-specific, hence, its numerical value, supporting data and theoretical justification will be reviewed on a case-by-case basis.

Finally, the non-steady state uncertainty depends in addition to the factors listed above, on the magnitude of the local power change, the time rate at which it takes place and the local power history. No numerical value is given, hence, it will have to be discussed on a plant-specific basis.

3. EVALUATION PROCEDURE

The review of topical report ScP-01, Rev. 4 has been conducted within the guidelines provided by Section 4.3 of the Standard Review Plan. Sufficient information was provided to permit the conclusion that the principle of the instrument, feasibility of the design, experimental verification and theoretical analysis are adequately documented and acceptable.

4. REGULATORY POSITION

Based on our review of the topical report ScP-01, Rev. 4, we conclude that it is acceptable for reference in PWR submittals. However, the use of these instruments as local power-measuring devices will be reviewed on a plant-specific basis.

A B S T R A C T

The γ -RADCAL[®] gamma thermometer (RGT) is proposed by the applicants as a replacement for any local power measuring instrument now in use in pressurized water reactors. The arguments and data supporting the use of this instrument originate with 20 years of direct large-scale experience with classic gamma thermometers in heavy water reactors and with the proven advances in structure and precision-of-calibration over classic gamma thermometers embodied in the RGT assembly.

Empirical and theoretical proofs of the close relationship of RGT sensor heat rate to local fuel power, and of the ability to accurately measure sensor heat rate, are presented.

The report deals quantitatively (for RGTs) with the two most basic uncertainties of any local power "measuring" system:

- 1) The uncertainty in sensitivity of the sensor (called σ_1 herein), which defines the proven ability of the instrument to measure the parameter it purports to measure (e.g., thermal neutron flux, gamma photon flux, or heat rate in a stainless steel sensor).
- 2) The "coupling" uncertainty (called σ_2 herein), which defines the uncertainty in the ratio of local fuel power around the sensor to the parameter purported to be measured.

The other measurement uncertainties, respectively: the spatial "extrapolation" uncertainty, σ_3 ; and the "non-steady state", or time-domain, uncertainty, σ_4 , are discussed primarily to inform NRC staff reviewers of the state-of-the-art in these two areas. These uncertainties are data processing system dependent and will be addressed in subsequent topical reports that are NSSS system and computer software specific, but remain plant generic (and are therefore best treated via topical report rather than plant docket).

TABLE OF CONTENTS

ABSTRACT

1. INTRODUCTION

- 1.1 Objectives of this Topical Report
- 1.2 Principles of Gamma Thermometry
- 1.3 History of Gamma Thermometry until 1974
- 1.4 The RGT Gamma Thermometer for PWRs
- 1.5 The History of γ -RADCAL
- 1.6 Intrinsic Advantages of RGT Gamma Thermometers

2. SUMMARY

3. DISCUSSION

- 3.1 Sensitivity of RGT's by Computation and Measurements
- 3.2 K_2 , The Ratio of Local Fuel Power to Gamma Heating in the Sensor and the Components of Uncertainty, σ_2
- 3.3 Completed Programs Demonstrating the Precision of Gamma Thermometry
- 3.4 GTIG-Related Programs Now underway to Reduce RGT Uncertainties
- 3.5 Programs Establishing Mechanical System Compatibility, Handling Technique, Integrity of Pressure Boundary, Consequences and Modes of Failure

APPENDICES

FIGURES

TABLES

DETAILED TABLE OF CONTENTS FOR SECTION 3 - DISCUSSION

- 3.0 DISCUSSION
 - The Sensitivity Uncertainty
 - The Coupling Uncertainty
 - The Spatial Extrapolation Uncertainty
 - The Non-Steady State Uncertainty
- 3.1 Sensitivity of RGTs by Computation and Measurements
 - 3.1.1 Description and Modelling of the Thermal Processes
 - 3.1.1.1 Relationships of Real Sensitivity, Indicated Sensitivity, and Response Times for Simple Systems
 - 3.1.1.2 Computer Model for Determining both S_r and τ (RADCAL/THERMAL)
 - 3.1.1.3 Application of the Model RADCAL/THERMAL
 - 3.1.1.3.1 Predicting Electric Calibration Results
 - 3.1.1.3.2 Conversion of Electric Calibration to Nuclear Calibration (Examples)
 - 3.1.1.3.3 Predicting Time Constants from a Step in Power
 - 3.1.1.3.4 Relationship of τ to S_r for RGTs
 - 3.1.1.3.5 Predicting Response to Plunge Testing
 - 3.1.1.3.6 Sensitivity Studies of Manufacturing Variables
 - 3.1.2 Methods and Results of Experimental Determinations of the Sensitivity of RGTs
 - 3.1.2.1 Response Time in Plunge Tests
 - 3.1.2.2 Direct Electrical Calibration and Power Step Response
 - 3.1.2.2.1 Reductions of the Uncertainty, σ_1
 - 3.1.2.2.2 Calibration Results Obtained
 - 3.1.2.3 "In Situ", or In-Reactor, Calibration Methods
 - 3.1.2.3.1 Determination of τ , S_r , and S_i from an Oscillation, Step Increase, or Reduction in Total or Local Power
 - 3.1.2.3.2 Loop Current Step Response

DETAILED TABLE OF CONTENTS FOR SECTION 3
(CONTINUED)

- 3.1.2.3.3 Installed Heater Cable
- 3.1.3 Effects of Reactor Exposure on Sensitivity
- 3.1.3.1 "Library" Studies
- 3.1.3.2 SRP Experience
- 3.1.3.3 HBWR, Halden Reactor Experience
- 3.1.3.4 Direct Testing of RGT at ORNL
- 3.2 K₂, The Ratio of Local Fuel Power to Gamma Heating in the Sensor and the Components of the Uncertainty, σ_2
- 3.2.1 Modelling via Neutron Physics and 3D Monte Carlo Shielding Calculations
- 3.2.1.1 The EdF/CEA Theoretical Programs
- 3.2.1.1.1 Specificity of Signal
- 3.2.1.1.2 Total Composition of Signal
- 3.2.1.1.3 Relationship of Sensor Heating to Fuel Power
- 3.2.1.2 Heat Rate of Gamma Thermometers During Non-Steady State Operation-CEA Studies
- 3.2.1.3 Extensions of Modelling to Other NSSS Systems
- 3.2.1.3.1 The ScP/CEA Proposals to EPRI for Extensions to Other NSSS Systems
- 3.2.1.3.2 The Oak Ridge National Laboratory Program
- 3.3 Completed Programs Demonstrating the Precision of Gamma Thermometry
- 3.3.1 Savannah River Plant, SRP, Experience
- 3.3.2 HBWR, Halden Reactor, Experience
- 3.3.3 The Otto Hahn Tests
- 3.3.4 EPRI/GE/Georgia Power Work at Hatch Nuclear Unit No. 1
- 3.3.5 AEG/KWU Gamma Thermometer Evaluation at KWL (Lingen)

DETAILED TABLE OF CONTENTS FOR SECTION 3
(CONTINUED)

- 3.4 GTIG-Related Programs Now Underway to Reduce RGT Uncertainties
- 3.4.1 The EdF Prototype Program
- 3.5 Programs Establishing Mechanical System Compatability, Handling Technique, Integrity of Presssure Boundary, Consequences and Modes of Failure
- 3.5.1 EdF Mechanical and Torture Testing of RGTs
- 3.5.2 RWE and DUKE Power Prototype Programs
- 3.5.3 ScP/IFA Tests Simulating Signal Failure Modes

APPENDICES

APPENDIX

- I Letter, 21 September 1977, Patrick M. Stafford of Duke Power Co., to R. D. Smith, Scandpower. "Self-Powered Neutron Detector vs. Gamma Thermometer Signal to Power Conversion."

CONSOLIDATED LIST OF FIGURES

Figure

- 1-1 First SRP Gamma Thermometer (Ca. 1953)
- 1-2 Today's SRP Gamma Thermometer (Ca. 1962 to present)
- 1-3 Standard Halden Type Gamma Thermometer
- 1-4 γ -radcal Gamma Thermometer Assembly (RGTA) for Pressurized Water Reactors
- 1-5 Enlarged Photograph of EdF γ -radcal Before Drawing on of Jacket Tube
- 1-6 Temperature Distribution and Heat Flow in PWR γ -radcal
- 1-7 Principle of Direct Electric Calibration of an RGTA

- 3.0-1 Contributions to Uncertainty in Sensitivity of Instrument
- 3.0-2 Contributions to Uncertainty in Ratio of "Measured" Parameter to Local LHGR

- 3.1-1 BWR γ -radcal Uses Pure Radial Heat Flow
- 3.1-2 Axial and Radial Split in RADCAL/THERMAL
- 3.1-3 Input Array for RADAL/THERMAL
- 3.1-4 Calculated Steady State Temperature Distribution
- 3.1-5 Predicted Response of Canne 3 and 4 by RADCAL/THERMAL
- 3.1-6 Logarithmic Plot of Power Step Response Curve
- 3.1-7 Relationship Between Real Sensitivity, S_r , and Dominant Time Constant of Junction, τ
- 3.1-8 Predicted Plunge Test Response - a Typical ORNL Specimen
- 3.1-9 Effect of Chamber Length Variations in ΔT
- 3.1-10 Effect of Axial Dislocation of Hot Junction in ΔT
- 3.1-11 Effect of Chamber Gas Filling in ΔT
- 3.1-12 Experimental Set-Up for Hot-Lab Plunge Tests at ORNL
- 3.1-13 Calibration of RGT Prototype at IFA (Air Filling)
- 3.1-14 Calibration of RGT Prototype at IFA (Vacuum Filling)
- 3.1-15 Calibration of RGT Prototype at IFA (Effect of Coolant Temperature)
- 3.1-16 Calibration of RGT Prototype at IFA (Effect of Coolant Velocity)
- 3.1-17 Calibration of RGT Prototype at IFA (Vacuum Filled Sensor Recalibrated After 5 Thermal Cycles up to 450°C)
- 3.1-18 Intertechnique Test Loop

CONSOLIDATED LIST OF FIGURES

(CONTINUED)

Figure

- 3.1-19 Canne No. 4, Sensor No. 1 - Calibration Results
- 3.1-20 Canne No. 4, Sensor No. 2 - Calibration Results
- 3.1-21 Canne No. 4, Sensor No. 3 - Calibration Results
- 3.1-22 Canne No. 4, Sensor No. 4 - Calibration Results
- 3.1-23 Canne No. 4, Sensor No. 5 - Calibration Results
- 3.1-24 Canne No. 4, Sensor No. 6 - Calibration Results
- 3.1-25 Canne No. 4, Sensor No. 7 - Calibration Results
- 3.1-26 Canne No. 4, Sensor No. 8 - Calibration Results
- 3.1-27 Canne No. 4, Sensor No. 9 - Calibration Results
- 3.1-28 High Temperature Calibration of Canne 2
- 3.1-29 Effect of Temperature on the Electrical Calibration
- 3.1-30 Interloop Comparison, Signal DT 11
- 3.1-31 Interloop Comparison, Signal DT 12
- 3.2-1 Use of Calibration Valve at Halden to Measure Fuel Power During Gamma Thermometer Calibration
- 3.2-2 Details of Calibration Valve
- 3.2-3 Ratio of Signals to Power
- 3.2-4 One-Eighth Sector of 17x17 Fuel Assembly Defining Pin Rows Used in CEA Calculations
- 3.2-5 Influence of a Transient in Power
- 3.2-6 Sensor Heat Rate Following Instant Rise to Full Power
- 3.2-7 Dynamic Response of Sensor Heating to 8 Hour Load Reduction
- 3.2-8 Fuel Power to Sensor Heating Ratio vs Burnup at Bugey 5
- 3.3-1 Change in Gamma Flux After a Power Change
- 3.3-2 Performance of SRP Gamma Thermometer
- 3.3-3 Failure Frequency of Instruments in HBWR
- 3.3-4 Specificity of Signal at HBWR
- 3.3-5 Effects of Nearby Control Rods in HBWR
- 3.3-6 Comparison of Gamma Thermometer Heating with Fast Flux in Axial Positions at HBWR

CONSOLIDATED LIST OF FIGURES

(CONTINUED)

Figure

- 3.3-7 Gamma Thermometer Assembly, Type A
- 3.3-8 Gamma Thermometer Assembly, Type B
- 3.3-9 Gamma Thermometer Assembly, Type D
- 3.3-10 Gamma Thermometer Assembly, Type E
- 3.3-11 All TIP Systems Require Normalization
- 3.3-12 TIP Devices Compared at Hatch 1 by GE/EPRI
- 3.3-13 AEG Gamma Thermometer
- 3.4-1 Calibration Comparison
- 3.4-2 EdF High Pressure Test Loop
- 3.4-3 Test Section in High Pressure Test Loop
- 3.4-4 Temperature Effect on Sensitivity
- 3.4-5 EdF γ -radcal Assembly
- 3.4-6 Photograph of "Exploded" Parts of EdF RGT
- 3.4-7 RGTAs in Bugey 5
- 3.4-8 RGTAs in Tricastin 2
- 3.4-9 RGTAs in Tricastin 3
- 3.4-10 Power Traces of RGT Sensors at Equal Core Elevations
- 3.4-11 RGT "Tracked" Power vs Calculated Power During Xenon Swing, Canne 5
- 3.4-12 Axial Processing
- 3.4-13 RGT Signal After Shutdown
- 3.4-14 Comparison of Gamma Heating and Incore Nuclear Power for Canne G9, detector 1, at Tricastin 3
- 3.4-15 Comparison of Gamma Heating and Incore Nuclear Power for Canne G9, detector 2, at Tricastin 3
- 3.4-16 Comparison of Gamma Heating and Incore Nuclear Power for Canne G9, detector 3, at Tricastin 3
- 3.4-17 Comparison of Gamma Heating and Incore Nuclear Power for Canne G9, detector 4, at Tricastin 3

CONSOLIDATED LIST OF FIGURES

(CONTINUED)

Figure

- 3.4-18 Comparison of Gamma Heating and Incore Nuclear Power for Canne G9, detector 5, at Tricastin 3.
- 3.4-19 Comparison of Gamma Heating and Incore Nuclear Power for Canne G9, detector 6, at Tricastin 3.
- 3.4-20 Comparison of Gamma Heating and Incore Nuclear Power for Canne G9, detector 7, at Tricastin 3.
- 3.4-21 Comparison of Gamma Heating and Incore Nuclear Power for Canne G9, detector 8, at Tricastin 3.
- 3.4-22 Comparison of Gamma Heating and Incore Nuclear Power for Canne G9, detector 9, at Tricastin 3.
- 3.4-23 Comparison of RGT and TIP Measurements for a Xenon Transient - Top Peak
- 3.4-24 Comparison of RGT and TIP Measurements for a Xenon Transient - Middle Peak
- 3.4-25 Comparison of RGT and TIP Measurements for a Xenon Transient - Bottom Peak
- 3.4-26 3-D Plot of Xenon Transient Using RGT Measurements
- 3.4-27 3-D Plot of Xenon Transient Using RGT Measurements
- 3.5-1 Cross Section of B&W SPND Unit
- 3.5-2 Detector Orientation in a B&W PWR
- 3.5-3 B&W Seal Flange Assembly
- 3.5-4 Westinghouse (Framatome) Arrangement of TIP System
- 3.5-5 Framatome Mechanical Test Facility
- 3.5-6 EdF RGTA
- 3.5-7 Disposal of Irradiated TIP Tubes or RGTA
- 3.5-8 Calculated Hot and Cold Positions of RGTs, Bugey 3
- 3.5-9 Details of DUKE RGTA Containing Calibration Tube

CONSOLIDATED LIST OF FIGURES

(CONTINUED)

Figure

- 3.5-10 DUKE RGTA
- 3.5-11 KKMK Seal Flange
- 3.5-12 Mechanical Alternative to Welded Seal Flange for KKMK
- 3.5-13 Pressure Barrier Considerations

CONSOLIDATED LIST OF TABLES

Table

- 3.1-1 Experimental Results for EdF, Canne No. 6
- 3.1-2 Summary of High Temperature Calibration of French Prototypes and Specimens, Canne No. 4-8
- 3.1-3 Summary of Low Temperature Calibration of French Prototypes and Specimens, Canne No. 3-12, Specimen No. 1-5
- 3.1-4 Schedule of Installation of Accelerated Irradiation Specimens in ORR
- 3.1-5 ORNL Tests: Post-Irradiation Results
- 3.1-6 Fast Neutron Exposure for the ORNL Specimens
- 3.2-1 Sources of Gamma Heating in Sensor
- 3.2-2 Distribution of Source Gamma Contributing to Sensor Heating
- 3.3-1 In-Core Instrument Status at Halden
- 3.4-1 GTIG Related Programs, listed by categories

DEFINITIONS

applicant	Scandpower on behalf of US utility members of GTIG: TVA, Duke Power, PSE&G, submitting this topical report.
APRM	Average power range monitor system which initiates the scram action in BWRs.
BBR	The B&W, Brown Boveri Co. consortium building KKMK for RWE.
B&W	Babcock-Wilcox Co., Lynchburg Virginia.
BWR	Boiling Water Reactor.
CE	Combustion Engineering Co., Windsor, Connecticut.
C _p	Specific heat, Watt-seconds/g°C or BTU/lb-°F.
cable pack	The ordered array of stainless steel clad, mineral insulated cables (thermocouples, difference thermocouples, double difference thermocouples, and nichrome heaters), running coaxially with the centerline of the RGTA and onto which the core tube is swaged or drawn.
canne	The French word for cane, or rod. It is used by EdF to identify the RGTA prototype series: canne no. 0 - a process development prototype rod canne no. 1 - a prototype rod for mechanical test canne no. 2 - prototype used for loop testing canne no. 3 - in Bugey 5, 12 June 1979 canne no. 4 - in Bugey 5, 12 June 1979 canne no. 5,6,7,8 - in Tricastin 2, June 1980 canne no. 9,10,11,12 - Tricastin 3, fall 1980
core rod, or tube	The central piece of stainless steel in an RGTA which is drawn or swaged onto the cable pack and into which sensor (chamber) annuli are ground or machined at selected measuring intervals along its first 4 meters of length.
DDT	Double Difference Thermocouple: a composite thermocouple assembly inside a single jacket containing four junctions: chromel-alumel (type K).
deconvolution	Mathematical methods to find the input when the output and transfer function are known.

DEFINITIONS

DT	Difference Thermocouple, a compound thermocouple containing both hot and cold junctions. Always has zero signal when both of its junctions are at the same temperature.
dry RGT	An RGTA that fits into a Westinghouse or GE TIP thimble rather than replacing it.
EdF	Electricite de France - sole power supplier for France, governmentally-owned corporation. World's largest utility, 45 nuclear plants operating or under construction by Framatome (Westinghouse PWR type).
EPRI	Electric Power Research Institute, Palo Alto, California.
g	specific heat rate in gamma thermometer sensor, W/g.
gamma thermometer	Any of the family of devices that uses the ΔT developed along a controlled heat path to measure the rate of heat being generated by absorption of gamma radiation energy.
GE	General Electric Co., San Jose, California.
GKSS	German utility operating the Otto Hahn nuclear ship.
GTIG	An information-sharing collaboration of companies in Europe, US, Japan doing RGT development individually and collectively (Gamma Thermometer Investigation Group) currently consisting of: Electricite de France, Duke Power Co., Rheinisch-Westfalisches Elektrizitatzwerk, Tennessee Valley Authority, Swedish State Power Board, Public Service Electric and Gas of New Jersey, Kansai Electric Power Co. and Exxon Nuclear, the newest member of the group which was started in November 1978.
Halden	See HBWR
HBWR	Halden Boiling Water Reactor, Halden, Norway. An international project operated jointly by 15 organizations under auspices of OECD, and owned by I.F.E. (Institut for Energiteknikk), Kjeller, Norway.

DEFINITIONS

I.F.E. (formerly IFA)	Institutt for Energiteknikk, formerly Institutt for Atomenergi, Norway.
in-situ	synonym for in-reactor.
k or λ	thermal conductivity of a material in consistent units usually W/ ^o C-cm.
K ₁	reciprocal of indicated sensitivity, 1/S _i , W/g of sensor heating per standard C of signal voltage.
K ₂	Ratio of local fuel power to "measured" parameter. In the case of RGT: local fuel power, W/cm, to sensor heat rate, W/g. For SPNDs, the ratio of LHGR to neutron flux.
KWU	Kraftwerk Union, originally a consortium of AEG and Siemens Nuclear Division, offering both BWRs and PWRs. PWRs are represented by RWE's Biblis A, B, C - 1300 MWe; BWRs are Brunsbuttel, Philipsburg, and RWE's Gundremmingen B, C. KWU is currently offering only PWRs.
LHGR	Linear heat generation rate in fuel pins, kW/ft or W/cm of fuel length.
LPRM	Local power range monitor which, in some BWR systems, initiates automatic rod withdrawal block.
LWR	Light Water (moderated and cooled) Reactor.
ORNL	Oak Ridge National Laboratory.
ORR	Oak Ridge Research Reactor at ORNL.
Otto Hahn	German nuclear ship, employing LWR fuel and operated by GKSS.
PSMS	Power shape monitoring system, EPRI project at Oyster Creek.
PWR	Pressurized Water Reactor.
q	specific heat rate in gamma thermometer sensor, W/cm ³ .
Q	heat rate, W.

DEFINITIONS

RGT	γ -Radcal gamma thermometer, refers to one sensor in an RGTA or the design concept.
RGTA	γ -Radcal gamma thermometer assembly - is the array of RGTs reaching from top of core to pressure seal flange (also referred to as "string" or "canne").
RWE	Rheinisch-Westfalisches Elektrizitätswerk, Germany's largest utility, Essen, second largest private utility in world with ca. 30,000 MWe, 10 nuclear plants operating or under construction. Major owner German Breeder, 17% participant in Super Phoenix.
γ -Radcal sensor	Acronym for LWR type gamma thermometers for light water reactors (radial heat flow, electrically <u>calibrated</u>).
S_i , indicated sensitivity	The indicated temperature difference (obtained using type K standard thermocouple curves) produced by a one watt per gram heating of the RGT sensor, std. °C/W-g.
S_r , real sensitivity	The true temperature difference produced between hot and cold junctions by a one watt per gram gamma heating of the RGT sensor. °C/W-g.
SPND	Self-powered neutron detector.
SRP	Savannah River Plant, Aiken, South Carolina; DOE facility operated by E.I. DuPont de Nemours and Co.
SSPB	Swedish State Power Board.
TIP	Travelling in-core probe.
TRAVCAL	GTIG name for a travelling gamma thermometer enabling substitution for and comparison with signals from Westinghouse travelling fission chambers.
TVA	Tennessee Valley Authority.

DEFINITIONS

WIRECAL	GTIG name for an assembly containing two RGTs and a tube for travelling wire or other probe. Originally specified for BWR, Big Rock Point, the scheme eliminates symmetry assumptions necessary in PWR tests to calculate "real" local powers in a RGT test position.
ΔT	Difference in temperature, °C.
ϕ_n	Thermal neutron flux, neutrons/cm ² -sec.
σ_c	Combined uncertainty (standard deviation) in the determination of the highest local LHGR in the reactor.
σ_1	Uncertainty (standard deviation) in the sensitivity of the detector (i.e., the uncertainty in the relationship of signal to the "measured" parameter ϕ_n , ϕ_γ , or gamma heat rate).
σ_2	The "coupling" uncertainty (i.e., the uncertainty in the ratio of "measured" parameter to fuel LHGR)
σ_3	The "extrapolation" uncertainty (i.e., the uncertainty involved in calculating local fuel power at a point remote from the measuring instrument).
σ_4	The "non-steady state" uncertainty (i.e., the uncertainty in local power "measurement" when local power is not constant.

LIST OF REFERENCES

- 1-(1) Nelson, Earl C., E.I. duPont de Nemours and Co., Savannah River Plant, Aiken, S.C. "Measurement of Neutron Flux Distribution", DPSPU 61-30-5.
- 1-(2) Asphaug, J.S., "Gamma Thermometer Development at Halden", HPR-35, July, 1964.
- 1-(3) Stutheit, E.I. duPont de Nemours and Co., Savannah River Plant, Aiken, S.C. "Fast-Response Gamma Thermometers", Nuclear Instruments and Methods, North Holland Publishing Co., 1968, pp. 300-306.
- 1-(4) Private communication: Scandpower ScPH Note 23, 11/9-73, from: Blomsnes, B.; Netland, K.; Smith, R.D. to: Ulfby (NVE), Lunde, Vik, Ager-Hanssen.
- 1-(5) HBWR Quarterly Progress Report, April to June 1970 (HPR 126), p. 71.
- 1-(6) Series of EPRI reports dealing with TIP development at Hatch Nuclear Unit 1:
 - a) EPRI NP-540, Dec. '77 "Special Tip Detector Measurements at Edwin I. Hatch Nuclear Plant Unit 1 Prior to End of Cycle 1".
 - b) EPRI NP-511, Aug. '78 "Gamma Scan Measurements at Hatch Following Cycle 1".
 - c) EPRI NP-561, Sept. '79 "Special TIP and Gamma Scan Comparisons from Hatch 1".
 - d) EPRI NP-562, Jan. '79 "Core Design and Operating Data for Cycle 1 of Hatch 1".
- 1-(7) Minutes of GTIG Meeting, Paris, France, 21 Feb., 1979.
 - a) Appendix B: "Programme EdF de Developpement Technologique de Cannes de Thermometres Gamma".
- 1-(8) Scandpower A/S, 30 Sept. 1974, "Appraisal of Developments in Control System Designs for LWRs" prepared for Framatome, Paris, France.
- 1-(9) EPRI, Jan. 1977, NP-337, "Review of In-Core Power Distribution Measurements - Technical Status and Problems".
- 1-(10) Meeting with NRC, Jan. 19, 1978, Scandpower U.S. Call Report 530. Attendance: ScP- Leyse, Smith, NRC- A.A. Johnson, D. Fieno, H. Richings, K. Kniel, R. Schemel.
- 1-(11) Scandpower U.S. Call Report 731, 3 Aug. 1978. Discussion: Leyse, Fieno.
- 1-(12) Nucleonics Week, April 10, 1980.

LIST OF REFERENCES

(CONTINUED)

- 3-(1) Papers presented to NRC by GE in securing ruling on conversion of Hatch Nuclear Unit No. 1 from travelling fission chamber to travelling gamma detector.
- (a) NRC Memo: H. Vandur Molen to R.L. Baer, Reactor Safety Branch, DOR, NRC, 23 Sept. 1977.
 - (b) Letter on docket No. 50-321, George Lear, Chief Br. No. 3, DDR to Georgia Power Co., 17 April 1978 - Gamma TIP Questions
 - (c) Letter of Docket No. 50-321, 22 May, 1978. "Gamma TIP Questions", C.F. Whitmer (Georgia Power) to Director NRR.
- 3-(2) Nelson, Earl C., E. I. duPont de Nemours and Company, Savannah River Plant. "Measurement of Neutron Flux Distribution", DPSPU, 61-30-5, June 1961.
- 3-(3) Weiss, Westinghouse Electric Corporation, "In Core Gamma Radiation and Neutron Flux Distribution in a Pressurized Water Reactor", Atomenergie (ATKE) Bd 15, 1fg 4.
- 3-(4) Stutheit, J.S., "Fast Response Gamma Thermometers", E.I. duPont de Nemours and Co., Savannah River Plant, 10 May 1968, Nuclear Instruments and Methods 63 (1968) North Holland Publishing Co.
- 3-(5) B. Aarset, "Power Measurements in a Natural Circulation Boiling Channel", HPR 35, Volume 1, August 1964.
- 3-(6) GTIG Meeting Minutes, Chattanooga, Tennessee, 11-12 October, 1979. Appendix G - "CEA Theoretical Work".
- 3-(7) K. Svanholm, December 1967. "Gamma Thermometer and Neutron Detector Application", HPR-73.
- 3-(8) Fordestrommen, N.T., "Discussion of an Incore Power and Safety System Consisting of Gamma Thermometers together with a Prompt Response Neutron Sensitive Detector Type". Meeting on Computer Control Fuel Research, Sanderstolen, Norway.
- 3-(9) Bid Specifications for Irradiation Test Specimens of RADCAL in Oak Ridge Research Reactor. Scandpower Technical Note 14, 1979.
- 3-(10) Experimental Procedure for RADCAL Testing at Oak Ridge. Prepared by Scandpower, February, 1980.

LIST OF REFERENCES

(CONTINUED)

- 3-(11) Thermometer Gamma Specimens ORNL. Plan de Control. Departement Telemesure Intertechnique ORSAY, DG/CC/CLS/02500, Mars 1980.
- 3-(12) TEC (Technology for Energy Corporation), Calibration Report on RADCAL Test Specimens for ORNL.
- 3-(13) Guillery, M., "Tests of Gamma Thermometer Prototype No. 2 in Electrical Loop at Renardier." Presented at GTIG meeting in Paris, February, 1979.
- 3-(14) Minutes from GTIG meeting at Oak Ridge, February 1980.
- 3-(15) Results of First In-Reactor Tests of RADCAL Gamma Thermometers at Bugey 5, EdF (report in preparation April 1980).
- 3-(16) Electrical Calibration of Prototype RGTAs, Cannes no. 3-12, EdF (report in preparation April 1980).
- 3-(17) Curtis, Thomas D., SPND Operating Experience at Oconee Nuclear Station. IEEE Conference Washington, D.C., March 1979.
- 3-(18) Stafford, P.M., "A Summary of the Program Leading to the Development of a Gamma Thermometer In-core Detector System." Nuclear Fuel Division, Duke Power Co., February 1978.
- 3-(19) Consumers Power - letter to DOE, 25 October, 1979.
- 3-(20) Tennessee Valley Authority - letter to DOE, 1 November, 1979.
- 3-(21) Power Peaking Nuclear Reliability Factors. BAW-10119, Topical Report, November 1977.
- 3-(22) Standard Technical Specifications for Westinghouse Pressurized Water Reactors. Westinghouse Electric Corporation. Nuclear Energy Systems, May, 1976.
- 3-(23) Duke Power Company, RADCAL Gamma Thermometers. Bid specifications prepared by Scandpower, Inc. spec. no. 904, 1978.
- 3-(24) Rheinisch-Westfalisches Elektrizitatzwerk AG RADCAL Gamma Thermometers, Type RW (prototypes). Bid specifications prepared by Scandpower A/S, January 1980.
- 3-(25) Bosio, J., "Experimental Results from Out-of-Pile Tests with an Electrical Heated Pre-prototype of RADCAL Gamma Thermometer, Wet-type." Scandpower A/S, 1977.

LIST OF REFERENCES

(CONTINUED)

- 3-(26) Garrett, Michael E., "Effects of Increased APRM Response Time on BWR Safety." Minutes from GTIG Meeting, Chattanooga, Tennessee, October 1979, Appendix C.
- 3-(27) Bosio, J., "Experimental Results from Out-of-Pile Tests with Electrical Heated Pre-Prototype of RADCAL Gamma Thermometer, Dry-type." Scandpower A/S, 1977.
- 3-(28) Normal Operating Control. BAW-10122A, Topical Report, November 1979.
- 3-(20) C-E Setpoint Methodology. C-E Local Power Density and DWB LSSS and LCO Setpoint Methodology for Analog Protection Systems. Combustion Engineering report CEWPD. 199, April, 1966.
- 3-(30) Process Computer Performance Evaluation Accuracy, General Electric, Topical Report, June 1979.
- 3-(31) Carroll, R.M. and Shepard, R.L., "Measurement of the Transient Response of Thermocouples and Resistance Thermocouples Using an In Situ Method." Oak Ridge Report ORNL/TM 4373, June 1977.
- 3-(32) Kerlin, T.W., "Analytical Methods for Interpreting In-Situ Measurements of Response Times in Thermocouples and Resistance Thermometers." Oak Ridge Report ORNL/TM 4912, March, 1976.
- 3-(33) Evaluation of the In-Pile Drift of Gamma Thermometer Signal Versus Time by Collecting Library Information. Scandpower Study. Fiche d'etude 3B, December 1979.
- 3-(34) Kollie, T.G. et.al. "Temperature Measurement Errors with Type K (Chromel vs Alumel) Thermocouples due to Short Ranged Ordering in Chromel." Rev. Sci. Instrum., Vol. 46 No. 11. November 1975.
- 3-(35) Herskovitz, M.B. and Hubbel, Jr., H.H., "Effects of Fast-Neutron Irradiation on Sheathed Chromel/Alumel Thermocouples", ORNL, TM-3803, August 1976.
- 3-(36) Final Report on Accelerated Irradiation Tests of Gamma Thermometers. ORNL, June 1981 under TVA contract.
- 3-(37) Calculation of RADCAL Gamma Thermometer Accuracy in Out-of-Pile Conditions. Scandpower study, fiche d'etude 3A, December 1979.

LIST OF REFERENCES

(CONTINUED)

- (38) Specifications Des Specimens De Thermometre Gamma Pour Reacteur Experimental Oak Ridge. Intertechnique, Department Telemesure. DG/CC/CLS/02446, Janvier 1980.
- 3-(39) 0-point Calibration of RADCAL Test Specimens in Accelerated Irradiation Test Program at ORNL, Scandpower Report, June, 1980.
- 3-(40) Bosio, J., "Radcal Parametric Study and Calculations." Scandpower A/S, June 1978.
- 3-(41) Beraud, G. and Sqalli, M.H. "Instrumentation interne fixe - Point sur l'interpretation des experiences Bugey 5 au 15," Septembre 1980.
- 3-(42) Beraud, G., Jouve, M.A., Squalli, M.H., "Etude de l'effet du houx d'irradiation sur le reponse des thermometres gamma de Bugey 5," (in preparation).
- 3-(43) Barral, J.C., Beraud, G., "Instrumentation interne, Analyse des performances de differents types d'instrumentation; E.SETB 8059 (aout 1980)."
- 3-(44) L'etude d'incertainties d'thermometre gamma relative definitive, Department Telemesure, Intertechnique, Mars 1979.
- 3-(45) U.S. Department of Energy Field Task Proposal/Agreement: "Gamma Thermometer Irradiation and Qualification" 6/20/79, Oak Ridge National Laboratory, Union Carbide Corporation.
- 3-(46) CEA Confidential Report, "Thermometre Gamma - 1ere partie - Etudes Concernant L'echauffement du thermometre carte des importances, Influence des Transitoires de Puissance, Dopage". Rapport SERMA/T/No358, L. Bourdet, Cladel, O. Hoclet, A. Le Dieu de Ville, J.C. Nimal, CEA.
- 3-(47) Bonnemay, A., et Fontana, X., CEA Confidential Report: Rapport SERMA/T/No358. "Thermometre Gamma 2eme partie - Etude de Faisabilite d'un filtre correcteur restituant le signal de puissance a partir du signal d'un thermometre gamma et perspectives de developpement".
- 3-(48) Unsolicited proposal to EPRI: "Development of Analytical Methodology for Power Distribution Monitoring in LWRS with Gamma Detectors", (prepared by CEA and ScP and submitted 4 September 1979 to Dr. A. Long, EPRI, on a visit to Saclay for this purpose).

L I S T O F R E F E R E N C E S

(CONTINUED)

- 3-(49) "Summary of Meeting with General Electric Company to discuss gammasensitive TIPS", NRC memorandum, H. Vander Molen, DDR to R.L. Barr, DOR, 23 September 1977.
- 3-(50) "Tests to Examine Stability of RADCAL Gamma Thermometer Signals through the Course of High Fast Flux Irradiation on Multiple Test Samples," Scandpower, 1 April 1979.
- 3-(51) Rheinisch-Westfalisches Elektrizitätswerk A/G, Radical Gamma Thermometers, Type RW, (Prototypes). Specification No. RWE 190618, rev. 1; Scandpower A/S, Halden, Norway.
- 3-(52) Program for RGT Qualification for BWR Use, Scandpower, February, 1981.
- 3-(53) Turnage, K.G., Development and Evaluation of PWR Vessel Liquid Level Instrumentation at ORNL, Oak Ridge National Laboratory, Oak Ridge, Tennessee.

1. INTRODUCTION

1.1 Objectives of this Topical Report

It is the objective of this Topical Report to elicit a statement from the NRC staff that, given appropriate data processing routines and equipment (to be defined on a system-by-system basis in subsequent topical reports), RGT gamma thermometer systems will measure local fuel powers with adequate accuracy to be used as the basic local power measuring in-core instrument in U.S. pressurized water reactors in compliance with operational Technical Specification requirements.

The applicants for review suggest that the work reported herein supports the accuracy of measurement attainable by this device and request that NRC staff concur with these conclusions. Applicants will provide all substantiating material requested during the course of NRC review.

1.2 Principles of Gamma Thermometry

Gamma thermometers depend upon the heating of a metal block by gamma rays (approximately 93 percent of the heating) and energetic neutrons (approximately 7 percent). The heat so generated is proportional to the specific power of nearby fuel rods. Heat generated in the block of metal (the "heater") is permitted to escape to a sink only through a controlled heat path of closely held dimensions. The temperature drop along that heat path is directly proportional to the volumetric heat rate (Watts/gram) in the heater, and therefore proportional to the power, not neutron flux, in the adjoining fuel rods.

A thermocouple, or thermocouples, arranged to measure the temperature drop along the controlled heat path, produces a signal proportional to this power. The usual material of construction is stainless steel. The heat rate in stainless steel at full power ranges from 0.5 to 6 W/g. Design temperature drops have been selected in the range from 4°C to 250°C at full reactor power. The thermocouple indication of ΔT

generated by one watt of heating per gram of material is called the "indicated sensitivity" of the gamma thermometer. The true temperature difference between the measuring points is called the "real sensitivity" of the gamma thermometer.

1.3 History of Gamma Thermometry until 1974

Gamma thermometers (single-sensor chambers) have been in routine use for power distribution measurement in the cores of heavy water moderated reactors at the DOE Savannah River Plant for over 25 years, Ref. 1-(1), and in the heavy water moderated Halden reactor since 1963, Ref. 1-(2).

Figure 1-1 illustrates the original gamma thermometer as devised and conceived at Savannah River Plant in 1953. The device replaced the original gamma ion chambers which proved to be unstable and short-lived devices.

Even in 1953 the designers of the gamma thermometer were cognizant that neutron flux* was an inferior parameter for measurement of local fuel heat generation rate, upon which all Savannah River Plant local control limits were based (i.e., surface temperature, burnout safety factor, and maximum local heat generation rate), Ref. 1-(3).

*Neutron flux peaks in water spaces, where no power is produced. It increases by large amounts as U_{235} burns up, even with constant fuel power.

Ref. 1-(6c), the EPRI report on recent Hatch Nuclear Unit 1 tests, documents recognition of the superiority of gamma over neutron measurement for local power determination in light water reactors:

"Relative to the thermal neutron TIP, calculated power distribution comparisons show that the gamma-sensitive TIP significantly reduces the apparent nodal and bundle power asymmetries. This reduction in asymmetry contributes to a 3 percent increase in the gamma TIP calculated thermal margins."

Figure 1-2 shows the present day gamma thermometer in use at the Savannah River Plant. Some 3,000 gamma thermometers have been used at SRP since 1961 with totally satisfactory results and a failure frequency under 3 percent, Reference 1-(4).

Figure 1-3 shows the gamma thermometer which has been used since 1963 in Halden reactor test fuel. These gamma thermometers, about 7 mm in diameter and 50 mm long, have survived with a mortality rate before removal of less than 3 percent, and have given signals proportional to surrounding fuel power without measurable drift for periods as long as 7 years and fuel exposure up to 26,000 MWd/ton, Reference 1-(5).

Note in Figure 1-2 that the present Savannah River Plant gamma thermometer employs what is referred to herein as a difference thermocouple. The heat being conducted along an iron pin, which is connected at its extremities to constantan wires, produces a ΔT and a difference thermocouple signal almost completely independent of the sink temperature and dependent only on the heat generation rate in the iron pin itself. In the absence of fission product gamma rays, the signal from this instrument will be zero at zero nuclear power, regardless of the temperature of the coolant outside the gamma thermometer. The Halden gamma thermometer of Figure 1-3 generally employs a standard type thermocouple, with only one junction. This is possible in the Halden Boiling Water Reactor because the sink temperature is essentially constant as determined by the saturation pressure in the vessel. Hence the local fuel power is proportional to the difference between the temperature measured in the gamma thermometer and the temperature corresponding to saturation pressure in the vessel.

The SRP and HBWR experience will be referred to in detail in later sections because the experimental verification of a local power instrument can be made more accurately in heavy water reactors than in light water reactors. In the SRP and Halden reactors the power in every fuel assembly can be measured calorimetrically (mass flow x C_p x temperature drop) with errors as small as $\pm 3/4$ percent at SRP and 2-1/2 percent at Halden. In-reactor calibrations of a new instrument in light water

reactors are, at the onset, subject to the uncertainties of the existing methods of measuring fuel power by thermal flux systems.

Not only is the gamma thermometer heating more nearly proportional to fuel power than the current from a well-behaved gamma ion chamber, as can be shown theoretically (Section 3.2), but the sensitivity, the signal per unit of heat generation (Section 3.1), is stable within narrow limits for indefinite life times in the reactor. Not only can sensitivity be accurately measured in the workshop but the sensitivity can be re-measured at will in the reactor without recourse to the cumbersome, inaccurate, time consuming systems such as travelling in-core probes. The solid stainless steel structure of an RGT system reduces the NSSS system exposure to pressure boundary disruption when compared to either TIP or SPND systems now in use in PWRs.

1.4 The RGT Gamma Thermometer for PWRs

The PWR γ -RADCAL assembly, RGTA, (Figure 1-4), is 7 to 8 mm in diameter and 7 to 9 detectors are located along its length. The assembly is constructed of stainless steel (Zircaloy is under investigation) and consists of three parts: the jacket tube; the core tube; and a set of difference thermocouples which are located in a cluster, or pack, in the small diameter bore of the core tube. The differential thermocouple construction is illustrated in the lower part of Figure 1-4. The cable pack sometimes also contains a nichrome heater cable used for in-reactor recalibration and one or more standard thermocouples. The difference thermocouples are of conventional, mineral insulated construction (preferably Al_2O_3), with stainless steel jacketing, and 0.5 or 1.0 mm outer diameter. The two chromel-alumel junctions are differentially connected as illustrated with hot and cold junctions separated by 3 to 5 cm. Each hot junction is located at the center of a detector section, and the thermocouples comprising the pack run parallel with the RGTA axis for total lengths up to 36 meters (in the large B&W systems). A dummy extension of thermocouple-type cable replaces the signal cable beyond its hot junction in order to provide an axially uniform cross section for the cable pack inside the bore of the core tube.

Several sensors (e.g., 6 to 9) are located along the first 4 meters of length of the RGTA core tube. A sensor (RGT) is produced by grinding a chamber (a heat transfer resistance) into the core rod. That is, the core rod is ground to a reduced diameter for an accurate length, (e.g., 26.5 mm) before the jacket tube is drawn onto the core tube. An annular gap of 0.3 to 0.5 mm thickness is thus produced for the length of the sensor. This gap creates the axial heat flow and the consequent measured ΔT .

The assembly sequence is as follows: The differential thermocouple cable pack is installed into the bore of the core tube in an ordered array and the core tube is then swaged or drawn onto the cable pack to achieve good heat transfer contact between the thermocouples and the core tube (Figure 1-5). The hot thermocouple junctions are then accurately located (as, for example, by X-ray) and the chamber sections are ground into the core rod at the identified locations. Finally, the jacket tube is slipped over the core tube and bonded over the length by drawing through dies or by swaging. The sensor chambers are filled with Argon during these assembly operations.

RGT manufacturing processes are simple. There are competitive and good sources of supply for mineral insulated thermocouples. The drawing and swaging processes involved in manufacture are relatively common art.

The heat transfer path and the temperature gradient within the gamma heated assembly are illustrated in Figure 1-6. The heat which is generated within the sensor section must flow axially from the center to each end where it then flows radially outward to the jacket tube. This is essentially the same heat flow path that has been illustrated for the Halden and the Savannah River devices, except that the heat flow is in two directions from the location of the hot junction. Since the temperature profile is relatively flat near the midpoint of the sensor section, it is not vital to achieve absolutely exact centering of the hot thermocouple junction in order to achieve an acceptable calibration characteristic. Likewise, since the cold junction is located in a flat (zero axial gradient) temperature region, the location of the cold junction

need not be accurate. However, the length of the sensor chamber must be carefully controlled since the total temperature gradient varies nearly as the square of the length of the chamber.

The γ -RADCAL gamma thermometer assembly, RGTA, is typically 15 to 36 meters long with an end seal and plug arrangement that are specific to the reactor application. The prototype assemblies constructed for Electricite de France are 16 meters long and are designed for installation in the PWR (Westinghouse-type) reactors Bugey-5 and Tricastin. Duke Power Company prototype assemblies are approximately 33 meters long and are designed for the Babcock & Wilcox reactor at the Oconee Station. The Duke prototypes have a central calibration tube (2.3 mm ID) and 7 sensors, as in the present self-powered neutron detector assemblies at Oconee, while the EdF assemblies have 9 sensors plus an additional differential thermocouple that measures the temperature rise across the core. The 36 meter long, RWE prototype design for the B&W plants, Mulheim-Karlich, contains heaters permitting direct in-core recalibration and employ double difference thermocouples one mm in diameter (see Section 3.1.1.3.6).

The gamma thermometers in the assembly (Fig. 1-7) can be simultaneously calibrated in the workshop by electric resistance heating of the 4 meter length while the assembly is cooled with flowing water at either atmospheric or PWR conditions. EdF has constructed a high pressure electrical calibration loop in which 10 RGT assemblies (90 chambers) have been calibrated at PWR conditions before reactor installation, Ref. 1-(7a). This resistance heating simulates the gamma heating in the reactor core and makes it possible to calibrate over the full range of PWR gamma heating rates and expected coolant conditions. This is a distinct advantage of all γ -RADCAL designs and will be discussed more completely in Sections 3.1.1 and 3.1.2.

1.5 The History of γ -RADCAL

The γ -RADCAL gamma thermometer for PWRs was an outgrowth of studies

conducted by Scandpower for Framatome and EdF in 1974, the essential conclusions of which were:

1. None of the local power instrument systems in use were of an accuracy and reliability that should satisfy plant owners, and
2. Gamma thermometers, long used in D_2O reactors, should be examined as practicable instruments for PWRs, offering both accuracy and reliability.

Framatome reported these ideas to Electricite de France, the governmentally owned national utility of France which commissioned further studies by Scandpower and the Norwegian Institutt for Atomenergi to determine the practicability of the use of gamma thermometers in light water reactors. Electricite de France's interest was in the possible replacement of the Westinghouse travelling, in-core probe type of instrumentation by the fixed, gamma thermometer type of instrumentation which would have the advantages of real time measurement and mechanical simplicity.

The hypothesis made at the time from D_2O reactor experience was that signal stability would be such that no on-line, in-pile recalibration would be necessary over the lifetime of the installed instrumentation. It was, however, recognized that fairly accurate in-pile recalibration of these thermal devices could be obtained upon any step increase or reduction of reactor power because, for gamma thermometers, the transient response to a step change in power (i.e., time constant) is closely and uniquely related to the real sensitivity of the instrument.

Scandpower's investigation of the applicability of the HBWR-type of gamma thermometer to the Westinghouse-type of light water reactor not only indicated the feasibility of the application of that type of gamma thermometer, but suggested that the PWR environment was, in fact, superior, not inferior, to the heavy water reactor environment for the application of gamma thermometers.

One primary difference was the higher specific gamma heat generation of approximately 1.5 W/g in the pressurized water reactor as compared to 0.5 W/g in the heavy water reactor. The high specific heat rate permitted miniaturization of the instruments without loss in signal strength.

A second advantage was the specificity of signal origin in the PWR lattice. Because of the closely spaced fuel rods (low moderator to fuel ratio) in the PWR, 92 percent of gamma heating in a gamma thermometer originates within the fuel bundle being measured. Eighty percent originates in the 110 fuel pins immediately surrounding the instrument (of 264 in a 17x17 bundle).

Signal strength is one of the primary advantages of the gamma thermometer. For example, the average, full-power, temperature difference in gamma thermometers is 40°C which produces a signal of 1.6 millivolts from a chromel-alumel difference thermocouple (strong enough to be routed directly from the reactor to the control room without intervening amplification). A gamma thermometer loses only 2 percent accuracy when cable resistance has dropped to 100×10^3 ohms.

Scandpower engineers recognized, as a common weakness of sensor systems employing discrete chambers or sensors, such as the fixed fission chamber system or the Halden gamma thermometer system, a vulnerability of the signal cable seals as they crossed the primary pressure barrier. A single monolithic rod-like structure became the objective. The earliest version of γ -RADCAL employed pure radial heat flow in a rod of stainless steel or Zircaloy in which multiple difference thermocouples could be imbedded at the desired number of levels in the core. This design is still the leading candidate for BWR RGTAs, (see Fig. 3.1-1). In the PWRs, however, where the diameter of such a rod was limited to 7.5 mm, the radial temperature rise was limited to about 4.5°C at the hot junction and for this reason the present PWR RGT design was developed. This design employs a combination of axial and radial heat flows and, in general, an average signal ΔT of 40°C has been selected. The gamma thermometer instrument referred to as the "PWR γ -RADCAL" is depicted in Figure 1-4.

The monolithic structures, which had been originally sought for mechanical and structural reasons, proved to offer the unique attribute of calibration by direct electrical resistance heating as depicted in Figure 1-7 and mentioned earlier. The ability to perform direct electric calibration makes it possible, if desired, to assure that all gamma thermometers, as they leave the workshop, will produce the same signal within 0.7 percent when exposed to the same gamma fields. (An alternative is to accept, say, a 2 percent variation in "as made" indicated sensitivity and individually bias signals a like amount in-reactor.)

The program conducted at Hatch Nuclear Unit 1 by GE, with EPRI funding, proved gamma flux measurement to be more accurate for local power determination than the fission chamber (i.e., thermal neutron flux) TIP system by using post-irradiation gamma scans as the reference or standard for local fuel powers, Figure 1-(6).

It is the position of the applicants that the Hatch work, backed by the D_2O calibration, by extensive theoretical treatment, and by a number of light water reactor programs complete and in progress, is sufficient to verify the high precision of local power measurement which can be attained by RGT gamma thermometers in PWR use. The intention is to minimize uncertainty at certain benchmark or reference points for which maximum calibration accuracy exists, and to prove that the extrapolation error, (i.e., the uncertainty at unbenchmarked or "off-reference" conditions), is small, because the total variation in the signal of gamma thermometers is small over the entire "parameter space" of operating conditions.

1.6 Intrinsic Advantages of RGT Gamma Thermometers

Direct Measure of LHGR

Foremost of the attributes of gamma thermometers is the very direct relationship of the output signal to the local fuel power, upon which all local operating limits most directly hinge (e.g., DNB, MLHGR, MCHFR, etc.).

Both theory and experience show that the raw signals from all core gamma thermometers can be converted to surrounding local fuel power values by the application of a single constant with an accuracy of about ± 10 percent regardless of fuel burnup, core configuration, or control rod position, and that this ratio of fission heat to sensor heat holds true indefinitely. It is expected that when full systems of RGTs have been installed in PWRs a simple summation of some 350 to 450 signals will yield a direct and quite accurate value for total reactor thermal power.

The readout systems under development for RGTs employ both a "straight through" signal channel and a "high accuracy" processing channel which employs normalization and obtains the highest possible accuracy of local power measurement from RGT sensors.

Constancy of Calibration

SRP gamma thermometers have exhibited constant calibrations over fast fluence corresponding to 5-1/2 years in a PWR (within 1-1/2 percent calibration accuracy). Halden gamma thermometers have held constant calibration over seven years of irradiation in HBWR with no observable changes in signal relative to the power in surrounding fuel. At HBWR the fuel loading is so variable and heterogeneous that the uncertainty associated with this observation is larger than at SRP, and is estimated by the applicants to be ± 5 percent.

A highly documented, well-controlled exposure test of RGT specimens has been undertaken in the ORR at Oak Ridge National Laboratory. It has been calculated that the 10 specimens being irradiated therein will change calibration less than 5 percent after a fast neutron exposure of 6.2×10^{21} neutrons per cm^2 , (equivalent to 3 years in a PWR).*

The overall correlation of RGT signal to fuel LHGR is dependent first upon the sensitivity of the RGT, S_i , signal/watt/gram of sensor heating

*Although the irradiation has been completed, as of July, 1981, experimental problems have delayed the post-irradiation calibration of the specimens. See Section 3.1.3.4.

(or its reciprocal K_1), and second upon K_2 , the fission-to-gamma heating ratio prevailing (LHGR in fuel per watt/gram of RGT sensor heating). The term gamma heating is used for convenience. Actually, 7 percent of the heating in an LWR gamma thermometer is due to n, γ reactions taking place in the sensor. Both of these ratios vary with time and core conditions within quite narrow bands (± 5 percent on K_1 and ± 10 percent on K_2).

Accurate Out-of-Pile Calibration

The sensitivity of RGT signals to heating of the sensors can be measured at the workshop by direct electrical heating or by time constant determination. Identity of chambers within ± 0.7 percent in sensitivity can be so attained. In practice, to date, a variation of $\pm 1-1/2$ percent in mean sensitivity has been accepted by EdF. Individual chambers have shown high linearity of signal (correlation coefficient greater than 0.9999 to the best fit straight line) in both room temperature and high temperature (300°C coolant) electrical heating calibrations (see Section 3.1.2.2). The second, independent, out-of-reactor calibration means, the dynamic type of calibration, is discussed in Section 3.1.2.1 and 3.1.2.2. The theoretical means for predicting the calibration is presented in Section 3.1.2.

Large Signals

RGTs produce meaningful signals (i.e., affected less than 2 percent) when cable resistance has fallen as low as 100,000 ohms. The signals can be led directly to the control room without intervening electronics (at Halden the signals are taken directly more than 100 meters). An average RGT signal at full power is 1.6 millivolts (40°C) from a thermocouple. EdF has reported usable RGT signals at 1 percent reactor power from prototypes in Bugey 5 with no noise problem.

RGTs can be used as fixed, in-core detectors to produce real time signals, which enhance the operator's knowledge of what is happening to critical core parameters at all times.

In-Core Recalibration Without TIP

Oak Ridge National Laboratory has developed a process called "Loop Current Step Response" in which small current steps are imposed upon in-reactor thermocouples and resistance temperature detectors to obtain transfer functions which are "deconvoluted" to show the response of the devices to external stimuli such as coolant temperature changes. This technique led Scandpower to propose to GTIG members that heater cables be incorporated in RGTs.

The initial tests using such heater cables in the RGT specimens for ORNL testing gave calibration curves with linearity and scatter as good as those obtained by direct electrical calibration.

In the application of the heater calibration technique, the heat being generated in any RGT string at any time (usually 0 to 3.0 W/g) is augmented by up to 3 watts per gram of electric heating via the mineral insulated nichrome cables imbedded in the cable pack. This full range recalibration can be done at any time required or desired, and at full or reduced reactor power.

2. SUMMARY

This report describes the use of RGTs in PWRs and the expected uncertainties associated with the use of RGTs to measure local power. The uncertainties currently established are summarized below.

Sensor Sensitivity (K_1) and its Uncertainty (σ_1)

The report and its references deal quantitatively with the uncertainty, σ_1 , in RGT sensor sensitivity after precalibration and irradiation. The values of this parameter are presently 1.9 percent for individual chambers upon installation and within 5 percent over sensor lifetime. Programs in place will probably reduce the uncertainty, σ_1 , to 1 percent and 2 percent, respectively, by a combination of well-documented exposure testing, upon which computer corrections can be based, and various means for accurate "in-situ" recalibration.

The Ratio of Fuel Power to Sensor Heating (K_2) and the Uncertainty (σ_2)

The report also deals with the ratio of local fuel power to gamma sensor heating, K_2 , and its associated uncertainty, σ_2 , when used in PWR fuel charges. The information presented herein, together with supporting reference material made available to NRC reviewers, establishes that the largest steady-state variation expected for K_2 within the PWR operating condition range is -12 percent and shows that the most important deviations from the reference value of K_2 occur where local fuel powers are suppressed (i.e., not possibly approaching local limits).

The report establishes that the most important limitation on proving experimentally the accuracy of K_2 (i.e., σ_2), is the accuracy of the installed neutron measuring systems from which K_2 must be benchmarked. The applicants show that the presently established value for σ_2 is ± 6.5 percent for this reason, but anticipate that efforts to benchmark

reference K_2 values will reduce σ_2 to ± 4.5 percent through various experimental programs under way from which data will be available within the course of NRC review of this report.

The limited range of variation of K_2 , proved by both theory and experiment, establishes that corrections to the final benchmarked values of K_2 are so small, and can be made with such high precision, that the increment in σ_2 introduced by such correction will be on the order of 10 percent of the basic uncertainty σ_2 experimentally proven at the benchmarked (reference) conditions.

A full core RGT system will enable accurate normalization of summed or average RGT power indication to total thermal power and thus provide the most important single reduction in the provable value of σ_2 . To arrive at this possibility for step improvement in demonstrable precision (i.e., a full core of RGTs), various programs (experimental and theoretical) comprising the attack on uncertainty σ_2 have been initiated and are defined.

The Spatial Extrapolation Uncertainty (σ_3)

The extrapolation uncertainty, σ_3 , represents an identical problem for neutron devices (SPND, TIP) as for the new fixed RGT system. It is both system specific and computer dependent and has little to do with the detector employed. This report deals with σ_3 only to the degree that the increased marginal returns of more sophisticated data processing, consequent upon the reduced σ_1 and σ_2 achieved by RGT systems, are illustrated. For example, the use of a high-speed on-line nodal physics simulator to interpolate between points of measurement can gain only 16 percent improvement in total uncertainty for a typical neutron-based system, but after RGT installation the same interpolation improvement can gain 38 percent of the remaining combined uncertainties for an RGT based system. The data processing, or extrapolation, uncertainties will be treated in subsequent submittals that are NSSS and RGT system generic but computer-code specific.

The Non-Steady State Uncertainty (σ_4)

Real-time core power distribution monitoring involves the non-steady state uncertainty, σ_4 , whose short term value can be fairly large for RGT systems, without signal deconvolution. This is due to the delayed part of the gamma sensor heating arising from fission product gamma. The uncertainty, σ_4 , is dependent upon the size of a local power change, the time over which it occurs and the recent local power history around the RGT position. The status of signal deconvolution development for RGTs is reported without arguing the final value of σ_4 attainable through analog or digital data processing. This uncertainty will be quantitatively addressed (as σ_4) in subsequent system specific, plant generic topical reports.

Signal Corrections

The RGT is so accurately characterized as made, and so little dependent upon complex on-line correction of signals, that the entire stream of 350 to 450 raw signals can be presented meaningfully and directly to the operator, without complex intervening data processing. The applicants propose to utilize this "straight-through" system attribute in all full scale applications, while the parallel, computer-processed data streams obtain the maximum accuracy of signal interpretation. All sensors now being made (to a particular design) exhibit mean sensitivities (K_1) within a ± 4.1 percent band (σ). The total range of variation in the uncorrected constant K_2 (the ratio of local fuel heat rate to sensor heating) is ± 3 percent in unrodded PWR cores (for the normal, baseload case).

The applicants conclude that a gamma responsive instrument such as RGT, requiring only small compensations during signal processing, intrinsically has an ultimate uncertainty in local power determination lower than that of any instrument responding to thermal neutron flux.

UNCERTAINTY STATUS

(All values are standard deviations, \pm)

A. With "Plant Accuracy" Line of Digital Signal Processing

	Currently ⁽¹¹⁾ established	Attainable from present programs (com- pleted during NRC review)	Attainable with full PWR core of RGT ⁽¹⁰⁾
σ_1 : Sensitivity uncertainty on K_1			
new RGTs	\pm 1.9 percent ⁽¹⁾	\pm 1 percent ⁽³⁾	\pm 1 percent
irradiated RGTs	\pm 5 percent ⁽²⁾	\pm 2 percent ⁽⁴⁾	\pm 2 percent
σ_2 : Coupling uncertainty on K_2			
at clean ref. conditions ⁽⁵⁾²	6.5 percent ⁽⁶⁾	4.5 percent ⁽⁸⁾	3.5 percent ⁽¹⁰⁾
at off ref. conditions	7.5 percent ⁽⁷⁾	5.0 percent ⁽⁹⁾	4.0 percent ⁽¹⁰⁾
σ_3 : Spatial extrapolation to hot points	X	per EDP rou- tines selected: same as SPNDs or TIPs (4.5 percent)	use of 3D nodal simu- lator 3.5 percent
σ_4 : Transient uncertainties	less than 6 percent with analog filters	6 percent for 20 sec. after 20 percent step (digital decon- volution)	dependent on BWR program

B. With "Straight-Through" Signal Processing⁽¹²⁾

σ_1 : new RGTs	4.1 percent	2.5 percent	2.5 percent
irradiated RGTs	6.5 percent	3.5 percent	3.0 percent
σ_2 : at clean ref. conditions	6.5 percent	4.5 percent	3.5 percent
at off ref. conditions	8.5 percent ⁽⁷⁾	6.0 percent	5.0 percent

(1) Based on EdF, ORNL calibration.

(2) Based on SRP, Halden, experience + "library" studies.

(3) Based on latest-made RGT specimens (ORNL). Process improvements underway (Duke, RWE).

(4) Based on ORNL tests, exposure corrections to K_2 , in situ recalibration.

(5) No nearby control rods or local poisons.

(6) Bugey 5 results.

(7) This reaches higher values for low powered (rodded, poisoned) fuel.

(8) Limits of accuracy attainable via Tricastin 2, 3, TRAVCAL and Oconee programs in 1981-82.

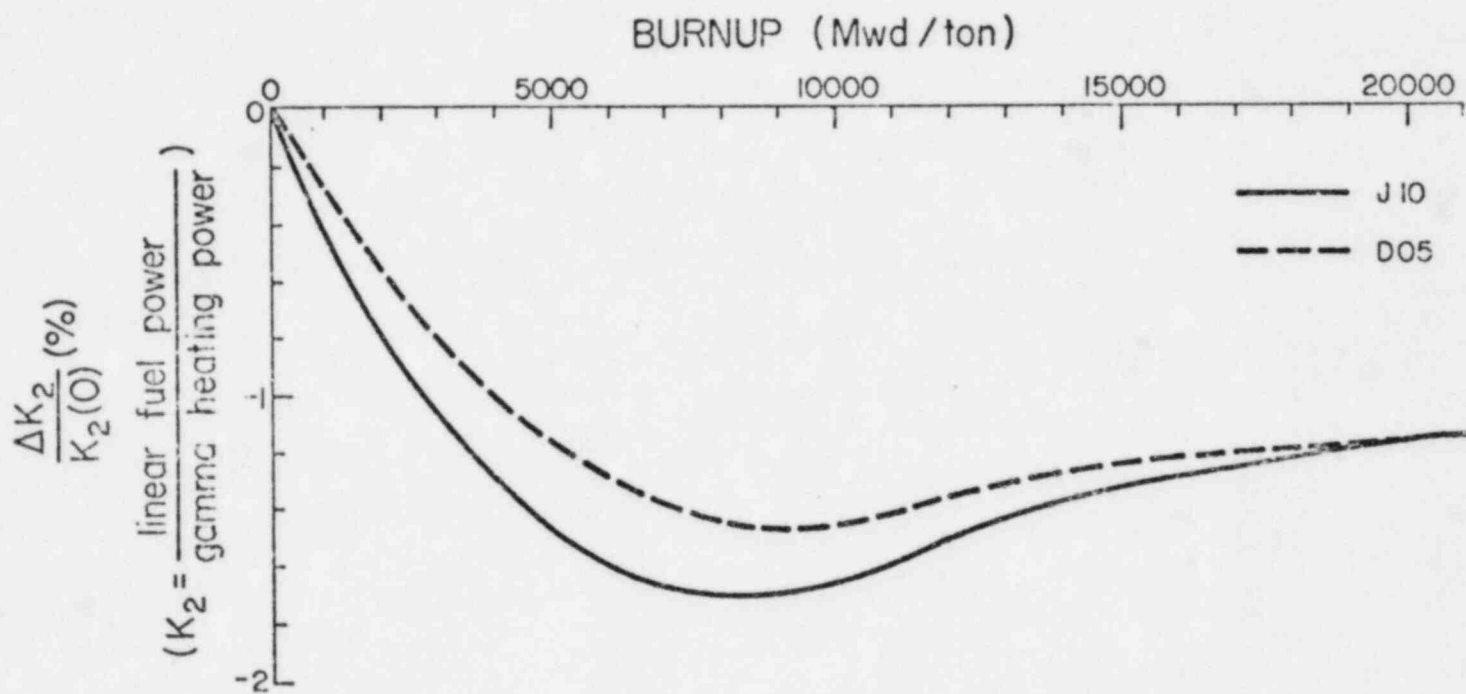
(9) Contributions from TRAVCAL, Tricastin, and theoretical (CEA, ORNL) programs.

(10) Requires normalization to thermal power - possibly P.I. gamma scans.

(11) Via this Topical Report and cited references.

(12) The systems selected for processing data from the "straight-through" signals will be a compromise between accuracy (smaller σ_3 and σ_4) and reliability (larger σ_3 and σ_4). Maximum attainable accuracy on σ_3 and σ_4 is that of the "plant accuracy" line. Selection of appropriate signal processing awaits more experience.

The following figure shows the effect of exposure on the value of K_2 , calculated for position D-5 in Bugey 5. For the exposure from 0 to 20,000 Mwd/t the ratio of computed fuel heat rate to sensor heat rate, K_2 , remains constant within 1.7 percent. (For this exposure range there would be nearly a 100 percent increase in neutron flux.)



Mechanical, Safety, and Other Considerations

Mechanical and pressure boundary compatibility of RGTAs with Westinghouse and Babcock-Wilcox NSSS systems has been demonstrated. Because of their solid, monolithic structure the RGTAs reduce the total system vulnerability (area exposed) to breach of the pressure boundary in both cases.

RGTs have the potential to measure core temperatures, heat transfer coefficients and tank level during loss-of-coolant-level accidents.

The lifetime of RGTs is not easily predicted because there are no known phenomena that should limit lifetime (equivalent PWR exposures of 5-1/2 years have been experienced). The premature failure rate should be much lower than the 3 percent experienced by some 3226 gamma thermometers used in D_2O reactors over the past 20 years because the RGT thermocouple sheaths are not exposed to reactor water. (Water penetration of thermocouple sheaths accounts for at least half of the 3 percent early failures experienced in D_2O plants).

Reduced frequency of handling of highly radioactive core instrument components arising from the long life expectancy of RGTs will reduce plant personnel exposure risk and critical path time lost for such handling during shutdowns.

3.0 DISCUSSION

There are four principal components of uncertainty (each complex) that must be addressed in qualifying any in-core detector for use in the determination of local fuel heat generation rates within the reactor core:

σ_1 : The Sensitivity Uncertainty

Question: To what accuracy is the sensitivity (i.e., the ratio of the signal to the "measured" variable) of the detector provable?

* The question may be restated as:

What are the uncertainties between the processed signals from the RGT sensors and the heat generation rate in the sensors at the point of measurement?

Answer:

$$g, \text{ sensor heat rate, W/g} = K_1 \cdot \text{signal} \pm \sigma_1$$

where K_1 has been determined individually and accurately for each sensor by electric calibration (i.e., $1/S_i$), and σ_1 is the uncertainty associated with K_1 .

There is as yet no known systematic correction applicable to the original out-of-reactor workshop calibration of an RGT. Conservative calculations using nominal materials property data indicate that a six year PWR irradiation of an RGT could have a maximum effect upon K_1 of +5 percent if the maximum postulated changes were combined unfavorably (Section 3.1.3). Past reactor experience (Section 3.3) has revealed no changes in K_1 . Since the total changes to K_1 are expected to be small, the uncertainty on K_1 is also small.

σ_2 : The Coupling Uncertainty In The Ratio Of The Local Fuel Power To The "Measured" Variable

Question: To what accuracy is the ratio of the local heat generation rate in surrounding fuel calculable from an accurate value of the measured parameter? (Since local fuel heat generation rate is the dominant variable in local operational limits derived from heat transfer burnout, maximum allowable surface temperature after LOCA, pellet clad interactions and all other phenomena which might damage fuel, LHGR is the parameter which should be directly measured if possible.)

* For gamma thermometers the σ_2 question can be restated as follows: Assuming the "measured" heating rate in the sensor is accurate, how accurately may the local powers of fuel rods in the immediate vicinity of the sensor be calculated?

Answer

$$\text{LHGR} = g \cdot \frac{f(\text{exposure, poison configuration})}{K_2} \pm \sigma_2$$

where g is the watts/gram of heating in the sensor and σ_2 is the uncertainty on K_2 .

Accurate measurements in D_2O reactors, where fuel thermal powers are directly measured calorimetrically, have shown that the total variances in K_2 , the ratio of LHGR to g , are extremely small over large fuel exposure ranges, (Sections 3.3.1 and 3.3.2), and are zero within the limits of detection at the HBWR up to 26,000 Mwd/t, and are within ± 2 percent in high exposure charges at SRP where the limits of detection of change are $\pm 3/4$ percent.

Theoretical work with PWR (Westinghouse-type) lattices by CEA, (SERMA at Saclay) has confirmed this stability of K_2 for the effects of fuel exposure, boron concentration, and burnable poison with the conclusion

that the ratio of local fuel power to gamma detector heating varies by less than ± 3 percent over the whole range of these kinds of variables in PWR cycles (Section 3.2). Because the range of variation of K_2 is small, the incremented uncertainty in calculational corrections away from experimentally benchmarked conditions is small, even if the predictive validity of the physics models were to be fairly poor in absolute terms.

This means that the sum of core gamma thermometer readings has the potential for agreement to total thermal power, without correction by normalization.

σ_3 : The Spatial Extrapolation Uncertainty

Question: To what accuracy are determinations of local fuel power in the region of sensors extrapolatable to local fuel power at locations remote from the sensors?

Answer:

This question is both reactor-system and computer-programming dependent. The most elegant methods of expansion of the measurements involve extrapolation on-line by streamlined three-dimensional core simulator models constrained to fit measurements at sensor locations in the nodal core structure.

There is diminishing marginal utility in such sophisticated methods, however, when other components of uncertainty are large. For example, consider that the simple "interpolate-and-ratio" scheme yields ± 6 percent for σ_3 , the spline-fit technique yields ± 5 percent, and the on-line simulator yields ± 3 percent. For sensor systems in which σ_1 is ± 5 percent and σ_2 is ± 5 percent, improvements in σ_3 have marginal pay off, e.g.:

$$\sigma_c^2(\text{combined}) = (.05)^2 + (.05)^2 + \sigma_3^2$$

For interpolate-and-ratio $\sigma_c = 9.2$ percent

For spline fit $\sigma_c = 8.6$ percent

For on-line simulator $\sigma_c = 7.7$ percent

Gain over poorest method: 16 percent

If RGT systems produce a σ_1 of 2 percent and σ_2 of 2 percent the value of the more elegant expansion processes increases:

For interpolate-and-ratio $\sigma_c = 6.6$ percent

For spline fit $\sigma_c = 5.7$ percent

For on-line simulator $\sigma_c = 4.1$ percent

Achievable gain from better expansion processing: 38 percent

Among the GTIG member utilities, SSPB already incorporates on-line simulators in its BWR data processing routines, and RWE is developing such a system for its Biblis PWR reactors, partially in anticipation of the reduced local power uncertainties to be derived from RGT gamma thermometer systems. EPRI has built fast, 3-D neutronics simulation into its power snape monitoring system at Oyster Creek.

The present report deals only with the accuracy of fuel power determination, in the vicinity of sensors, obtainable with RGT gamma thermometers and with the components of uncertainty related to instrument sensitivity S_i or, $K_1 \pm \sigma_1$, and the LHGR-to-gamma-sensor heating ratio, $K_2 \pm \sigma_2$.

Subsequent topical reports will address both σ_3 and σ_4 on NSSS and computer software-specific bases, for referencing in individual plant licensing cases.

σ_4 : The Non-Steady State Uncertainty

Question: To what extent is the ratio of LHGR-to-measured parameter (i.e., K_2), made more uncertain when power or power distribution is changing or has recently changed?

Answer:

This is an uncertainty not necessarily addressed for base loaded systems. For example, the Westinghouse full core power mapping system takes from 3/4 to 1-1/2 hours to execute with TIP, and stable steady

state operation is a prerequisite for accurate use of the system (i.e., σ_4 is large if power is changing).

The present PWR-type RGTs have a relatively short response time* to changes in sensor heat rate (i.e., 17 seconds compared to about 60 seconds for SRP gamma thermometers and 2-1/2 minutes for SPNDs), but exhibit a delay somewhat comparable to that of SPNDs in the transfer function relating fuel power to gamma heating of the sensor. Stutheit of SRP, Reference 1-(3), reports that:

"For a step increase in reactor power in a D₂O moderated reactor, gamma flux will increase by 65 percent instantly (following the prompt gamma resulting from fission) and after 100 seconds (the increase) will be at 90 percent of its final value."

Sophisticated calculational methods not available to Stutheit 12 years ago enable the delayed component of gamma heating to be "deconvoluted" to the degree that 90 percent of the final value is "measured" within 10 seconds of a step change.

The French theoretical program (Section 3.2.1.1) and the reactor prototype program aim aggressively at minimizing σ_4 through analog numerical filter programs or deconvolution on the process computers. The underlying reason for this attention to the non-steady state uncertainty for PWRs is the eventual necessity for load follow operation of many PWRs (Section 3.2.1.2) in, for example, France.

* Size of signal is exchangeable for response time in an RGT. See Section 3.1.1.1.

Corrections to Signals

Figures 3.0-1 and 3.0-2 illustrate the components of uncertainty that affect the RGT gamma thermometer method of determination of LHGR. An important point is that the raw signal from an RGT gamma thermometer is directly meaningful at all times during the reactor cycle and in whatever fuel exposure zone of the reactor it is located, (i.e., using single values of K_1 and K_2 for 450 instruments). The expected total computer corrections to raw RGT signals to achieve minimum uncertainty in local power measurement will not exceed 10 percent. As presently made for EdF, the nine RGT sensors within an RGTA exhibit the same sensitivities within a 2σ band of 3 percent. The average sensitivities for all 90 sensors in 10 assemblies agree within 7 percent (2σ). The scattering of calibration data for a particular sensor is very small ($\sigma = \pm 0.7$ percent) with a linear correlation coefficient greater than 0.9999 for a 7-point calibration. The measured sensitivities and time constants of sensors are as predicted by Ohm's Law and the laws of heat conduction.

Reliability of Signals

The conversion of the Hatch Nuclear Unit 1 TIP system to gamma ion chambers (from fission chambers) constituted the first serious recognition in the LWR industry that gamma flux was superior to neutron flux as an indication of LHGR, although isolated instances of recognition of the utility of gamma indicating devices in LWRs had occurred prior to Hatch 1. In Reference 3-(3), H. Weiss of Westinghouse Nuclear Energy

Systems, concluded a paper on gamma ion chamber measurements in Connecticut Yankee reactor by saying:

"The presented results may be considered as an attempt towards the application of the in-core gamma radiation for monitoring the cores of large power reactors under steady-state conditions. . .

The main advantage of the gamma technique is the constant sensitivity of the gamma detector which does not suffer from burnup of neutron sensitive material. As a consequence of this, frequent recalibration which is inevitable using neutron detectors may be omitted."

The question of the possible effects of irradiation upon sensitivity (i.e., increases in σ_1 after RGTs are in use) in gamma thermometers has been attacked in several ways (Section 3.1.3):

- 1) The examination through the computer model (parametrically) of all known or suspected effects of irradiation upon properties that could affect sensitivity such as: radiation vs thermocouple decalibration; radiation vs gas gap composition; and radiation effects upon thermal conduction and geometry of stainless steel parts (Section 3.1.2.3).
- 2) Examination of all available long-time irradiation vs calibration data on argon-filled, stainless steel gamma thermometers, principally from Savannah River and Halden (Sections 3.3.1 and 3.3.2).
- 3) Institution of high-accuracy, well-characterized "Accelerated Tests of Irradiation Effects on RGT Gamma Thermometer Sensitivity at ORNL." This test program was specified in April 1979, test specimens fabricated in the first quarter of 1980. Irradiation began in July 1980 and ended in July 1981. Most of the results of sensitivity change after a three year equivalent PWR irradiation

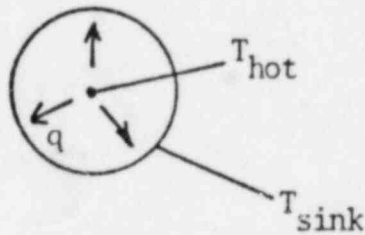
have been delayed due to experimental difficulties with the post-irradiation calibration. More complete results are expected in mid-1982 (Section 3.1.3.4).

- 4) Center line electrical heaters capable of doubling the full power heating have been incorporated into recent RGT prototypes (Sections 3.4.1 and 3.4.4). Initial out-of-pile tests with these heaters give calibration results that agree with direct electrical calibration results. Thus an accurate method of in-reactor recalibration already exists, if it proves to be necessary to minimize σ_1 . The heater cables also improve the ability of the RGTs to be used for level indication and core coolant heat transfer measurement during abnormal situations.

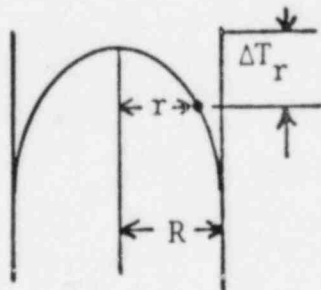
3.1 Sensitivity of RGTs by Computation and Measurements

3.1.1 Description and Modelling of the Thermal Processes

The ideal gamma thermometer would use pure metallic heat conduction for developing the signal temperature difference, and, if the signal were great enough, (i.e., W/g were high enough), the ideal geometry would use pure radial heat flow, as:



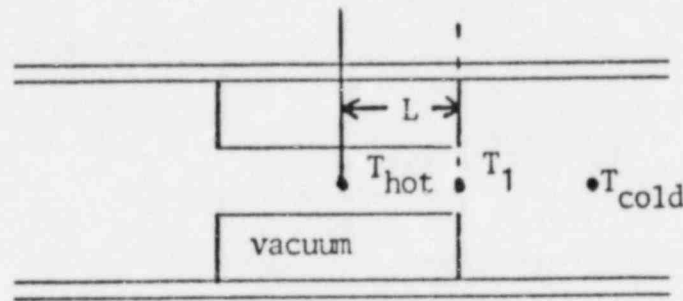
In this case the temperature distribution away from the central measuring point is parabolic:



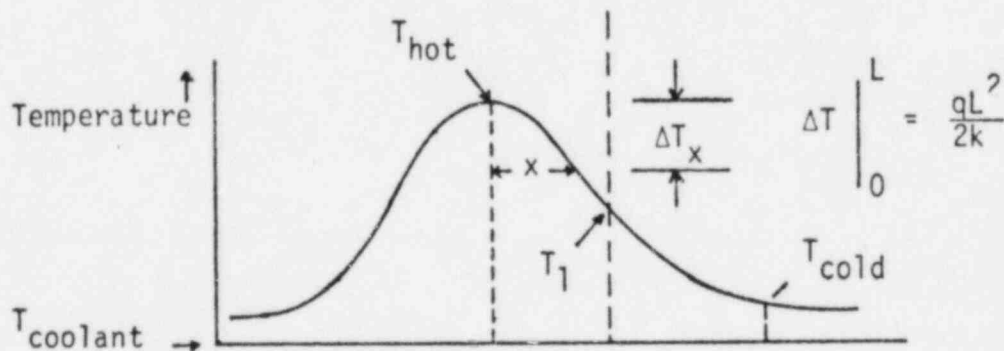
$$\Delta T_r = \frac{qr^2}{4k} \text{ and } \Delta T_{\text{signal}} = \frac{qR^2}{4k}$$

the variability in k (thermal conductivity of stainless steel) with temperature is known and reproducible. Only second order corrections to k are required when signal ΔT 's are small (i.e., in the region from 4°C to 100°C) and an average k corresponding to $T_{\text{sink}} + 2/3$ of ΔT_{signal} gives quite accurate prediction.

Pure radial heat flow as depicted above is in consideration for BWR RGTs which must have relatively low ΔT s to respond quickly enough to power changes. (See Figure 3.1-1.) However, for the smaller diameter PWR instrument (OD limit 7.5 mm in Westinghouse and Babcock & Wilcox PWRs) a larger signal is desired than can be achieved by pure radial heat flow. In this case axial heat flow is established, as:



Ideally, the annular space would be totally evacuated thus allowing only radiation heat losses to occur across the gap. These are, however, negligible below $500^\circ\text{C } T_{\text{hot}}$. In such a case the temperature profile is:



where q is the volumetric heat generation rate and k is the thermal conductivity in appropriate units. There are two practical considerations that led RGT designers away from this "ideal" design:

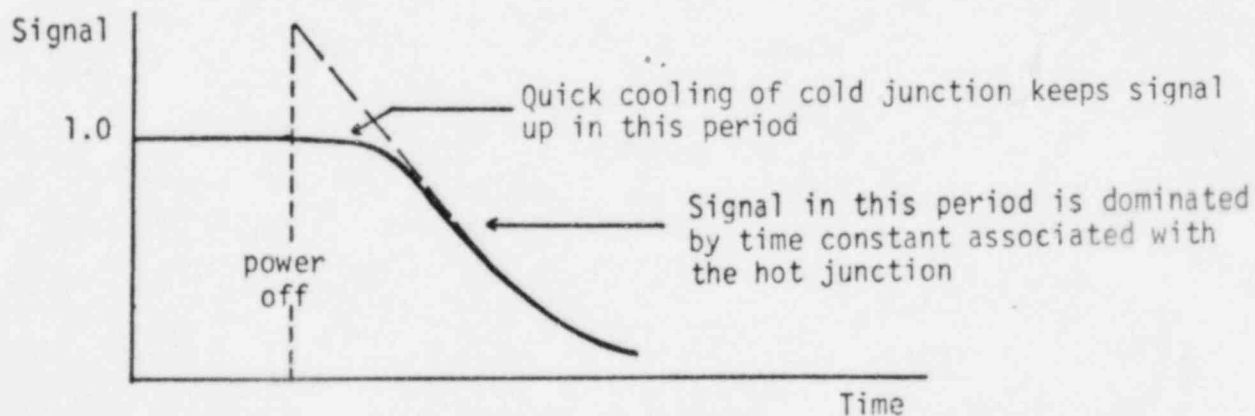
1. A cold junction located at T_1 would have to be very accurately located, for sensor reproducibility, because it is in the region of steepest temperature gradient. Thus, the cold junction has been moved to a point where its temperature is dominated by pure radial conduction (as described on the previous page) and the axial temperature distribution is flat. The signal ΔT from an RGT with vacuum in the annular space would thus be:

$$\Delta T \text{ signal} \approx \frac{qL^2}{2k} + (T_1 - T_{\text{cold}})$$

where the second term gives a small addition to signal from radial heat flow that is also linearly proportional to q .

2. Stainless steel jacket tubes are permeated rapidly by hydrogen in a PWR environment and hydrogen is an excellent heat conductor. Thus, all practical gamma thermometers of stainless steel have used inert gas (argon) filler. The "price" for this is a 15 percent heat loss through the gap. The benefit for it is that the presence or absence of small amounts of hydrogen negligibly affects gap thermal conductivity.

The time response of practical PWR RGTs (sensitivity of 40°C/W/g of heating) is thus composed of two components, that of the cold junction (~ 2 sec.), and that of the hot junction (~ 17 sec.), i.e.,



The difference in these two time constants leads to their easy separability in the plunge testing type of calibration to be discussed in Section 3.1.2.1. It need only be stated here that signal response to a step change in power or coolant temperature (with power zero) is uniquely related to the real sensitivity (ΔT vs W/g) for all gamma thermometers, as will be shown.

The practical departures from ideal construction (argon fill instead of vacuum), variable conductivity of steel vs temperature, variable conductivity of argon with temperature, location of the cold junction making a 2-dimensional thermal distribution, etc., have led to the development and use of a computer code, which is designated as RADCAL/THERMAL, to predict accurately the signals received during electric calibration, plunge test or transient calibration, and in-reactor heating. The primary use of the computer code is in the prediction of response to transient type calibrations and to appraise the sensitivity of the instrument to manufacturing tolerances and non-idealities of various kinds. The accuracy with which electric calibration results can be predicted by RADCAL/THERMAL is strongly dependent on the accuracy to which the properties k (thermal conductivity) and r (electrical resistivity) are predetermined for both the jacket tube and the core rod of the RGT being tested.

3.1.1.1 Relationships of Real Sensitivity, Indicated Sensitivity, and Response Times for Simple Systems

Definition of Sensitivity:

The RGT and some earlier gamma thermometers employ difference thermocouples (DTC) which cannot be easily calibrated in isothermal baths (i.e., they always give a zero signal). The variation in signal response for a given ΔT between the junctions would be expected to be on the same order as that for two remotely connected standard type K (chromel-alumel) thermocouples, ≈ 1 percent.

In considering gamma thermometer sensitivity (ΔT per W/g of sensor material) it is important to distinguish between what the applicants refer to as the "real" and "indicated" sensitivities of the sensors:

S_r = real sensitivity - true sensor ΔT per W/g of heating

S_i = indicated sensitivity = $\frac{\mu V \text{ signal from DTC}}{\text{standard } \mu V/^{\circ}C}$ per W/g of heating

This distinction is important because the transient methods of calibration (i.e., where time response is measured to yield sensitivity) give only the real sensitivity unless very special measures are taken. On the other hand, S_i , the indicated sensitivity, is that which must be used by the reactor power distribution system.

It is possible to manufacture RGTs whose real sensitivities to heating are within ± 0.5 percent with good process control, and the measured time responses will so agree. When the same units are directly calibrated by Joule testing (I^2R heating) the indicated sensitivities, S_i 's are measured and the achievable standard deviation among sensor calibrations increases to 1.0 percent. This is a direct measurement of the variability in signal of the differential thermocouples. Electrical calibration methods are accurate to at least ± 3.8 percent, 2σ , at the present state-of-the-art and are being improved with a target accuracy of 1 percent in the RWE prototype program.

Aproximate equations for the real ΔT of a PWR Gamma Thermometer RGT

Real ΔT (with vacuum in gap):

$$\Delta T = \frac{qL^2}{2k}$$

where: ΔT = ideal real temperature difference with axial conduction only
 q = heat rate, watts/cm³
 L = half length of the sensor, cm
 k = thermal conductivity, W/ $^{\circ}C$ -cm

Gap Conduction:

In the practical case there will be heat loss by conduction (though radiation is negligible) across the gas gap. The radial heat loss can be approximated by:

$$Q_{\text{leakage}} = \frac{2\pi k_g L \Delta T_A}{\ln \frac{d_2}{d_1}}$$

where:

- Q_{leakage} = heat loss by radial conduction, watts
- k_g = thermal conductivity of gas, W/°C-cm
- d_2 = inside diameter of jacket tube, cm
- d_1 = outside diameter of sensor, cm
- ΔT_A = average temperature difference between jacket tube and sensor. Can be taken as 2/3 ΔT sensor
- L = half length of RGT sensor, cm

Real ΔT with Gas in the Gap:

When radial gas gap heat conduction is combined with axial conduction along the sensor:

$$\Delta T_{\text{signal}} = \frac{q}{\frac{2k_s}{L^2} + \frac{20}{3(d_1)^2} \cdot \frac{k_g}{\ln \frac{d_2}{d_1}}}$$

where both k_g and k_s are somewhat temperature dependent and an iterative solution of ΔT_s is required. For type 316 ss and argon gas, the properties normally used are:

	$k_{T_{\text{ref}}}$	α	T_{ref}
316 stainless steel	.131 W/cm-°C	$10 \times 10^{-4} / ^\circ\text{C}$	20°C
argon	.000164	.00267	0°C

and for other temperatures:

$$K_T = K_{T_{ref}} [1 + \alpha (T - T_{ref})]$$

The above equation embodies the approximation that the effective ΔT across the gas gap is 2/3 of the sensor ΔT . This is accurately true only where the axial temperature distribution is truly parabolic.

Gamma Heat Absorption:

$$q = 16.03 \frac{\phi_\gamma E \mu_C}{\rho} \times 10^{-14}$$

where: $q = W/cm^3$
 $\phi_\gamma =$ no. of photons/cm²-sec.
 $\mu_C =$ absorption coefficient for energy E
E = photon energy in MeV
 $\rho =$ density g/cm³

The effective gamma energy is sometimes approximated as 1.5 MeV. For 1.5 MeV radiation $\frac{\mu_C}{\rho}$ for most materials is about 0.02/cm. Using these two

approximations the equation may be rewritten:

$$q = 11.7 \phi_\gamma \rho \times 10^{-15}$$

Since a flux of 3.8×10^5 photons/cm²-sec of 1.5 MeV energy is 1 R/h the equation may be expressed as:

$$q = 4.6 \rho r \times 10^{-9}$$

where:

r = the field in R/hr.

Having measured $q = 11.9 \text{ W/cm}^3$ in a PWR, the approximate radiation field is thus $3.3 \times 10^8 \text{ R/hr}$.

Neutron Heating

-- fast neutrons

Energy from collision from fast neutrons is:

$$q = 16.03 \phi \sigma_s \frac{2A}{(A+1)^2} E \times 10^{-14}$$

where:

$$q = \text{W/cm}^3$$

$$\phi = \text{flux in n/cm}^2\text{-sec}$$

$$\sigma_s = \text{elastic scattering cross section}$$

$$\frac{2A}{(A+1)^2} = \text{fraction of energy transferred to the target atom}$$

$$A = \text{atomic weight of the target atom}$$

$$E = \text{energy of the neutron group, MeV}$$

The amount of heat from fast neutron collision is less than 1 percent of the total and fast flux is directly proportional to fission rate.

-- Neutron Capture

The heat from neutron capture must be calculated for each material and for the spectrum at hand. Heat from n, α and n, β reactions in the sensor is, however, negligible.

Heat from n, γ Reactions in Sensors:

$$q = 16.03 \phi \mu_c E f \times 10^{-14}$$

where:

$$q = \text{W/cm}^3$$

$$\phi = \text{neutron flux n/cm}^2\text{-sec}$$

$$\mu_c = \text{absorption cross section}$$

$$E = \text{energy of } \gamma \text{ ray given off}$$

$$f = \text{probability of self-absorption of } \gamma \text{ ray}$$

The self-absorption factor for internally generated gamma rays in a thin rod is:

$$f = 1.3 \mu r$$

where: μ = linear absorption cross section

r = radius of rod in cm

Since the absorption cross section for neutrons varies greatly with energy the neutron energy distribution must be known. For the Westinghouse PWR neutron spectrum CEA has calculated that an average of 7.4 percent of total q comes from these neutron reactions (see Section 3.2) inside the sensors.

Time Response

For a gamma thermometer with no radial heat losses the response time τ is:

$$\tau = \frac{C_p \rho L^2}{2K}$$

where:

τ = time constant in seconds

C_p = heat capacity of thermometer material, W-sec/ $^{\circ}$ C

ρ = density

L = half length of sensor

K = thermal conductivity in W/cm-°C

Relationship of τ to Real Sensitivity (no gap losses)

By combining the equation for sensitivity (ΔT) and that for τ , one obtains:

$$S_r = \frac{\Delta T \rho}{q} = \rho \frac{L^2}{2k} \quad \text{and}$$

$$\tau = \frac{C_p \rho L^2}{2k} \quad \text{and}$$

$$S_r = \frac{\tau}{C_p}, \text{ where } S_r \text{ is the real sensitivity, } ^\circ\text{C/W/g}$$

This relationship suggests how step changes in either power or in coolant temperature could be used to determine S_r if the gamma thermometer employed ideal axial heat flow, i.e., no gap losses. In fact, the relationship is very general between τ and S and computer studies with RADCAL/THERMAL (next section) show that the relationship holds over large ranges of gap size and conductivity and is independent of various dimensional parameters (see Section 3.1.1.3). Only the specific heat controls the ratio of S/τ until the gamma thermometer is made so fast acting that the outside coolant film heat transfer coefficient (normally greater than 2 W/cm²-°C) begins to play a role.

To determine the very important S_i , indicated sensitivity, from plunge tests the exact temperatures of the bath must be known. The real sensitivity, back-calculated from the time response to a step change (e.g., a "plunge" test changing coolant temperature) would be the same whether an iron-constantan or a type-K DTC had been inserted to sense temperature. Non-idealities of the measuring DTC cannot be determined from τ alone, and plunge tests designed to measure indicated sensitivity must contain provision for quantification of both amplitude and response time (Section 3.1.1.3.5).

3.1.1.2 Computer Model for Determining both S_p and τ : RADCAL/THERMAL

Although the equations presented in the previous section enable an approximate calculation of instrument sensitivity and time response, it is necessary to have a more extensive computer code to interpret alternative ways of calibrating the instrument and to make detailed studies of different design options. For these purposes, the RADCAL/THERMAL code has been developed. The code solves the heat transfer equations in space and time using a finite element method and integrating in time by the Euler method. The code has been written in standard FORTRAN-IV language and is available to NRC staff upon contact with Scandpower.

Geometrical Description

Figure 3.1-2 shows how the RGT sensor is spatially divided in the RADCAL/THERMAL code. Axially the sensor is considered to consist of three distinct regions, the upper sink region, the heater region, and the lower sink region. The heater region consists of the outer jacket tube, the gas chamber, and the core tube with cable pack. If axially symmetric conditions have been assumed, the code calculates the temperature distribution in the upper sink region and half of the heater region, as the symmetrical part is thermally identical. If asymmetric conditions are to be considered, (i.e., different heat transfer conditions in the upper and lower sink regions), the code calculates the temperature distribution in all three regions.

Each of the three main axial regions can be divided into 90 axial elements.

Radially the sensor is divided into 11 annular regions. The jacket tube is divided into two annular rings designated radial elements 1 and 2. The sink material corresponding to the chamber thickness is divided into another two parts, called radial elements numbers 3 and 4. The heater tube, and corresponding regions of the sink, are divided into three rings called radial elements numbers 5, 6 and 7.

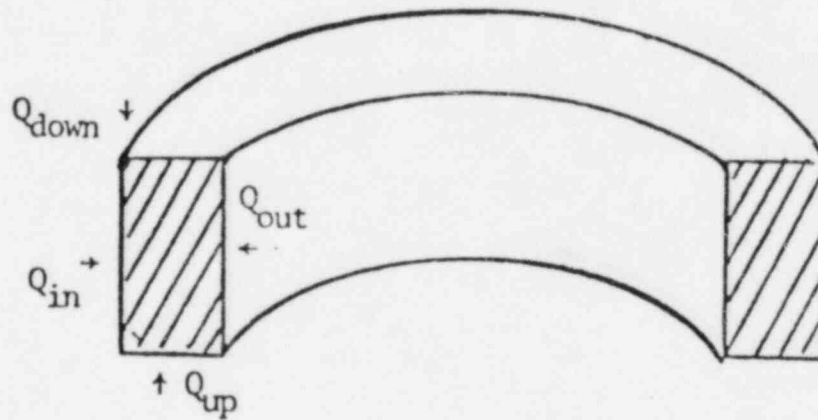
The centrally located cable pack is treated as four regions. The peripheral thermocouples constitute regions 8 and 9. Here the sheath of the cables is region 8 and the insulation with the lead wires, region 9.

The central cable (thermocouple or heater) is treated as region 10 and 11. The sheath is the region 10 and the insulation with the wires, region 11.

The heat transfer between regions 8 to 11 is described by contact area and heat transfer coefficient inputs.

Mathematical Formulation

The code is two-dimensional in the sense that rotational symmetry around the axial center line is assumed. The differential heat transfer equation is therefore formulated for rings as sketched below where four heat flow components are considered:



The equation is written:

$$M_i \frac{dT_i}{dt} = Q_{up} + Q_{down} + Q_{in} + Q_{out} + Q_{heat}$$

here:

M_i = thermal capacity of the element (volume $\times \rho \times C_p$)

T_i = temperature of the element

Q_{heat} = heat generated within the element (electrical heating or nuclear heating)

The heat conducted from the neighboring elements is calculated using the equation:

$$Q = k \frac{A \cdot \Delta T}{\Delta L}$$

where:

k = thermal conductivity

A = contact area between neighboring elements

ΔL = linear distance between the centers of the two elements

ΔT = the temperature difference between the center of the neighboring element and the center of the element considered

In cases where discontinuities exist on the border between two neighboring elements or where the neighboring element does not exist, other heat transfer equations are used. In the following, some of the more special calculations of heat transfer are shown:

Heat Transfer from Radial Element No. 1 to Coolant

RADCAL/THERMAL was designed for situations where the mode of cooling is forced circulation by subcooled water flowing longitudinally along the RGTA surface.

The equation:

$$Nu = 0.023 \times Re^{0.8} \times Pr^{0.4} \quad (Nu = \text{Nusselt number}) \text{ is}$$

assumed to apply.

The non-dimensional Prandtl number, Pr, has the value of 0.97 at 300°C.

The non-dimensional Reynolds number is given by the equation:

$$Re = \frac{\rho VD}{\mu}$$

where:

- ρ = water density
- V = coolant flow rate, typical value = 2 m/sec
- D = hydraulic diameter for the coolant flow passage outside of RGT (typical value = 0.003 m)
- μ = dynamic viscosity of the coolant water (typical value at 300°C = 0.91×10^{-4} kg/m-sec)

With the above values the following value for Reynolds number is obtained:

$$Re = \frac{\rho VD}{\mu} = \frac{712 \times 2 \times 0.003}{0.91 \times 10^{-4}} = 46,945$$

Using the relationship:

$$Nu = \frac{HD}{k}$$

Where:

- H = heat transfer coefficient on the water cooled surface
- k = thermal conductivity of water (0.54 W/m-°C at 300°C)

The heat transfer coefficient H then becomes (at 300°C):

$$\begin{aligned} H &= \frac{Nu \cdot k}{D} \\ &= 0.023 \times Re^{0.8} \times Pr^{0.4} \times k/D \\ &= 2.2315 \text{ W/cm}^2\text{-}^\circ\text{C} \end{aligned}$$

Heat Transfer from Radial Element No. 3 to Element 2 in Sink Region

A temperature step could conceivably exist at the border between radial region 3 and 2. The sheath and core rod material are drawn down, not welded, together. Various RGT fabricators have, in the course of process development, applied a range of "draw-down" ratios in final assembly. Reduced inter-molecular bonding during draw, or impurities in the gap, could produce detectable thermal and electrical gap resistance. The equation used is:

$$Q_{\text{out}} = \frac{(\text{TEMP}(3) - \text{TEMP}(2)) \times P3 \times DL}{\frac{(D3 - D4)}{4 \times \text{CONDA}} + \frac{1}{\text{HTA}} + \frac{(D2 - D3)}{4 \times \text{CONDA}}$$

The diameters D1, D2, D3 . . . are defined in Figure 3.1-2 and P3 is the contact perimeter. The first term in the denominator represents the resistance to heat flow from the center of element 3 to the boundary. The second term in the denominator represents a possible resistance at the boundary, and the last term represents the resistance from the boundary to the center of element 2. The heat transfer coefficient at the boundary, called HTA, is an input which can be varied for each of the three axial subregions in the sinks (Figure 3.1-2) to investigate how a variation in the contact situation would influence the measured ΔT .

Heat Transfer Across the Gas Gap (from Radial Region 5 to Region 2)

Heat is assumed to be transported by two parallel and independent mechanisms:

- by conduction across the stagnant gas in the gap
- by radiation across the gap

The equation for the conduction is:

$$Q = \frac{(P4 \times DL \times (\text{TEMP}(5) - \text{TEMP}(2)))}{\frac{(D5 - D6)}{4 \times \text{CONDA}} + \frac{(D3 - D5)}{2 \times \text{CONDA}} + \frac{(D2 - D3)}{4 \times \text{CONDA}}$$

The first term of the denominator represents the resistance to heat flow from the center of radial element 5 to the surface, the second denominator term represents the resistance over the gas gap and the last term, the resistance from the inner surface of radial element 2 to its center.

The equation for the radiant heat transfer is:

$$Q = P4 \times DL \times RADCONS \times \left(\left(\frac{T(5) + 273}{100} \right)^4 - \left(\frac{T(2) + 273}{100} \right)^4 \right)$$

Where:

$$RADCONS = \frac{0.0005672}{\frac{1}{EMIS} + \frac{D5}{D3} \times \left(\frac{1}{EMIS} - 1 \right)}$$

EMIS is the emissivity of the two surfaces, and is an input value. It takes values between 0 and 1, where 1 means a non-reflective surface. The range expected in RGT is 0.2 - 0.4, but the exact value is unimportant below 500°C operating temperatures.

Heat Transfer from Radial Element 8 to 7

This is the transport of heat from the cladding of the outer thermocouples (usually 6) to the inner surface of the core rod. This is treated as a possible temperature step occurring where the sheath contacts the core rod, using the equation:

$$Q_{out} = \frac{P8 \times DL \times (TEMP(8) - TEMP(7))}{\frac{1}{HTB} + \frac{D7 - D8}{4 \times CONDA}}$$

The total contact perimeter is input as P8 and the heat transfer coefficient as HTB. Different values for HTB can be input for various axial regions.

Heat Transfer from Radial Element 9 to 8

Radial region 9 is the insulation material together with the thermocouple wires of the outer thermocouples. There is also modelled a possible temperature step at the contact boundary, calculated by the equation:

$$Q_{out} = P9 \times DL \times (TEMP(9) - TEMP(8)) \times HTC$$

P9 and HTC are input.

Heat Transfer from Radial Element 10 to 8

This is calculated by the equation:

$$Q_{out} = P10 \times DL \times (TEMP(10) - TEMP(8)) \times HTD$$

where P10 and the array HTC are input.

Heat Transfer from Radial Element 11 to 10

Radial element 11 represents the insulation material and thermocouple wire of the centrally located thermocouple. The possible temperature step on the contact surface is calculated by the equation:

$$Q_{out} = P11 \times DL \times (TEMP(11) - TEMP(10)) \times HTF$$

where P11 and the HTF array are input.

Heat Transfer from Radial Element 10 to 7

A heat transfer path from a centrally located body represented by element 10 over to the surface of the core rod is allowed for. This is computed by the equation:

$$Q_{out} = P12 \times DL \times (TEMP(10) - TEMP(7)) \times HTG$$

where P12 and the array HTG are input.

Heat Input

Two options for heat input exist, nuclear heating (by gamma rays) or electrical heating. In the case of nuclear heating, the heat rate in W/g of material is directly input. For electrical heating (i.e., calibration), the total current, I, is an input. In the heater region the current splits between the core and the jacket tube. The split is calculated based upon the input resistivity of the core part and the jacket tube in the heater region.

When calculating the resistances, the coolant temperature (T_{water}) is used to represent the sheath temperature, while the core temperature is calculated as:

$$T_{\text{core}} = T_{\text{sink}} + \frac{2}{3} (T_{\text{max}} - T_{\text{sink}})$$

where:

$$\begin{aligned} T_{\text{sink}} &= \text{temperature of sink at beginning of heater} \\ T_{\text{max}} &= \text{temperature in the center of the core} \end{aligned}$$

The radial element no. 6 is chosen to represent the temperature of all radial elements for calculating resistance. This is a good approximation because radial temperature profile is flat in this region.

As a special option of the code the central thermocoax cable (radial element 10 and 11) can be treated as a heater element with linear heat rating (W/cm) given as an input.

Method of Solution

The code starts by assuming that all elements have temperature equal to the coolant temperature. The heat input is then stepped up to any specified value and the temperature rise of each element is calculated for short time steps. Initially there is no heat flow as all elements are at the same temperature, but gradually temperature differences build up and heat flow increases.

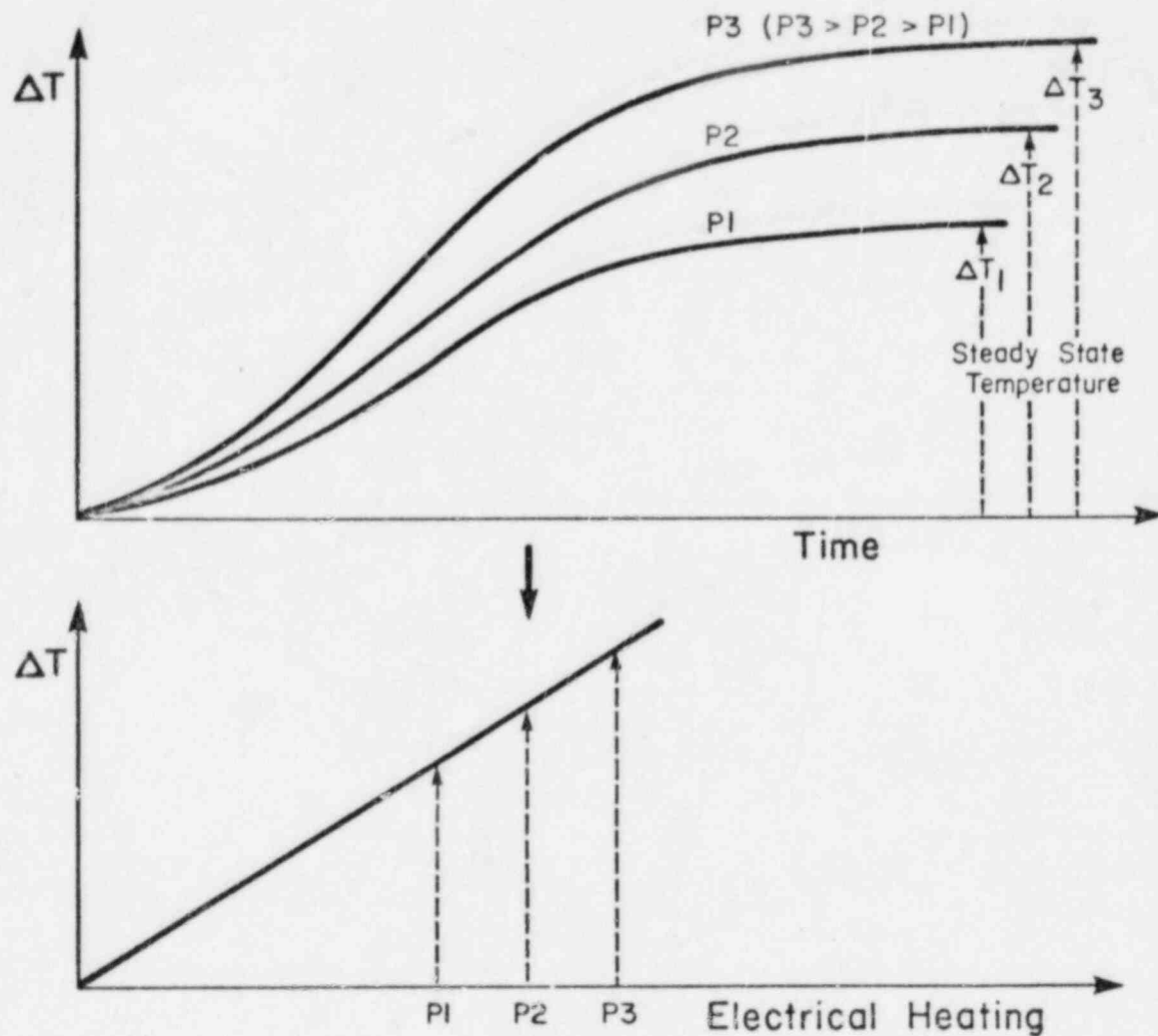
Figure 3.1-3 shows an array of the input data to the model and Figure 3.1-4 shows the calculated steady state temperature distribution.

Use of the Model to Predict Electrical Calibration Results

The electrical calibration of the RGT sensor is predicted by simulating power steps with the code. This means that the electrical current is switched on and the code calculates the temperature response. The real sensitivity is found by dividing the final, steady state temperature difference, ΔT , (between hot and cold junction) by the final heat input (W/g).

Both calculation and experiment have shown that there is an almost perfectly linear relationship between real ΔT and heat input, and that it is not necessary to calculate the sensitivity for more than one value of the power step.

In the sketch below is shown how the RADCAL/THERMAL results are converted into the calibration curve as obtained during direct electric calibration of the RGT sensors.



3.1.1.3 Application of the Model RADCAL/THERMAL

3.1.1.3.1 Predicting Electric Calibration Results

Figure 3.1-5 shows how the RADCAL/THERMAL code was used to predict the low temperature (11°C coolant) electrical calibration of the EdF prototype, Canne no. 6, in the Intertechnique test loop. Table 3.1-1 shows the scatter of the individual RGT sensor mean sensitivities with respect to the overall mean (40.65), and the standard deviations of the eight

data points from which each RGT mean sensitivity was determined by the method of least squares.

From the calculations, the steady state nominal value of the temperature difference is 40.38°C with a power input to RADCAL/THERMAL of 1.017 W/g. This gives:

$$S_r = \text{Real Sensitivity} = \frac{40.38}{1.017} = 39.71 \text{ } ^\circ\text{C/W/g}$$

The average indicated sensitivity, S_i , for the RGTs in this assembly was:

$$\bar{S}_i = 40.65 \text{ } ^\circ\text{C/W/g with } \sigma_{\text{means}} = 2.64 \text{ percent}$$

Experimental values for 90 RGTs in 10 French prototype assemblies are given in Table 3.1-3.

The overall average (low coolant temperature) sensitivity for the 90 RGTs tabulated was 40.87 °C/W/g. The approximate equations given in Section 3.1.1.1 give 40.31 °C/W/g for the nominal EdF type RGT (26.0 mm long sensor, 0.4 mm thick argon gas gap).

It can be seen from Tables 3.1-1 and 3.1-3 that the variation among sensors is considerably larger than the scatter of calibration data for a single sensor. In prototype no. 6, for example, the RGTs exhibit mean sensitivities that differ by 2.64 percent (standard deviation of the means) while the eight data points (i.e., increasing electric calibration current) scatter around the best fit (least squares) line by standard deviations ranging from 0.11 percent (RGTs 4, 5, 6 and 9) to 0.21 percent for RGT no. 8.

Sensor-to-sensor mean indicated sensitivity variation has two main sources: First, the variation in Seebeck coefficient of the difference thermocouples is estimated to produce a 2 percent ($\pm 2\sigma$) variation in

signal for a given ΔT . Second, the variation in gas gap thickness between the sensor and the jacket tube is estimated to be ± 0.1 mm (2σ) resulting from variations in "as-made" jacket tube dimensions. This gap variation alone accounts for ± 4.6 percent ($\pm 2\sigma$) variation in real sensitivity among chambers. These two variations alone account for much of the range of inter-sensor variation.

The RGT also has potential for "trimming," or tuning out, the intersensor variation mechanically. So far, this has not been practiced, because "as-made" variations were small. Several methods for such "tuning" have been developed.

The two key properties of the materials of construction (i.e., for prediction purposes) are thermal conductivity and heat capacity. These properties can vary substantially among various types of stainless steels and within types according to chrome and nickel content. A good prediction of sensitivity therefore depends upon good characterization of these parameters. Values normally used for high quality type 316 ss are:

$$\begin{aligned} k &= 0.131 \text{ W/cm-}^\circ\text{C at } 20^\circ\text{C} \\ \alpha &= 10 \times 10^{-4} / ^\circ\text{C in } k_T = k_{20}(1 + \alpha(T - 20)) \\ C_p &= 0.51 \text{ at } 100^\circ\text{C} \\ \alpha &= 3.9 \times 10^{-4} / ^\circ\text{C} \end{aligned}$$

For very accurate prediction of calibration sensitivity, the values of k and C_p for the material actually in use can be measured.

For proper interpretation of electrical calibration results the resistivities of the core rod and jacket tube must be very accurately measured to enable accurate calculation of the current in the sensor (i.e., for a given total current) and for calculation of the power, W/g

from $(I_{\text{sensor}}^2 \times R_{\text{sensor}})$.

EdF has commissioned a complete study of the sources of variation in both manufacture and electric calibration, Reference 3-(44), and has concluded that, with their present techniques (i.e., used by Intertechnique after manufacture and EdF in the high temperature and pressure loop), the

absolute combined error which could exist in power determination (W/g), is 1.9 percent at the 1σ level (68.2 percent confidence level), and the relative error in such power determination (i.e., W/g of any one data point to any of the others) is 0.45 percent at the 1σ level.

These accuracies are not fundamentally limited and could be improved by a factor of at least two if the economic incentives existed to do so.

Section 3.1.2 presents alternate methods of experimental determination of RGT sensitivity that are purely thermal and hence not subject to the uncertainties in the direct electric calibration that arise from uncertainties in electrical resistivity measurement. For the ORNL test specimens (Section 3.4.1), multiple calibrations of both electrical and pure thermal types were employed.

3.1.1.3.2 Conversion of Electric Calibration to Nuclear Calibration (Examples)

In principle there is no difference between heating the gamma thermometer electrically or by gamma irradiation. The sensor output will be a temperature difference between the hot and cold junctions caused by heat generated within the core part of the sensor (core tube and cable pack).

The heat generation is, however, slightly differently distributed in the two cases.

In the nuclear case, the same heating in W/g is developed in both the core tube and the cable pack (sheath and insulation), and is temperature independent.

In the electrical case, there is no heating in the insulation and leads of the thermocouple. The effect of this difference upon S_i at a particular W/g is quite small because the product of the area and the thermal conductivity of the insulation and leads is small. The ΔT calculated by RADCAL/THERMAL is only about 0.15°C lower in the electrically heated case than in the nuclear, at 1.0 W/g.

The cold junction temperature will be about 2°C higher with nuclear heating, at 1.4 W/g, than with electrical heating. This is because, for an electrically generated sensor heat rate corresponding to a given value of gamma heating, the heating in the sink region is lower than that in the sensor. (In nuclear heating the heat rate in the sink is the same as in the sensor.) This is because the electric resistance of the sink region is lower than that of the heater section. The controlled variable is the total current. When this is so adjusted that the heating in the core part corresponds to a particular rate of gamma heating in the sensors, the sink heating is lower due to its lower resistance. Model calculations show that for a 1.4 W/g heating in the core, the sink region heating is 0.9 W/g.

The difference in sink heat rates (i.e., between electrical and nuclear cases) is shown, however, to have no significant influence on the measured signal for a given W/g in the sensor.

3.1.1.3.3 Predicting Time Constants from a Step in Power

From the calculated response of the RGT to power steps, time constants can be extracted for comparison to test data. Time response is closely related to sensitivity, as explained in Section 3.1.1.1, and is free of the uncertainties of electrical resistance.

Figure 3.1-5 shows that the response curve is that of a higher than first order system. If the response is approximated by a second order system, the response can be expressed in the time domain as:

$$\Delta T = \Delta T_{\infty} \left(1 + \frac{\tau_1}{\tau_2 - \tau_1} e^{-t/\tau_1} - \frac{\tau_2}{\tau_2 - \tau_1} e^{-t/\tau_2} \right)$$

Where τ_1, τ_2 = time constants
 ΔT = final, steady state value

As $\tau_2 \gg 1$, the response can be approximated for $t > 10$ sec. to

$$\Delta T = \Delta T_{\infty} \left(1 - \frac{\tau_2}{\tau_2 - \tau_1} e^{-t/\tau_2} \right)$$

and this equation can be transformed into:

$$\ln \left(1 - \frac{\Delta T}{\Delta T_{\infty}} \right) = -\frac{t}{\tau_1} - \ln \left(1 - \frac{\tau_1}{\tau_2} \right)$$

In Figure 3.1-6 this equation has been plotted using the response value from Figure 3.1-5. From the slope and intercept of the plotted curve the time constants are found to be:

$$\begin{aligned} \tau_1 &= 2.1 \text{ sec.} \\ \tau_2 &= 17.8 \text{ sec.} \end{aligned}$$

The average of the "measured" time constants, i.e., τ_2 's, reported for the EdF prototypes in Table 3.1-3 is 17.27 seconds.

3.1.1.3.4 Relationship of τ to S_r for RGT's

From the expressions for the real sensitivity and time constant derived in Section 3.1.1.1, it can be shown that for simple geometries these two are related as:

$$\frac{\text{Real sensitivity}}{\text{Time constant}} = \frac{1}{C_p}$$

where:

C_p = specific heat of gamma thermometer material

To check how this applies to real systems, RADCAL/THERMAL has been used to do calculations in which different basic parameters have been varied relative to a reference condition. The variations studied have been:

- heater length
- gas filling and emissivity of chamber inner surface
- thermal conductivity of steel

The results of the calculations are shown in Figure 3.1-7.

From this figure it is seen that there is a linear relationship between real sensitivity and dominant time constant, τ_2 , over large variation ranges and that this applies independent of which parameter has been changed.

Since the slope of the linear part of the curve is the reciprocal of the specific heat of the gamma thermometer material, the sample curve is valid for cases where no changes in specific heat take place. This means that the sample curve shown would not be used, for example:

- for high temperature cases (300°C) (C_p varies by ~ +12 percent from 20°C to 300°C for type 316 stainless steel)
- for gamma thermometers of different material (e.g., zircaloy)

The curve shown is constructed in such a way that to obtain the real sensitivity of a gamma thermometer from its time responses, the curve must be entered with the two time constants of the response signal. The difference in sensitivity obtained from the curve for the two time constants is the real sensitivity of the gamma thermometer. An example is shown of how the sensitivities for Canne No. 4 to 8 can be obtained (see calculated time constants in Section 3.1.1.3.2). Determinations of S_r made in this way are dependent only on the least variable of the physical properties (i.e., C_p) and independent of the values of either thermal conductivity or electrical resistivity.

3.1.1.3.5 Predicting Response to Plunge Testing

In plunge testing the sensor is in thermal equilibrium at one temperature (e.g., in an ice bath of 0°C) and then suddenly is moved to another ambient temperature (e.g., boiling water at 100°C). As the two junctions of the difference thermocouple will reach the new, steady state temperature at different rates, an intermediate output signal is obtained from the sensor while it is stabilizing at the new temperature. The measured output signal contains information about the time constants and the differential thermocouple calibration for a particular sensor.

The plunge test response can be predicted by the RADCAL/THERMAL model. In the calculations, the coolant temperature is changed in a step corresponding to the difference between the two temperatures of the baths used in the plunge test. In Figure 3.1-8 is shown, as an example, a prediction made by RADCAL/THERMAL for the response of a specimen used in the plunge tests at ORNL. From the measured plunge response, the time constants of the gamma thermometer can be calculated. By approximating the thermal behavior of the sensor by a second order function, the response can be expressed in the time domain as:

$$\Delta T = \Delta T_w (B e^{-t/\tau_1} + A e^{-t/\tau_2})$$

where:

ΔT_w = temperature step in plunge test (difference in bath temperatures).

A and B are constants calculated from test data along with τ_1 and τ_2 .

From the evaluated time constants the sensitivity of the gamma thermometer is found using Figure 3.1-8 as explained in Section 3.1.1.3.4.

Separating S_{real} from $S_{\text{indicated}}$

In the model calculations it is the real temperature of the gamma thermometer that is predicted. This leads to the notation "real sensitivity."

In the measurement the temperatures found are those "seen" by the thermocouple. Depending upon variations in the difference thermocouple sensitivity ($\mu\text{V}/^\circ\text{C}$) the measured, or "indicated" sensitivity of the gamma thermometers may vary although the real sensitivity is constant. (An iron-constantan difference thermocouple would yield the same "real sensitivity" from time constants as a chromel-alumel one. The indicated sensitivities however would differ by 20 percent in μV signal per W/g.)

Special control of the plunge testing makes it possible to determine both the real sensitivity, S_r , and the indicated sensitivity, S_i . In order to take variations in the thermocouple calibration into account, the equation above should be formulated:

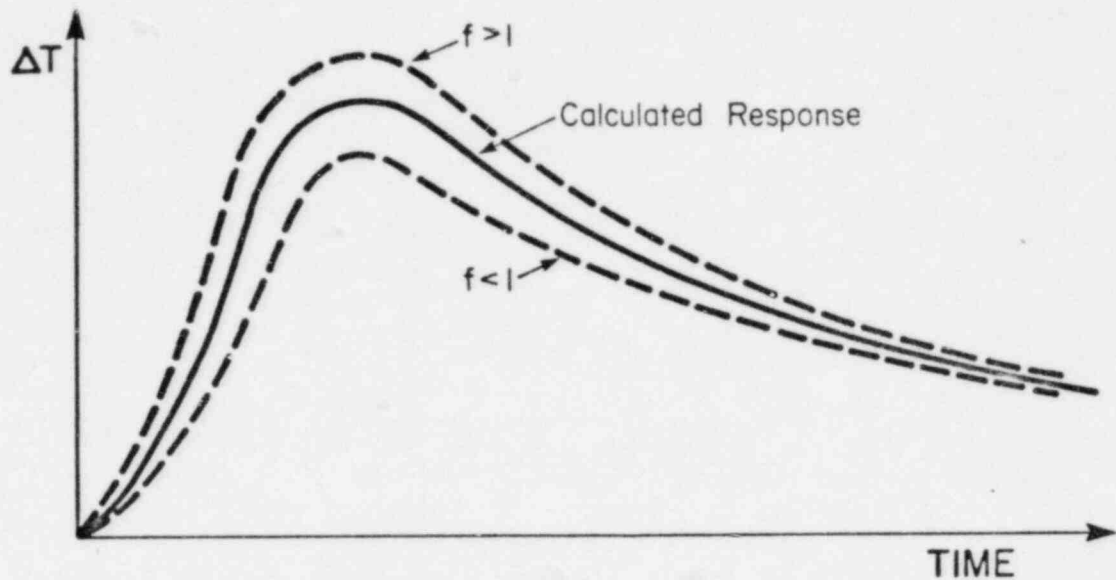
$$T = \Delta T_w f (B e^{-t/\tau_2} + A e^{-t/\tau_1})$$

where:

f = ratio of actual thermocouple sensitivity to nominal (handbook) sensitivity (NBS 25 for type K thermocouples is used in all RGT work).

Variation in f will only shift the response curve up or down, but not alter the shape of the curve. The time constants are not changed by thermocouple characteristics.

If, therefore, ΔT_w is well controlled and accurately measured, the value of f can be determined by comparing the response obtained to the response predicted for the actual ΔT_w , A , B , τ_1 and τ_2 .



When f is known, the indicated sensitivity of the gamma thermometer is directly found from the real sensitivity as:

$$S_i = f \cdot S_r$$

3.1.1.3.6 Sensitivity Studies of Manufacturing Variables

The RADCAL-THERMAL model has been used to do studies of the sensitivity of ΔT to variations in design parameters. Such studies are useful for the optimization of the sensor design, specification of manufacturing tolerances, and establishing uncertainty. Studies of this kind are represented by the calculations made for the French prototypes (see Section 3.1.1.3.1). In this particular study the effect on ΔT from variations of the following parameters were evaluated, Reference 3-(37):

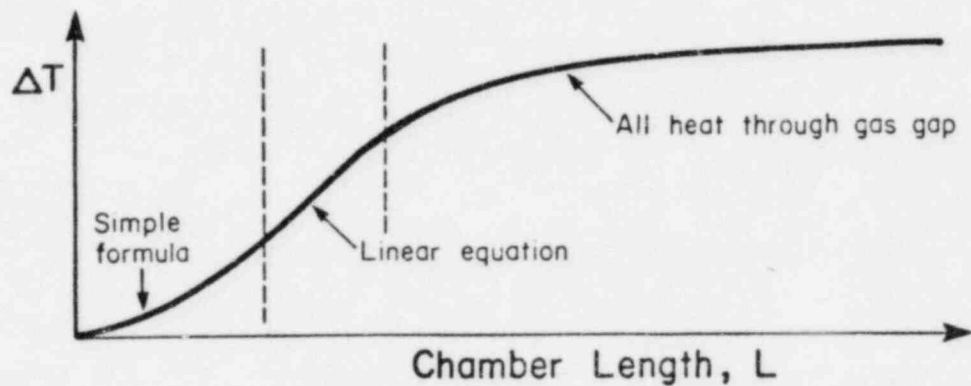
- length of chamber
- gas chamber inner and outer diameter
- fill gas thermal conductivity
- steel thermal conductivity
- hot junction location displacement

The following results are extracted from the study:

Chamber Length Variations

The chamber length was varied ± 2 mm around the nominal length of 26 mm. The effect on ΔT is shown in Figure 3.1-9.

For the chamber length studied, there is a linear relationship between ΔT and chamber length. The simple formula for ΔT , neglecting gas gap heat transfer, says that ΔT is proportional to L^2 . Gas gap conduction will "straighten out" the relationship, and for very long chamber lengths, ΔT will be independent of L (most heat goes through the gas gap). In the sketch below the relationship of ΔT to L is indicated.



It is no problem to maintain manufacturing tolerances that make the chamber-to-chamber variations in ΔT due to length differences negligible.

Hot Junction Location Displacement

Figure 3.1-10 shows the axial temperature distribution along the sensor near the thermocouple hot junction. It is seen that a displacement of the hot junction by 1 mm would change the ΔT (indicated sensitivity) by 0.37% or 0.8 percent.

When the chamber is machined after locating the hot junction by X-ray, it is possible to hold tolerances on the distance from the junction to the sensor to closer than ± 0.25 mm. This is a factor of 4 smaller than indicated in the figure (i.e., ~ 0.2 percent).

Gas Thermal Conductivity Variations

Calculations have been made assuming the gas space being:

- evacuated to 10^{-6} atm.
- argon filled
- hydrogen filled

The results of the calculations are shown in Figure 3.1-11. As seen from the figure, evacuation to below 10^{-6} atm. gives a substantially higher sensitivity than argon filling does. Hydrogen filling, on the other hand, would greatly reduce the sensitivity of the sensor. Thus, a drastic shift of sensitivity would occur if the sensor was initially evacuated and made from stainless steel. Diffusion of hydrogen molecules through the stainless steel sheath into the gas chamber would, after a relatively short time, give a sensitivity corresponding to hydrogen filling. An evacuated sensor, made from Zircaloy (which is hydrogen impervious) has been tested at ORNL (Section 3.1.3.4) in the Oak Ridge Research Reactor.

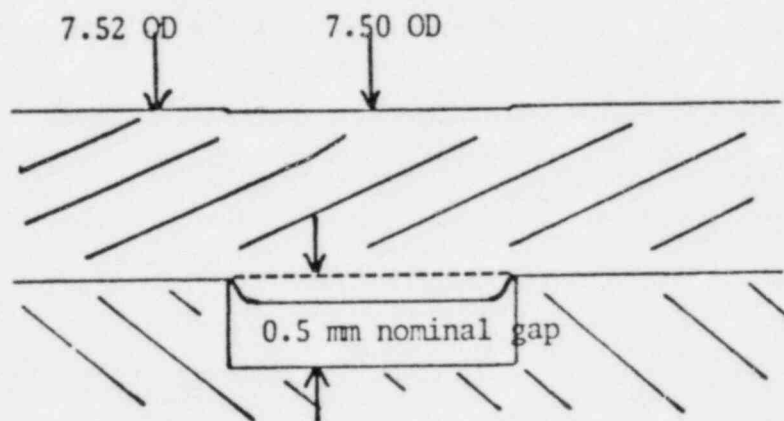
It is a peculiarity of the thermal conductivity of mixed gases that, while the presence of 10^{-6} to 10^{-4} atmospheres of hydrogen by itself in the chamber space would drop the signal drastically, the same quantity of Hydrogen in the presence of 2 atmospheres of argon has no deleterious effect on gas gap conductivity, which is dominated completely by the argon molecules. The conductivity of the gas gap is independent of argon pressure over a range of 10^{-4} to 10 atmospheres.

High gas gap conduction is undesirable for several other reasons: 1) temperature changes gas conductivity more than it does that of stainless steel; 2) gas properties are the least stable of those properties for which high stability is sought in gamma thermometers - the larger the percent gap conduction, the less certain the long term stability; and 3) gas gaps can be contaminated. Accordingly, very strict process controls on the argon gas fill have been developed for RGTA manufacture.

The figure also shows the effect of steam or air filling in the gas gap. Leakage at PWR conditions would result in the chamber being filled with water. Because the thermal conductivity of water is much higher than that of steam, the resulting ΔT would become so low the signal would disappear. It has been shown to be easy to detect such water leakages. To date investigations have shown only such "hard failure" mechanisms for RGTs. These are much to be preferred to "soft failures" in which it is difficult to tell whether a reading is true or faulty.

Chamber Inside and Outside Diameter

The gas gap thickness is the most difficult of the RGT critical dimensions to control accurately because the final manufacturing step (i.e., drawing or swaging the jacket tube onto the core rod) produces some extrusion of jacket tube material into the nominal chamber cavity as:



Because the jacket tubes vary somewhat in wall thickness and draw dies wear out, the distance to which this extrusion occurs is somewhat non-reproducible. For example, for EdF specimens having a nominal gas gap of 0.5 mm, highly magnified photo cross sections of several RGT sensors destructively examined show a mean value of actual gas gaps of 0.40 mm (0.1 mm less than nominal).

Such measurements, together with data from accuracy resistance measurements of the completed RGTs, indicate that the expected $\pm 2\sigma$ variation in

gas gap thickness is $\pm .10$ mm around 0.4 mm (nominal 0.5 mm). The $\pm 2\sigma$ effect of this $\pm .10$ mm on real RGT sensitivity is ± 1.6 percent for chambers 26 mm long.

Effects of Variations in Coolant Velocity on Sensitivity

The coolant velocity in the instrument tubes of PWRs is in the region of 1-2 meters per second. Experiments by IFA and tests by Intertechnique and EdF on full scale prototype RGT assemblies show the sensitivity of RGT sensors to be independent of velocity over the range from 0.5 meter per second to 2.5 meters per second.

RADCAL/THERMAL calculations verify that the variation in sensitivity over this velocity range will not be detectable in tests having an accuracy (2σ) of $\pm 3/4$ percent. The variation in coolant velocity results in a change of coolant film temperature of only 1-3°C. The difference thermocouple junctions rise by almost equal amounts and the ΔT remains constant. The effect on the signal of 1-3°C changes is limited to that produced by the absolute temperature change on conductances internal to RGT (i.e., ~ 20 percent for a 300°C change in absolute temperature).

The outside film coefficient can however effect the accuracy of plunge test calibrations and good bath agitation must be provided.

Effects of Crud Deposit, Uniform - Non-Uniform

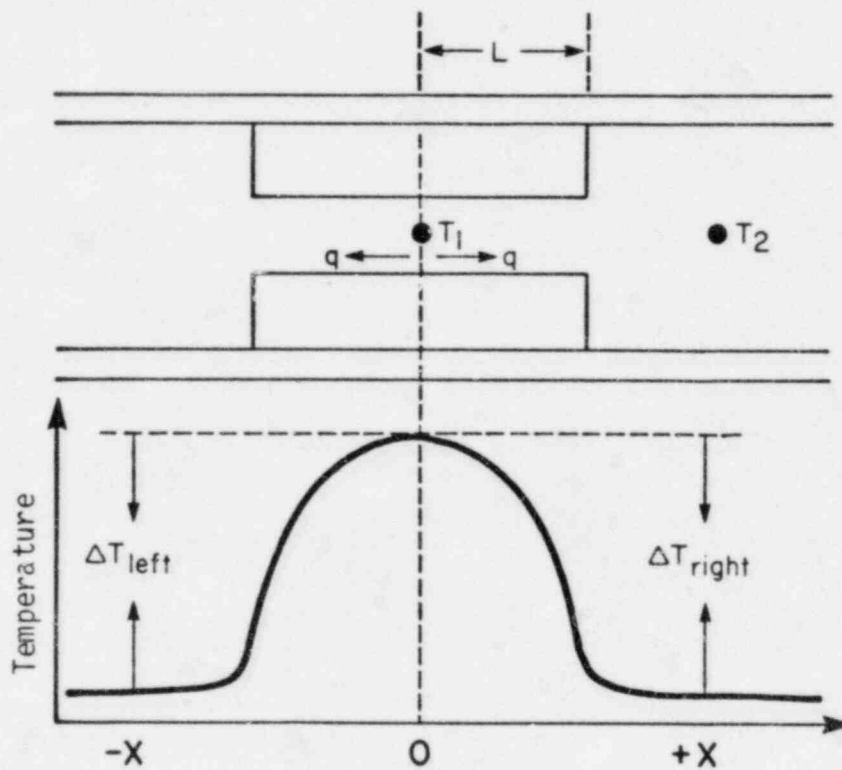
There is no report of crud or scale buildup on SPND rods or TIP thimbles in PWRs. This, of course, does not preclude that crud deposits could be occurring.

The crud deposits, if uniform, along the RGT jacket, would have the same effect upon RGT signal as a reduction of coolant velocity (i.e., negligible) because both junctions are raised in temperature the same amount and this increase could not be large enough to affect sensitivity.

Non-uniform deposits, however, could render the heat flow asymmetric from the RGT center line and affect sensitivity.

In order to attack this source of uncertainty, several (i.e., ORNL and RWE) RGT prototypes (see Section 3.1.3.4) are employing double difference thermocouples which not only double the signal strength, without increasing τ , but also eliminate possible error deriving from asymmetric heat flow. This is shown by the illustration which follows:

1) Consider RGT with a single difference thermocouple:



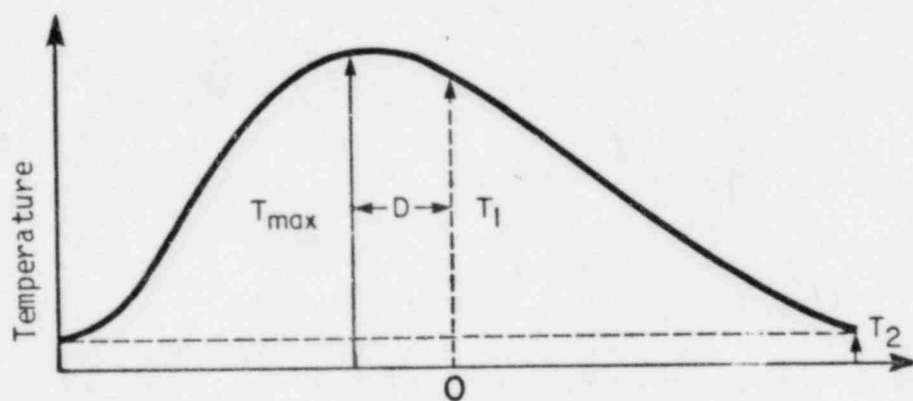
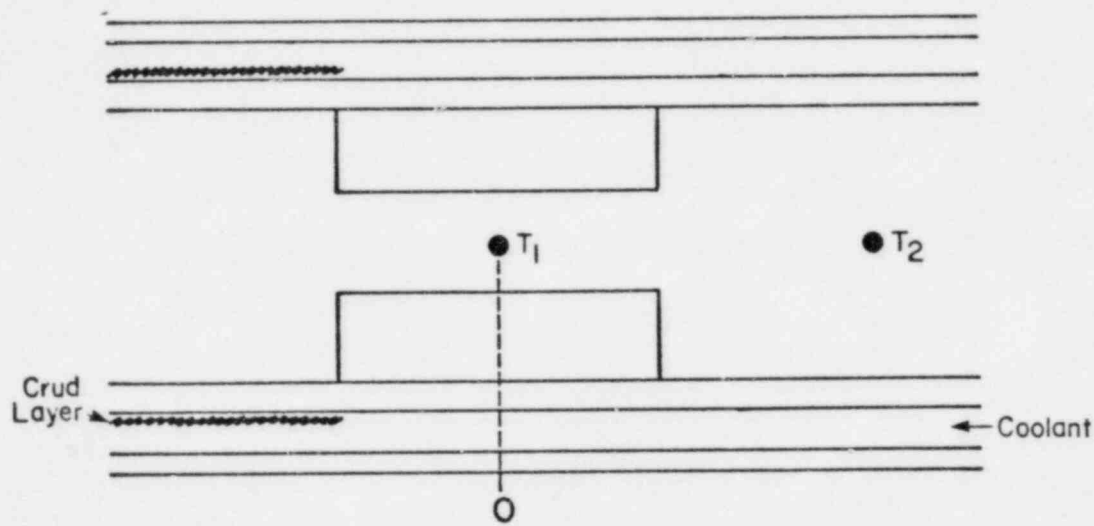
If heat flow is ideal (i.e., symmetric about center line), then $\Delta T_{\text{left}} = \Delta T_{\text{right}}$ and T_{max} occurs at $X = 0$.

For average PWR conditions ΔT_{signal} is designed for about 40°C by choosing appropriate L and the equation for $T_{\text{max}} - T_x$ is:

$$(T_{\text{max}} - T_x) = \frac{qx^2}{2k} \quad \text{and} \quad \Delta T_{\text{signal}} \approx \frac{qL^2}{2k}$$

Now, this holds true only if heat splits identically to right and left of the center line (where the hot junction is located). RGTs with single difference thermocouples are dependent upon such symmetry.

2) Heat flow in an RGT can be disturbed (i.e., rendered non-symmetric) by asymmetric heat transfer resistance to the coolant sink. This could occur if crud deposited on one end only of the sensor, as:



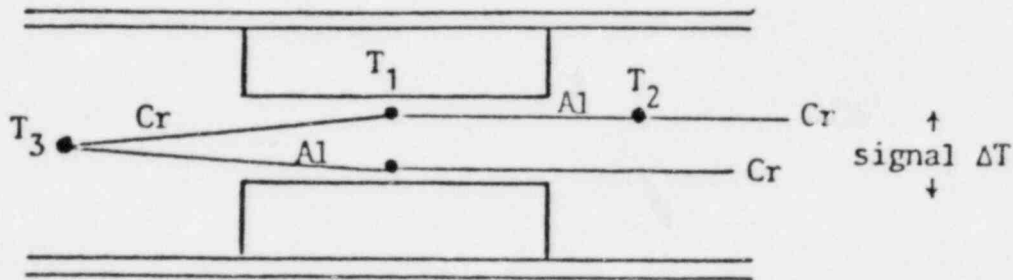
In this case heat transfer will be impeded between the outer jacket tube of the RGT and the coolant at the left and heat will flow preferentially toward the good conductor with the resulting skew in temperature distribution.

In this case the signal ΔT , $T_1 - T_2$, becomes:

$$\frac{qL^2}{2k} + \frac{qDL}{k}$$

and the power, q , is incorrectly calculated if the signal ΔT is used without consideration of the additional term, $\frac{qDL}{k}$.

3) If one uses, however, instead of a single difference thermocouple, a double difference thermocouple, as:



Then the "signal ΔT " in the symmetrical flow case becomes:

$$\Delta T = (T_1 - T_2) + (T_1 - T_3) = 2(T_1 - T_2), \text{ or } 2(T_1 - T_3)$$

NB! Signal is doubled without increase in chamber length.

For the non-symmetric heat flow case of 2) above, the signal ΔT becomes:

$$T_{\text{ddt}} = 2 \times \frac{qL^2}{2k} = \frac{qL^2}{k}$$

This is exactly twice the "true" theoretical ΔT for a single difference junction in the symmetrical case! The heat rate, q , is accurately measured whether heat flow is symmetrical or not.

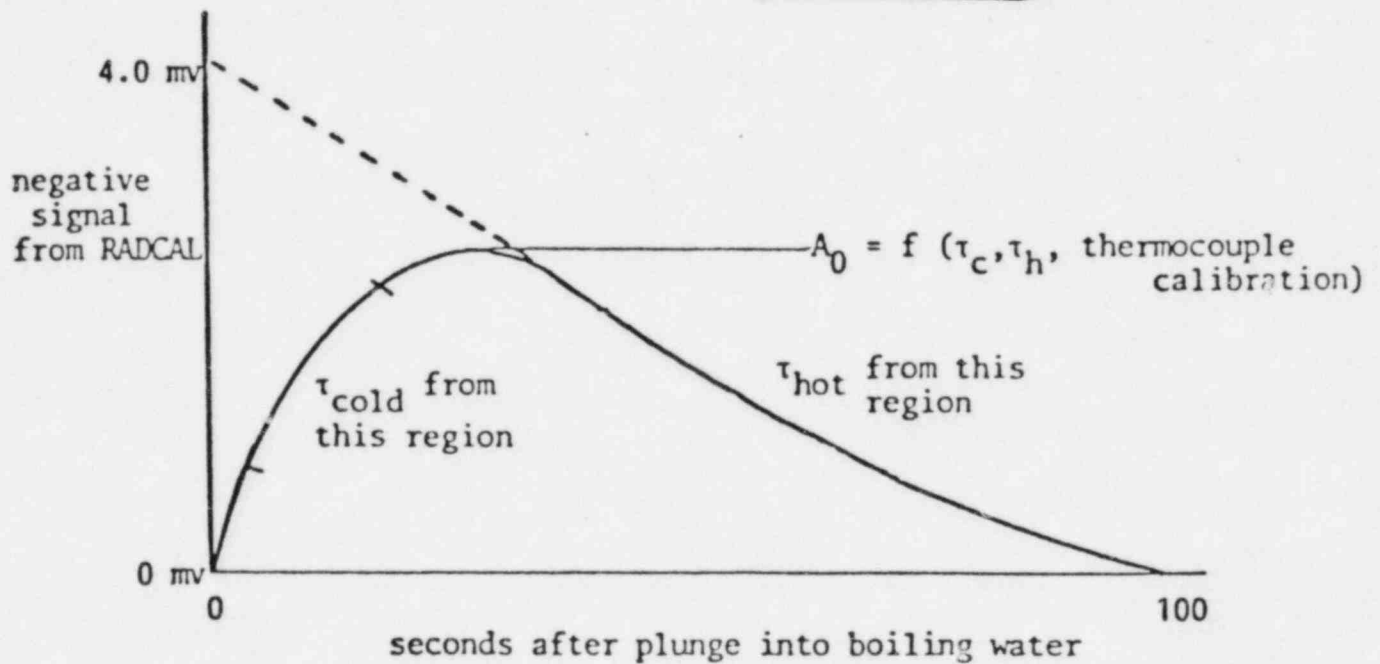
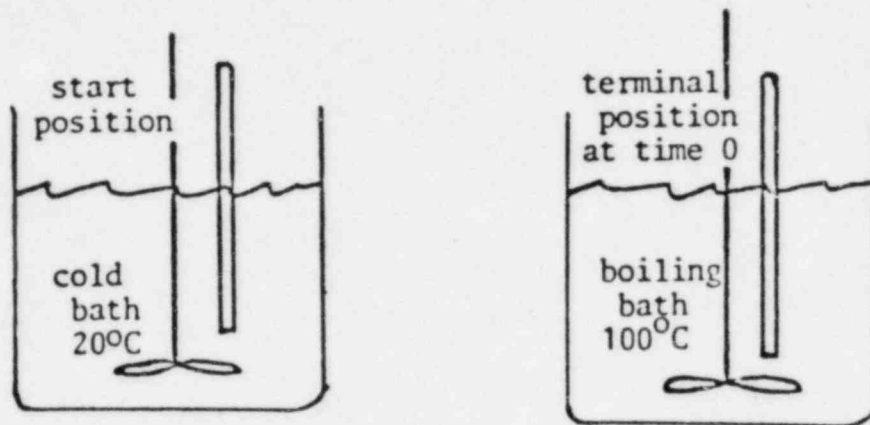
3.1.2 Methods and Results of Experimental Determination of the Sensitivity of RGTs

Plunge testing has been used as the basic workshop calibration technique for classic SRP and HBWR gamma thermometers. In plunge testing the specimen (without internal heating) is moved rapidly from one stable ambient environment to another, making certain that outside film coefficients in the second ambient condition are high enough not to affect the dominant heat transfer processes.

For example, the ORNL calibrations and post-irradiation recalibrations (Section 3.4.1) have been done by plunging the specimens from a cold water bath to a boiling water bath.

Halden calibrates their gamma thermometers by plunging from air to boiling water. (Since absolute thermocouples, rather than difference thermocouples, are used, the signal rises from 20°C to 100°C and stays there.) The same test with an RGT starts with zero signal and ends with zero signal. The shape of the response curves yields both hot and cold junction time constants and by careful interpretation of the maximum

amplitude of the response, indicated sensitivity can be obtained if both terminal temperatures are accurately known:



3.1.2.i Response Time in Plunge Tests

Plunge testing of gamma thermometers has earlier been used as a manufacturing test and then mainly as a means to select sensors of very similar sensitivity. For such somewhat rough tests (e.g., for Halden gamma thermometers), it has been sufficient to plunge the sensor from ambient air to boiling water.

In the irradiation program at ORNL the plunge test has been used to detect irradiation induced changes in the gamma thermometers. An accurate plunge testing program of the sensors is then necessary before and after the irradiation.

The proposed experimental set-up for the hot lab plunge testing at ORNL is illustrated in Figure 3.1-12. The gamma thermometer specimens were plunged from a cold bath of 20°C temperature into a boiling water bath of 100°C. Sufficient mechanical agitation of the baths was provided for.

The selected direction of plunging was preferred because it is easier to obtain a good surface heat transfer in boiling water (good, natural agitation, higher Prandtl number).

A manipulator was used to obtain a well-controlled and reproducible transfer from the cold bath to the hot bath. The manipulator was designed for a transfer time less than one second.

Five of the 15 specimens tested at ORNL served as "library" specimens and did not undergo irradiation. These specimens were used to "standardize" the plunge test procedure and the experimental set-up. Prior to the start of the calibration campaign, these specimens were used to determine the accuracy and repeatability of the plunge test itself.

After the irradiation (July 1981), a new standardization was the first part of the plunge test series, and again the library specimens were used. The purpose of the test was to serve as a reference and verify that the same results were obtained at identical conditions for the same, unirradiated specimens one year later.

The data obtained during a plunge test were digitally recorded and processed by computer.

It was expected that the indicated sensitivity of the gamma thermometer could be determined with an accuracy better than 1.5 percent. The determination of sensitivity from a plunge test response is explained in

Section 3.1.1.3.5. The plunge testing as made at ORNL therefore makes possible detection of irradiation induced changes in S_i for the gamma thermometers larger than 1.5 percent over the irradiation period (fast test fluence corresponding to three years irradiation at PWR conditions). For S_r , a one percent level of detectability of change was anticipated (95 percent confidence). Reference 3-(39) gives pre-irradiation plunge test calibration data. The status of the ORNL program is described in Section 3.1.3.4.

3.1.2.2 Direct Electrical Calibration and Power Step Response

3.1.2.2.1 Reductions of the Uncertainty, σ_1

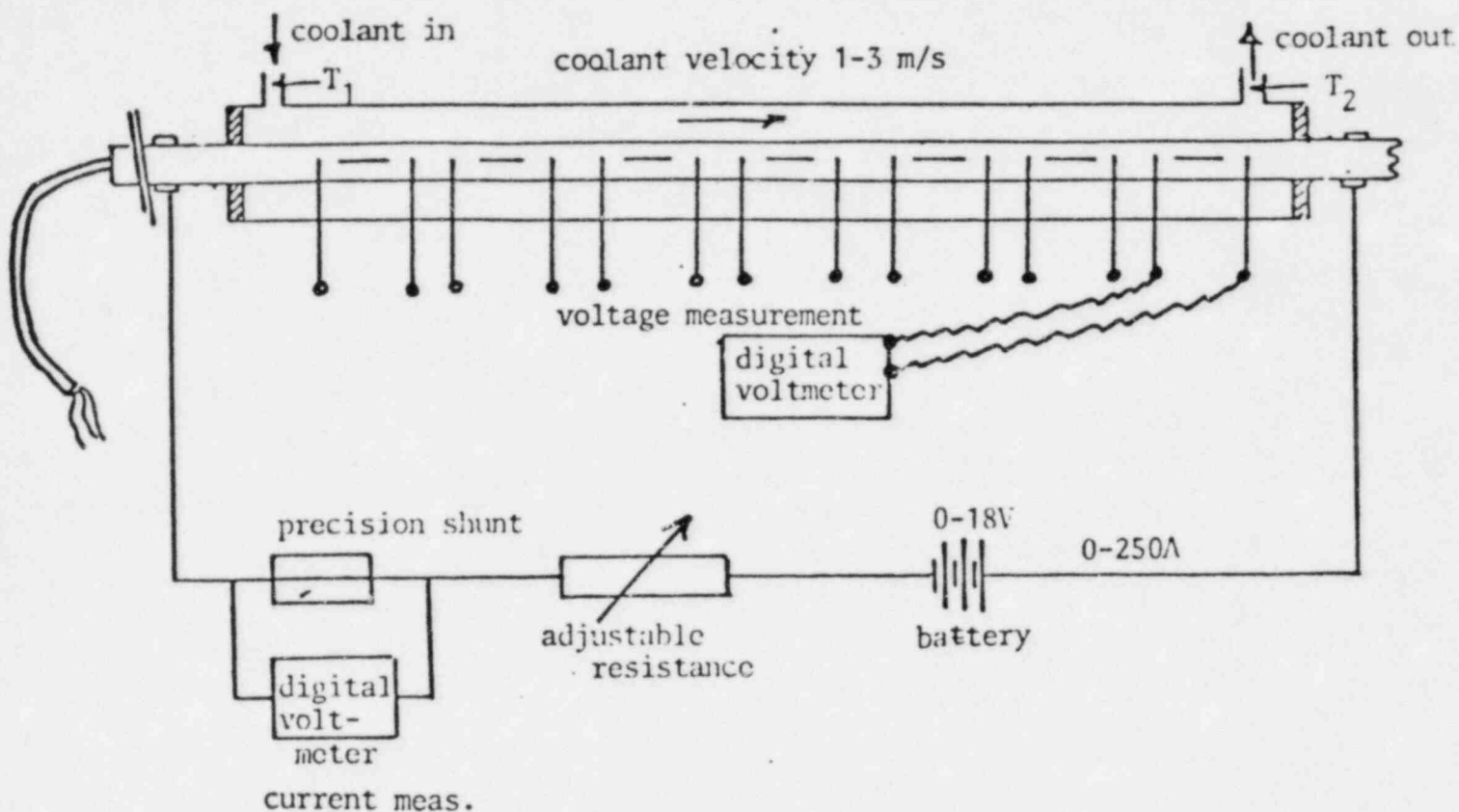
In contrast to the earlier designs of the gamma thermometer (Savannah River, Halden) the RGT gamma thermometer can be electrically calibrated both at low temperatures and at temperatures corresponding to PWR conditions (300°C). This out-of-pile calibration is a powerful attribute of the RGT that serves to reduce the uncertainty σ_1 related to variations in sensor design parameters and properties.

The low temperature electrical calibration is rather straightforward and can be made by any well qualified workshop. Experimental rigs and equipment required for this type of test are not elaborate.

The high temperature calibration requires a high pressure loop and is presently possible at EdFs experimental facilities. Every RGT sensor for reactor use is calibrated at both high and low temperatures.

Low Temperature Testing

In the sketch below is shown the principal design of the low and high temperature loops as applied at IFA, EdF, TEC, etc. Electric current is passed through the RGT string over the active length (where the sensors are positioned). In all the calibrations so far DC current has been applied.



The electrical current going through the RGTA is measured by the voltage drop over a high accuracy shunt.

The current is adjusted by a variable resistance. The resistance is normally a water cooled tube and the part of the tube entering the electrical circuit is adjusted by moving clamps on the tube.

The RGTA is cooled by water having a velocity of 1-3 m/s. The inlet and outlet temperature of the water is recorded.

Accuracy determination of the W/g of sensor heating can be attained by use of individual voltage taps as shown. Alternatively, the pre-measured sensor resistivities may be used.

Data Recorded During Static Electric Calibration

The table below indicates the most important data to be recorded during a direct electrical calibration of the RGT sensors. (In addition, dimensions and electrical resistances must be known.)

Approx. amperes	Actual amperes	Voltage drop sensors 1 to n			μ V signals** sensors (DTCs) 1 to n			T_I^*	T_O^*
		1	2	3	1	2	3		
30	_____	_____	_____	_____	_____	_____	_____	_____	_____
60	_____	_____	_____	_____	_____	_____	_____	_____	_____
90	_____	_____	_____	_____	_____	_____	_____	_____	_____
120	_____	_____	_____	_____	_____	_____	_____	_____	_____
150	_____	_____	_____	_____	_____	_____	_____	_____	_____
180	_____	_____	_____	_____	_____	_____	_____	_____	_____
210	_____	_____	_____	_____	_____	_____	_____	_____	_____
240	_____	_____	_____	_____	_____	_____	_____	_____	_____

* T_I and T_O are coolant inlet and outlet temperatures respectively.

** The sensor signals are read as μ V (or mV) and converted to nominal temperature drop using the conversion factors for type K thermocouples from NBS 25.

Calculation of Indicated Sensitivity

The indicated sensitivity of the sensor is expressed as $S_i = \Delta T_i / P$ where:

P = electrical heat dissipated per gram in the core of the sensor (core and cable sheath).

ΔT_i = measured signal divided by standard conversion to temperature at $\frac{T_I + T_O}{2}$

The heat generation is not directly measurable, but it can be calculated from the formula:

$$P(W/g) = I^2 \frac{R_S}{M} \left(\frac{R_J}{R_S + R_J} \right)^2$$

where:

- I = total electrical current
- M = mass per cm length of sensor (core + cable sheath) at operating temperature
- R_S = electrical resistance per cm length of sensor (core + cable sheath) at operating temperature
- R_J = electrical resistance per cm length of jacket tube over sensor at operating temperature

Determination of Resistance

The resistances entering the formula are measured and corrected to the actual temperature during calibration using the following formula:

$$R_S = R_{S0} (1 + \alpha (T_W + 2/3 T - T_R))$$

$$R_J = R_{J0} (1 + \alpha (T_W - T_R))$$

where:

R_{S0} and R_{J0} = resistances measured at reference temperature, T_R

α = temperature coefficient of resistivity

$$T_W = \frac{T_I + T_0}{2} = \text{coolant temperature}$$

The two resistances are measured as follows:

R_{S0} is measured on the core rod in the chamber region before the jacket tube is installed.

R_{J0} is measured in an excess piece of the jacket tube after drawing.

A check on the estimation of the resistances at reference temperature can be obtained by measuring the resistance over the chamber section in the completed sensor. This resistance should be the resultant of R_{SO} and R_{JO} :

$$R_{ch} = \frac{R_{SO} \times R_{JO}}{R_{SO} + R_{JO}}$$

As an example, the following values were found for one of the EdF-type RGT specimens to be irradiated at ORNL:

R_{SO} measured	:	$0.729 \times 10^{-3} \Omega/cm$
R_{JO} measured	:	$0.306 \times 10^{-3} \Omega/cm$
R_{ch} measured	:	$0.216 \times 10^{-3} \Omega/cm$
R_{ch} calculated	:	$0.2155 \times 10^{-3} \Omega/cm$

For this case the combined resistance measurement checks the composite of the two component resistances within 0.2 percent.

Determination of the Mass of the Core per cm Length

The mass of the core per cm length is determined using the measured inner diameter of the core chamber prior to mounting of the jacket tube. The diameter is measured at several points and the average value is used in the calculations. Destructive examination has shown that the diameter of the sensor is unaffected by drawing on of the jacket tube.

Accuracies Obtainable from Direct Electric Calibration

The calibration of the French prototype RGTAs has shown that the indicated sensitivity S_i of a particular sensor can be calibrated relative to all others with two standard deviations of 0.9 percent. The measured standard deviation among 89 sensor sensitivities, as made, is 3.67 percent. Components of this are estimated to be: thermocouples 1 percent, gas gap 2.3 percent, method 1.9 percent, material conductivity (rod-to-rod) 1.9 percent; all $\pm 1\sigma$.

High Temperature Calibration

In principle, the high temperature calibration is identical to the low temperature one. The same set of data is recorded in the two cases. The main difference is the demand on the test rig design due to the high temperature (and pressures) involved. Figure 3.4-2 shows a sketch of the EdF test rig used for the high temperature calibration of the French reactor prototype RGTs.

3.1.2.2.2 Calibration Results Obtained

IFA Bench Tests

Experimental investigations of the RGT gamma thermometer started with bench tests at the Institutt for Atomenergy (IFA), Norway. In these tests a specimen embodying two sensors was used. The gas chamber was either air-filled or evacuated by a vacuum pump.

The objectives of the testing were to investigate:

- electrical calibration of RGTs.
- sensor stability (constant heating).
- sensor reproducibility (power cycling).
- thermal cycling (electrical heating without coolant to 450 C in sensor body).
- influence of coolant flow and temperature.

In Figures 3.1-13 to 3.1-17 are shown sample results from the tests. The sensors respond linearly to heat ratings up to a factor of four higher than those experienced at PWR conditions. The scatter of the measured data is very low, Reference 3--(40).

Calibrations at EdF/Intertechnique

Description of Renardieres Test Loop

Figure 3.4-2 shows the high temperature test loop at Renardieres, and Figure 3.4-3 shows the "active" part of a full prototype stringer mounted in the high pressure loop.

The operating range for the loop is:

Temperature	:	30 - 300°C
Pressure	:	up to 155 bars
Coolant velocity:		0.5 - 4 m/s
Current	:	0 - 255A

Description of the Intertechnique Test Loop

The Intertechnique company manufactures the French RGTAs and performs low temperature, direct electric calibration of the sensors prior to delivery to EdF.

Essentials of the Intertechnique test loop are shown in Figure 3.1-18.

The electric power is supplied by a high accuracy power supply.

In the Intertechnique case the voltage across the part of the assembly installed in the loop is of secondary importance. The dissipated power is calculated from the measured current and the measured resistance of the sensors. The resistance is measured during manufacture of the RGTA and is adjusted to the calibration temperature by applying the correction formula given earlier in this section.

Low Temperature Calibration

Figures 3.1-19 to 3.1-27 show the results of the low temperature calibration of the nine sensors of one of the French prototypes (canne no. 4).

The signal varies linearly with heating power in the whole calibration range (up to 3 times the average heat rating at PWR conditions). The scatter of the data is very small. Table 3.1-3 shows the calibrations (S_i , τ , σ) obtained at low temperature for a number of French reactor prototypes, numbers 3 through 12, and the five specimens made by Intertechnique for ORNL. The average indicated sensitivity, S_i , for the 89 chambers is 40.88 std °C/W/g. The 1σ variation in mean sensitivities of the 89 chambers is 3.67 percent and the average standard deviation for data from each sensor is 0.7 percent.

High Temperature Calibration

The high temperature direct electric calibration has shown the same quality of results as those obtained at low temperature. This is true both with respect to linearity and scatter of the experimental results.

Table 3.1-2 lists the results obtained for prototypes calibrated at high temperature.

Figure 3.1-28 shows calibration curves obtained for representative French prototypes from high temperature calibration tests in the Renardieres loop (see Figure 3.4-2). Calculations show that for all sensors shown in Figure 3.1-28 the correlation coefficient is better than 0.9999, Reference 3-(16).

Data in Figure 3.1-29 show how the sensitivity of a sensor is lower at PWR temperature than at room temperature. (This is predictable with RADCAL/THERMAL.) Note that all PWR use of RGTs is in the relatively narrow region of 300° to 340°C. For the 45 sensors reported in Table 3.1-2, the standard deviation of mean sensitivities measured at 300°C, electrically, was 4.3 percent compared to the 3.67 percent σ reported above for 89 sensors on the cold calibration.

Data Recording During Power Step

As a supplement to the static, direct electrical calibration of the RGT sensors, a dynamic measurement is made by switching on or off the electric current. From the sensor response, time constants can be calculated as explained in Section 3.1.1.3.3.

The measured response is recorded on an X-Y strip-chart recorder and/or by a computer system. To evaluate the time constants to the highest accuracy, computer codes using regression analysis are applied. Graphic analysis based upon logarithmic plots of the response curve provide results with slightly larger uncertainties.

For the French reactor prototypes (cannes 5, 9, 11, 12) such power step determinations were made by the supplier (Intertechnique) with standard deviations between sensors in these rods of, respectively, 2.16 percent, 2.5 percent, 1.3 percent, and 1.48 percent. The standard deviations of the means by direct electric calibration were, respectively, 3.6 percent, 1.42 percent, 1.43 percent and 1.58 percent. The average for a step change was 1.86 percent and for direct electrical calibration 2.0 percent.

Interloop Comparisons

A very important proof of the accuracy and adequacy of the direct electric calibration has been obtained in connection with the ORNL program (see Section 3.1.3.4). The RGT test specimens (15 in number) were first electrically calibrated in the manufacturers' workshop. Thereafter, the calibration was repeated at TEC where the irradiation resistant signal connector plug was installed.

For the ORNL test specimens only, the RGT sensors each employ two difference thermocouples. (This was for measurements of the contribution of thermocouple calibration to variance in S_i .)

Five of the ORNL specimens were manufactured and first calibrated in France by Intertechnique. Upon delivery to Knoxville, they were

The data for specimen 1 are compared graphically in Figure 3.1-30 and 3.1-31.

For other ORNL specimens, the Intertechnique data, Reference 3-(38), can be summarized as follows:

The mean sensitivity and standard deviation of the eight best fit sensitivities for the four stainless steel RGTs (two difference thermocouples each) is:

$$\bar{S}_i = 28.69 \text{ std } ^\circ\text{C/W/g}$$

$$\sigma, \text{ percent} = 1.5 \text{ percent (between sensors - best fit } S_i \text{'s)}$$

$$\text{average } \sigma \text{ percent for the data on the best fit lines} = 0.88 \text{ percent.}$$

3.1.2.3 "In Situ", or In-reactor, Calibration Methods

There are three entirely distinct methods which have potential for in situ recalibration of RGT sensitivity, in-reactor, that are totally independent of the need for TIPs. Two of these methods reveal real sensitivity, S_r , and the third yields the more important indicated sensitivity, S_i .

3.1.2.3.1 Determination of τ , S_r , and S_i From an Oscillation, Step Increase, or Reduction in Total or Local Power

The precisions attainable by these in-reactor calibrations are best guesses at present, until the methods have been reactor tested. As has been explained in Section 3.1.1.3.4, the dynamic response characteristics of an RGT are tightly related to the real sensitivity, S_r . A step change in either gross power or in local power, corrected for late arrival of delayed fission product gamma, yields the true response of the RGTs exposed to this change, which can be directly converted to the real

sensitivity of the instrument with an estimated uncertainty of ± 4 percent. The uncertainty is due in part to the inaccuracies in accounting for lagging sensor heat generation rate.

The uncertainty in real sensitivity during in-reactor dynamic recalibration can be reduced to about 3 percent by transfer function analysis of local power oscillations of high enough frequency as to be predominantly influenced by the ~ 75 percent of sensor heating which is prompt relative to the 15 second τ_{apparent} of the RGT.

With this method there remains the uncertainty associated with the correction of S_r to S_i (correction for the variability of difference thermocouple characteristics). It can be shown that, because both junctions are equally irradiated in a difference thermocouple, most of the postulated irradiation damage effects are cancelling and that by applying pre-irradiation differences between S_i and S_r the additional uncertainty imposed to convert S_r (± 3 percent) to S_i is at the 3/4 percent level.

A thermocouple correction curve can be initially associated with each RGT and used to convert reactor-determined S_r 's to S_i 's without significant loss of accuracy.

The oscillation method is burdensome on the reactor operator, and more often, tracking of signals during quick nuclear shutdowns would be used (expected uncertainty on $S_i \sim 4.5$ percent). Tracking RGT signals after scram could be more accurate for detecting changes in sensitivity than for absolute measures of sensitivity.

3.1.2.3.2 Loop Current Step Response

ORNL, References 3-(31) and 3-(32), described methods (now used in PWRs to recalibrate important RTDs and T/Cs) called "loop current step response" in which small pulses of power are applied to the signal leads of thermocouples or RTDs. The response transfer functions of the instruments following such pulses are analyzed, or deconvoluted, in such a way

that the transfer functions for response to externally imposed steps (such as occur in plunge testing) can be extracted. Thus, the τ , and in the case of RGTs, S_r , is determined. ORNL has proposed to DOE, Reference 3-(45) and Section 3.2.3.2, that this method be qualified for in-reactor recalibration of RGTs.

The expected uncertainty in the determination of S_r by this method, which neither disrupts operation nor requires special hardware in the RGTA is about ± 5 percent on S_r plus the uncertainty of about 3/4 percent in converting to S_i , related to difference thermocouple calibration. The underlying limit on accuracy is the small value of the power pulses, relative to the magnitude of the range of gamma sensor heat rates (e.g., .05 W/g vs 1.5 W/g), that can be imposed without risk through tiny thermocouple wires.

3.1.2.3.3 Installed Heater Cable

A 1 mm stainless steel jacketed, nichrome heater cable has been installed in the center of the cable pack in some of the ORNL test specimens. Through this cable a heat of up to 10 W/cm may be applied at will. This corresponds to an additional 10 W/g of RGT sensor heating. The heat may be applied in discrete steps, oscillations, or in ramps, and can be superimposed upon in-reactor gamma heat rates ranging from 0 to 3 W/g.

Figure 3.4-1 compares a direct calibration obtained by use of the internal heater with that obtained by direct joule heating. The heater cable can also be used in dynamic tests to determine τ and S_r to an estimated accuracy of $\pm 1-1/2$ percent.

Since no estimation of difference thermocouple calibration is required to find S_i when direct in situ recalibrations are done with the heater cable, the accuracy of this method is almost as good as the direct electrical workshop calibration when the relationship between heater cable power and RGT sensitivity is determined on an individual basis.

3.1.3 Effects of Reactor Exposure on Sensitivity

3.1.3.1 "Library" Studies

A study, Reference 3-(33), has been made to evaluate possible effects of irradiation on the sensitivity of the gamma thermometer (both real and indicated sensitivity). The study is referred to as a library study since the first step was a literature search for reported experience on variations to be expected in critical material properties. Using the estimated variations as input to the RADCAL/THERMAL code, the possible effects on sensitivity have been calculated.

The changes to be expected during in-pile operation can be divided into two groups:

- changes that influence only the indicated sensitivity of the instrument (i.e., changes in the thermocouples during irradiation).
- changes that influence the real sensitivity (and thereby also the indicated sensitivity) of the instrument, (i.e., changes in the thermal properties and the geometry of the sensor).

Irradiation Effects on Thermocouples (Effect on S_i Alone)

Extensive experiments have been carried out at ORNL to measure possible changes in type K thermocouples (chromel-alumel) during in-pile operation, References 3-(34) and 3-(35). In these experiments the effect of temperature alone and the combined effect of temperature and neutron irradiation have been studied. The measurements conducted show that type K thermocouples experience a slight increase in the Seebeck coefficient and thereby the EMF when operated in the temperature range 200-500 °C without irradiation. The effect is attributed to so-called "short-range ordering" in the chromel lead. The alumel does not undergo such changes. The observed increase in the Seebeck coefficient is about one percent. The changes disappear if the thermocouple is annealed at temperatures above 500 °C.

The neutron irradiation seems to have the opposite effect of the temperature alone and results in a lower value of the Seebeck coefficient. The irradiation effect is also of the order of one percent and it can be annealed out at higher temperatures.

Detailed investigations show that while the temperature effects mostly occur in the chromel lead, it is the alumel lead that experiences irradiation damage. Further, most other irradiation effects that have been postulated (but never proven) cancel out in difference thermocouples where damage that adds to the signal in one lead, subtracts from the signal in the other.*

The ORNL tests are expected to confirm these conclusions to within the accuracy of those determinations of thermocouple sensitivity.

Irradiation Effects on Thermal Properties and Geometry (Affecting Both S_r and S_i)

During in-pile operation the irradiation from thermal and fast neutrons causes minor changes in the materials of the RGTA (stainless steel) and argon gas). The material changes show up as:

- transmutation of argon atoms
- lattice damage of structural metals

The thermal neutrons are responsible for the transmutation and this change is irreversible. Lattice damage is mainly caused by fast neutrons and it can be annealed out at higher temperatures.

* Actually, chromel-alumel thermocouples that have resided in the HBWR for up to 14 years still give signals that correspond to within 1/2°C of the accurately known saturation temperature of the heavy water moderator.

Thermal Conductivity of Steel

For the steel used, a maximum reduction in the conductivity of 4 percent may occur at the end of six years of operation of RGTs at PWR conditions. The change is mainly caused by irradiation induced pores in the steel body.

Calculations with the RADCAL/THERMAL code show that the estimated decrease in thermal conductivity would result in a 2.8 percent increase in real sensitivity.

Thermal Conductivity of Argon

The study shows that a small amount of the argon gas may undergo transmutation into potassium (K_{41}). This will not influence the heat transfer in the gas chamber.

The potassium may, however, plate out on the surfaces of the chamber and thereby influence the emissivity.

Conservative calculations show that if all the potassium plates out, a surface layer corresponding to 120 atom layers (.00001 mm) of potassium builds up, having no significant effect on the gap dimensions. In the calculations, a change of the emissivity from 0.3 to 0.4 was attributed to the deposit. The calculation shows that a less than one percent decrease in sensitivity would result.

Geometrical Changes

Swelling

The pore formation responsible for the reduction of the thermal conductivity of the steel, also results in swelling of the steel body. It is estimated that the dimensional increase will not be more than one percent in any direction. Calculations with the code show that such changes in the geometry could increase the instrument sensitivity by 1.6 percent.

Creep Down

Creep down of the jacket tube on the core rod in the chamber section is found to be negligible (i.e., less than 0.5 percent reduction of gap size at the end of six years of operation at PWR conditions). Such a change has negligible influence on the sensitivity of the sensor.

Conclusions

Even if it were assumed that only effects that increase the sensitivity would occur, the study shows that the instrument could change sensitivity by a maximum of 5 percent after six years at PWR conditions. If the negative effects are included this could be reduced to zero to three percent. Such a change in sensitivity would become an uncertainty on the sensitivity only if:

- no in-reactor recalibration of sensors was possible (i.e., in situ calibration cable inoperable).
- no compensation for sensor drift by slight adjustments of constants in the signal processing was practicable.
- no recovery of irradiation damage by heat treatment was provided for. (The incorporated heater cables can be used to anneal both the thermocouple pack and the RGTA itself by applying heat when the RGTAs are uncooled.)

3.1.3.2 SRP Experience

The experience with gamma thermometers at SRP is reported fully in Section 3.3.1. Gamma thermometers having had an exposure corresponding to 5.5 years of PWR operation showed a change of 2 percent in local power indication relative to calorimetric determination of local power. Within this 2 percent, changes in both instrument sensitivity ($1/K_1$) and in the ratio of local heat generation to gamma heating (K_2) are included.

3.1.3.3 HBWR, Halden Reactor Experience

The Halden (HBRW) experience with gamma thermometers is reported fully in Section 3.3.2. At Halden the gamma thermometer signal can be compared to the local power determined calorimetrically. At Halden the ratio of local fuel power generation to gamma heating has been constant within the limits of detection of such change, (about 3 percent).

3.1.3.4 Direct Testing of RGT at ORNL

Highly documented and well-characterized accelerated irradiation experiments have been performed at ORNL. These tests give the possibility to accurately measure the effects of irradiation on the RGT sensitivity (K_2). The sensors used in these tests have been so designed that it is possible to evaluate which parameters or properties have undergone changes, if any.

The test involves special, short RGT specimens, each of which contains only one chamber. Several different RGT designs have been tested - they are identified by the prototype programs for which they were developed. Thus, the Duke (or Oconee) type are designed to be compatible with the B&W in-core system and include a central, hollow tube that would permit, in reactor prototypes, a travelling SPND to be inserted for cross-calibration. The RWE-type are designed to Mulheim-Karlich dimensions and include double difference thermocouples and an internal heater cable. The EdF-type are the same as the EdF prototype RGTs.

On April 10, 1980, the delivery of 15 RGT specimens to ORNL was initiated. Five were of the EdF type, four of the Duke Power (Oconee) type, three of the RWE (Mulheim-Karlich) type and three of the BWR type. One of the EdF type specimens was made of Zircaloy and employs an evacuated sensor cavity (i.e., rather than argon filled).

All specimens had been electrically calibrated for S_i and power transient calibrated for S_r (except those with removable thermocouple packs). The five EdF type specimens had been twice calibrated, first by

Intertechnique and later by TEC of Knoxville (who produced seven other specimens and also installed the irradiation resistant connection plugs on all specimens and produced seven other specimens). Some of the calibration data were shown in Section 2.3.1.3 to illustrate the high degree of reproducibility of direct electrical calibration (Joule testing).

A selection of five "library" specimens has not been irradiated at all, but are used in "standardization" campaigns before and after the one year's irradiation to prove the reproducibility of the ORNL plunge test method of calibration.

Ten specimens entered the ORR on the schedules shown in Table 3.1.4 to be irradiated for one year to a fast neutron exposure of 6.21×10^{21} mvt (equivalent to three-year service in a PWR). From both library studies and D₂O reactor experience it was predicted that the resultant shift in sensitivity would be less than 5 percent when the 10 irradiated specimens are recalibrated. The experimental design, however, provided for separation of effects which may have caused any unforeseen changes in sensitivity, Reference 3-(36).

The detailed design of the specimens appears in Reference 3-(9) and the acceptance criteria for plunge test calibration are given in Reference 3-(10). The results of the Intertechnique calibration and the TEC calibration are documented in References 3-(11) and 3-(12), respectively. Results of the initial ORNL plunge test calibration are given in Reference 3-(24).

Post-irradiation testing has not yet been completed due to problems encountered with the special electrical connectors used on these test specimens. The ceramic connectors experienced cracking apparently due to irradiation and/or handling effects. (Note that these ceramic connectors are used only for the ORNL test specimens and are not used with any RGT for in-reactor use.) The possible failure of these connectors was provided for in the test plan, since the connectors were of an original and unique design. The failure of the connectors has resulted in broken

thermocouple leads and the consequent inability to obtain measurements from the affected thermocouples. Efforts are now underway to recover the thermocouple signals by removal of the existing ceramic connector and the installation of new leads.*

Despite the connector problems some post-irradiation data have been obtained, as shown in Table 3.1-5. The sensitivity, S , is determined from the time constants using the relationship illustrated in Figure 3.1-7. The data show a change in sensitivity of less than 1 percent. This change is a consequence of irradiation equivalent to 3 years in a PWR. The actual fluences are shown in Table 3.1.6. More complete data analysis and results from other specimens following connector repair work are expected to confirm these results.

*This work will be carried out at the hot cells of the CEGB (at Berkeley, England) which are well equipped to handle this type of work.

3.2 K₂, the Ratio of Local Fuel Power to Gamma Heating in the Sensor and the Components of the Uncertainty, σ₂

The gamma thermometer was, in the first twenty years of its use in heavy water reactors (1935-1973), a purely empirical instrument. At SRP, where the concept originated, and at Halden (HBWR), it was neither anticipated nor required that the instrument indicate fuel LHGR directly for long periods without correction to K₂. Both Halden and SRP had the luxury of recalibration at will.

SRP (as previously discussed) continually measures the power of every fuel assembly to $\pm 3/4$ percent accuracy with flow (orifice ΔP) and temperature rise (four thermocouples) and can, at will, determine the axial neutron flux shape by running TWFM (Travelling Wire Flux Monitor) Traces. Thus, the gamma thermometer was not originally intended as an accurate measure of local power but rather as a continuous multi-source axial power shape indicator that could be recalibrated at will to read channel power (the sum of seven readings) and relative axial flux (or LHGR) distribution on a nearly real-time basis. For the short (one month) SRP fuel cycles for plutonium production, the difference between neutron flux shape and power shape (LHGR) was itself small. It was observation, not theory, (there was no theory developed) that proved the long-term constancy of the Fuel-Power-to-Sensor-Heating ratio, K₂, even in year-long tritium production cycles in which thermal neutron flux shape had departed dramatically from LHGR shape. Recalibration was not necessary, except in isolated cases where the sensitivity of instruments had shifted for mechanical reasons, (e.g., shift in thermocouple position). Stutheit, Reference 3-(4) reported:

"Response is linear with average reactor power (not flux) and changes in sensitivity as a result of irradiation are small. Of fifteen gamma thermometers which were used to monitor flux levels for a year in a neutron flux of more than 10^{15} n/cm²-sec, only three required compensation for sensitivity changes of 5-10 percent."

Awareness of the SRP experience in 1963 led the HBWR technical staff to select gamma thermometers as the best instrument to monitor the power of

individual test fuel assemblies. As at SRP, the construction of the HBWR instrument fuel enabled direct calorimetric recalibration of these instruments against measured thermal power of the fuel element as shown in Figures 3.2.1 and 3.2.2, extracted from Reference 3-(5). These show pictorially how a device called the "calibration valve" is used at HBWR to convert normally boiling coolant to sensibly heated (non-boiling) coolant in order to measure individual fuel element power at an accuracy of ± 3 percent. Again it was observation, not theory, that led to the conclusion that the ratio of the heat generated in the fuel to the heat generated in a gamma thermometer sensor remained constant within very narrow limits.

For instance, the instrumented fuel assembly IFA-4 was installed in HBWR early in 1964 and its three gamma thermometers were recalibrated from time to time until the assembly was finally removed in 1971. The same gamma thermometer signal factors ($K_1 \times K_2$) were being used when the fuel was removed only because they were observed to be the same (within the limits of detection of change which, because of signal contribution from other fuel and control configuration, was estimated to be ± 6 percent). HBWR experience is described further in Section 3.3.2.

The initial theoretical work on the use of gamma thermometers in LWRs was performed by SERMA (Service d'Etudes des Reacteurs et Mathematiques Appliques), a division of the French National Atomic Energy organization, CEA, located at the Saclay center outside Paris.

To enlarge and extend the basic work of CEA to other types of LWRs and benchmark the predictions resulting, Scandpower and CEA submitted a joint proposal to EPRI in September 1979, which is still under review at EPRI, (Section 3.2.1.3). Additional independent work has been performed by the Oak Ridge National Laboratory (Reference 3-54).

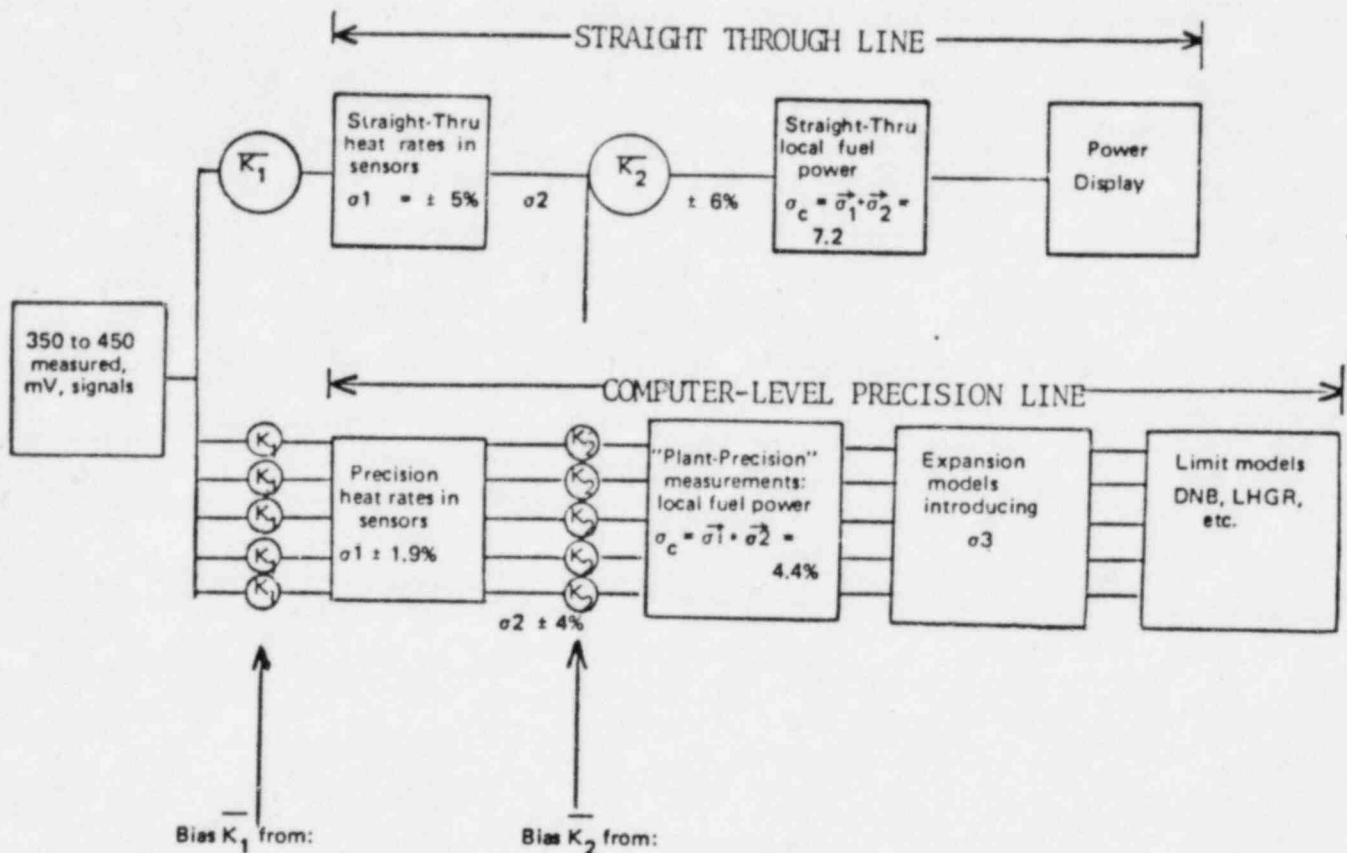
3.2.1 Modelling via Neutron Physics and 3D Monte Carlo Shielding Calculations

Goals of the Physics Modelling

The goals of the physics modelling efforts are to show fairly good absolute predictive validity, to assess the magnitude of the corrections applicable to K_2 for "off-reference" core conditions, (such as "rods-in"), and, finally, to provide software, practicable for plant computers, to make the desired small corrections automatically to any of the 350 to 450 values of K_2 when core conditions there are "off-reference" (i.e., different from the conditions at which the basic value and uncertainty of K_2 was established).

The readout system construct supporting the steady-state use of fixed RGT sensors in light water reactors is depicted below:

DUAL SIGNAL PROCESSING



- individual bias from precalibration to an accuracy of $\pm 1.9\%$
- max. correction to $K_1 \approx 5\%$

- LHGR to γ heat models: $\left\{ \begin{array}{l} \text{core condition corrections, } K_2\text{'s} \\ \text{time domain corrections, } K_2\text{'s} \end{array} \right.$
- normalization to thermal power attainable $\sigma_2 \approx 4\%$

The calculational approach to establishing both the values of the corrections to the single best value, K_2 , the ratio of local fuel to sensor heating, and estimating the accuracy thereof, must use the most accurate off-line neutronics and shielding theory available. The problem is initiated in reverse order to its ultimate final use, i.e., to predict values of K_2 and to extrapolate beyond them rather than to interpolate K_2 between benchmarked points:

- Given a distribution of known local fuel powers, compute the sensor heating resulting in gamma sensors under a variety of burnup, control rod, boron and burnable poison distributions.
- Use the models to bracket extreme influences on the ratio of fuel-to-sensor heating, K_2 , over such core-condition "feature space" (i.e., sensitivity studies).
- Benchmark the models to the highest accuracy possible in TIP or SPND "measured" LWR cores.
- From the prediction accuracy provable at benchmark points estimate the accuracy of (i.e., uncertainty in) extrapolation.

The provable accuracy in K_2 at reference conditions (e.g., clean core, steady state, no control rods, low burnup, etc.) will improve as larger and larger groups of RGTs are inserted in PWR cores for comparison of RGT measured fuel heat rates with the best values otherwise obtainable. Full core installation will permit direct determination of the accuracy of K_2 by comparing the sum of LHGKs "measured" to the total thermal power independently measured.

The uncertainty of the extrapolation to "off-reference" conditions can be satisfactorily developed by good theoretical models (whose expected provable absolute accuracy is ± 10 percent). The models can show the size of the variation on K_2 to be expected over feature space and, if this is small, the error in K_2 corrections for off-reference conditions becomes very small. If, for example, K_2 is measured at reference

conditions with an uncertainty of ± 10 percent and the absolute predictive validity of the models for several extreme cases was shown to be ± 12 percent, then the corrections to K_2 for off-reference conditions could be relied upon to ± 12 percent. If the theoretical models showed that a ± 8 percent correction should be applied to the value of the benchmarked K_2 (accuracy ± 10 percent) for, say, control rods in the vicinity, then the error in K_2 -rodded would be:

$$\sqrt{+10^2 + (8 \times .12)^2} = 10.05 \text{ percent}$$

The incremental uncertainty produced by off-reference conditions would be only 0.05 percent. This arises from two important facts:

- 1) The theoretical model was good on an absolute basis (± 12 percent).
- 2) The change in K_2 due to the off-reference condition is small.

Given that the best possible accuracy of benchmarking is about the same for any local power instrument (whether by post-irradiation gamma scan, total power normalization, comparison to TIP, etc.), there is one criterion that governs the ultimate accuracy of measurement by any instrument at any reactor condition, namely:

The single key to the ultimate reduction of the uncertainty of LHGR measurements by an in-core device is the magnitude of the corrections which must be applied to the signal to account for "off-reference" core condition changes, i.e., operation away from the condition at which the ratio, K_2 , between LHGR and the measured parameter can be most accurately established experimentally.

This principle was alluded to, though perhaps not articulated in this way, when Georgia Power and GE presented to NRC staff the advantages of gamma measurement over neutron measurement depicted in Figure 3.2-3, extracted from Reference 3-(1).

The figure shows, along one axial distribution, that the raw signals of a gamma detecting device required less correction for various influential parameters than did the thermal neutron or fast neutron sensitive devices. It is evident therefore that the ultimate accuracy of the gamma device will be better (i.e., the corrections to raw signal will be smaller). It is notable that in this case the "dice are loaded" toward the thermal neutron device because the denominator of the ratios being plotted (i.e., actual local power) was obtained from computations made upon the signal from the thermal neutron device itself.

The applicants (herein) can draw upon the body of experimental work submitted by GE and Georgia Power Company establishing the intrinsic superiority of gamma measurement to either fast or thermal neutron measurement. Measurements need not be made to demonstrate (as GE has already done) that gamma signal deviates less from true LHGR of surrounding fuel than the signal from thermal neutron devices. This can be shown by modelling. The changes in K_2 , the local fuel heat rate to sensor heating ratio, are shown both by theory and past experiment, to be so small that any necessary approximate corrections to K_2 result in an insignificant increase in the total uncertainty of K_2 .

Measurement campaigns reported herein, therefore, are those necessary to establish the accuracy of the LHGR measurement at reference core conditions, and to try to minimize resident uncertainties imposed on the new instrument by the in-place reference systems to which it must be calibrated. The predictive validity of the theoretical models will be ascertained for each reference case (the first such data reported herein are from Bugey 5 (Section 3.4.2), an EdF (Westinghouse-type) PWR.

The small variance of the fuel-to-sensor heating ratio, K_2 , makes possible the "straight-through-line" of signal processing in which single-valued constants, $\overline{K_1}$ and $\overline{K_2}$, are applied hard-wired, without individual bias, directly to the raw signals from 350 to 450 RGTs. The "straight-through-line" of LHGR surveillance is a feature of gamma thermometry which is unachievable by TIP, SPND, fission chamber or previously installed in-core systems of any kind.

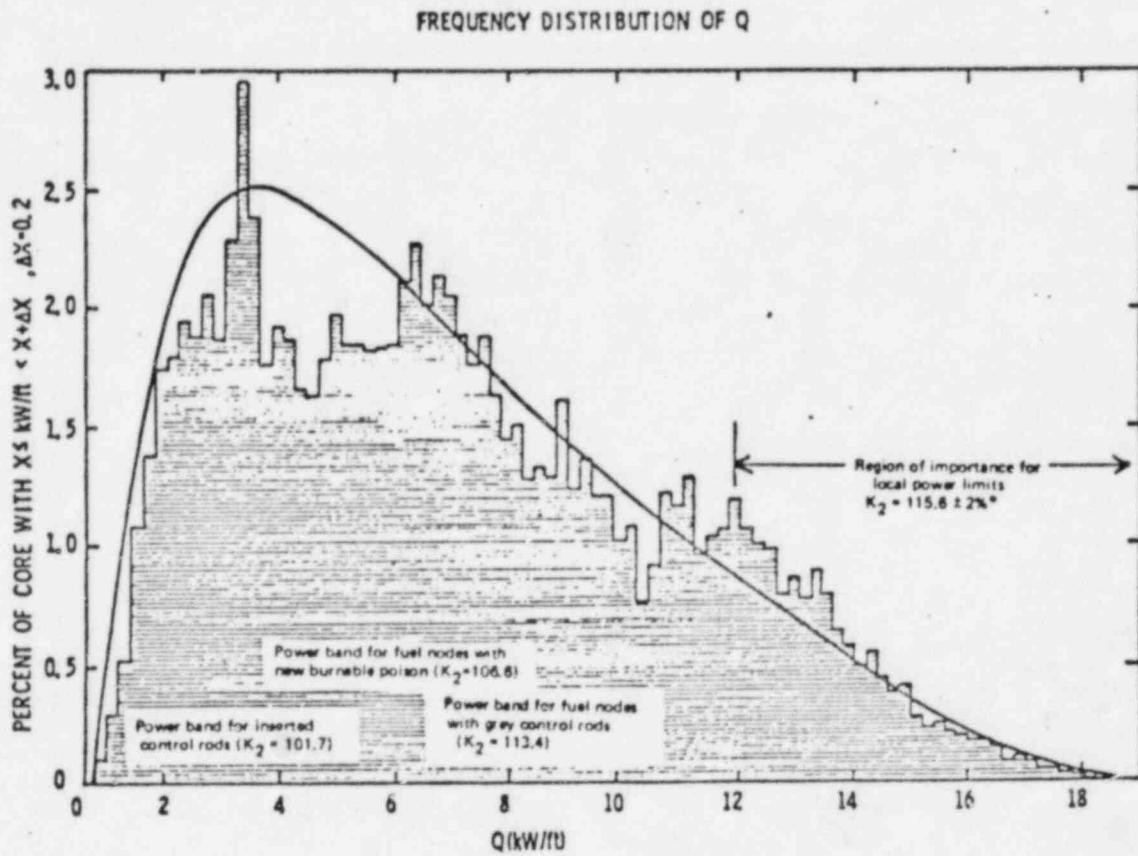
In evaluating the uncertainties in nodal power which would be associated with direct reading instruments biased only by $\overline{K_1}$ and $\overline{K_2}$, (i.e., the "straight-through" line), it is necessary first to select a philosophy for selecting the single value to be used for $\overline{K_2}$.

It is calculated by CEA that all poisons that tend to lower power in particular individual assemblies, such as control rods, burnable poison shim rods, and grey control rods, have the similar effect of adding a little gamma heating to the RGT sensor for a fixed power in the fuel rods (i.e., lowering K_2 for these core nodes). When a $\overline{K_2}$ value is selected for unpoisoned assemblies, the power in the poisoned nodes is conservatively overestimated.

In no case can an overestimate of local LHGR originate from fuel which is at or near local limits for LHGR. For example, the new consumable poison suppresses power in its fuel assembly by about 15 percent relative to "unpoisoned" assemblies. A regular control rod cluster suppresses power by 50 percent or more, relative to unrodded fuel nearby. In the case of such a control rod insertion in the assembly containing RGTs, the real value of K_2 would be reduced to 101.7 W/cm/W/g. Using a global reference $\overline{K_2}$ of 115.6 in this case would give a "measured" power of 102 W/cm for the rodded assembly when the actual power was 90 W/cm. Meanwhile the average LHGR in the adjoining unrodded assemblies, where K_2 of 115.6 is accurate, are being measured at 180 W/cm or greater.

Thus, if the philosophy of setting the average $\overline{K_2}$ value at 115.6 (reference "clean" value) were adopted, the error in any local power measurement would lie in the region between -0 and +12 percent. However, the portion of the fuel in which local limits can occur lies within a much narrower uncertainty band of -0 to +4 percent. Thus, in discussing errors resident in the straight-through system, it is more meaningful to refer only to errors in measurement for the fuel with LHGRs lying within the highest 50 percent of the LHGRs in the core.

The figure below is qualitative only but illustrates the low importance of errors in K_2 occurring in or near poisoned or controlled assemblies: The conservatism resulting from use of 115.6 for $\overline{K_2}$ would have no effect on the accuracy of power "measurements" for fuel closest to any local limits.



* Expected 68/68 confidence limit after normalization core wide to thermal power.

Gamma Heating

The sources of heat production in the gamma thermometer sensors are absorption of direct gamma radiation from surrounding fuel rods (emanating directly from fission, fission product decay, and $n-\gamma$ reactions in U_{235} and U_{238}), a variety of gamma radiations from secondary sources (such as neutron captures in control rods, borated water, fuel cladding), elastic collision of fast neutrons in the gamma thermometer itself, and $n-\gamma$ absorptions in the gamma thermometer itself. In the tightly packed PWR lattice, the shielding provided by nearby fuel rods is quite effective in reducing the range from which source gammas can originate.

The gamma sources depend upon fuel burnup, void, and the structural materials present in the core. The spectrum of source gammas covers a range from a few eV to 10 MeV. (As suggested in Section 3.1.1.1, rough shielding calculations characterize the spectrum at 1.5 MeV average.)

The transport of gammas from their point of origin involves scattering, absorption and electron pair production. Scattering processes include Compton scattering and other types of diffusion. The probability that a given source gamma, born at a known point, will contribute to gamma heating in the RGT sensor position also depends upon the lattice type and upon the operating parameters mentioned above (e.g., boron, burnable poison).

3.2.1.1 The EdF/CEA Theoretical Programs

The CEA approach to the problem involves 2D neutronics codes which define the neutron reactions taking place: fissions, absorptions, diffusion, slowing down in fuel pins, water and structural materials (including the sensor itself). This S_n, j, k (geography, energy group, and nature of neutron reaction) information is then transformed through nuclear data libraries, to S_γ, j, k information for source gamma rays, which are tracked from points of origin through their journeys and scatterings to

arrive at the probability of incidence on, and absorption in, the sensor. All sources are summed and the signal determined. Monte Carlo codes for gamma transport carry within the processing routines an estimate of the uncertainty associated with the absorption probabilities being arrived at. The CEA effort described below quickly established the validity of use of simpler methods known as "integration of line-of-sight point attenuation kernel" as substitutes for the more exact but more costly Monte Carlo diffusion codes, such as TRIPOLI.

TRIPOLI is a general, three dimensional Monte Carlo program, which treats the slowing down and the diffusion of neutrons or gamma. For neutrons, TRIPOLI can solve criticality problems, problems with a given source, or time dependent problems. The geometry is described as a combination of volumes, bounded by portions of first or second degree surfaces. The orientation in space of these volumes is arbitrary. Repetitive geometry by translation, symmetry or rotation can be processed. The program itself can control the consistency of geometry data.

For shielding calculations, the neutron or gamma cross sections are represented in a multigroup mode, with the number of groups as large as necessary. Usually used are 240 neutron energy groups from 14 MeV to thermal energy and 61 gamma energy groups between 10 MeV and 10 KeV. Multigroup data are derived from a library tape (LINDA) containing pointwise data taken from the UKNDL library. For core calculations, neutron cross sections are pointwise defined with 40000 points between 6 KeV and 5 eV; above 6 KeV and below 5 eV, the code uses fine multigroup cross sections. The following interactions are taken into account: for neutron, elastic collision, with any anisotropy order, (n, n') and $(n, 2n)$ reactions, fission, capture and thermalization; for gamma problems, TRIPOLI takes into account the Compton diffusion with exact anisotropy, pair effect, and photoelectric effect. The program can solve deep penetration problems using variance reduction techniques based on the exponential transformation and biasing of angular scattering laws. The distribution of sources can be any arbitrary function of space, energy and direction. The program calculates spectra and activities averaged in specified volumes or areas.

The neutron heating in gamma thermometers is composed of components due to n, γ reactions in the sensor itself (followed by some self-absorption), and from elastic scattering of fast neutrons (which source is negligible and proportional to nearby fission rates, anyway). TRIPOLI, described above, has been used in neutron, as well as gamma heating, calculations.

The onset of EdF/CEA involvement in gamma thermometry in 1976 marked the first attempt to build detailed theoretical models capable of predicting accurately every aspect of gamma thermometer performance with regard to sensitivity in workshop calibration, the basic physics governing the relationship of sensor heating to LHGR, and the thermal processes governing signal (ΔT) production and drift.

The first concern to EdF physicists before expending a large effort on the development of a theory from which to develop reactor software for correcting K_2 was specificity of signal. Did the sources of heat in the instrument come from nearby rods mostly, or were they a "smear" from all over the reactor? It was found that 91.5 percent of externally generated gammas producing sensor heating came from within the instrumented fuel assembly, (in fact, 81 percent of such heat production came from the first five rows of rods surrounding the sensor). Vertically, a control rod or spacer grid more than 10 cm away from the sensor caused less than 1/2 percent variation in heat rate and could be neglected.

The next activity was to actually predict the LHGR-to-sensor heat ratio, K_2 , using high accuracy 3D Monte Carlo methods, TRIPOLI, and at the same time benchmarking with TRIPOLI less expensive codes (a first step toward plant usable software). For Bugey 5 prototypes, at reference conditions, K_2 was 115.6 W/cm fuel per W/g of sensor heating. This value was used to design EdF RGTs for an average signal of 40°C (at 178 W/cm) with 26.0 mm sensor length.

The third theoretical activity was to assess the impact of such "off-reference" conditions as control rods nearby, high burnup fuel, burnable poison nearby, etc., upon K_2 . This was the first theoretical effort to verify for H_2O reactors a phenomenon which had been observed

in D₂O reactors (i.e., the constancy of the relationship of signal to heat production in surrounding fuel). The table below summarizes the magnitude of various effects calculated by SERMA.

CASE	External γ W/g at 178 W/cm	Internal γ from n, γ W/g	K_2 W/cm W/g	Change percent of K_2
Reference (equilibrium γ from fission products, 100 hrs after startup)	1.43	.11	115.6	--
Rods in	1.69	.06	101.7	-12.0
Consumable poison in	1.56	.11	106.6	-7.8
Grey control rods	1.46	.11	113.4	-1.9
Exposure 20,000 Mwd/t Reference 3-(42)	1.44	.11	114.8	-0.7

In applying the "straight through" system (e.g., use of $K_2 = 115.6$ for all gamma thermometers) one would overestimate local fuel power in the three cases: control rods in the same assembly, burnable poison fingers in the same assembly, grey control rods in the same assembly, as has been discussed.

Only if an effort were made to normalize to total thermal power the sum of all local powers, "measured" using \bar{K}_2 (as is done for neutron instruments) would an overestimate in "off reference" (low power) parts of the core lead to underestimates in the high power (limiting) parts of the core. For example, if 1/4 of the core contained fuel assemblies with consumable poison and a normalized reference value were used for \bar{K}_2 , then power in 1/4 of the core would be overestimated by 8 percent, and, through normalization, local powers in other parts of the core would be underestimated.

In the example below, the operator attempts a correction of his best estimate of global \bar{K}_2 (i.e., 115.6) by normalization to total thermal

power. The lower real values of \overline{K}_2 in the 1/4 core that contains poison causes his new normalized \overline{K}_2 (113.5) to produce a -1.7 percent error in high power regions of the core where use of the original \overline{K}_2 (benchmarked in reference, no poison cases) would have resulted in only a 0.1 percent overestimate in the "reference" region representing 3/4 of the core and including the highest power fuel.

ILLUSTRATION OF NORMALIZATION ERROR

<u>Actual Conditions</u>	<u>Known to Operator</u>
Mwth: 3500	Mwth: 3500
Average LHGR in "poisoned" 1/4 core = 158.3 W/cm	Avg. signal in poisoned region = 1.48 W/g
Avg. LHGR in 3/4 core at reference conditions = 195.5	Avg. signal in reference region = 1.69 W/g
Actual K_2 in poisoned region = 106.6	Best estimated global \overline{K}_2 = 115.6
Actual K_2 in reference region = 115.5	
Length of fuel: 188 km	Length of fuel : 188 km

Consequences of Normalization to Adjust Operator's Value of K_2 before Calculating W/cm in "High Power" Reference Regions of Core:

- 1) Σ of RGT readings x 115.6 x 188 km = 3566 Mwt
- 2) $\frac{3500 \text{ Mwt}}{3566} \times 115.5 = 115.5 = 113.5 = \text{normalized } K_2$
- 3) Computation of max power = 1.69 x 113.5 = 193.1 W/cm
 Error in max LHGR arising from inclusion of poisoned part of core in normalization = $\frac{193.1 - 195.5}{195.5} = 1.7 \text{ percent}$

NB! Error if not "normalized" = $\frac{115.6 - 115.5}{115.5} = +0.1 \text{ percent}$

This type of error can be avoided with RGTs since the RGT signals can be used directly, without normalization, to indicate local power.

A fourth EdF/CEA theoretical effort has been to determine the inaccuracies resulting from transients in local power and how easily the raw signals could be "deconvoluted" by analog or digital means to minimize the effects of delayed fission product gammas.

The present topical report does not deal quantitatively with uncertainties during transients for RGT systems because this is an NSSS system-specific and computer-specific matter that will be dealt with in forthcoming topical reports. Nonetheless, this report contains a status report on signal deconvolution and the state-of-the-art regarding attacks on the time-domain uncertainties, σ_4 , without defining the signal processing methods which will be presented and defended in subsequent system-specific (plant generic) topical reports. Both analog and digital processes for deconvoluting the delayed fission-product gamma signal exist and are being evaluated.

3.2.1.1.1 Specificity of Signal

Of first concern to EdF physicists was the specificity of signal. Would heating in gamma sensors be from sources so wide spread as to render the reading non-local? CEA theoreticians approached this problem for a 17x17 PWR lattice (Figure 3.2-4) and arrived at the positive result that the sources of gamma signal were as specific as the sources of thermal neutron flux feeding the present instrument systems.

Table 3.2-1 reports information contained in a report given by M. Chabrillac at the Chattanooga meeting (11-12 October 1979) of the GTIG group, Reference 3-(6). Ninety-one and one-half percent of the gamma heating signal comes from the bundle within which the detector is located. In fact, sources within the first five rod rows (cells) contribute 80.9 percent of the gamma heating of the sensor. The total heating of the sensor itself, from neutron scattering and n, γ reactions, followed by self-absorption, comprises 6.8 percent of the sensor heating and is prompt.

The distribution of heat sources from the first and eighth pin rows is about the same as is indicated by Table 3.2-2 (which considers only gamma

rays from within the fuel rods). Table 3.2-2 also shows how well the simpler code MERCUR IV reproduces results from the complex code TRIPOLI (see Section 3.2.1.3 for code descriptions and References 3-(46) and 3-(47).

A series of calculations were made to decide if the 11 gamma energy groups in use (matrix of j's) were adequate to describe the contribution of the gamma rays having energies less than 500 KeV, i.e.:

<u>j</u>	<u>MeV Range</u>
1	8.5 - 7.5
2	7.5 - 6.5
3	6.5 - 5.5
4	5.5 - 4.5
5	4.5 - 3.5
6	3.5 - 2.75
7	2.75 - 2.25
8	2.25 - 1.75
9	1.75 - 1.25
10	1.25 - 0.75
11	0.75 - 0.5

To do this the energy region between 500 KeV was twice again subdivided in TRIPOLI and reference cases rerun with nearly identical results (difference = 0.43 percent).

3.2.1.1.2 Total Composition of Signal

Having tested the computational tool in various ways, CEA computed total composition of the signal in the base or reference case (i.e., no control rods, equilibrium fission product, high boron (low exposure)) as follows:

gamma from fissions	35.4 percent	
decay gamma from fission products	32.6 percent	{ 22.8 percent prompt 9.8 percent delayed

gamma from n capture in U_{238}	15.8 percent
gamma from n capture in U_{235}	5.6 percent
gamma from n capture in cladding	1.85 percent
gamma from n capture in borated H_2O	1.85 percent
gamma heating from n, γ in sensor	6.8 percent*

Of this total heating source only 9.8 percent could be called delayed relative to the 18 second response time of the signal.

3.2.1.1.3 Relationship of Sensor Heating to Fuel Power

When the average power within a 17x17 assembly was input as 178 W/cm (the average LHGR for Bugey 5), the heating from external gamma in the RGT sensor was computed to be 1.43 W/g with an additional .11 W/g arising from self-shielding of gammas produced by n, γ reactions within the sensor (1.54 W/g total).

This prediction has been confirmed so far to a accuracy of ± 6.5 percent for the 18 sensors installed in Bugey 5 on June 12, 1979 (see Section 3.4.1).

Equally important to the ultimate predictive validity are many of the differential effects which now can be analysed by the CEA tools. The most severe distortion of K_2 could be produced by inserting control rods directly into the assembly in which the RGT was installed. In fact, control rods are not used in any high power regions of the PWR core, being inserted only slightly at full power.

The effect of a control rod in the region of the sensor would be to lower K_2 by 12 percent. If the rod tips are more than 10 cm above a given sensor there is negligible effect on K_2 . If one used the fixed K_2 of

*The small contributions of direct heating from fast neutron scattering in the sensor and from low energy gammas originating from neutron capture in fission products are prompt and can be considered lumped into the 6.8 percent, although they were not separately calculated.

the straight-through system (115.6), power would be underestimated in rodded areas by 12 percent. However, since the real power in rodded areas is suppressed to 52 percent of that in surrounding, unrodded fuel the underestimate is of no consequence except if attempting to normalize, as discussed above. Local power limits do not occur in fuel in which control rods are embedded.

The next condition calculated was the inclusion of 15 rods of burnable poison. This lowered K_2 by 7.8 percent relative to an unpoisoned bundle of equal power, (i.e., raised sensor heating). This would lead to a conservative overestimate of local power by +7.8 percent in poisoned bundles by the straight-through signal interpretation system.

EdF reactors may use "grey" control rods. These raise the sensor heat rate by 1.9 percent (i.e., lower the value of K_2 which should be used). Again the overestimate of local power which would occur in the straight-through system is of no consequence because the actual power of fuel in the area is suppressed.

The effects of long fuel exposure upon K_2 are negative and variable as shown in Figure 3.2-8. At 8500 MWd/t, K_2 goes down a maximum of 1.7 percent, and is down by 1.2 percent at 20,000 MWd/t. However, the effect is more than offset by boron reduction in the water, the from which contributes 1.85 percent of the signal early in core life. The reduction in boron concentration is itself partly off set by increasing contribution of n, γ reactions in fission products.

3.2.1.2 Heat Rate of Gamma Thermometers During Non-Steady State Operation - CEA Studies

After a change of power in either direction, a portion of the heating in gamma thermometers is delayed while fission product gamma emission reaches an equilibrium state for the new condition.

As shown earlier, 32.6 percent of the heating is caused by fission product gamma, much of which may be considered prompt relative to the 18 second time constant of the instrument.

The delay in heat generation in the instrument after restoration of initial conditions is a function of the time for which non-equilibrium conditions have persisted. For example, Figure 3.2-5 shows a power event in which real power is reduced to 54 percent and restored over a period of 30 minutes.

At the root of the power transient, the gamma thermometer heating is +18 percent higher than it will eventually be. At the instant of reestablishment of full power, the heat rate from the gamma thermometer is 4 percent lower than its equilibrium heating rate (which is reached about 1/2 hour later).

The sensor heat rate excess immediately following a local power reduction produces a conservative "measure" of local power.

The short-time sensor heat rate deficit following an increase in local power is a function of:

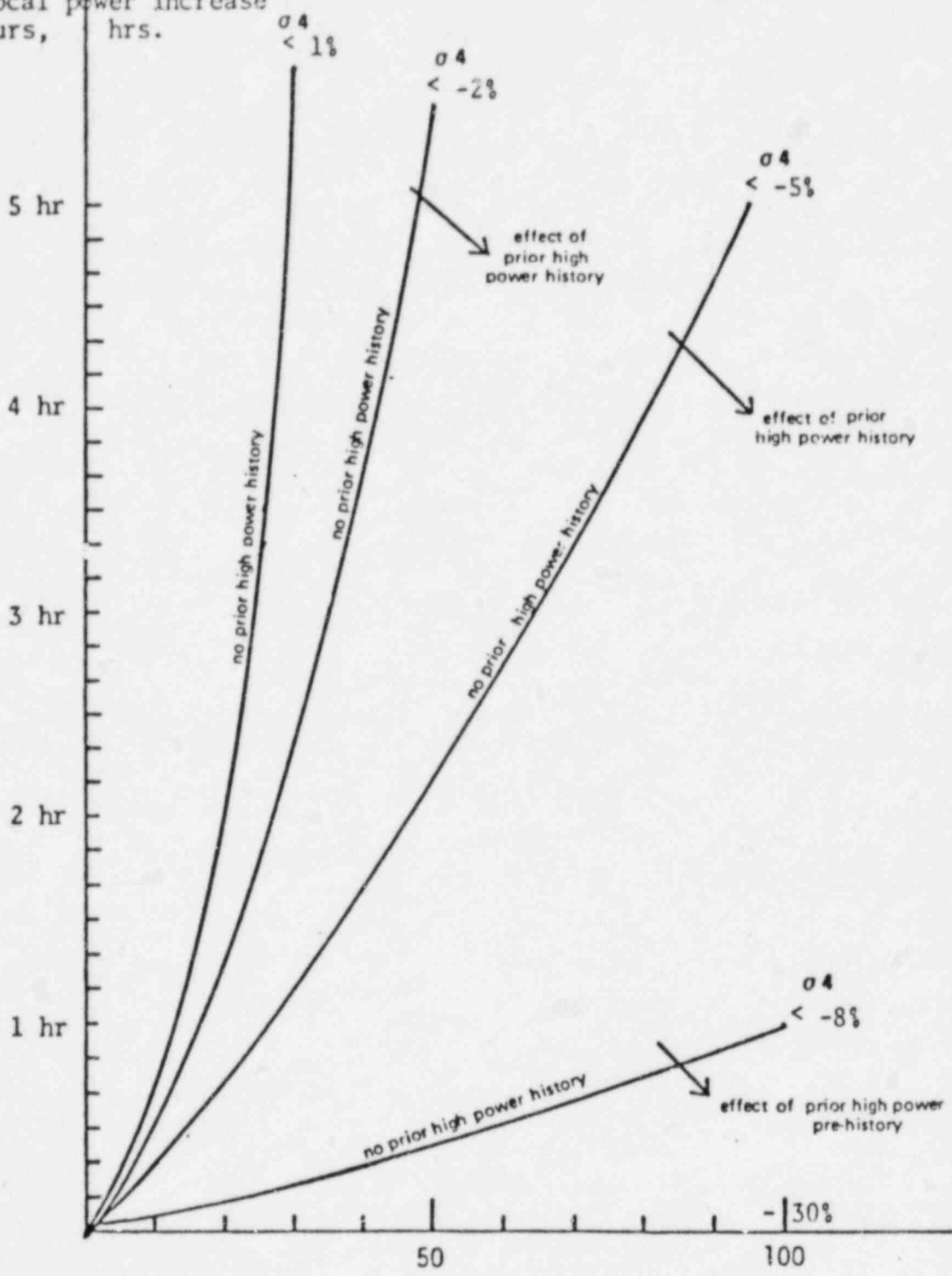
- time over which the increase occurred (ramp rate).
- time during which the fuel around the sensor had been at a lower power. If the lower power had been sustained long enough for fission product gamma equilibrium to exist, then the contribution of historical fission product γ is nil and the error is maximum.
- the magnitude of the increase in power.

The uncertainty associated with direct use of a gamma thermometer signal during or after a power change is referred to by the applicants as σ_4 .

"Deconvolution" of transient signals consists principally of inserting into the data processing circuits a false (positive or negative) signal which fades away in proportion to the time elapsed since a power change event. Deconvolution methods are being investigated (for cost/benefit) along several lines including both analog and digital signal processing.

Time during which
a local power increase
occurs, hrs.

Instantaneous signal (W/g) deficit following
events in which power is increased



% of full (100%) power increase during the Event

The σ_4 situation without deconvolution can be depicted qualitatively by the following diagram showing line of constant signal deficit after a power increase as a function of size of the variance, and time during which it took place.

The pictorial description of a complete matrix of such deficits would require that such functions be developed for a number of starting powers, with each such deficit map having subsidiary "maps" lowering the "iso-deficit" curves, to account for any recent high power history preceding the lower start point power.

The "straight-through" line of signal processing depicted earlier in Section 3.2 will be subject to such deficits in local power indication after local power increases of the approximate characteristics depicted in the figure.

For most variations in local power occurring in a base-loaded PWR plant, the dynamic reduction in accuracy of the straight-through signal processing line is not great. Drifts in local power due to xenon redistribution, for example, fall well within the < 1 percent deficit line. Increases resulting from boron dilution would be equally well tracked.

To quickly administer local power limits in the vicinities of control rod withdrawals, however, some form of signal deconvolution will be applied in the "plant-accuracy" line of signal processing.

In Figure 3.2-6 is depicted a theoretically "clean" case, in which real power is raised instantaneously from 0 to 100 percent. The sensor heating instantly reaches 65 percent of its equilibrium value (since this computation does not include n, γ in the sensor itself which is prompt, the "instant" signal is actually 72 percent of the equilibrium value).

In the case depicted, unlike that in Figure 3.2-5, there is no residual fission product gamma to contribute to the heat rates. In six minutes, 84 percent of signal is present and in 12 minutes 86 percent. About 30 hours after this the heat rate is within 1 percent of its final equilibrium.

A third type of transient is depicted in Figure 3.2-7 in which power is reduced to 30 percent in 1/2 hour, held for eight hours, and restored in a 1/2 hour period. In this case fission products are contributing an extra 21 percent to signal when the lowest power is reached at -23.5 hours, and γ sensor heating is at 93 percent of equilibrium when full power is again reached at -15 hours (a 7 percent underestimate of local power in the absence of dynamic correction or normalization to thermal power). The signal deficit drops to 3.5 percent in 20 minutes.

The discussion in this section has been included to give a general picture of the magnitude and direction by which gamma thermometer signals lag local fuel power under dynamic circumstances.

For this topical report review, however, the staff is asked to examine only the questions of inherent uncertainties in the knowledge of the ratios K_1 (heating in sensor to signal from sensor) and K_2 (heating in fuel to heating in sensor) with the hypothesis that fuel power is not varying dynamically. The time domain uncertainty, σ_4 , is recognized, however, and will be treated in later NSSS system-specific topical reports in relationship to the particular signal deconvolution methods selected.

3.3 Completed Programs Demonstrating the Accuracy of Gamma Thermometry

An underlying problem in experimentally demonstrating in an LWR the precision of any new local power measuring device, such as the gamma thermometer, is that the local powers in light water reactors measured by the presently installed reference systems are dependent upon highly corrected and normalized readings from various neutron flux measuring devices in which the accumulated signal corrections often exceed the signals themselves (Appendix I).

In the matter of experimental demonstration of instrument accuracy, the heavy water moderated and cooled reactors are superior to either PWRs or BWRs for one main reason: The fuel elements are separated and susceptible to very accurate measurement of both coolant flow and coolant temperature rise, thereby providing an accurate and independent calorimetric measure of individual fuel element thermal power. At the Savannah River Plant, for example, the coolant flow through every fuel assembly is measured by pre-calibrated end fitting orifices to $\pm 1/2$ percent. The 40 °C temperature rise of the coolant is measured to within $\pm 1/4$ °C by the average of four thermocouples measuring every channel outlet stream. Thus, SRP engineers have the capability to directly measure fuel element power while LWR operators must use complex physics codes combined with very indirect measurements.

The gamma thermometers are empirically conceived and proven instruments. Until recently (see Section 3.2.1) the question of calculating accurately how much heat is developed in a stainless steel part as a consequence of fission in adjoining fuel rods had not been necessary to address theoretically. Both SRP and HBWR engineers, having the "luxury" of accurately measured individual fuel element powers, could simply set the sum of four or five gamma thermometer signals equal to measured channel power at the start of a cycle and wait to see what happened. Actually, nothing happened. The sum of the four or five gamma thermometer signals has shown the same relationship to local fuel powers at cycle end that it had at the start (the gamma thermometer calibration process at HBWR is

explained in Section 3.3.2). Calibration is more complicated and less accurate at Halden than at SRP for two reasons:

- 1) The fuel load is very heterogeneous and large fractions of the gamma thermometer signals come from very dissimilar fuel assemblies.
- 2) The instrumented channel must be converted from boiling to non-boiling to measure thermal power during gamma thermometer calibration.

The estimated calibration accuracy at HBWR is ± 3 percent and at SRP $\pm 3/4$ percent.

Unlike the D_2O reactors, where the proof of gamma thermometer accuracy can be made directly and empirically, in LWRs any new instrument must be calibrated against the existing neutron-sensitive devices. There have been a few special experiments constructed for LWRs that provide proof that unprocessed gamma thermometer signals are more representative of local fuel power than existing neutron flux-to-LHGR constructs. One of these is the Otto Hahn work reported in Section 3.3.3. Another is the comparison of post irradiation gamma scan to the signals from travelling fission chambers and travelling gamma detectors at Hatch reported in Section 3.3.4.

3.3.1 Savannah River Plant, SRP, Experience

During the 1950's and early 60's, all work at SRP was classified, militarily, and virtually no publications relating to operating experience entered the open literature. Even in 1961, Reference 3-(2) and in 1968, Reference 3-(4), publications were carefully edited to avoid disclosures of protected information. Thus, though summary statements such as those by Stutheit, Reference 3-(4), could be made, the highly qualified data which would back such conclusions were largely omitted:

"-- long life with constant sensitivity

- rugged, simple, economical
- satisfactory operating experience
- γ t's achieve optimum fuel burnup and preclude hot spots
- produce strong signal without power supply
- gamma flux is proportional to local power generation
- gamma flux is at 90 percent of its final value in 100 seconds
- for protection, a fast γ t can operate safety circuits".

At SRP, some of the 61 instrument positions in five reactors can be equipped with rods containing seven equally spaced gamma thermometers and a thimble for a travelling wire monitor. These aluminum instrument rods are replaced every three to five years in a preventive maintenance program aimed at minimizing effects of aluminum component damage (corrosion, vibration).

The SRP gamma thermometer design was described in Section 1, Figure 1-2. Since introduction of this design in about 1962, nearly 3000 gamma thermometers have been used with a premature failure rate of about 3 percent, Reference 1-(4). The preceding paragraphs explained that at SRP individual fuel powers are measured to accuracies of $\pm 3/4$ percent, calorimetrically. The super-position of travelling wire axial thermal neutron flux traces, with the real time gamma thermometer signals allow accurate measurements of LHGR in the fuel assemblies.

Individual SRP gamma thermometers are calibrated as-made by the plunge test method (Section 3.1.2) and are required, for acceptance, to exhibit response times (τ s) within a ± 3 percent band (1σ) of the median (18 seconds). While RGT manufacturing acceptance criteria have not yet been set, EdF prototype instruments have exhibited sensitivities within a 1σ band of ± 4 percent and exhibit τ s of 17 seconds.

SRP technical staff, Reference 1-(4), have advised the applicants that, although sensor reproducibility (i.e., of τ) better than ± 3 percent appeared achievable, such a requirement was not considered to be economically expedient in view of the operational scheme. At installation, all SRP gamma thermometer signals are biased (within the ± 3 percent band) to

produce signals which can be converted directly to local fuel powers. During the short plutonium production cycles, the signals are closely proportional to the thermal neutron fluxes measured by travelling wires. Re-biasing is not required for the instruments and they are used to automatically initiate control rod reversal should local core power limits be approached (minimum burnout safety factor, maximum LHGR, etc.).

In the much longer (higher burnup) tritium production cycles, thermal neutron flux departs substantially from its original proportionality to power in the fuel, rising the most in the highest burnup portions of the core. Gamma thermometers continue to accurately report local fuel power, independent of fuel burnup status, while travelling wire neutron flux determinations converted to local power become progressively less accurate.

The most LWR pertinent case reported to the applicarts during the investigation of SRP gamma thermometer performance was a year-long high-flux irradiation, producing Californium, during which the gamma thermometers were exposed to a fast neutron fluence of 1×10^{22} nvt (a fast neutron dosage equivalent to five calendar years of PWR exposure). During the period the driver fuel element powers were "determined" in four ways:

- 1) The basic calorimetric determination ($WC_p \Delta T$) enabled by channel flow and temperature instrumentation at SRP; $\sigma = (\pm 3/4 \text{ percent}) : P_1$
- 2) The pure calculational determination from neutron physics codes with no correction from travelling wires: P_2
- 3) Physics calculations of power adjusted to fit thermal neutron flux wire traces of Φ_n : P_3 (this is a typical LWR procedure).
- 4) Direct readings (summed) from gamma thermometers using the start of cycle constant, $C_\gamma = \frac{P_1}{\Sigma GT \text{ signals}} : P_4$

All methods were normalized to fuel element power P_1 at cycle start:

Ratio to P_1	Start of Cycle	End of Cycle
P_2/P_1	1.00	1.40 "pure" calculation
P_3/P_1	1.00	1.25 neutron flux "measured"
P_4/P_1	1.00	1.02 gamma thermometer measured

These were the averaged results for a group of fuel elements, individually monitored and calculated. Variances for individual fuel assemblies were not given but were reported to be small.

During this period the highly enriched fuel was about 35 percent depleted (i.e., thermal neutron flux doubled at constant power). This corresponds to very high LWR fuel exposures with no significant change in the ratio of fission power to gamma sensor heating, K_2 .

The results agree with CEA theoretical studies (Section 3.2.1.1) for PWR (Westinghouse) lattices with codes MERCUR IV and TRIPOLI. These indicate similarly that in spite of shifts in fission spectra and build-in of fission product gamma emitters, the heating rate in a stainless steel gamma thermometer sensor per unit of LHGR in nearby fuel, K_2 , remains essentially constant, (i.e., within 0.7 percent) during fuel lifetime. This constancy is more pronounced for heat production by gamma absorption than for beta current production from miniature ion chambers such as those used for power distribution measurement in Hatch Nuclear Unit I, because gamma ion chambers pick out photons above certain threshold values in energy, while gamma thermometers respond to the entire spectrum.

The stability and reliability of gamma thermometers at SRP was discussed in Section 1.2 of the Introduction. Figures 3.3-1 and 3.3-2 show results reported by Nelson, Reference 3-(4) for early SRP gamma thermometers. Note that in Figure 3.3-1 the prompt heating transient measured after a power step agrees very well with that computed for the LWR lattice by CEA (Section 3.2.1.1).

Figure 3.3-2 shows the level at which thermal radiation losses begin to make the gamma thermometer response non-linear as sensor temperature rises (i.e., $\sim 480^\circ\text{C}$). Linearity is a desirable, but not necessary, characteristic and RGT designers decided that an average signal ΔT of 40°C (sensor temperature $\sim 365^\circ\text{C}$) was sufficient. (The SRP sink temperature was about 80°C and they were reading a signal of 400°C .) Electrical calibration results of RGTs exhibit almost perfect linearity over the working range with correlation coefficient greater than 0.999.

Note also from the SRP data points that the scatter in data is actually around two "best-fit" lines (one for each sensor) and that the difference between these lines is a measure of the variation in indicated sensitivity of the two sensors including thermocouple calibration difference. There are several factors that are important when examining these data:

- This is the early type instrument of Figure 1-1. Because no difference thermocouple is employed, scatter can be introduced by the measurement and subtraction of sink temperature.
- The requirement for inter-sensor sensitivity agreement has been ± 3 percent on τ (time constant) since the newer design of Figure 1-2 was developed at SRP. As was pointed out earlier, τ measures real sensitivity, S_i . With direct current calibration (as opposed to response time) RGT sensors display a standard deviation between mean (best fit) sensitivities (S_i) of 4 percent and the standard deviation of calibration data points for a given sensor is 0.9 percent. SRP has not (openly) published data like that of Figure 3.3-2 for newer gamma thermometers.
- The choice of axes in Figure 3.3-2 carries with it an inherent problem. Neutron flux (a very difficult quantity to measure accurately) is plotted on the abscissa. How much of the point scatter is due to inaccuracies in the X value of data points? (The Otto Hahn data in Section 3.3.3 suggest that neutron flux measurements with LSPNDs scatter more widely than gamma thermometer measurements when total reactor power is varied.)

Only when SRP sums all seven gamma thermometers in a string to compute adjacent fuel channel power (which is comparable to accurately measured fuel assembly thermal power), can the uncertainty associated with neutron flux measurement be eliminated. In the case depicted in Figure 3.3-2, the axial isolation of γ ts makes this type of calibration impossible.

3.3.2 HBWR, Halden Reactor, Experience

The history of application of gamma thermometers at Halden was presented in Section 1.2, and the standard design shown in Figure 1-3. The theoretical treatments upon which actual design features (gap, length, fill gas, materials) were selected in 1963 are treated by Asphaug in Reference 1-(2).

Table 3.3-1 is a record of instruments installed at Halden and shows that through 1978 a total of 226 gamma thermometers had been used in-core.

Figure 3.3-3 shows the performance record of various sorts of instruments in use at Halden, classified by year, type of fault (electric or mechanical) and whether the failure was indicated by absence of signal or faulty signal. The best performance (i.e., the lowest in-reactor failure rate) is from low temperature thermocouples and has been consistent for four years at five percent. These thermocouples are mostly 1 mm inconel jacketed, supplied by SODERN. All thermocouples are exposed throughout their core length to 230°C, 30 atmosphere heavy water. The thermocouples being reported upon have had an average exposure of three years with a σ on exposure time of two years.

The category "flux thermometers" in the table includes not only the standard gamma thermometer, but a like number of experimental instruments (neutron flux thermometers, special gamma thermometers, etc., tested since 1964), and shows a failure rate in the whole category of 7.5 percent. For standard gamma thermometers, with water-exposed thermocouple cables, the rate of failure has been about 5 percent with exposure lifetimes of about three years.

The RGT gamma thermometer (Figure 1-4) employs a configuration in which the thermocouple sheaths are entirely dry and much lower failure rates are thus anticipated (moisture in cables has been the most frequent cause of both thermocouple and gamma thermometer failure at Halden, accounting for at least half of the failures for which a cause has been determined). Thus, a projected premature failure frequency for RGTs of 2-1/2 percent is considered realistic.*

Some 220 self-powered neutron detectors have been used at Halden. They have exhibited a premature failure frequency of 13.5 percent.

HBWR engineers have published a number of papers describing use and performance of gamma thermometers at Halden where, due to the open lattice and heterogeneity of the fuel load, the sources of signal for a detector in a given fuel assembly lack the specificity characteristic of SRP or LWR applications. Asphaug, Reference 1-(2), showed the various HBWR fuel configurations under consideration at that time, see Figure 3.3-4. Since that time, corrections for lack of specificity have been even greater because many single-rod fuel assemblies have been tested. In these cases less than 20 percent of the gamma thermometer signal comes from the source being "measured" and frequent recalibrations are required as the assemblies in the adjoining lattice positions are shifted, control rods inserted, etc. The lack-of-specificity problem affects both gamma thermometer and SPND power measurements at Halden. Various tests have indicated that SPNDs require somewhat smaller corrections for the surrounding environment than do gamma thermometers. (The problem, unique to HBWR, perhaps explains why HBWR staff did not recognize the value of gamma thermometers for use in LWRs.)

* The importance of individually failed RGT sensors is related to the number and location of sensors in an assembly. The EdF program has included an analysis of the errors introduced in axial power shape determinations by the failure of one or more sensors as a function of the number originally installed. This work is reported briefly in Section 3.4.2, but is primarily related to the uncertainty of σ_3 (the extrapolation uncertainty) which will be reported subsequently.

Figure 3.3-5 shows the effect of nearby control rods on the relationship between the sum of three gamma thermometer readings and the calorimetrically determined assembly power. The calibration slope changes by about 20 percent. For a PWR lattice, where the signal specificity is much greater, this effect is smaller: CEA has shown a 12 percent increase in signal when control rods are in the instrument assembly.

Figure 3.3-6 shows a comparison between fast flux taken from a wire after shutdown and gamma thermometer readings at the locations shown.

The depression in power which would have been calculated from the fast neutron flux wire previously used is obviously not real. The fuel rods in IFA-3 and 4 had been deliberately misplaced (lifted a few cm) to show the high specificity of gamma thermometer signal.

Halden publications through the years 1964 to 1974 dealt extensively with reliability and specificity. Svanholm, in 1967, Reference 3-(7), related the variety of gamma thermometers which had been tested at Halden. Figures 3.3-7, 3.3-8, 3-3.9 and 3.3-10 show these. Svanholm described the relationship between time response and real sensitivity, i.e.:

$$S_{\text{real}} = \frac{\Delta T_{\text{real}}}{q \text{ (heat rate)}} = \frac{\tau}{C_p \text{ (specific heat)}}$$

Svanholm did not, however, deal with differences in thermocouple sensitivity, which affect S_i , but not S_r . He reported τ determinations for the various detector designs ranging from 46 to 104 seconds.

Regarding in-core gamma thermometer experience, Svanholm reported:

"Approximately eighty gamma thermometers of type B have been used to date and most of them have performed very well. The failure rate has been very low: one instrument has given indication of leakage, while three more have failed because of thermocouple failures."

In June 1974, Fordestrommen, of the HBWR staff, Reference 3-(8), proposed a hybrid instrument system for BWRs composed of gamma thermometers replacing the TIP system (for the LPRM function) and fast response neutron detector (for the APRM function). His paper was important because it summarized the surprisingly good accuracy results from Halden gamma thermometers, though they had been made with little attention to σ_1 , the uncertainty in K_1 , the ratio of signal to heat rate (this σ_1 has been reduced to low levels for RGT sensors):

"The gamma thermometer (GT) consists of a tube with heater, heat bridge and heat sink inside. The hot thermocouple is fixed in the heat bridge while the reference thermocouple is mounted in the heat sink near the outer surface of the tube. The heater is isolated by argon gas or vacuum. The electronics are very simple and rugged, giving a low resistance voltage signal about 3-5 mV. The time constant is approximately 20 sec., found experimentally. During a period of approximately eleven years, about 230 GT's in 95 different fuel assemblies have been used in-core. Of these, only 5 percent have failed, mainly because of fuel handling operations, like fuel rod exchange, and not due to any in-core irradiation damage effect. Average in-core time is about 10,000 MWd/tUO₂ and a maximum of 36,000 MWd/tUO₂."

"In order to test if the sensitivity of the GT is changing with irradiation time (for instance, due to thermocouple deterioration), the signals have been compared relative to the signals of self-powered Vanadium neutron detector, which is known to have a very small burnup rate. No change in the sensitivity* could be seen during a period of 2 years of irradiation, within an accuracy of ± 3 percent."

* The Halden engineers often mix two ratios when they refer to sensitivity. In RGT parlance the indicated sensitivity, S_1 , is the ratio of the output signal to the heat generation rate in the sensor, $(1/K_1)$, while K_2 is the ratio of local fuel power (W/cm) to heat generation in the RGT sensor.

"In order to see if the GT is giving a good description of the axial flux (power) profile, average signals over the last month of irradiation for a number of fuel assemblies have been compared to the gamma scan curves of the fuel rods obtained from post-irradiation examination (PIE). Eighteen IFAs have been examined, and the GTs had an average deviation from the gamma scan curve equal to ± 3 percent, and a maximum of ± 12 percent. This result becomes more impressive when one realizes that the GTs are used without any out-of-pile calibration, that is: one assumes all the GTs to be identical."

The assumption of identical sensitivity is one that the applicants do not choose to make. RGTs can be accurately calibrated out of pile either with electrical heating or plunge testing (Section 3.2.1). In-core recalibration of RGTs can be provided without use of a TIP system via in situ heaters (section 3.1.2.3).

Fordestrommen further reports on matters of specificity at HBWR, and alludes indirectly to the ability to account for the delayed fraction of the signal through deconvolution.

"The GT-signal is caused by two heat sources in the heater:
a) neutron flux absorption; b) gamma flux absorptions."

Their relative magnitude depends on the heater material and the specific reactor design. For the gamma thermometers in HBWR, the neutron absorption heat is roughly calculated to account for approximately 10 percent of the total GT-signal.*

The gamma radiation escaping the fuel rods originates from different physical processes, Table I below gives their relative importance in a typical power reactor, together with their approximate percentage contribution to the total GT-signal.

* For PWR 17x17 lattice the n, γ component is computed to be 6.8 percent.

PROCESS		GAMMA RADIATION (%)	GT-SIGNAL (%)
	Fission	28.8	~ 26
Prompt	Captured in U-235 and Pu (n, γ)	13.1	~ 12
Gammas	Captured in U-238 (n, γ)	16.7	~ 15
	Captured in structure and fission products (n, γ)	12.7	~ 11
Delayed Gammas	Gamma radiation from fission products	28.7	~ 26
Neutron Absorption		—	~ 10
		100.0	100.0

"Of the delayed gammas, only approximately 1/5 comes from radioactive gamma emitters with half-lives bigger than minutes in magnitude. Furthermore, of these, only a minor part has half-lives bigger than one year in magnitude. Therefore, it will be only a small build-up of constant gamma flux signal as burnup increases, about 1-2 percent of the total signal over the range of 1-30,000 MWd/tUO₂. These results are found by comparing GT- and ND-signals in fuel assemblies with different burnup during shutdown ramps and shutdown periods."

With respect to the appropriate reference point for in-core determination of the ratio of sensor heating to fission power, in particular, the remarks:

"New fuel assemblies in HBRW are usually calibrated before the build-up of fission products has reached equilibrium. The gamma flux will therefore continue to increase some time after the calibration work is finished. In this way, the GTs will show somewhat too high power. Theoretically, the error can be as big as 26 percent,* see table, but for actual cases in the HBRW, the error most probably does not exceed 10 percent, since the fuel is always irradiated some days before the calibration is performed. This assertion is supported by the PIE-results mentioned, and can also easily be checked in-core by performing a recalibration a few weeks after start-up."

* I.e., after an instant power rise, see Figure 3.2-6 for this value computed for a PWR by CEA. In the PWR such error is negligible after 100 hours. In any event, deconvolution will be applied in the plant-accuracy line of data processing.

3.3.3 The Otto Hahn Tests

This particular series of tests is valuable in that it permits direct comparison of the scatter in "measurement" of local power by SPND and gamma thermometer, and special devices such as the central oxide temperature thermocouples.

The Otto Hahn program of instrument calibration was a cooperation between GKSS (the German utility responsible for the Otto Hahn ship operation), and the Halden Project, which prepared instrumentation for a fuel assembly installed in the second cycle of the second core in August, 1976. The Otto Hahn core employs standard PWR type fuel pins at standard lattice pitches.

In addition to an assembly of four gamma thermometers of the Halden type B (Figure 3.3-8), a corner fuel assembly was equipped with the following additional instruments:

- 2 fission chambers (type I)
- 2 fission chambers (type W)
- 4 SPND detectors (Cobalt)
- 1 KWU Aeroball tube (Neutron flux detector)
- 2 Tungsten-Rhenium thermocouples (inside fuel pieces)

In the following paragraphs, the item on the Otto Hahn test results has been extracted from HPR-198 "OECD Halden Reactor Project Quarterly Progress Report, July to September, 1976 and is reproduced in its entirety, with clarifying footnotes introduced by the applicants.

Experiments with Gamma Thermometers in the NS "Otto Hahn" Reactor Core

Introduction

In cooperation between GKSS and the Halden Project, four of the Halden type gamma thermometers were installed in the core of the German nuclear powered ship "Otto Hahn" during its stay in Hamburg

for core reloading and general overhaul. During its subsequent commissioning runs, a series of measurements with the gamma thermometers were successfully performed. A brief introductory review of the experiments and results is given in the following.

Installation and Experiments

The four Halden type gamma thermometers were located in a corner assembly as shown in Figures P-1 and P-2, where also the location of other flux sensors are shown. Signals from the gamma thermometers and other flux sensors were measured together with thermal reactor power both during experiments in the Hamburg harbour, and during trial runs in the North Sea, during the period 8th to 24th August.

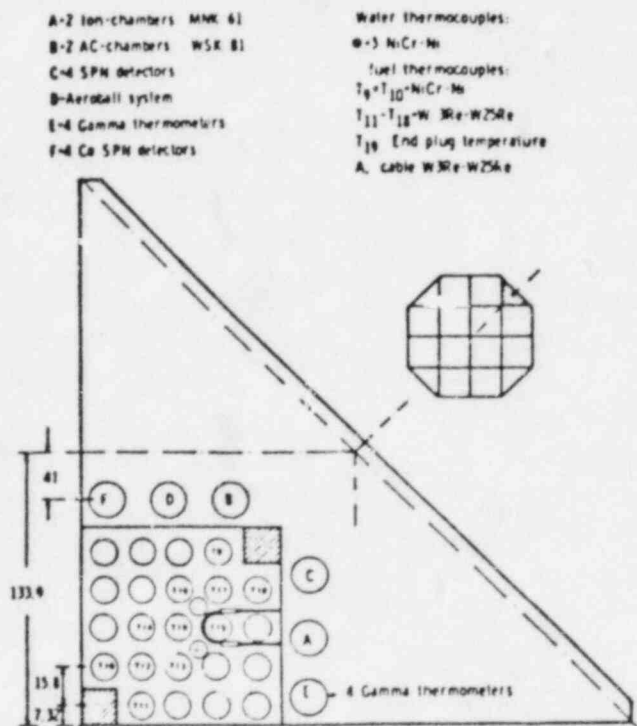


Fig. P-1. Instrumented corner assembly; NS "Otto Hahn" reactor

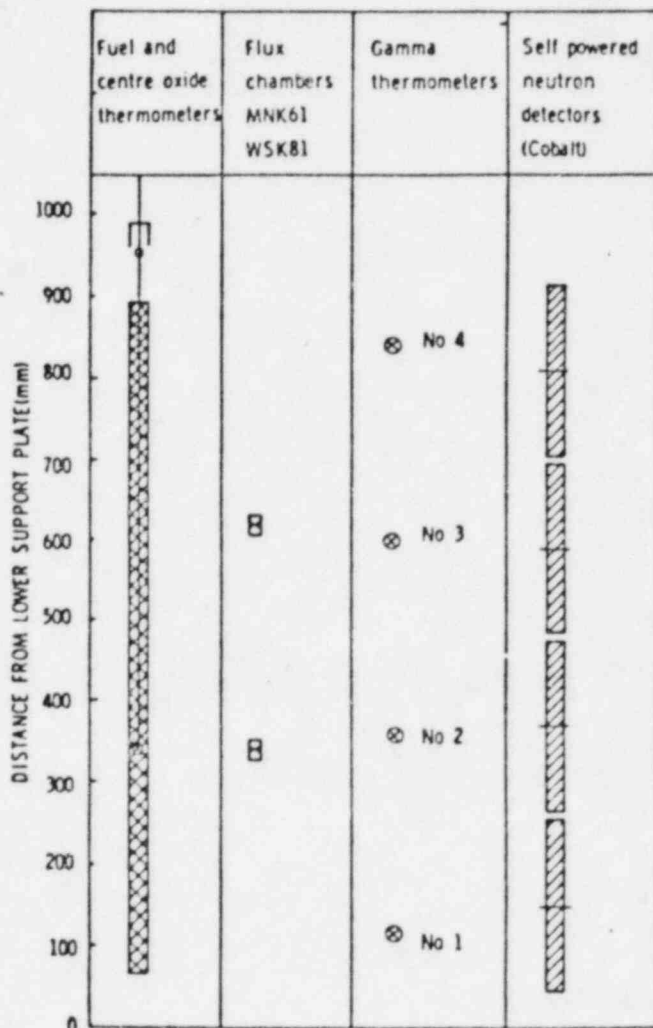


Fig. P-2. Vertical location of in-core instruments

Results and Evaluation

In order to evaluate the gamma thermometers, their signals were compared to those simultaneously obtained from self-powered neutron detectors (cobalt), fuel temperature measurements and reactor thermal power determinations.

In Figures P-3, P-4, and P-5, the reference signals are plotted versus the signals from gamma thermometer no. 2 (near the axial reactor flux maximum). Because of difficulties with the read-out systems during the period up to 16th August (half-way through the initial slow ramp up in power), only the measurements from 25 to 38 MW reactor power are considered reliable during this period.

Due to the working principle of the gamma thermometer, there is a slight non-linearity in the relation between heat rate and signal (1). This is due to the temperature dependence of the thermal conductivity of the instrument fill gas.

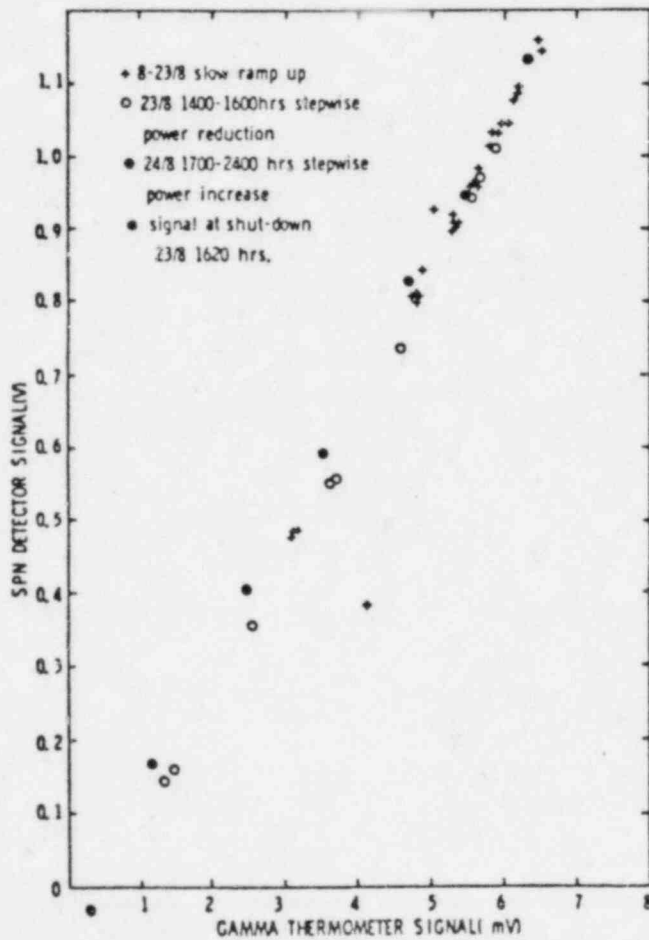


Fig. P-3. Cobalt detector signals vs. gamma thermometer signals

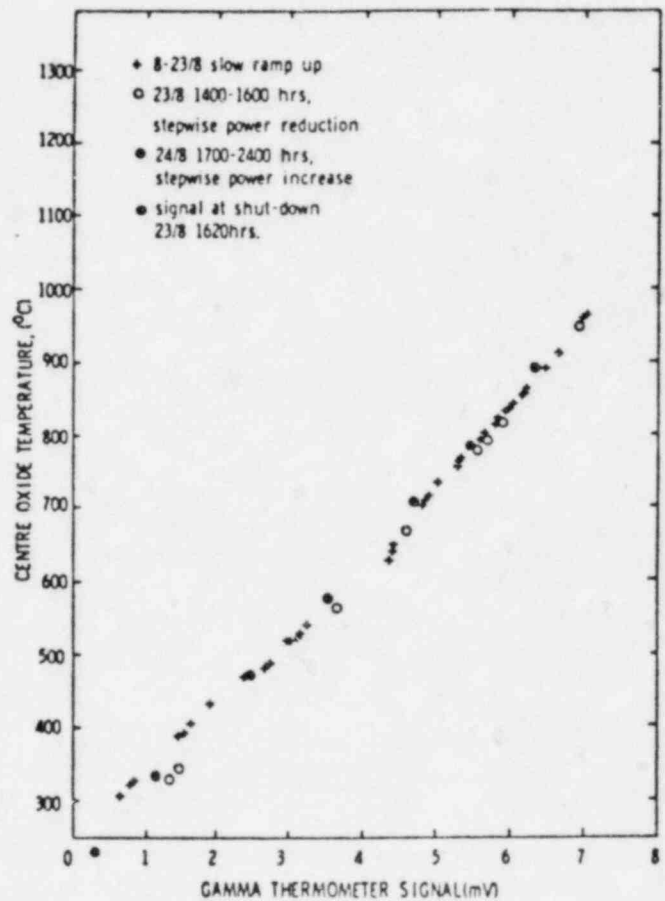


Fig. P-4. Centre fuel temperature vs. gamma thermometer signals

Figure P-6 shows the calculated heat rates versus instrument signal. The thermal conductance of the instruments was calculated from measurements of the thermal time constant prior to installation in the core (2).

Figures P-3 through P-5 show similar non-linearity as does the calculated heat rate in the gamma thermometer. This observation leads to two conclusions (3):

--the heat rate in the stainless steel heater of the gamma thermometer is proportional to reactor neutron flux and power, and

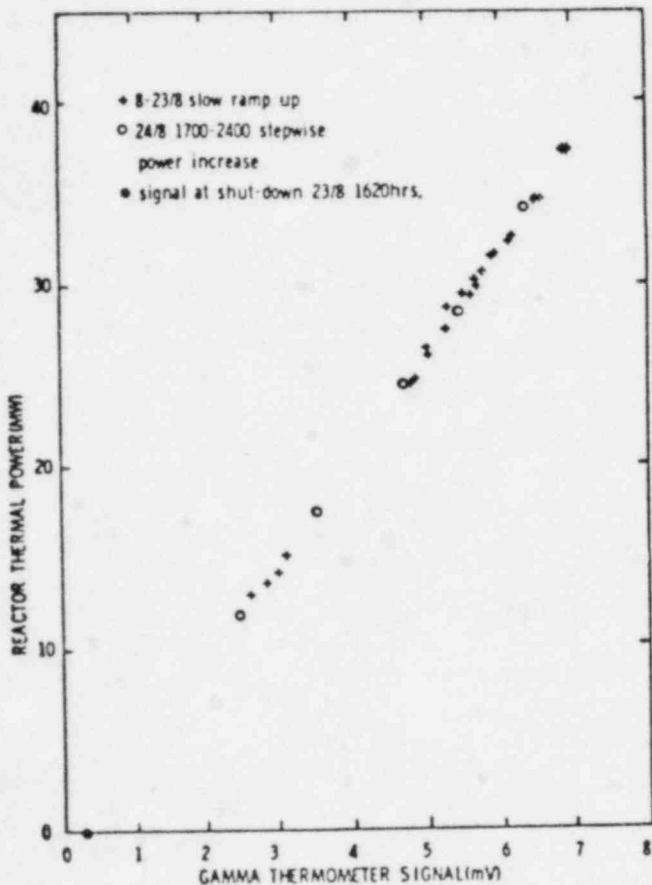


Fig. P-5. Thermal reactor power vs. gamma thermometer signals

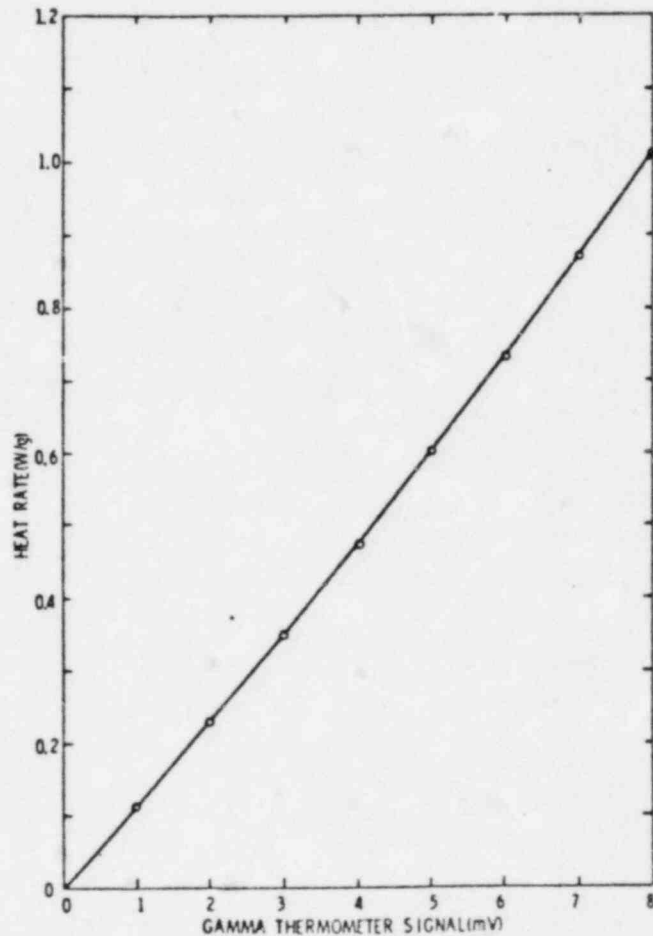


Fig. P-6. Heat rating in gamma thermometer as function of signal

--the heat transfer mechanism in the gamma thermometer is primarily conductive up to the temperatures experienced (340°C average, 425°C at heater), while convection and radiation are of negligible importance.

Axial Heat Rate Profile

The relative heat rates (normalized) in the gamma thermometers are plotted against their respective axial core positions in Figures P-7 and P-8. Since there were no other simultaneous measurements of axial flux distribution, the resulting heat rate profile cannot be directly verified, but the comparisons to aeroball profiles (2) measured at the end of the 1st cycle of the second core and to theoretically calculated profiles (3) show close agreement.

Gamma Thermometer Signal during Reactor Shutdown

Figure P-9 shows the signal from gamma thermometer no. 2 at shutdown of the reactor from ca. 8 MW to subcritical conditions. Figure P-10 shows the development of the signal in the following 24 hours. Most of this time, the reactor was kept at temperature by nuclear heat, but the periods at full shutdown provides information about the reactor decay heat generation rate, which can be expressed in terms of the gamma heating rate in stainless steel (4). Quantitative use of such information should be made with caution, as even small changes in the thermocouple calibration may distort the result.

Extrapolating the decay heat function back towards the moment of shutdown makes it possible (in Figure P-9) to estimate the time constant in the gamma thermometer signal. It is found to be about two minutes, as found in the tests prior to installation in the reactor.

Conclusions

The initial operational experience with the gamma thermometers in the "Otto Hahn" reactor has verified the characteristics of this instrument. The linearity and stability over short time periods were very good. The results make it possible to quantify the specific gamma heating rate in stainless steel in the core and to obtain data on the rate of decay heat generation. The tests also

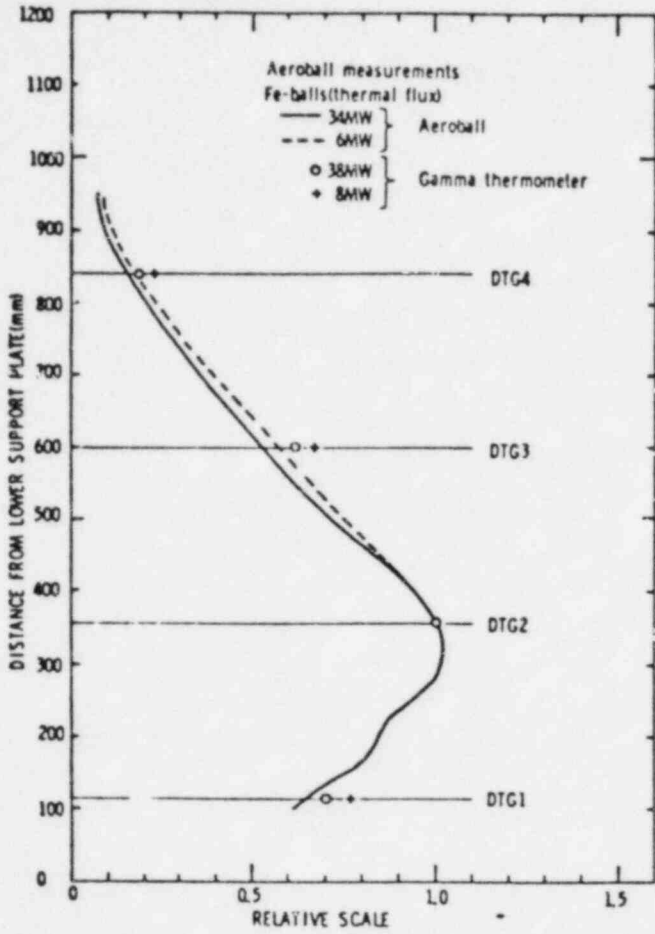


Fig. P-7. Axial thermal flux profile measured 9-11/2-74 compared to gamma thermometer signals

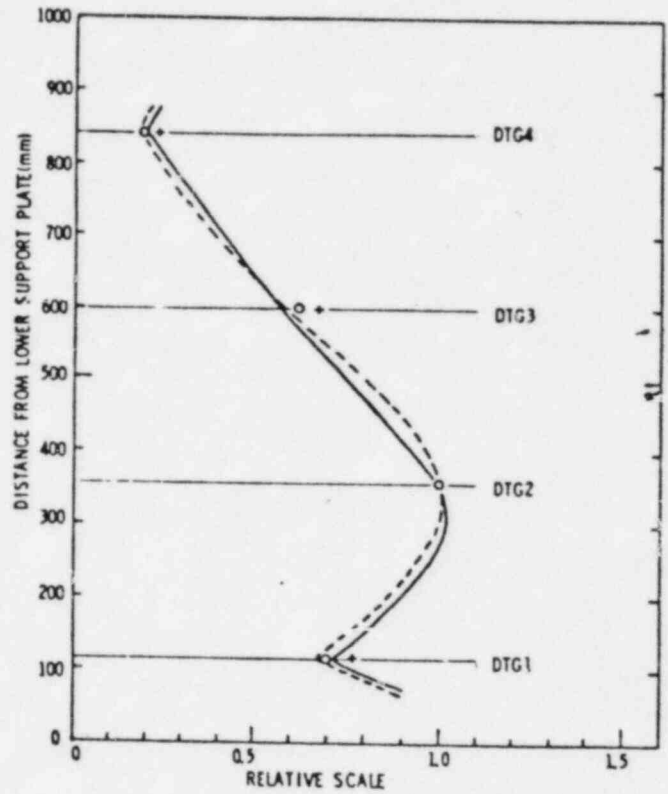


Fig. P-8. Comparison of gamma thermometer signals and calculated thermal flux profile

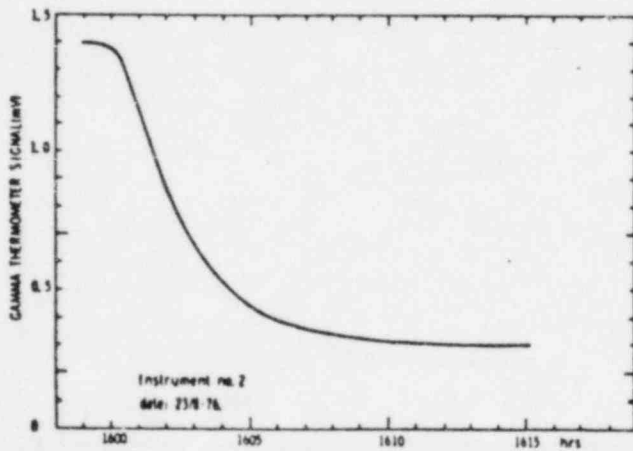


Fig. P-9. Gamma thermometer signal transient at reactor shutdown from ca. 8 MW

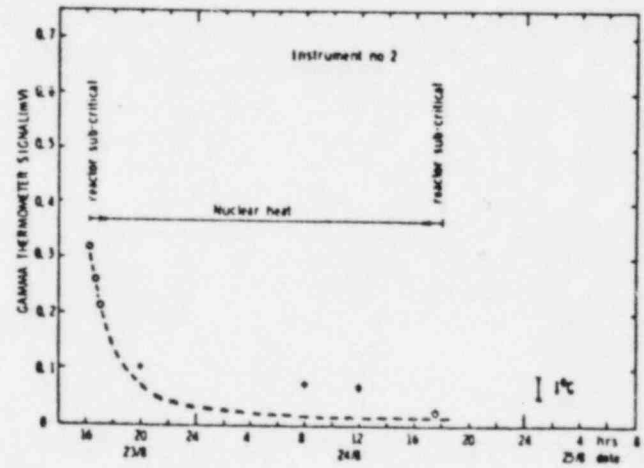


Fig. P-10. Gamma thermometer signal after shutdown

demonstrated the advantages of instruments not requiring complicated electronic amplifier systems for signal treatment.

Future Work

The overall design of the "Otto Hahn" reactor makes possible measurement of reactor thermal power with very good reproducibility. It is therefore recommended that measurements of gamma thermometer signals and reactor thermal power should be repeated at increasing burnup levels to assess the drift and/or decalibration of the instruments. (5)

* * * * *

COMMENTS OF THE APPLICANT

- (1) The non-linearity referred to is smaller for RGTs for several reasons: the signal selected is less (40°C for RGT vs 200°C indicated here); RGT uses difference thermocouples that virtually eliminate effects of sink temperature variations. The "curve" comparable to P-6 for RGT is given in Section 3.1.2.2 and the linear correlation coefficient is 0.9997.
- (2) Since, as explained in Section 3.1.1, the time constant method of calibration yields the real sensitivity, S_r , not the indicated sensitivity, S_i , some of the curvature of P-6 might be attributable to thermocouple signal non-linearity (this is not revealed by τ calibrations, but is revealed by direct electric calibration).
- (3) Although Figures P-3, P-4, and P-5 do exhibit the same degree of upward concavity as the gamma thermometer calibration curve, the next step in analysis of the data would be to present sensor heat rate (W/g) using the calibration curve of P-6 instead of the raw signal. This step would have eliminated the upward curvature and shown even more clearly the linear relationship between W/g and nuclear power.

There is a second important observation to be drawn by examination of P-3, P-4, and P-5, which all depict GT signal on the abscissa. Of the three experimental quantities depicted on the ordinates (i.e., SPND signal, central oxide temperature, and reactor thermal power, successively), the probable error resident in the Y coordinate of the data points is diminishing, (i.e., SPND signal (P-3) is least accurate, central oxide temperature moderately so, (P-4), and reactor thermal power is known to $\pm 1/2$ percent (P-5).

The variance of the data from the best fit lines is obviously, in P-3 and P-4, being produced by the Y coordinates of the data points, not the gamma thermometers. Both SPND signal and central oxide temperature are less accurate measures of power than the gamma thermometer.

P-5 data shows a σ of ~3 percent, P-4 of ~8 percent, and P-3 of ~16 percent. Thus, the error contribution of the gamma thermometer can be "determined" from P-5 as:

$$\sqrt{x^2 + (1/2 \text{ percent})^2} = 3 \text{ percent} \quad x = \sigma_{GT} = 2.96 \text{ percent}$$

and the scatter contributions of the signals to which the gamma thermometers are referred can be calculated, for P-4:

$$\sigma \text{ central temp.} = \sqrt{(8)^2 - (2.95)^2} \quad \sigma_{CT} = 7.4 \text{ percent}$$

and for P-5:

$$\sigma \text{ SPND} = \sqrt{10^2 - 2.95^2} \quad \sigma_{SPND} = 9.6 \text{ percent}$$

- (4) The decay curves of P-9 and P-10 are also of interest to RGT proponents in other ways (the heat generation rate in the sensor is predicted by the methods of 3.2.1). Of major interest is the readability of signal to levels below 50 micro-volts without interference by noise. This agrees with EdF observations in Bugey 5 that RGT signals are usable without noise disturbance at local fuel powers down to one percent of nominal. RGT difference thermocouples always give zero signal with zero sensor heat generation.
- (5) This recommendation is indeed being followed but (as is the rule for both SRP and HBWR) the distinction is not drawn between the two components governing the relationship between fuel power and gamma thermometer signal, i.e.,

Both K_1 and K_2 could conceivably change. The value of K_2 at any time and its associated uncertainty σ_2 are determined by benchmarking to the best available reference conditions and extrapolation by physics models. The value of K_1 and its associated uncertainty, σ_1 , is addressed by direct electrical calibration, ORNL irradiation tests, the various prototype programs and the in situ recalibration developments.

In RGT terminology the two uncertainties, σ_1 and σ_2 are referred to as the "sensitivity" and "coupling" uncertainties.

Given the size of the σ_1 involved in these tests, (i.e., +2.5 percent), the inference can be drawn that the total uncertainty in gamma thermometer measurement of power is 3 percent, and the inference can also be drawn that the variability in K_2 is limited to 1.7 percent over the range represented by these tests. If calibrated RGT sensors had been used ($\sigma_1 = 0.9$ percent when new) the value of combined uncertainty in GT measurement of power would have been:

$$\sigma_2 = \sqrt{(.91)^2 + (1.7)^2} = 1.93 \text{ percent}$$

3.3.4 EPRI/GE/Georgia Power Work at Hatch Nuclear Unit No. 1

The program carried out at Hatch Nuclear Unit No. 1 by GE and Georgia Power Company is documented by References 1-(6a), 1-(6b), 1-(6c), and 1-(6d), published by EPRI, and the summary of that work was quoted in the introduction (Section 1.2), to the effect that use of gamma ion chambers instead of fission chambers resulted in smaller uncertainties in local power determination when used in BWRs.

The use of gamma sensors in TIP systems has been initiated as a consequence of the work at Hatch. The neutron fission chambers in the TIP system have been entirely replaced by gamma sensitive chambers in the TIP systems at Hatch I, Duane Arnold, Muhleberg, and other GE plants. These actions have been undertaken, without reexamination of the plant licenses, under CFR-50.59, for operating plants.

The Hatch work was presented to NRC staff on September 23, 1977, Reference 3-(49). The work supports the applicants' position that gamma flux is a better measure of local fuel power distribution, with smaller ultimate uncertainty in local power distribution determination, than any system based upon measurements of neutron flux.

In being applied in the GE TIP systems, the gamma ion chamber becomes the fundamental source of information on local fuel power distribution to which the individual fixed fission chambers of the LPRM are repeatedly recalibrated.

The empirical evidence from the Hatch program establishes the superiority of measurement of gamma flux to measurement of neutron flux for local power determinations. Figure 3.3-12 is extracted from Reference 1-(6a) and shows the three TIP devices compared at Hatch 1.

The applicants have three main points to make in connection with the entire Hatch 1 program:

- a) It establishes the validity of the applicants' claim that gamma radiation is the proper parameter to "measure" if local fuel power is the objective.
- b) Because the work was done with a device whose sensitivity to the gamma flux is neither known nor calibratable before it is inserted into the reactor, the requirements for mechanically cumbersome processes of total and inter-sensor normalization are preserved intact after Hatch 1.
- c) It is considered unfortunate that in such an extensive and unique effort (one of the very few that is not totally dependent on existing neutron devices and calculations to calibrate new and better devices), the travelling gamma thermometer (called TRAVCAL by GTIG) was not included in the comparison among fast flux chamber, thermal flux chamber, and gamma ion chamber.

3.3.5 AEG/KWU Gamma Thermometer Evaluation at KWL (Lingen)

Description of Gamma Thermometer

The AEG gamma thermometer is shown in Figure 3.3-13. In principle, there is no difference in design between AEG's gamma thermometer and their neutron thermometers. In both cases, heat generated within a nickel encapsulated block is measured by two thermocouples connected to constitute a difference thermocouple.

When one of these devices is designed as a gamma thermometer, gamma radiation heats a solid nickel block (or a nickel encapsulated heavy metal block). To be used as a neutron thermometer, a piece of U^{235} is embedded in the nickel block.

The heat generated in the nickel block is conducted to the heat sink along a heat path made up of CrNi. An Inconel jacketed cable containing two nickel leads penetrates the detector housing and the leads are terminated, one on the nickel block and one on the inside of the nickel housing. The nickel leads together with the nickel housing constitute the nickel part of the thermocouple pair while the heat path constitutes the CrNi part. The hot junction is the interface between the nickel block and the heat path, while the cold junction is the heat path/bottom plug interface.

Testing of Detectors

The development program included irradiation in the test reactors at Seibersdorf and Kahl. During these tests the linearity and sensitivity of the detectors were established. For the gamma thermometers, a sensitivity of $2.5 \text{ mV}/10^9 \text{ R/h}$ was found.

A power plant program was undertaken by installing 28 detectors in the Lingen BWR plant. In that case, however, the detectors were used as neutron thermometers.

A decision was later taken within AEG to base the in-core instrumentation on miniature fission chambers. This decision stopped the further development and testing of the AEG gamma thermometer in the German reactors. Therefore, no data from full-scale operation of the gamma thermometers are available.

Ironically, the decision to use fission chambers reflected the poor experience with those devices rather than the good experience with gamma thermometers. It was assumed at that time that the gamma thermometer could not be made fast enough for APRM scram functions and for this reason a certain number of fission chambers would have to be used. Since fission chambers had a high failure rate it would be necessary to install at least twice as many as required for the APRM function if all were working. Thus, the unreliable fission chamber literally crowded the reliable gamma thermometer out of the in-core system.

3.4 GTIG-Related Programs Now Underway to Reduce RGT Uncertainties

3.4.1 The EdF Prototype Program

The EdF programs for RGT development, initiated in 1974, have been designed for careful documentation in every phase. For example, the bench tests carried out in 1974-76 by ScP/IFA at Kjeller, Norway, were documented by five reports covering: the manufacturing process for the specimens, the design of the test apparatus, the calibration results for the wet type, the calibration results for the dry type, the analysis of the results and recommendations. Not only the test reports were shipped to EdF, however; the test specimens themselves were transferred and the calibrations replicated and reported by EdF's Chatou Laboratories.

EdF's own program of pre-reactor calibration of RGTs is marked by replication, verification, and documentation.

The Electricite de France program is the earliest and so far largest of the efforts to convert from systems based on neutron detectors to systems based on fixed RGT gamma thermometers. The selected supplier, Intertechnique (Paris) has manufactured 12 full-length RADCAL assemblies 15 meters long, each containing nine sensors. Two of the first were employed in extensive mechanical compatibility testing (Cannes No. 1 and No. 2) (reported in Section 3.6) and enabled the development of both the low temperature (Intertechnique) electrical calibration loop and the high temperature electrical calibration loop at EdF's Renardieres Laboratories (Figures 3.4.2, 3.4.3).

Every one of the RGT assemblies (each containing nine sensors) is calibrated by the manufacturer, Intertechnique, at low coolant temperature and is accompanied by a detailed report documenting dimensions, properties, and calibration results on each chamber. The calibrations are repeated at Renardieres and are first performed at low temperature to verify the results from Intertechnique. Then every sensor is calibrated at temperatures and pressures corresponding to PWR operation (150 bar and 300°C).

Figure 3.4-4 illustrates data obtained at the Renardieres loop giving the sensor calibration for one sensor as a function of temperature. Data points are not visible because they are essentially perfect fits on the calibration lines. M. Guillery of EdF's R&D division reported in Reference 3-(13) linear correlation coefficients for the five sensors in Canne No. 2:

<u>Chamber</u>	<u>Correlation Coefficient, r</u>
1	0.99999
2	0.99998
3	0.99998
4	0.99997
5	0.99997

The agreement between Intertechnique calibrations at low temperature and Renardieres electrical calibrations at low temperature has been on the same order ($\sigma \sim 2$ percent) as the agreement between TEC and Intertechnique calibrations of specimens for the ORNL tests (see Table 3.4-3).

Results and statistics of the low temperature calibrations of cannes 3 through 12 are tabulated in Table 3.1-3, in which the total 1σ variation in sensitivity is 3.67 percent and the average scatter of calibration data around individual sensor mean lines is 0.5 percent (1σ).

Cannes No. 3 and 4 were installed in Bugey 5 on June 12, 1979, and the 18 sensors have been generating usable data since about September when the reactor reached power. The exact design of the EdF RGT assemblies and sensors is given by Figures 3.4-5 and 3.4-6. The nine sensors are 26.5 mm long and employ a nominal gas gap of 0.5 mm (fabrication reduces average gas gap to 0.4 mm). They employ ten difference thermocouples, nine of which are 1/2 mm in OD and surround a central 1 mm thermocouple with its two junctions at the top and the bottom of the active core, (measuring core ΔT).

Four more prototypes, cannes No. 5 through 8, were inserted into Tricastin 2 reactor in the summer of 1980. Four additional RGTA's, cannes Nos. 9 through 12, were installed in Tricastin 3 in October, where the effects of "grey" control rods will be measurable for comparison with CEA predictions. EdF alone is irradiating 90 sensors now.

Figure 3.4-7 shows the two RGTA locations in Bugey 5 and the corresponding symmetric TIP locations. These locations have been chosen to:

- have symmetrical positions to those used by movable fission chambers (TIP).
- insert into fuel assemblies with in-core fixed thermocouples measuring exit coolant temperature.

Figure 3.4-8 shows the locations of four RGTAs in Tricastin 2 and the symmetric TIPs. The effects on K_2 to be measured are:

- influence of control rods.
- influence of reflector.
- influence of enrichment.
- influence of burnable poisons.

Figure 3.4-9 shows locations for the four RGTAs in the Tricastin 3 core. The objectives here are to measure the effects on K_2 of grey control rods.

Results from the two RGTAs in Bugey 5 confirm the prediction of K_2 of CEA (115.6 W/cm of fuel per W/g of sensor heating) to an accuracy of ± 6.5 percent (1σ). Signals will be taken directly to the readout equipment without intervening amplifiers and accuracy of the confirmation of K_2 is expected to be somewhat improved.

Figure 3.4-10 shows "paired" signals from RGT sensors at the lower elevation (no. 1) in positions J10 and D5 in the Bugey 5 core as reactor

power varies over an 80 hour time period. They illustrate the tracking capability of the sensors during routine power variations and are simply excerpts showing raw data of the type being recorded at Bugey 5. Note that the scale is directly in W/g of sensor heating. (Thus, the average LHGRs at these positions, using a K_2 of 115.6, are 162 W/cm at J10 and 141 W/cm at D5.)

At the Oak Ridge meeting of GTIG, Reference 3-(14), EdF displayed traces made during xenon oscillations at 75 percent power. EdF pointed out that many more RGTs would be required to track simultaneous azimuthal and vertical oscillations but presented Figure 3.4-11 to show how the gross vertical oscillations computed from ex-core chambers and infrequent TIP traces compared to actual local power variations tracked by the RGTs. In this figure it is shown that the peak power in a 12 hour cycle is over-estimated using normal plant data compared to real time local data from the RGT.

Figure 3.4-12 shows that at time $t = 0$ the axial power trace reconstructed from nine RGT signals in position D5 agrees almost exactly with the TIP trace. At a later time, however, the axial distribution shows a shift which would not be detected by TIP readings taken once a month.

Figure 3.4-13 compares computed and observed RGT signals for the first four minutes after a reactor shutdown at Bugey 5 where fission product gamma keeps the signal up to 9 percent of its full power value while actual thermal power falls below 0.5 percent. The CEA model would have predicted a signal of 11 percent after four minutes in this case.

The Bugey 5 tests have also shown an almost non-existent signal noise with RGT signals being readable and proportional to power at levels as low as 1 percent of nominal reactor power (16 μ V signal). Reference 3-(42) gives a summary of Bugey 5 results to date. Reference 3-(43) compares RGT performance with that of other in-core systems (TIP, SPND, etc.).

The signals from all 90 prototype sensors have been analyzed by EdF. Comparing the gamma heating (W/gm) to the local nuclear power (W/CM) obtained from the TIP system, EdF found a very good correlation (this comparison is an evaluation of K_2).

The linearity of K_2 was found to be excellent with a $\sigma \leq 1.6$ percent and the origin intercept was within $\pm 2\sigma$. This considered all flux maps obtained so far by EdF, with no corrections made for transient or burn-up effects. These results are illustrated in Figures 3.4-14 through 3.4-22. These data are for an RGT string loaded in Assembly G-9 of Tricastin 3 and are for all flux maps obtained from 0 to 7,000 MWd/t burnup.

The ability of the RGT to accurately follow the core power during xenon transients is shown in Figures 3.4-23 through 3.4-25. These figures compare the RGT measurements to TIP measurements at three times during a xenon transient. Figures 3.4-26 and 3.4-27 show how the continuous RGT signals can be used to generate video graphic 3-D plots for tracking of xenon, or other, transients.

3.5 Programs Establishing Mechanical System Compatability, Handling Technique, Integrity of Pressure Boundary, Consequences and Modes of Failure

The RGTA looks from the outside exactly like the presently installed instrument. For Westinghouse PWRs, the jacket tube of the RGTA is the same outside diameter and wall thickness as the pressure thimble through which TIPs are inserted. In fact, Intertechnique, who makes RGTAs for EdF, uses pressure thimble tubes (purchased from Framatome) for the RGTA jackets.

For B&W pressurized water reactors, the present SPND array is shown inside its jacket tube in Figure 3.5-1. The seal location is shown in Figure 3.5-2 and a seal detail in Figure 3.5-3. The seal flange is defined as an element in the primary pressure boundary and is subject to Class I quality assurance and regulations under 10 CFR 50.51, Appendix B.

In the newest Westinghouse system the TIP tubes make only one bend as they are led from beneath the reactor to the seal flange array (Figure 3.5-4). The use of the solid RGT assembly to replace the dry TIP thimble tubes eliminates these 50 tubes as components of the primary pressure boundary, and eliminates the need for emergency isolation valves (and the complexity of the TIP drive system). The use of the essentially solid RGTA reduces the risk of leakage relative to that of the B&W SPND assembly.

CE has, in its System 80 plants, gone to bottom entry systems similar to those of B&W and Westinghouse. RGTA installation would also be similar.

The EdF mechanical compatability program is well advanced. Before insertion of the first two RGTAs in Bugey 5, the entire spectrum of handling and system compatability questions was dealt with.

3.5.1 EdF Mechanical and Torture Testing of RGT's

Thermal Cycling

The first prototype RGTA made by Intertechnique (canne No. 0) was three meters long. This was a successful extrapolation of the manufacturing process from the earlier, shorter, drawn specimens, containing two sensors, made by ScP/IFA. The specimen was cycled more than 50 times through severe cycles from room temperature to 550°C. No thermocouple signal was lost and destructive examinations revealed no disturbance in position of jacket tube, core rod, or sensors.

Mechanical Testing

The first full length prototype RGTA (canne No. 1) was 14.2 meters long and was used in the Framatome test facility, Figure 3.5-5. The insertion and removal techniques were found adequate. Forty insertions and removals showed no damage to either the RGTA or the guide tube mockups. Figure 3.5-6 gives the mechanical details of the EdF RGTA.

The forces required to insert and withdraw the RGTA were measured and found acceptable and consistent with TIP tube experience.

Hydrostatic pressure tests were performed and thermal cycling repeated within the limits of the facility (i.e., temperatures not as high as those of canne No. 0).

After satisfactory completion of non-destructive testing, canne No. 1 was processed through the disposal equipment in accordance with standard test specifications for the TIP thimbles.

The disposal machine (Figure 3.5-7) removed a TIP thimble and coiled it into about a 2/3 meter diameter (a destructive process). After this treatment, the sensor thermocouples of canne No. 1 were still functioning.

Positional Accuracy of Sensors

Both theoretical and experimental work were conducted by Framatome (on behalf of EdF) to determine the accuracy to which locations of RGTs could be calculated.

The distance from the bottom reference plane of the fuel core to the top of the RGTA was calculated to be 3875 mm in cold conditions and 3915.5 mm in hot conditions and the nine RGT positions distributed accordingly (Figure 3.5-8).

Actual measurements were performed in Bugey 3 where a TIP was used to "find" the top of a mock-up RGTA (i.e., a TIP thimble) and relate it to known positions of fuel spacers. This was done for core positions D-5 and J-10 (the same positions used for Cannes No. 3 and No. 4 in Bugey 5). In position D-5 the top was at 3918 mm measured and 3916.5 mm calculated. Positional uncertainties on the measurement are ± 15 mm.

Experience

The installation of Cannes No. 3 and No. 4 in Bugey 5 took place on June 19, 1979, where EdF replaced TIP thimble tubes in core positions J-10 and D-5. No problems were encountered in insertion or sealing. Subsequent successful installations have taken place in eight core locations of Tricastin 2 and 3.

3.5.2 RWE and Duke Power Prototype Program

The substitution of RGTAs for SPND strings in B&W reactors as regards insertion, removal, handling, transport, and disposal causes virtually no change. The Duke Power prototypes are to be shipped on reels used for SPNDs and supplied to Reuter Stokes by Duke (who owns them).

At Oconee the four prototype RGTAs (see Figures 3.5-9 and 3.5-10) will employ the same seal flanges, Bendix connectors and cabling as have been used for the SPND assemblies they displace.

For RWE's KMKK plant (startup 1984), the seal flanges are of an improved BWR design which may also be employed for the RGTA's (Figure 3.5-11). However, an advanced "no welds" design which employs mechanical fittings, arranged doubly for back-up pressure tests, is also being considered to eliminate welds on the RGTA jacket tube (Figure 3.5-12).

A series of qualifying mechanical tests are embodied in the purchase specifications for both sets of prototypes. Both Duke, Reference 3-(23), and KMKK (RWE) bid specs, Reference 3-(24), will be provided to NRC reviewers upon request.

There exist two schools of thought regarding termination of the RGTA core rod. The first opinion is that the core rods inside the RGTA's should be continuous and uninterrupted from top of the core to the seal flange (36 m). The alternative is to end the core rods somewhere below the reactor vessel and allow the cables to proceed inside the seamless jacket tube to the seal flange. Generally, buyers prefer the former alternative, while suppliers prefer the latter.

Figure 3.5-13 illustrates three degrees of conservatism with respect to primary system leakage after a crack occurs in the jacket or sheath tube:

- 1) In the present SPND design a crack anywhere in the jacket tube feeds water directly into the inter-cable space from which it proceeds to confront the gold braze seals around each SPND cable.
- 2) In the buyer-preferred RGTA design, a jacket tube crack anywhere along the entire 36 m length of the RGTA means nothing. High pressure helium tests impressing 3000 psi on a short section of an RGT have produced no detectable helium leakages along the path of the drawn joint between jacket tube and core rod. Further, even a core rod crack does not result in primary coolant out-leakage because the thermocouples are held so tightly within the drawn down core rod, (see Figure 3.4-6). The KMKK mechanical testing specs (seismic) for RGTA's call for a complete destructive fracture of the RGTA cross-section of the pressure side of the seal flange and no

leakage is allowed (such a fracture of an SPND would open the calibration tube to the in-core instrument pit).

- 3) In the supplier-preferred RGTA design, the core rod terminates outside the reactor core. In this case a leak developing in the jacket tube, between the reactor and seal flange, would result in primary pressure at the cable penetration seal much as in case 1 above. The proponents of this middle alternative argue that jacket tube leaks are far more probable in the high temperature high-coolant velocity core region of the RGTA than in the static, low temperature region inside the guide pipe. Since the SPND is vulnerable to such cracks also in the core region, as well as outside, proponents of arrangement (3) argue that "much less vulnerable" is good enough. Proponents of configuration (2) argue that the RGTA offers the opportunity to remove the full area of 52 pressure tubes from the surface area retaining the primary pressure, and "why go only half way?".

At this point in RGT development, mechanical testing necessary to qualify RGTAs to replace Westinghouse TIP thimbles is complete. Mechanical testing of various kinds will be carried out by Duke Power and RWE but the fact is clear that reduced exposure to primary system leakage is brought about where any PWR instrument system is converted to RGTAs.

3.5.3 ScP/IFA Tests Simulating Signal Failure Modes

The ways in which RGTs can fail or give erroneous signals is more limited than for either the SPND or the fission chambers. It has already been pointed out that lead-to-sheath resistance can drop to 100,000 Ω before a 2 percent signal error occurs. The modes of failure or signal degradation for fission chambers and gamma ion chambers are several and degradations are difficult to detect.

There are two known types of failure for RGTs:

- 1) Cable defects which are those common to all low temperature thermocouples: lead interruption (detectable by loop resistance measurement); lead grounding (detectable by lead-to-sheath resistance); and moisture in insulation (detectable by lead-to-sheath resistance).
- 2) Water in the annular gas space arising from jacket tube failure. In a PWR any crack in the jacket tube (over a sensor cavity) will fill the sensor space with water, not steam. Tests in 1975 and 1976 at IFA, Reference 3-(25), showed that the presence of water in the annular space completely eliminated (made zero) the RGT signal.

There are no known non-detectable (i.e., "soft") failure modes for RGTs. The signals are either correct or the instrument can clearly be shown to be inoperative.

Use of heater cables for in situ calibration of RGTs eliminates the necessity for insulation resistance measurement to detect failure.

APPENDIX

DUKE POWER COMPANY

STEAM PRODUCTION DEPT.
 GENERAL OFFICES
 422 SOUTH CHURCH STREET
 CHARLOTTE, N. C. 28242

TELEPHONE AREA 704
 373-4011

P. O. BOX 2178

21 September 1977

Mr. R.D. Smith
 Scandpower, Inc.
 4853 Cordell Avenue
 Suite B-2, Triangle Towers
 Bethesda, Maryland 20014

Subject: Self-Powered Neutron versus Gamma Thermometer
 Signal to Power Conversion
 File No.: GS-532.00

Dear Bob:

In response to your question concerning the probable compatibility and feasibility of utilizing gamma thermometers where we currently use self-powered neutron detectors (SPND), I offer you the following information.

The signal to power conversion process which we now perform on our process or Operator Aid Computers is quite involved utilizing 7 major programs that contain 13 subroutines within them. Their functions are as follows:

1) Program 1 provides for:

- (i) Instrument Leakage Calibration
- (ii) Depletion Correlation
- (iii) Replacement of Inoperable Instruments
- (iv) Background Correlations
- (v) Experimental Normalizations

2) Program 2 provides processing whereby the raw signal is converted to power by:

- (i) Burnup Correlation
- (ii) Enrichment Correlation
- (iii) Xenon Correlation
- (iv) Boron Correlation
- (v) Rhodium Depletion Correlation
- (vi) Moderator Temperature Correlation
- (vii) Geometry and Spectrum Correlation for Rodded, Non-Rodded and LBP Assemblies

3) Program 3 processing includes:

- (i) Calculation of quadrant tilt using all symmetric segment powers
- (ii) Surface fit functions for deviations in quadrant tilt and symmetric ring values

21 September 1977

- 4) Program 4 constructs a representation of the power in all fuel assemblies from the detector readings.
- 5) Program 5 performs the following:
 - (i) Calculates Assembly Powers
 - (ii) Calculates Nuclear Core Power
 - (iii) Converts Heat Balance Power to Megawatts
 - (iv) Calculates Heat Balance to Nuclear Power Normalization Factor
 - (v) Normalization of Segment and Assembly Powers
 - (vi) Performs an Axial Least Squares Fit of Each Assembly
 - (vii) Sums Polynomial Coefficients for Each Level
 - (viii) Integration
 - (ix) Calculates Quadrant Relative Powers
- 6) Program 6 calculates:
 - (i) Core Power History
 - (ii) Segment Power History
 - (iii) Assembly Power History
 - (iv) Time Integration
- 7) Program 7 calculates the depletion of the incore or SPND emitter material.

All of the above presupposes of course, that the required correlations and conversion factors are available, the determination of which is not trivial and must be performed for each cycle. The calculational flow for each γ factor or correction term is shown in Attachment I, and involves large amounts of man and computer time to execute.

It is my opinion that whatever software and conversion factor work would have to be performed for signal to power conversion of gamma thermometer signals, that work could not be greater in magnitude than that performed for SPND signals, and in all probability would be less, based upon what I now know of both systems.

It is this probability plus the promise of higher dependability and longer lifetime that would, once proven, allow Duke Power to provide its resources in a cooperative effort toward an integrated gamma thermometer system, both hardware and software.

Mr. R.D. Smith

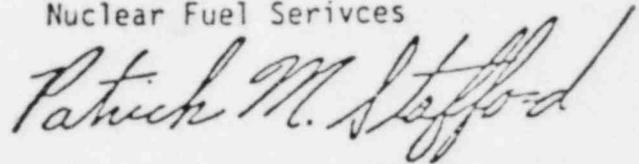
-3-

21 September 1977

I hope that this collective effort shall come to pass with you and our fellow European utilities, and look forward to an effort which shall be beneficial to all involved.

Yours very truly,

H.T. Snead, Manager
Nuclear Fuel Services

A handwritten signature in cursive script that reads "Patrick M. Stafford".

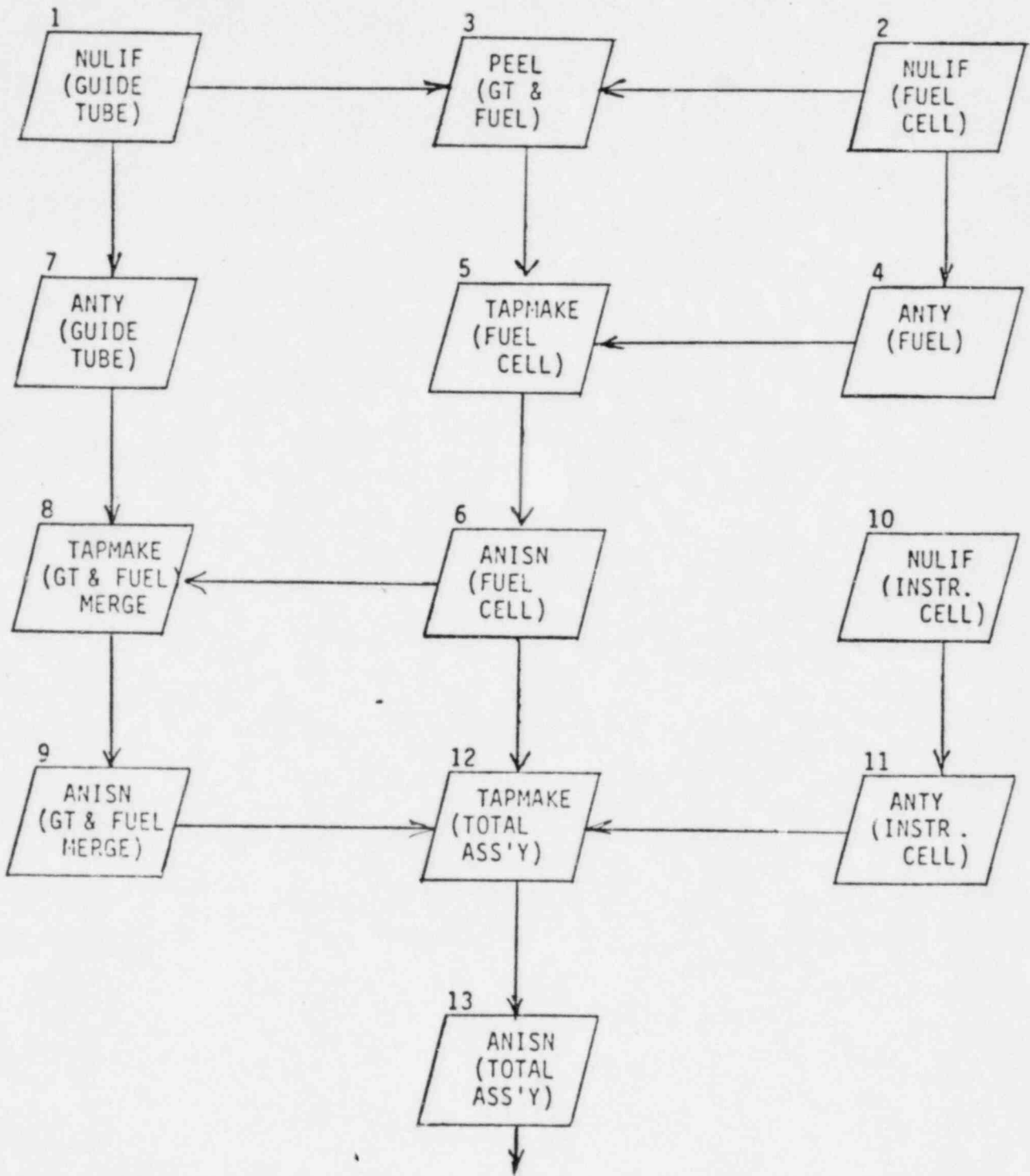
BY: Patrick M. Stafford
Assistant Engineer
Core Performance

PMS/plc

Attachments

CC: J.D. Kortheuer
H.T. Snead

ATTACHMENT I



CALCULATE Y FACTOR

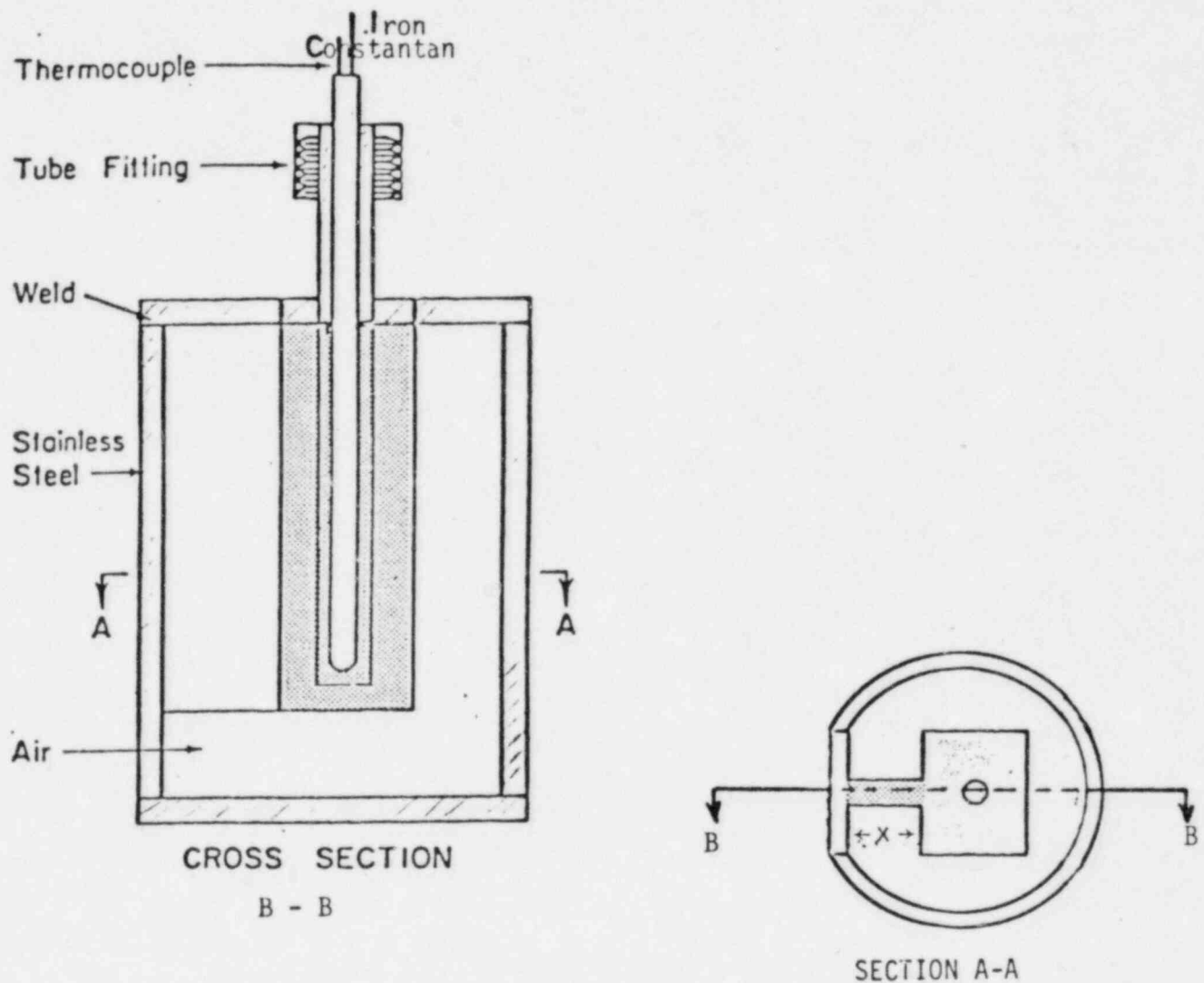
Note:

TAPMAKE and PEEL are automation codes which reduce draftically the manapwer required for y factor generation.

FIGURES

FIGURE 1-1

FIRST SRP GAMMA THERMOMETER (CA. 1953)



$\bar{g} = 0.5 \text{ W/g} =$

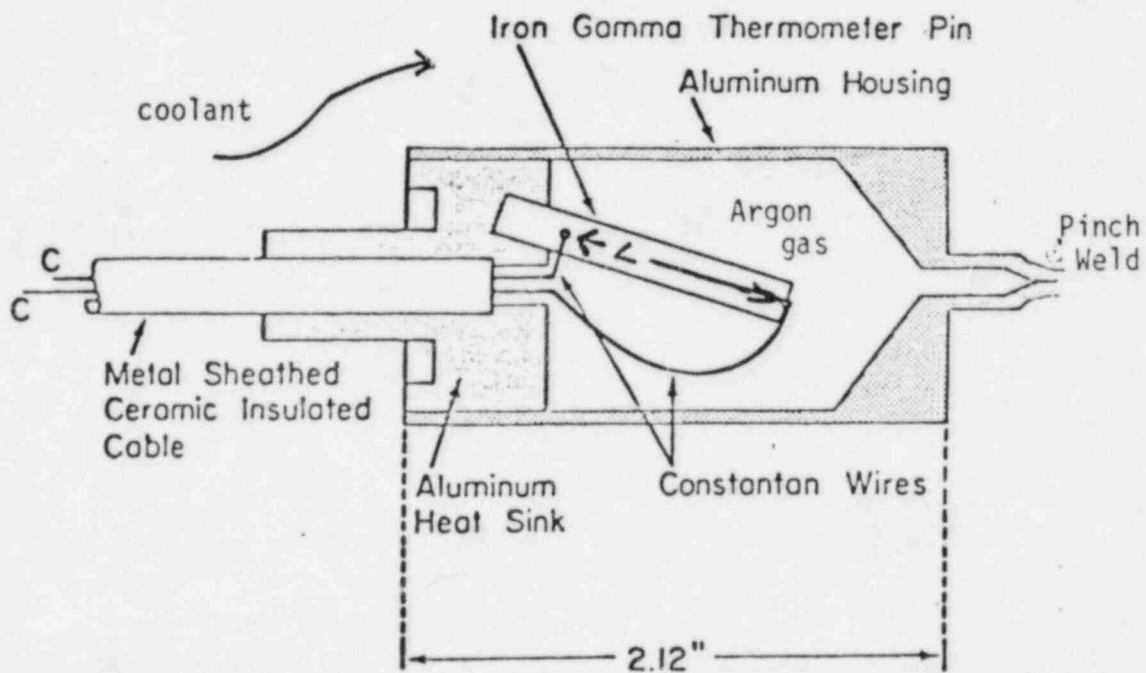
- 65% prompt fission γ
- 25% fission product γ (70% "prompt")
- 10% fast neutron heating

$$\Delta T \approx \rho g x / kA \quad (40^{\circ} \text{ to } 150^{\circ} \text{C.})$$

In this device, about one inch in diameter, the majority of gamma heating was produced in the central block of stainless steel. The device was long enough so that the temperature measured was controlled by radial heat path (X) which also generated a little heat.

FIGURE 1-2

TODAY'S SRP GAMMA THERMOMETER (CA. 1962 TO PRESENT)

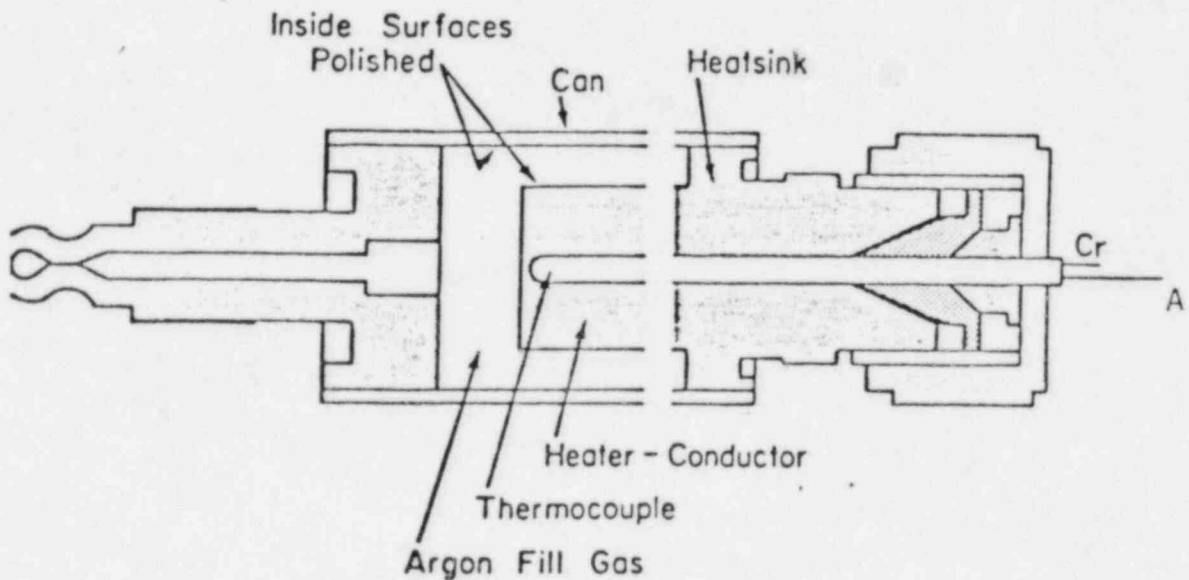


$$\Delta T \approx \rho g L^2 / 2K \quad (40^\circ \text{ to } 150^\circ \text{C.})$$

This embodiment, of which some 3000 have been used, was the first to use principles of the difference thermocouple. The signal is zero at zero power regardless of coolant temperature. The units are made identical within $\pm 3\%$ response time on plunge testing. (This is the same as $\pm 3\%$ on real ΔT sensitivity to heating.) They are then signal biased in-core within this $\pm 3\%$ range by cross calibration with wire monitor and flow $\times \Delta T$ measurement. Although normally replaced yearly, SRP reported fast fluence exposures up to 10^{22} nvt (5½ operating PWR years) without change in ratio of fuel power to gamma thermometer signal. Failure before removal is reported for less than 3% of the units.

FIGURE 1-3

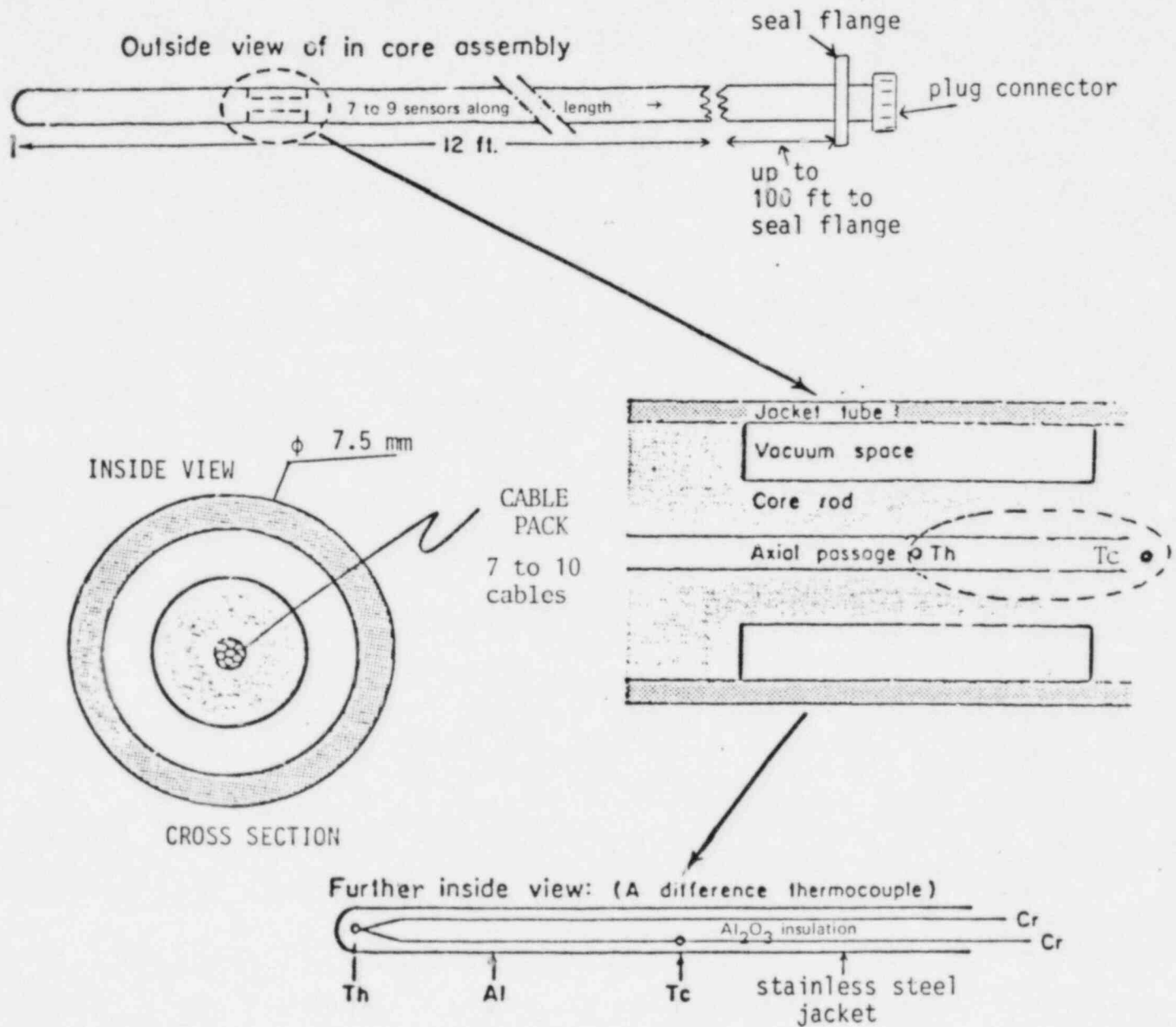
STANDARD HALDEN TYPE
GAMMA THERMOMETER



These units are about 1/3 inch in diameter and about 3 inches long. They are of stainless steel and are cylindrical. Since 1964 226 such units have been employed and only 3% have failed before their removal. They are plunge tested at manufacture and accepted if within $\pm 1\frac{1}{2}\%$ on measured response time (τ is uniquely related to real sensitivity, $^{\circ}\text{C}/\text{Watt}/\text{gm}$). A set of 5 gamma thermometers installed in Instrumented Fuel Assembly, IFA-4 in 1964 were removed with IFA-4 in 1971 after a fuel burnup of 26,000 MWd/t, and showed no change in calibration over this period. Note that thermocouple cables (as at SRP) are exposed to reactor coolant, and are therefore more vulnerable to premature failure than the RGT design.

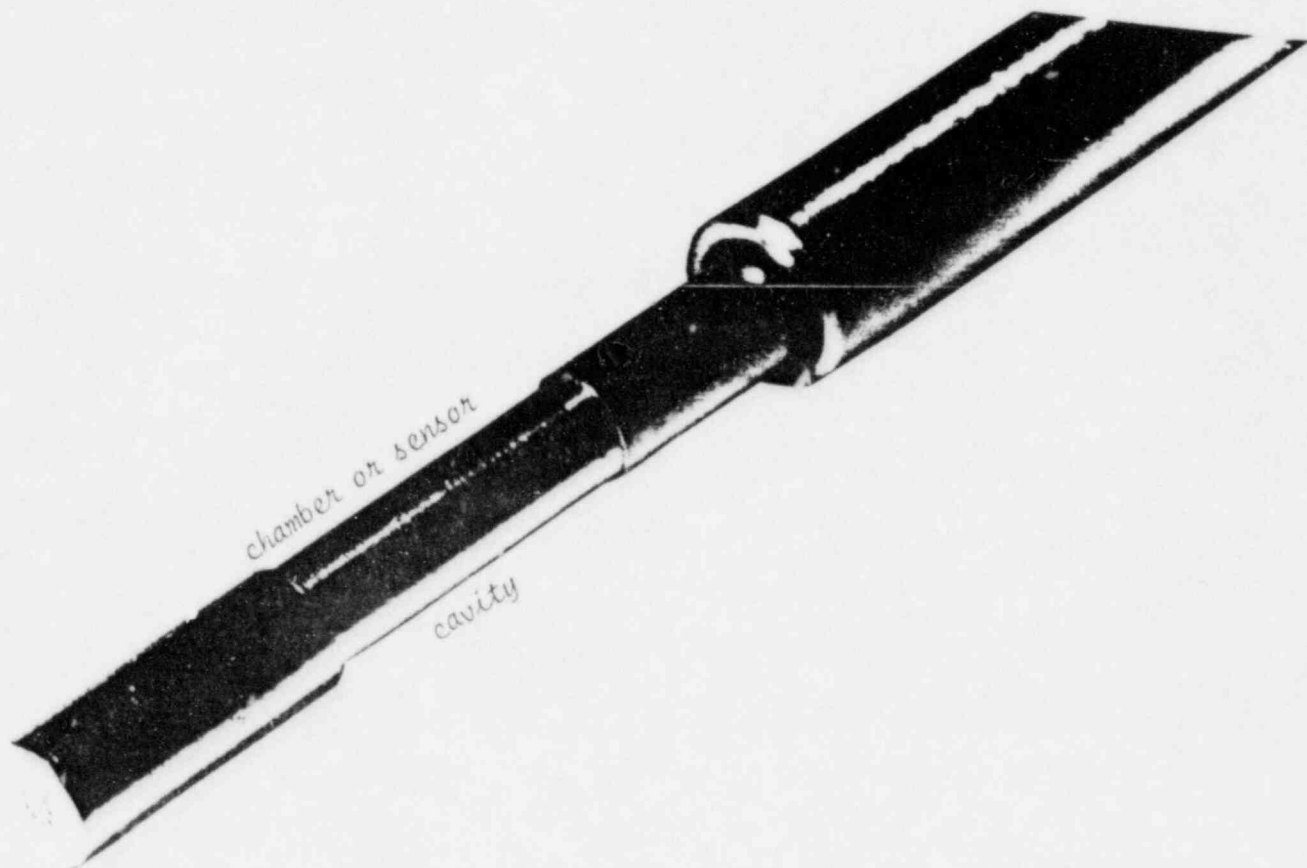
FIGURE 1-4

γ -RADCAL GAMMA THERMOMETER ASSEMBLY (RGTA) FOR
PRESSURIZED WATER REACTORS



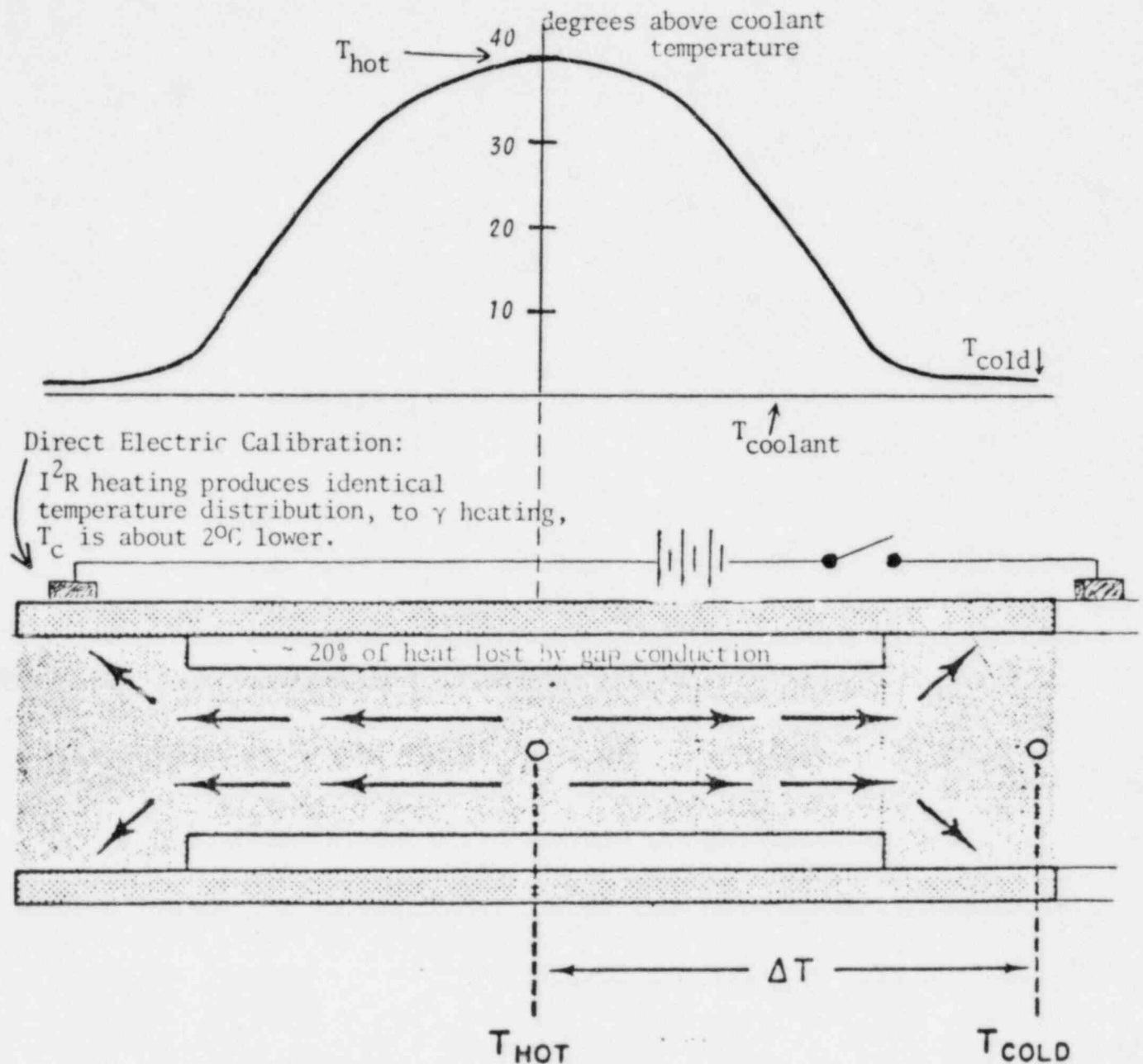
Details of these designs are given in Section 3.4. They differ very little in outside appearance and substitute directly for in-core pressure thimbles in Westinghouse plants and for SPND assemblies in B&W plants. The Duke γ RGT employs a central calibration tube. The RWE γ RGT uses a central heater cable that permits in situ recalibration at will. Some γ RGTs use double difference thermocouples to double signal without lengthening time of response. (τ is 17 seconds for the $\text{E}^{\text{r}}\text{F}$ γ RGTs compared to 150 seconds for Rhodium self-powered neutron detectors). BWR γ RGTs will be much faster and will be augmented by signal deconvolution electronics to give apparent τ 's of 0.25 seconds. The monolithic stainless steel construction keeps thermocouples dry, improves pressure boundary integrity in all PWRs, and permits workshop calibration to $\sigma: \pm 1.0\%$ by direct electrical heating (I^2R). Introduction of a nichrome heater cable into the cable pack permits full-range in-situ recalibration.

FIGURE 1-5
ENLARGED PHOTOGRAPH OF EDF_Y RADCAL BEFORE DRAWING ON
OF JACKET TUBE.



The core tube is drawn or rotary swaged tightly onto the cable pack before sensor cavities are ground on outside of core rod. Intimate metal-to-metal contact is achieved. Torture tests by EdF / Intertechnique have failed to loosen thermocouples or impair thermal contact. This specimen contains 9 $\frac{1}{2}$ mm difference thermocouples arrayed around one 1mm difference thermocouple whose hot junction is at coolant outlet and whose cold junction is at coolant inlet. In the next process step the jacket will be drawn tightly onto the core rod with Argon gas in the sensor cavities.

FIGURE 1-6: TEMPERATURE DISTRIBUTION AND HEAT FLOW
IN PWR_γRADCAL



The unit is relatively insensitive to locations of hot and cold junctions because of flat temperature gradients in junction regions. A specific two dimensional code RADCAL/THERMAL has been developed by Scandpower to predict steady state signals and transient response to step change or plunge test. Both electric and gamma heating modes are accurately modelled. Tests and theory show insensitivity of response to coolant velocity over a wide range. Responses to power exhibit a correlation coefficient > 0.9999 to the best fit straight line. A sensitivity change of about -30% occurs when coolant temperature increases from $20^\circ C$ to $300^\circ C$. This is accurately modelled in RADCAL/THERMAL code.

FIGURE 1-7: PRINCIPLE OF DIRECT ELECTRIC CALIBRATION OF AN RGTA

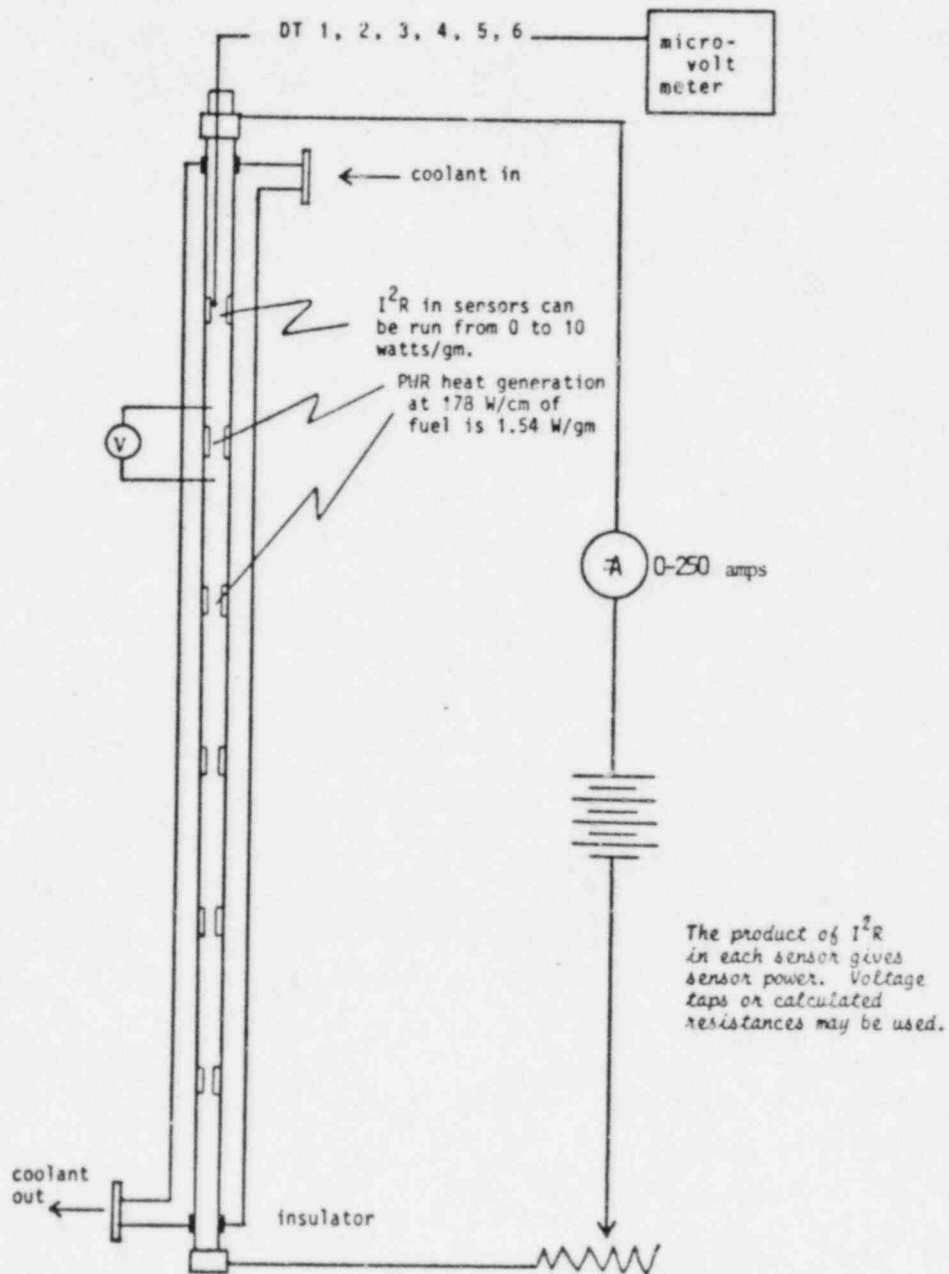


FIGURE 3.0 - 1.

UNCERTAINTY σ_1

$$\text{RGT: } q = \text{RGT millivolts} \times \left[\begin{array}{l} \text{small individual} \\ \text{sensor corrections} \end{array} \right] \pm \sigma_1$$

The range of gamma thermometer sensitivities is proven to be within $\pm 2.5\%$ as they leave the shop calibration. No effect of irradiation has been detected during long irradiations at SRP and HBWR. High precision tests to verify this are now in progress at ORNL.

FIGURE 3.0 - 2
 CONTRIBUTIONS TO UNCERTAINTY IN
 RATIO OF LOCAL LHGR TO "MEASURED" PARAMETER,
 K_2

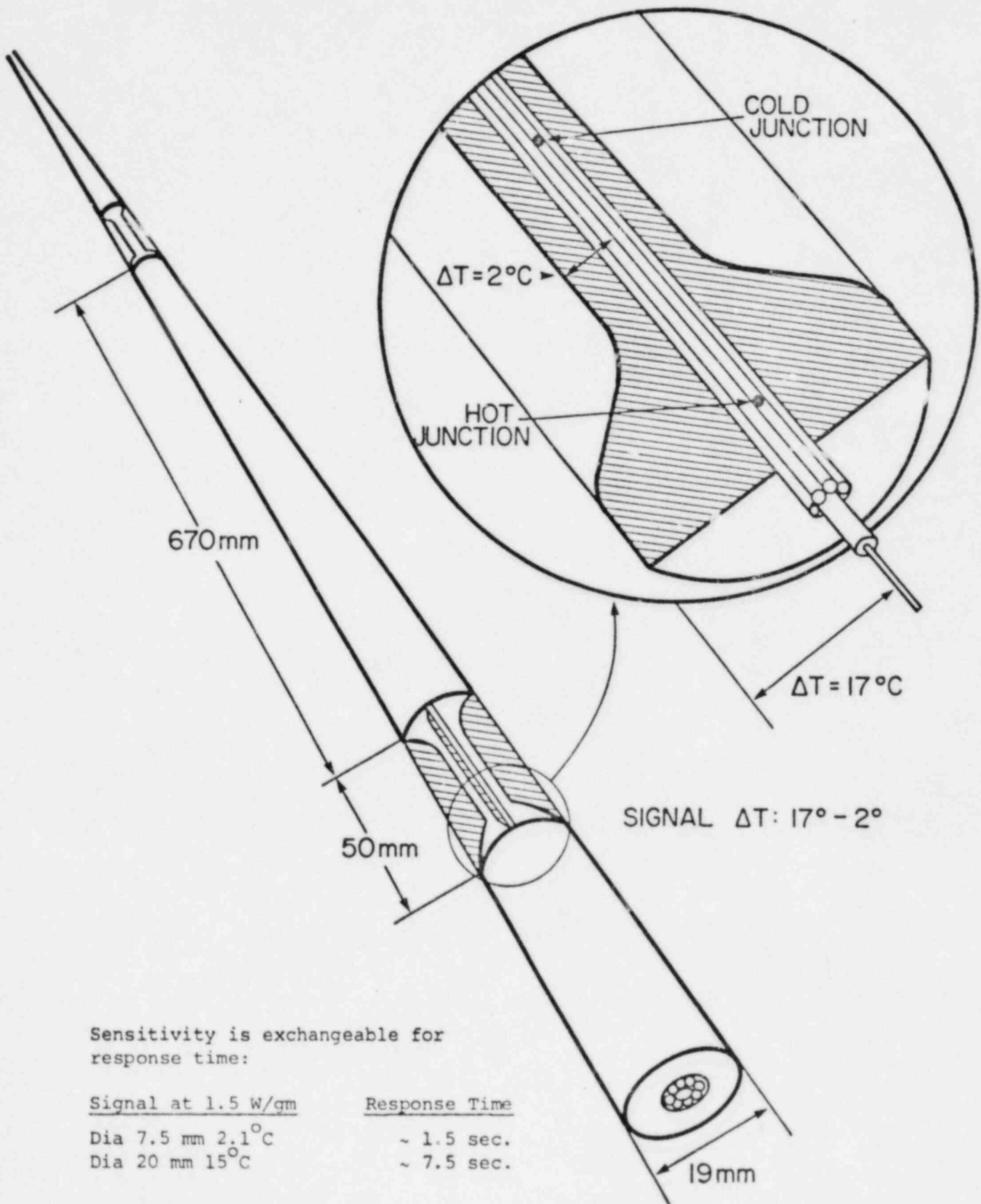
UNCERTAINTY 2

How well does K_2 define local power of fuel adjoining a detector?:

$$\text{RADCAL HEAT} \times \left[\begin{array}{l} K_2 \text{ corrected for: Small} \\ (< 6\%); \text{ Corrections as found} \\ \text{by experimental and} \\ \text{theoretical work.} \end{array} \right] = \text{LHGR} \pm \sigma_2$$

To date, both experiment and theoretical calculations indicate that total corrections smaller than $\pm 3\%$ need to be applied to relate gamma thermometer heat rate to the highest possible precision to LHGR in surrounding fuel in a PWR, regardless of exposure, enrichment or distributed poison. Slightly larger corrections, in a minus direction, may be needed for low power fuel near embedded control rods. Avoidance of normalization yields truly independent local power determination.

FIGURE 3.1-1: "BWR" γ -RADCAL Uses PURE RADIAL HEAT FLOW

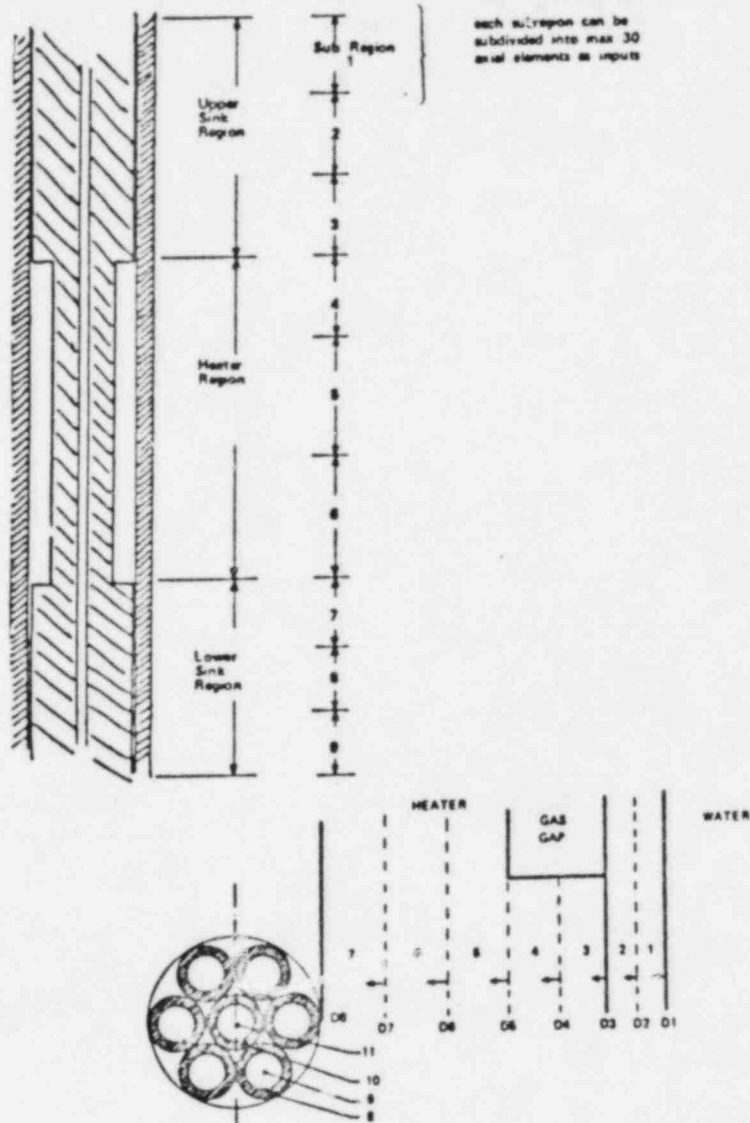


Sensitivity is exchangeable for response time:

Signal at 1.5 W/gm	Response Time
Dia 7.5 mm 2.1°C	~ 1.5 sec.
Dia 20 mm 15°C	~ 7.5 sec.

The Radial-type RADCALs are simpler and avoid the gas gap.

FIGURE 3.1 - 2
 AXIAL AND RADIAL SPLIT IN RADCAL/THERMAL



The figure shows how the RADCAL/THERMAL code splits the γ-radial sensor in axial and radial direction to integrate the thermal heat transfer equation in space.

FIGURE 3.1 - 3

INPUT ARRAY FOR RADCAL/THERMAL

INPUT-VALUES:

```

NO. OF ELEMENT-LINES:  A  6  6  10  10  10  6  6  6
COOLANT WATER TEMP      1  300.0      C
TIMEPERIOD              1  121.00     SECS
TIMESTEP                1  0.200     SECS
TESTVALUE               1  0.0000
TEMPVALUE               1  0.100      C
PRINTOUT EVERY          1  10.00     SECS

OUTER SLEEVE-DIAMETER:  0.75000     CM
INNER SLEEVE-DIAMETER:  0.52000     CM
INNER HEATER-DIAMETER:  0.19000     CM
OUTER HEATER-DIAMETER:  0.42000     CM
HYDRAULIC DIAMETER     1  0.30000     CM

HEAT TRANSFER AREAS A-11:  0.007500  0.010200  0.001000  0.006100  CM2
WATER SECTION LENGTH   1  2.000     CM
UPPER/LOWER SINK LENGTH:  2.000     CM

HEAT TRANSFER PERIMETERS A-12:  0.30000  0.75400  0.10470  0.12570  0.00000  CM

DENSITY 1-5            1  7.84  8.33  3.93  8.33  3.93  G/CM3

GAMMA/ELECTRIC HEAT RATES  1  0.00  1.40  1.40  0.00  0.00  0.00  0.00  0.00
CORRESPONDING TIME VALUES  1  0.00  1.00  121.00  0.00  0.00  0.00  0.00  0.00

ENIGIVITY              1  0.30
WATER DENSITY          1  726.0   KG/M3
WATER CONDUCTIVITY     1  0.0054  W/CM-C
WATER VISCOSITY        1  0.0001000  KG/M-S
PRANDTL-CONSTANT       1  1.00
COOLANT FLOW           1  2.00   M/S

      TEMP1  SPECIFIC HEAT1  TEMP2  SPECIFIC HEAT2
A1  100.00  0.5100  400.00  0.5700
N1  20.00   0.4400  315.00  0.5300
C1  0.00    1.0500  400.00  1.0500
O1  20.00   0.4600  315.00  0.5500
E1  0.00    1.0500  400.00  1.0500

      TEMP1  CONDUCT1  TEMP2  CONDUCT2
A1  20.00  0.15900  300.00  0.18400
N1  20.00  0.12000  315.00  0.16000
C1  20.00  0.40000  300.00  0.17500
O1  20.00  0.12000  315.00  0.16000
E1  20.00  0.40000  300.00  0.17500
S1  300.00  0.00025  500.00  0.00010

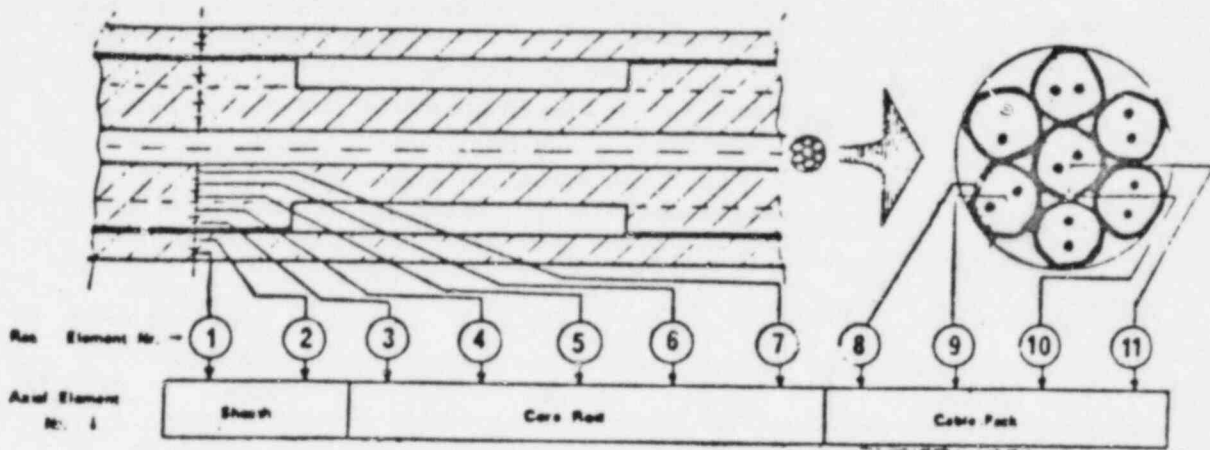
HTA=HTR=...=HTB1
  1  2.00  2.00  2.00  2.00  2.00  2.00  2.00  2.00  2.00
B1  2.00  2.00  2.00  2.00  2.00  2.00  2.00  2.00  2.00
C1  2.00  2.00  2.00  2.00  2.00  2.00  2.00  2.00  2.00
O1  2.00  2.00  2.00  2.00  2.00  2.00  2.00  2.00  2.00
E1  2.00  2.00  2.00  2.00  2.00  2.00  2.00  2.00  2.00
F1  2.00  2.00  2.00  2.00  2.00  2.00  2.00  2.00  2.00
G1  2.00  2.00  2.00  2.00  2.00  2.00  2.00  2.00  2.00

TEMP1= 0.00  RESISTIVITY1= 0.0000750 OHM-CM
TEMP2= 400.00  RESISTIVITY2= 0.0001000 OHM-CM
REF1 = 1.000  RFL2 = 1.000
    
```

The figure shows the input data that are necessary to give to the RADCAL/THERMAL code. Data given are geometry of the sensor, thermal and electrical properties, type of heating.

FIGURE 3.1 - 4

CALCULATED STEADY STATE TEMPERATURE DISTRIBUTION



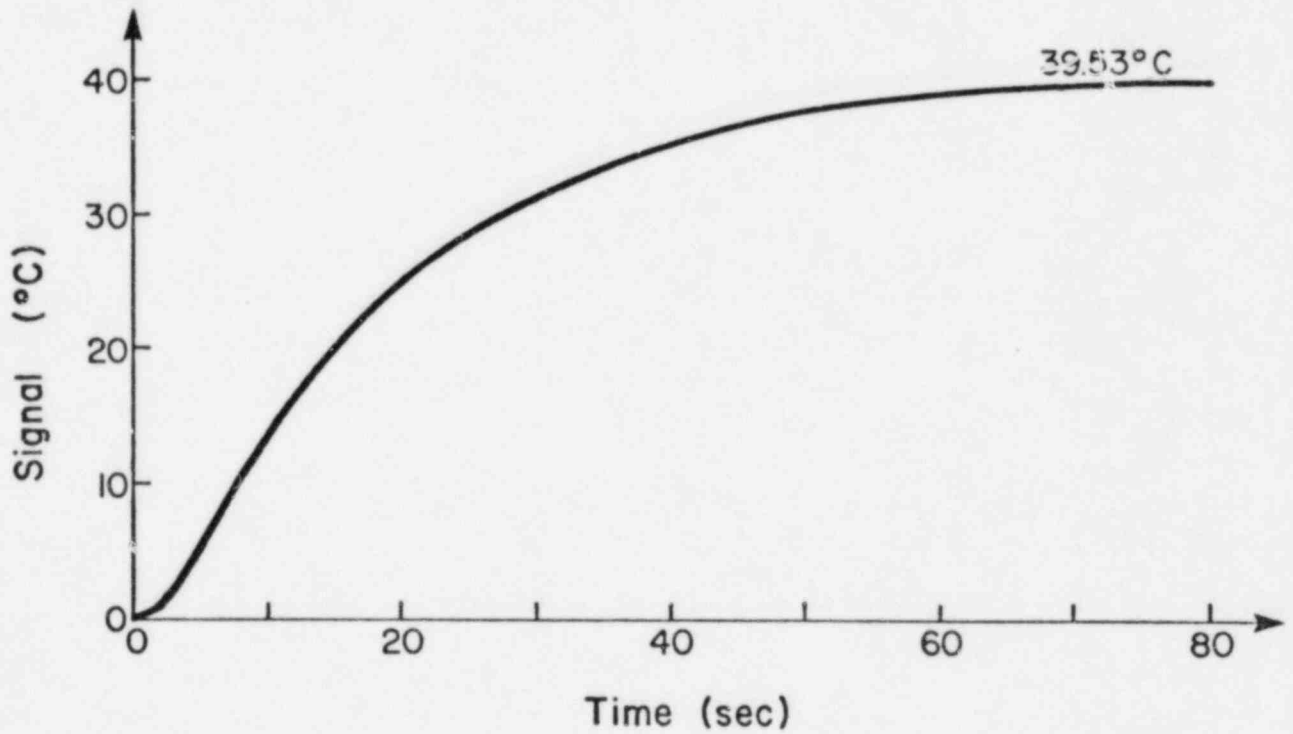
TEMPERATURE TABLE:

1:	1.26	1.7A	2.76	2.94	3.11	3.29	3.41	3.81	3.85	4.07	4.21
2:	1.26	1.7A	2.7A	2.91	3.12	3.29	3.41	3.81	3.85	4.07	4.21
3:	1.26	1.79	2.75	2.97	3.10	3.29	3.41	3.81	3.85	4.08	4.21
4:	1.26	1.7A	2.80	2.89	3.13	3.29	3.42	3.82	3.85	4.08	4.21
5:	1.26	1.79	2.74	2.99	3.10	3.30	3.42	3.82	3.86	4.08	4.22
6:	1.26	1.79	2.81	2.87	3.15	3.29	3.42	3.82	3.86	4.09	4.22
7:	1.26	1.79	2.73	3.02	3.10	3.31	3.43	3.83	3.87	4.10	4.23
8:	1.27	1.79	2.63	2.88	3.17	3.31	3.44	3.85	3.88	4.11	4.25
9:	1.27	1.80	2.75	3.05	3.13	3.34	3.46	3.87	3.91	4.14	4.28
10:	1.28	1.81	2.87	2.91	3.21	3.35	3.49	3.91	3.95	4.18	4.33
11:	1.29	1.84	2.81	3.11	3.20	3.41	3.54	3.97	4.01	4.26	4.41
12:	1.31	1.87	2.97	3.02	3.32	3.48	3.62	4.07	4.12	4.38	4.54
13:	1.35	1.93	2.98	3.28	3.39	3.62	3.76	4.25	4.30	4.59	4.77
14:	1.41	2.02	3.23	3.33	3.64	3.83	3.99	4.54	4.60	4.93	5.15
15:	1.50	2.16	3.44	3.74	3.93	4.20	4.38	5.04	5.11	5.50	5.78
16:	1.63	2.37	3.95	4.16	4.52	4.81	5.04	5.88	5.97	6.47	6.82
17:	1.76	2.62	4.65	5.05	5.46	5.91	6.23	7.34	7.47	8.07	8.51
18:	1.76	2.72	5.71	6.33	7.28	8.04	8.53	9.86	10.03	10.65	11.11
19:	1.27	1.70	0.00	0.00	13.03	13.15	13.29	13.95	14.03	14.44	14.73
20:	0.99	1.28	0.00	0.00	17.86	17.90	17.95	18.24	18.26	18.49	18.63
21:	0.85	1.10	0.00	0.00	22.19	22.21	22.24	22.37	22.37	22.49	22.54
22:	0.79	1.02	0.00	0.00	26.10	26.13	26.15	26.22	26.21	26.27	26.28
23:	0.76	0.99	0.00	0.00	29.64	29.68	29.70	29.74	29.74	29.77	29.75
24:	0.75	0.98	0.00	0.00	32.83	32.86	32.88	32.93	32.92	32.94	32.92
25:	0.75	0.98	0.00	0.00	35.67	35.70	35.73	35.78	35.77	35.79	35.77
26:	0.76	0.99	0.00	0.00	38.17	38.21	38.23	38.29	38.28	38.31	38.29
27:	0.76	0.99	0.00	0.00	40.34	40.38	40.41	40.47	40.47	40.49	40.48
28:	0.76	1.00	0.00	0.00	42.19	42.23	42.26	42.33	42.33	42.36	42.35
29:	0.77	1.00	0.00	0.00	43.72	43.77	43.80	43.88	43.88	43.91	43.90
30:	0.77	1.01	0.00	0.00	44.94	44.99	45.02	45.11	45.10	45.14	45.13
31:	0.77	1.01	0.00	0.00	45.86	45.91	45.94	46.03	46.02	46.06	46.06
32:	0.77	1.01	0.00	0.00	46.47	46.51	46.55	46.64	46.64	46.67	46.67
33:	0.77	1.02	0.00	0.00	46.77	46.82	46.85	46.94	46.94	46.98	46.98

The figure shows the temperature distribution of the sensor of steady state. The number above the columns refer to the corresponding section of the γ -radial sensor.

FIGURE 3.1 - 5

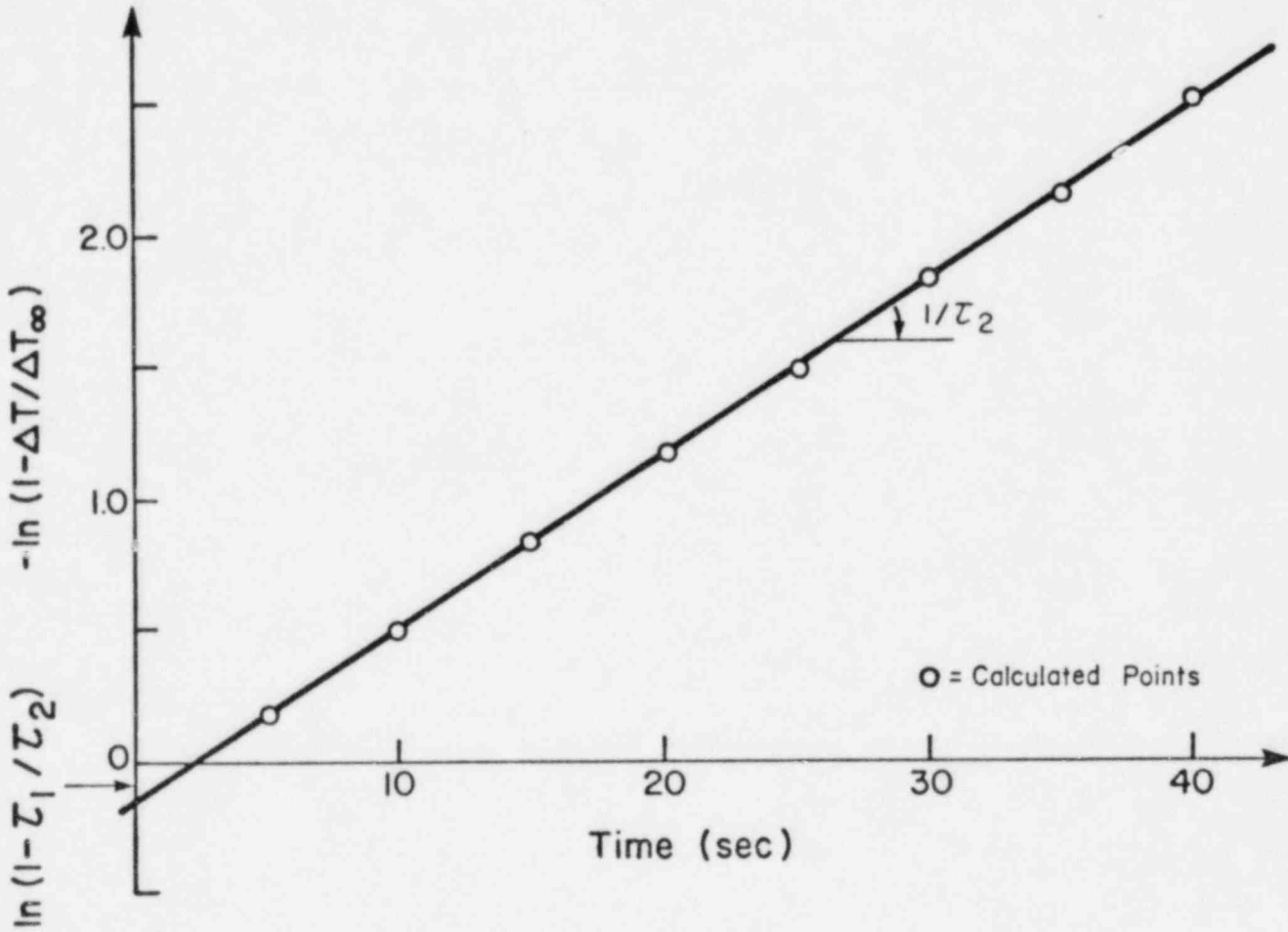
PREDICTED RESPONSE OF CANNE 4 THROUGH 8 BY RADCAL/THERMAL



The figure shows the predicted response of Canne 3 and 4 to a step in electrical heating from 0 to 1.4 W/g. Cooling water 15°C.

FIGURE 3.1 - 6

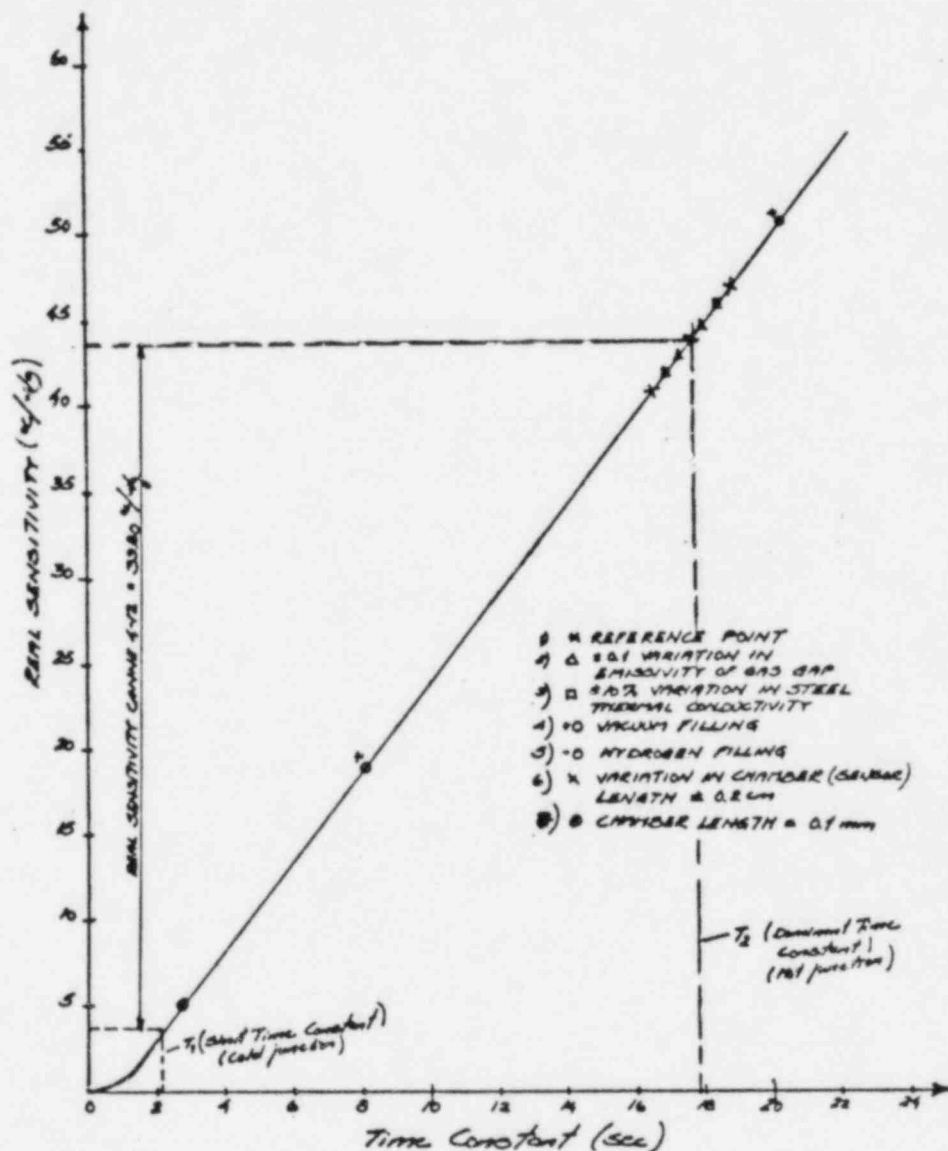
LOGARITHMIC PLOT OF POWER STEP RESPONSE CURVE



The logarithmic plot of the response curve shows that the system is a higher order system, at least of second order. The highest time constant (dominant eigen value) is found from the slope of the curve. The intercept provides information about the lowest time constant if the system is treated as a second order system.

FIGURE 3.1 - 7

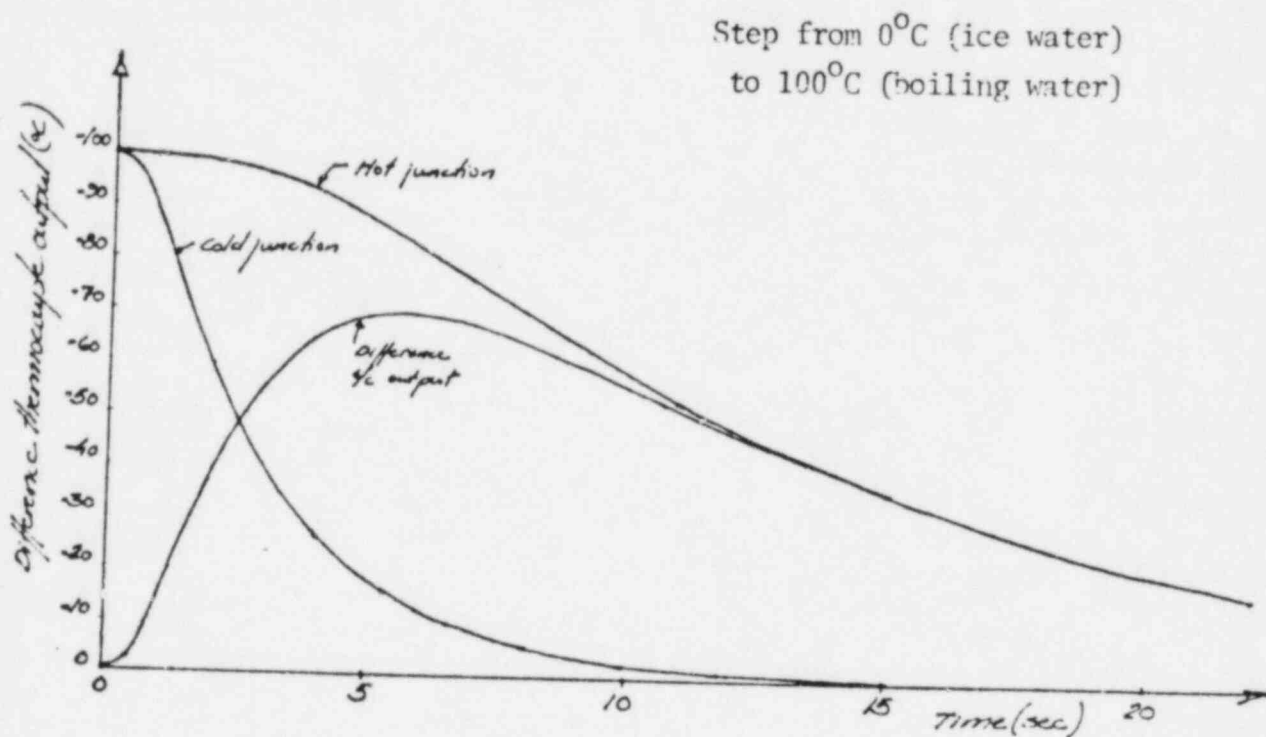
RELATIONSHIP BETWEEN REAL SENSITIVITY, S_R ,
AND DOMINANT TIME CONSTANT OF JUNCTION, τ



The curve shows the relationship between the real sensitivity and the time constants of an RGT. The curve has been constructed by calculating sensitivity and time constant when basic parameters have been varied around a reference value. Knowing the time constants of the two junctions of the RGT sensor (e.g., from plunge test), the curve can be used to find real sensitivity.

FIGURE 3.1 - 8

PREDICTED PLUNGE TEST RESPONSE - A TYPICAL ORNL SPECIMEN

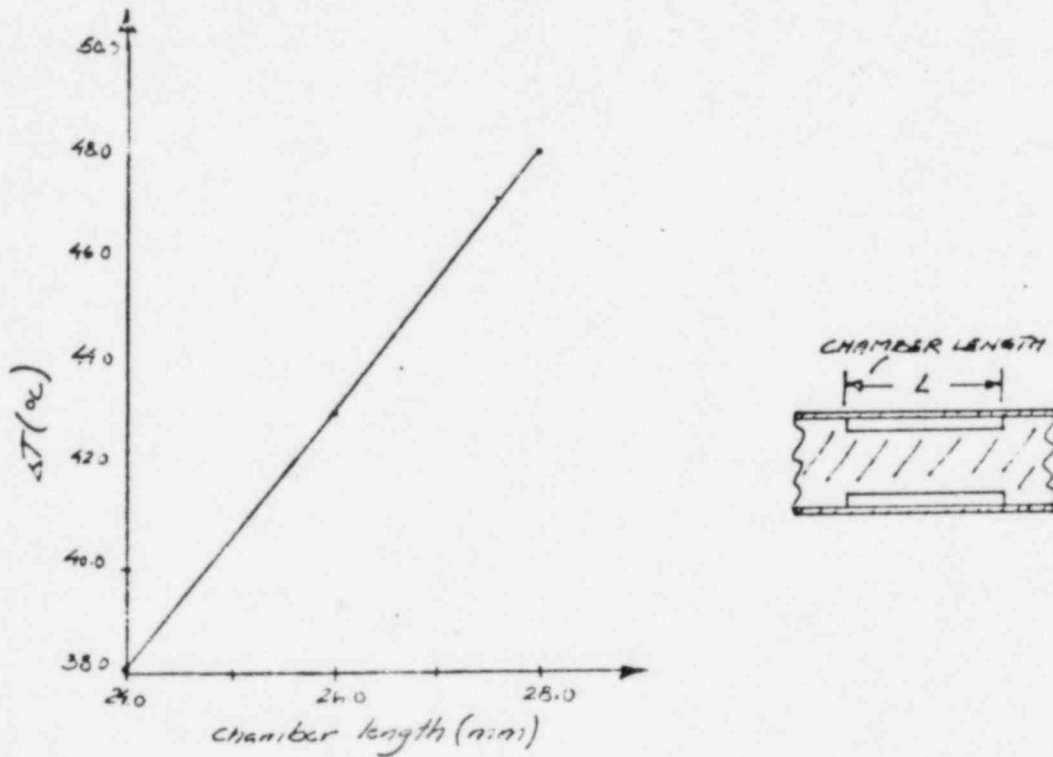


The observed signal is the algebraic difference of the two individual response curves. If the two bath temperatures are well controlled, the experiment also yields *t/c* calibration (i.e., amplitude of the response).

NB! Actual ORNL tests were done from a stirred 20°C bath to a stirred 100°C bath. See section 3.4.1.

FIGURE 3.1 - 9

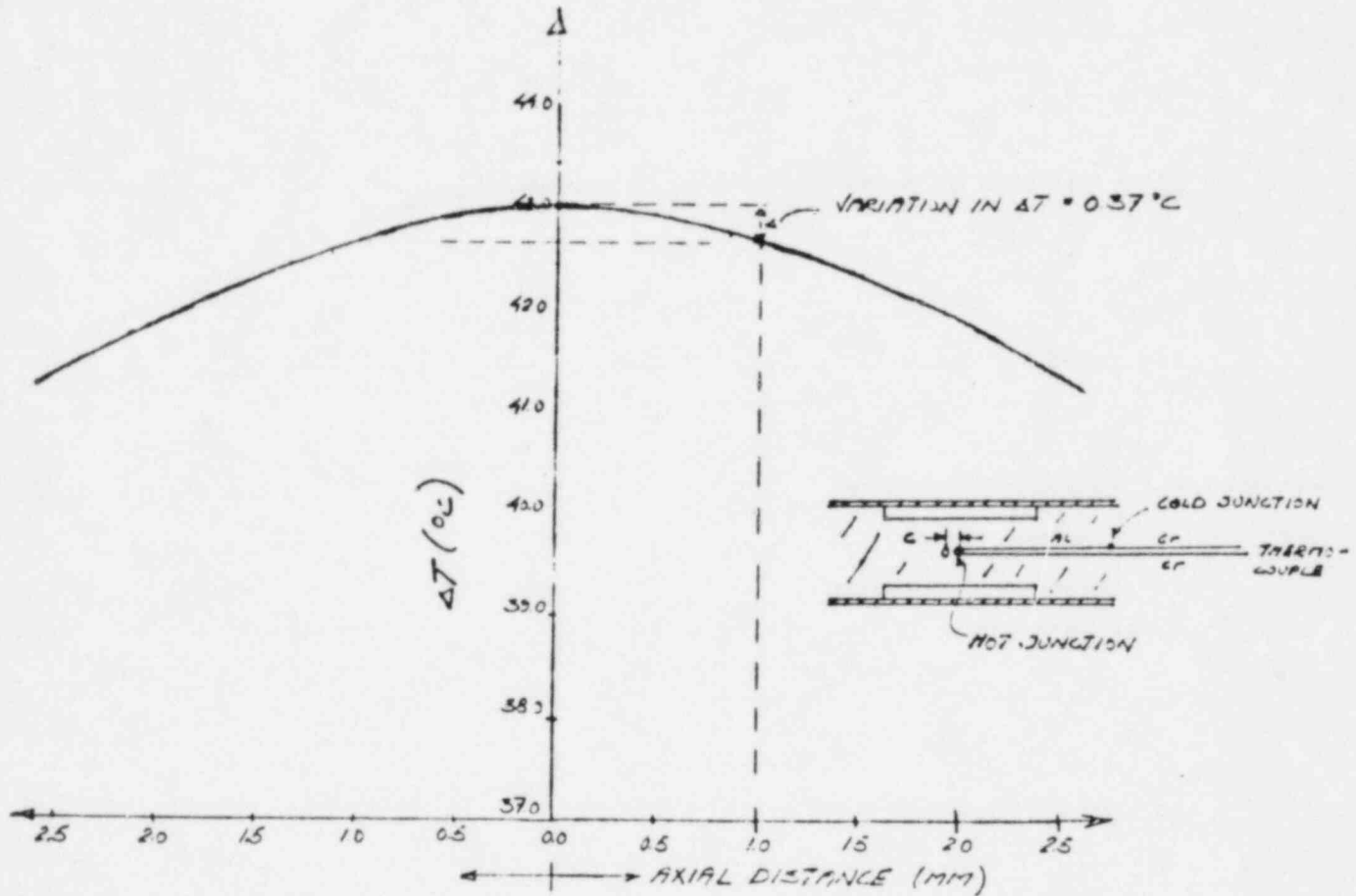
EFFECT OF CHAMBER LENGTH VARIATIONS ON ΔT AT 300°C



The figure shows how the output signal ΔT changes if the chamber length is varied by ± 2 mm around 26 mm. It is worth noticing the linear relationship between ΔT and chamber length. At this particular length the gas conduction is important to the degree that response is no longer proportional to L^2 .

FIGURE 3.1 - 10

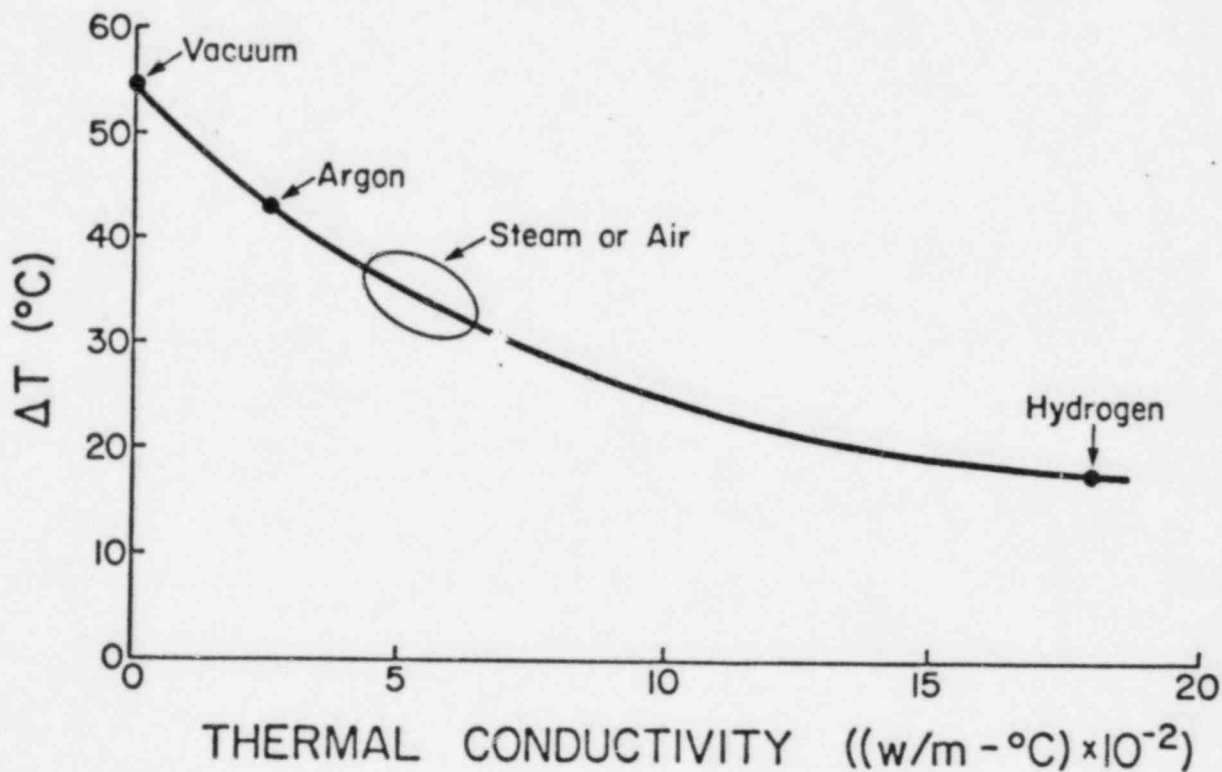
EFFECT OF AXIAL DISLOCATION ON HOT
JUNCTION IN ΔT



The figure shows the axial temperature distribution in the RGT sensor. It is seen from the figure that, as the curve is rather flat in the region of the hot junction, minor displacement of the junction in axial direction does not influence the signal very much. Tolerances of ± 0.25 mm are held in practice.

FIGURE 3.1-11

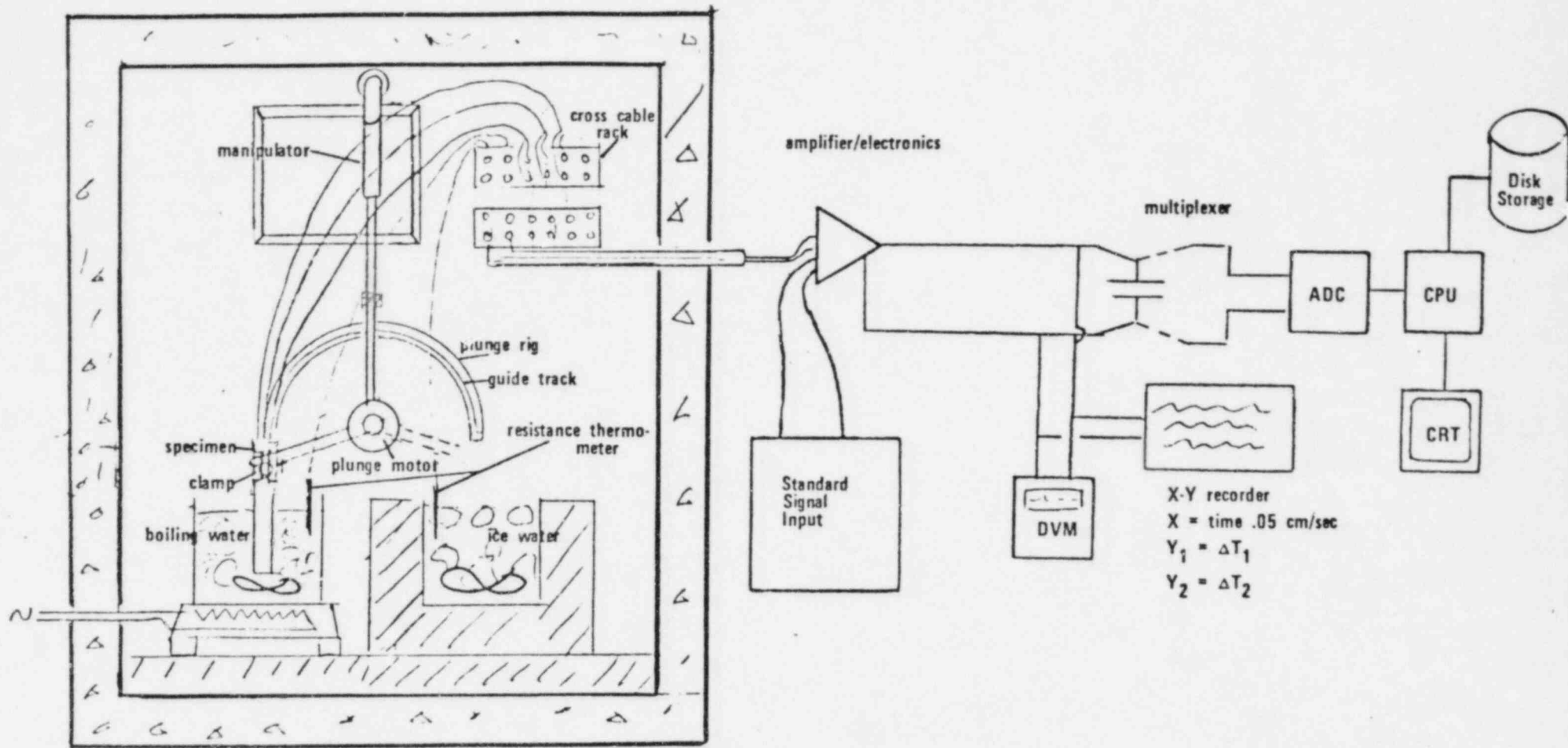
EFFECT OF CHAMBER GAS FILLING ON ΔT
 WITH 300° C SINK
 TEMPERATURE



The figure shows how various types of gas filling influence the sensor signal ΔT . Conductivity is independent of pressure, over a wide range (10⁻⁴ to 10 ata). A consequence of this is with 2 ata of argon and 10⁻³ ata of hydrogen the conduction is dominated by argon. With pure hydrogen, however, even at 10⁻⁴ ata, the sensitivity would be only 20° C/watt/gm.

FIGURE 3.1 - 12

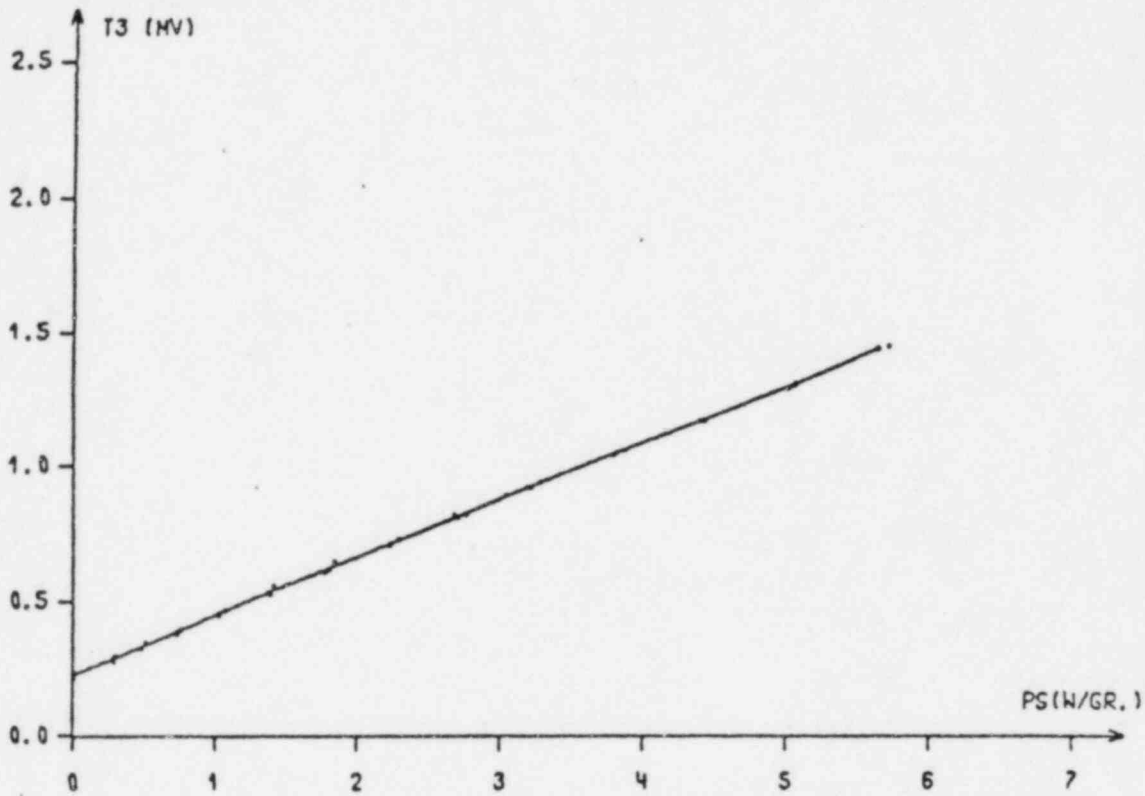
EXPERIMENTAL SET-UP FOR HOT-LAB PLUNGE TESTS AT ORNL



The figure shows the experimental set-up specified for the plunge testing in hot lab of R G T specimens at ORNL. In the test the specimens will be quickly transferred from ice bath (0°C) to a boiling water bath (100°C).

FIGURE 3.1 - 13

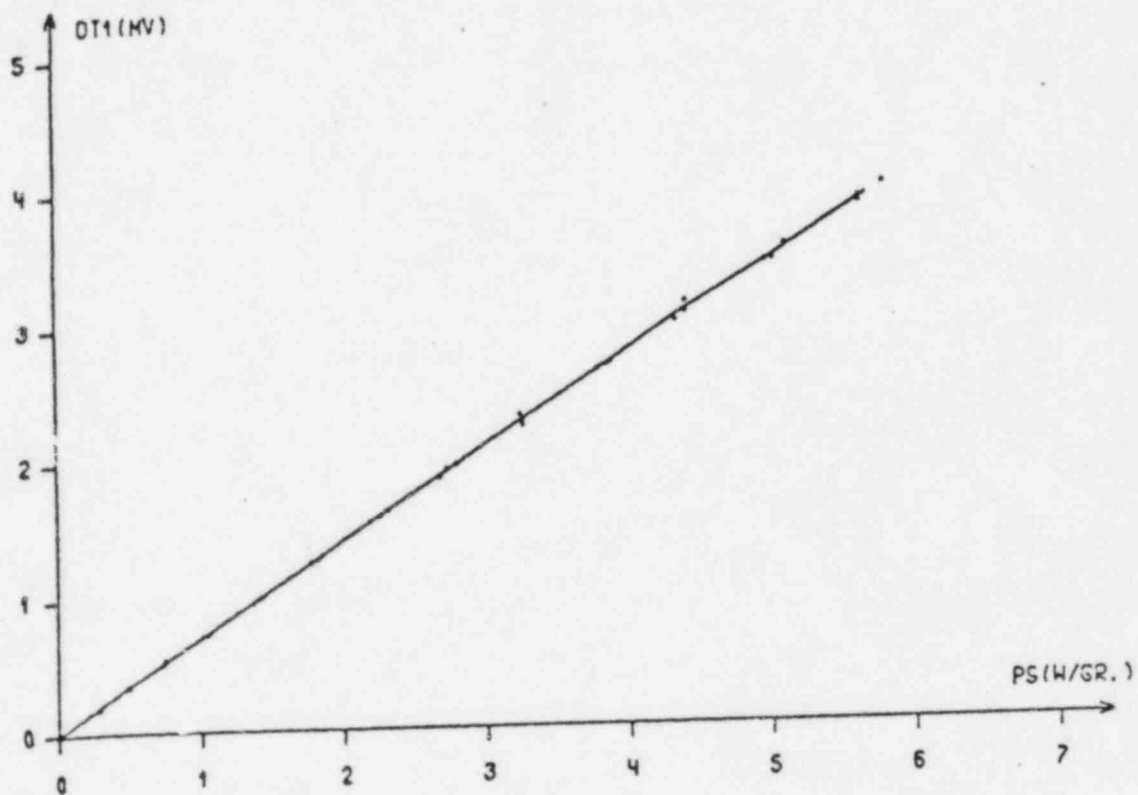
CALIBRATION OF γ RGT PROTOTYPE AT IFA (AIR-FILLING)



Figures 3.1-13 through 3.1-17 show results from electrical calibration of an early prototype of the RGT. The critical experiments done by ScP/IFA established methods of manufacture, tested failure mechanisms, and exposed specimens to severe thermal cycling ($\sim 550^{\circ}\text{C}$). The direct electrical calibration techniques were piloted.

FIGURE 3.1 - 14

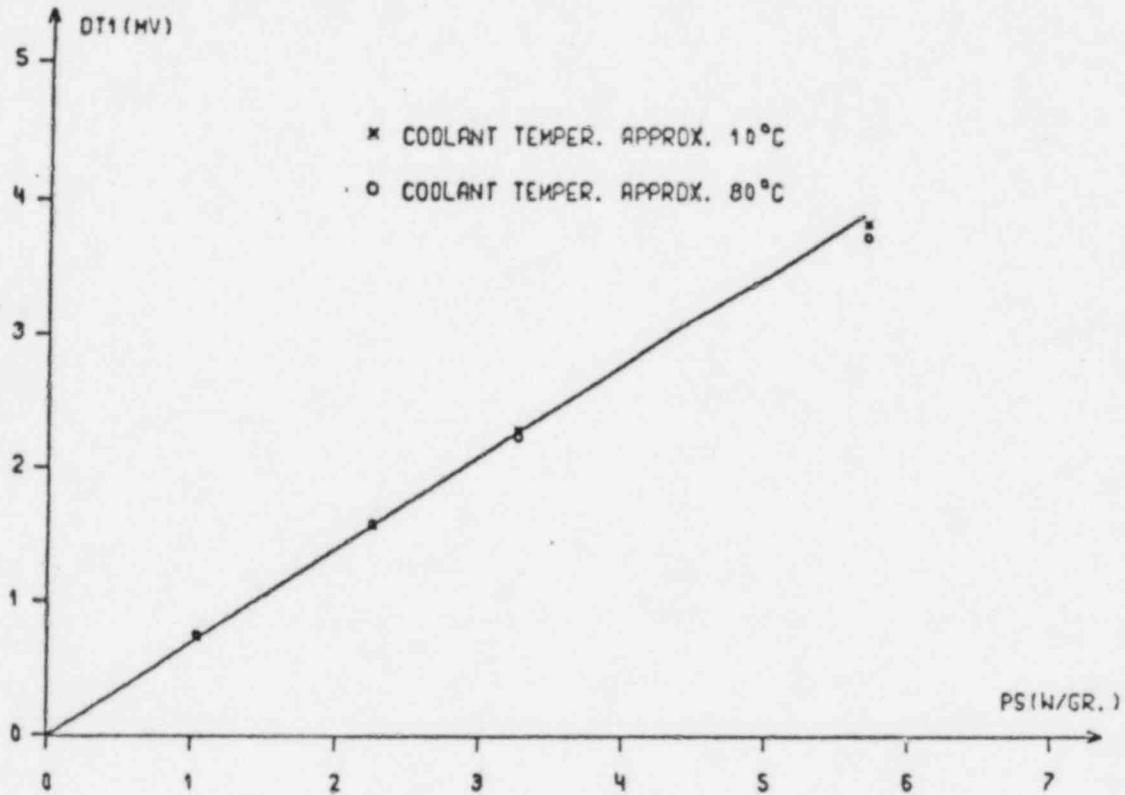
CALIBRATION OF γ RGT PROTOTYPE AT IFA (VACUUM FILLING)



An evacuated chamber doubles the signal over the air filled chamber but in PWR environment, an evacuated chamber quickly fills with hydrogen which penetrates the stainless steel jacket tube until equilibrium with partial pressure in the coolant is reached.

FIGURE 3.1 - 15

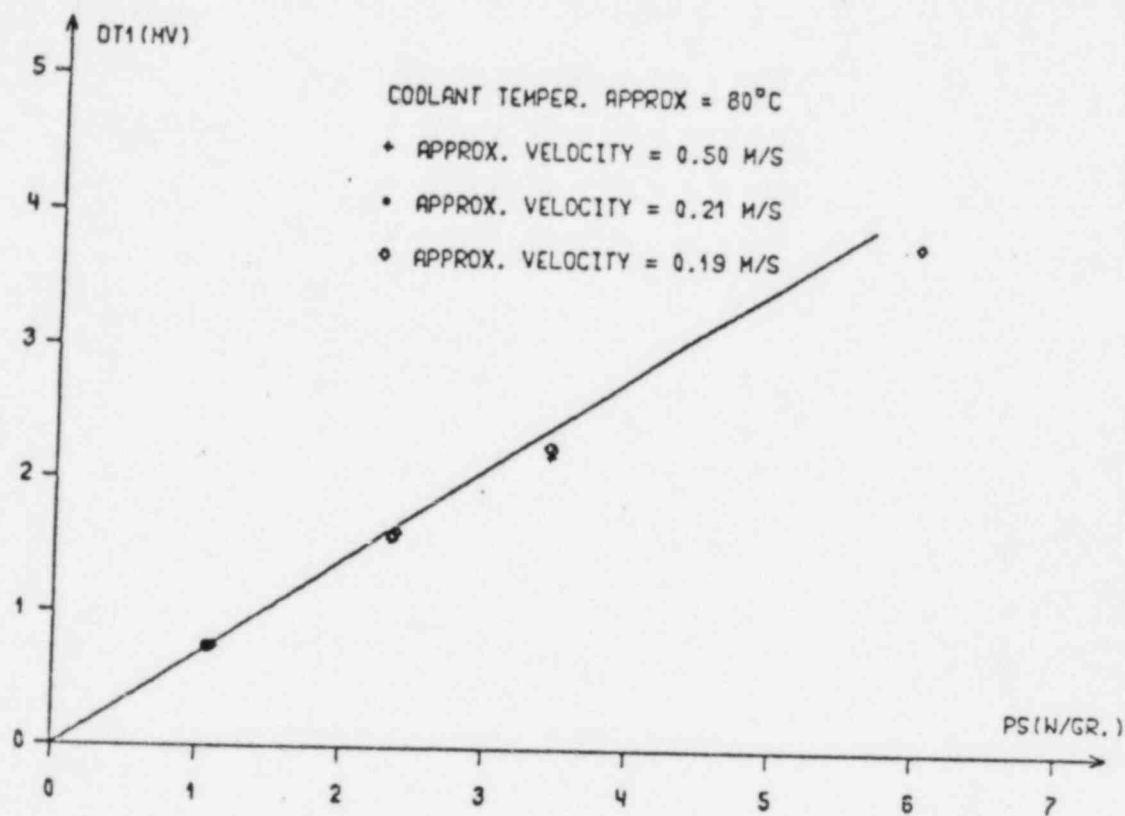
CALIBRATION OF γ RGT PROTOTYPE AT IFA (EFFECT OF COOLANT TEMPERATURE)



Over the 40°C range of coolant temperatures which occur in a PWR, the change in sensitivity is slightly larger than between 10° and 80° but it is very closely predictable.

FIGURE 3.1 - 16

CALIBRATION OF γ RGT PROTOTYPE AT IFA (EFFECT OF VERY LOW COOLANT VELOCITY)

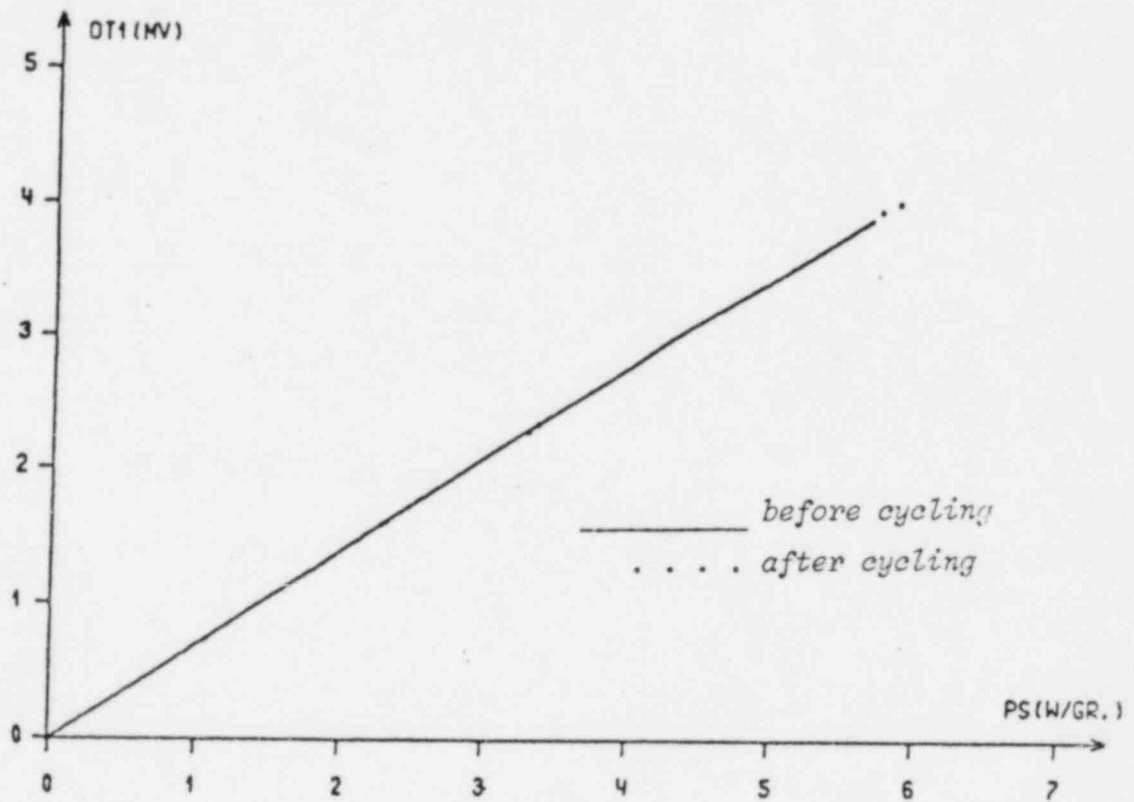


Calibration does not begin to depend upon coolant velocity until velocity is lower than 0.2 m/sec. In the curve above, both power and velocity are varied below 0.5 m/sec. The velocity of coolant in the PWR case is 1.3 m/sec.

FIGURE 3.1 - 17

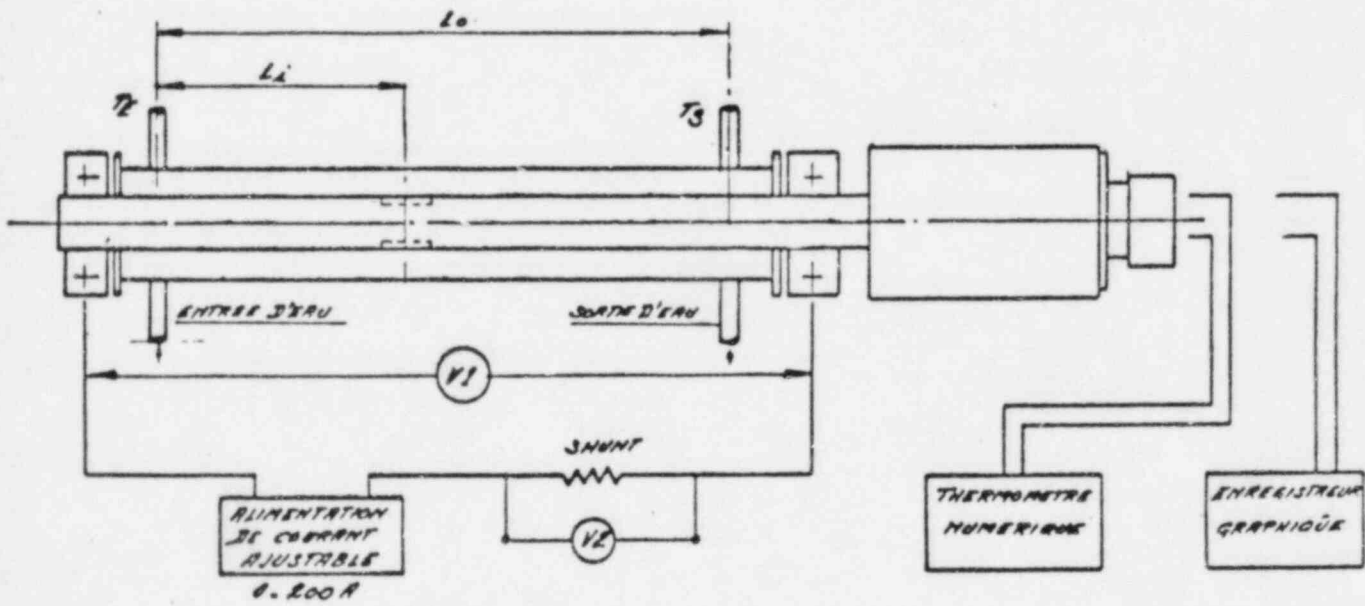
CALIBRATION OF γ RGT PROTOTYPE AT IFA

VACUUM FILLED SENSOR RECALIBRATED AFTER 5 THERMAL CYCLINGS UP TO 450°C



Severe thermal cycling did not affect calibration

FIGURE 3.1 - 18
 INTERTECHNIQUE TEST LOOP



EQUIPEMENT DE CALIBRATION
ELECTRIQUE

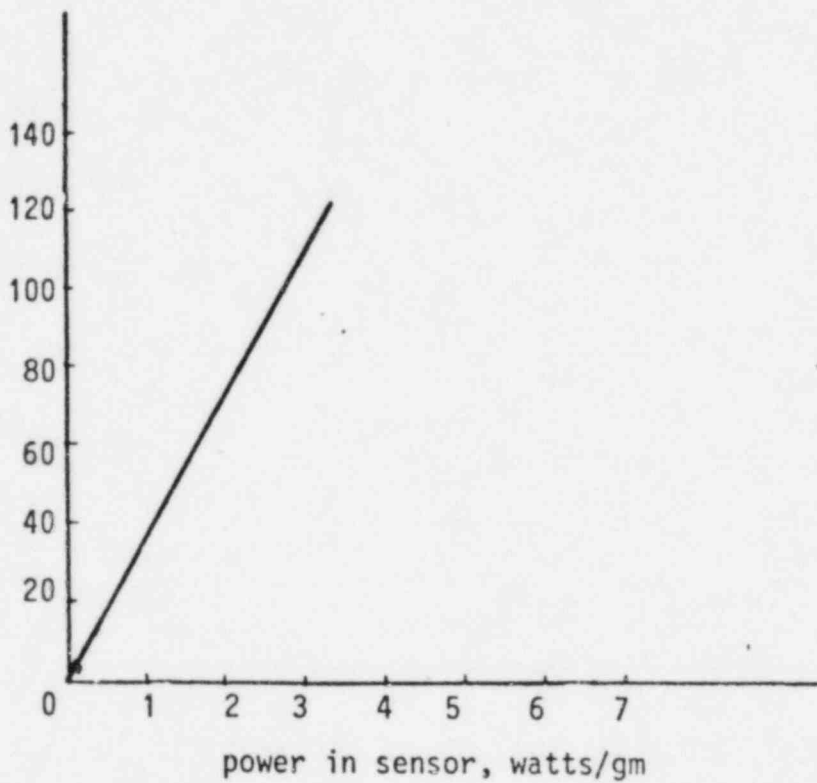
TECHNIQUE
 INTERNATIONAL

Ce document est la propriété de "INTERTECHNIQUE" et ne peut être reproduit ou communiqué sans autorisation.

FIGURE 3.1 - 19

$$\text{signal } \frac{\mu\text{V}}{40.6} = \text{ }^{\circ}\text{C}$$

$$\text{Best fit } S = 38.47$$



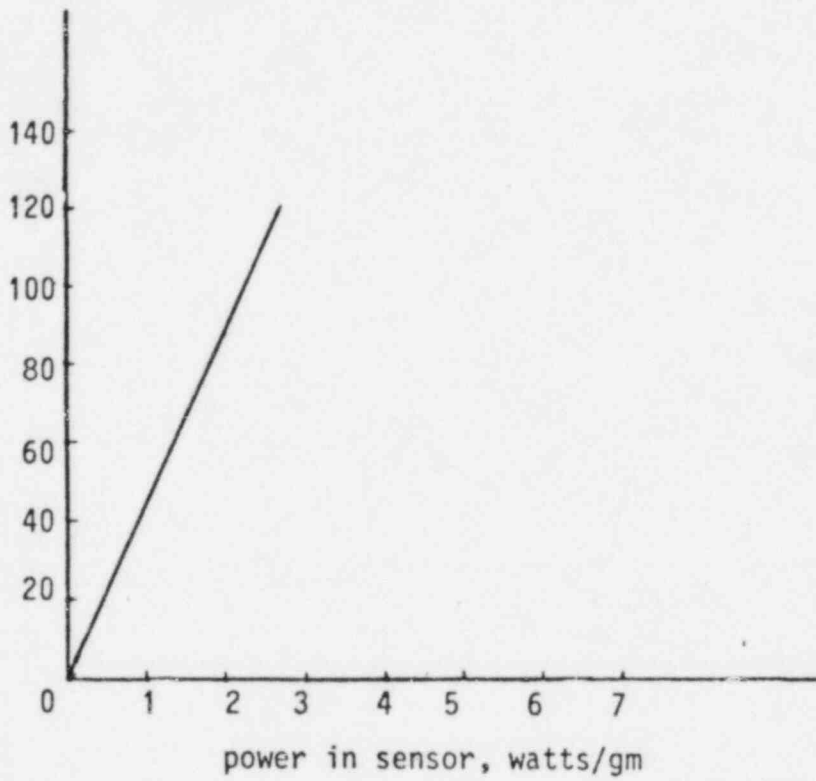
CANNE NO. 4, SENSOR NO. 1

Figures 3.1-19 through 3.1-27 show the low temperature electrical calibration of the sensors in Canne No. 4. Scatter of data around best fit line is too small to see. Variations in sensor-to-sensor sensitivity (slope) have been greatly improved for later cannes. See table 3.2-3. Overall sensitivity variation for 10 RGTAs (90 sensors) is 3.67%.

FIGURE 3.1 - 20

signal $\frac{\mu V}{40.6} = ^\circ C$

Best fit $\delta = 42.34$

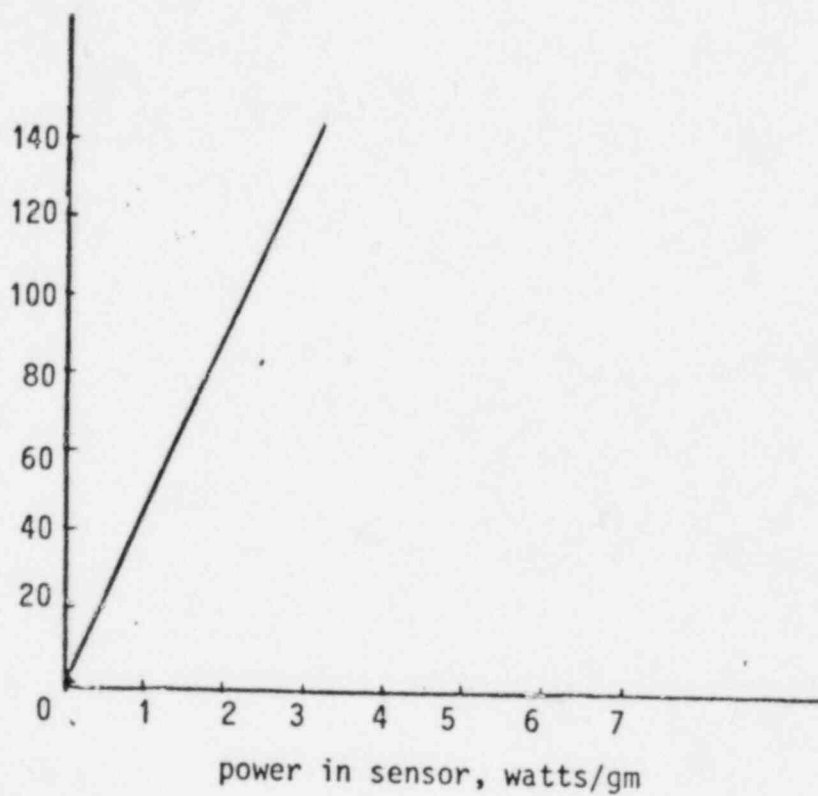


CANNE NO. 4, SENSOR NO. 2

FIGURE 3.1 - 21

signal $\frac{\mu V}{40.6} = ^\circ C$

Best fit S = 41.70

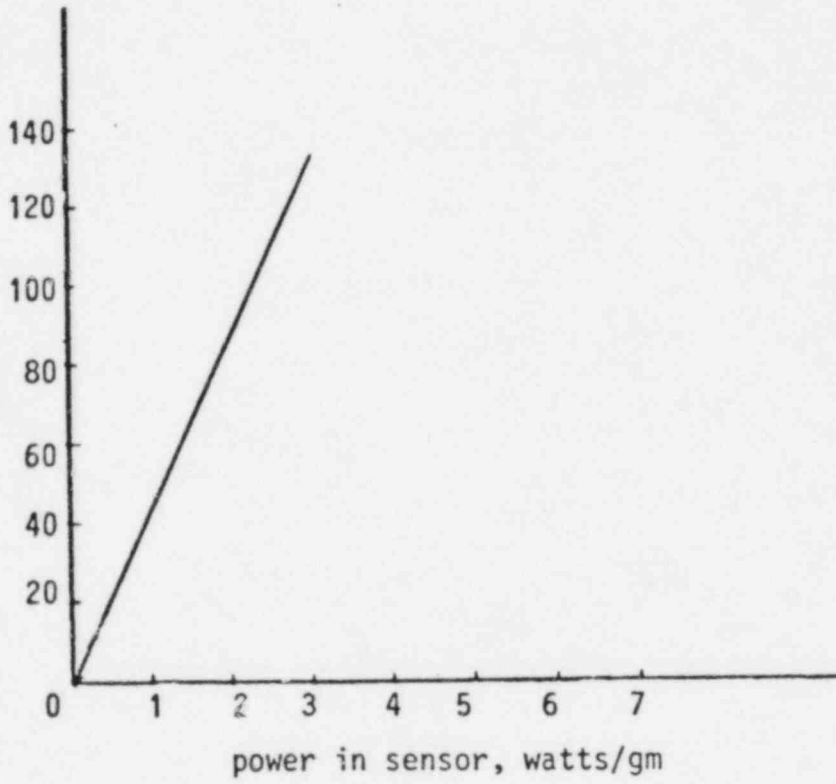


CANNE NO. 4, SENSOR NO. 3

FIGURE 3.1 - 22

signal $\frac{\mu\text{V}}{40.6} = \text{ }^{\circ}\text{C}$

Best fit S = 40.66

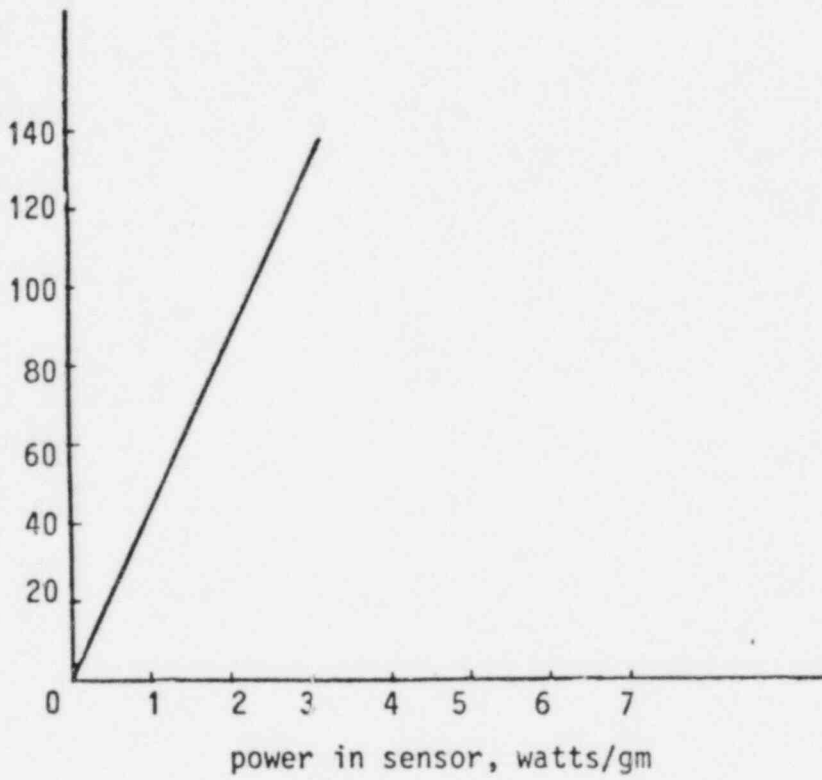


CANNE NO. 4, SENSOR NO. 4

FIGURE 3.1 - 23

signal $\frac{\mu\text{V}}{40.6} = \text{ }^{\circ}\text{C}$

Best fit S = 42.89

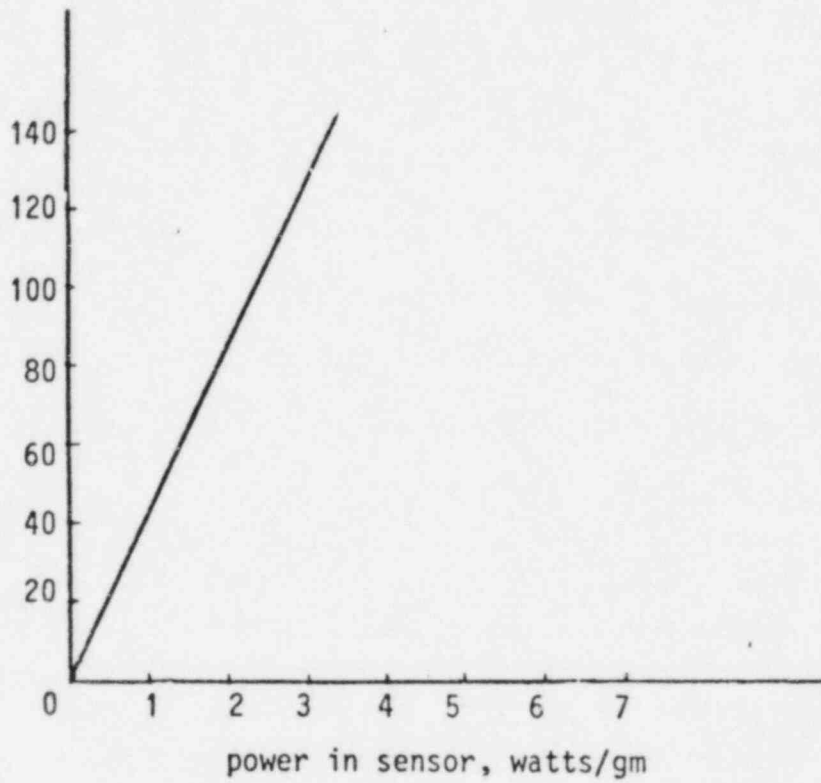


CANIE NO. 4, SENSOR NO. 5

FIGURE 3.1 - 24

signal $\frac{\mu\text{V}}{40.6^\circ\text{C}} = \text{ }^\circ\text{C}$

Best fit S = 42.68

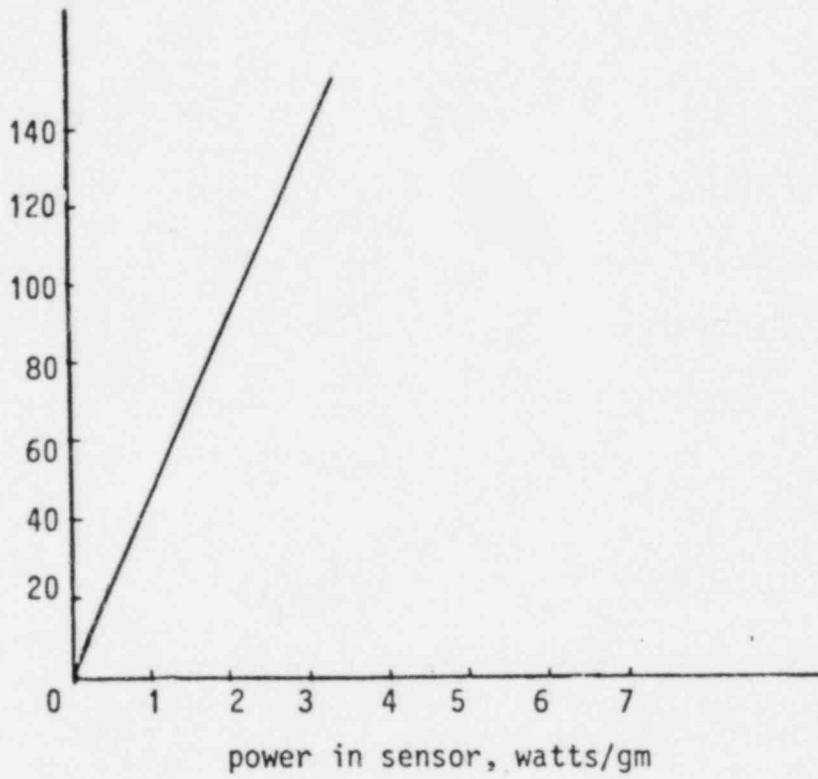


CANNE NO. 4, SENSOR NO. 6

FIGURE 3.1 - 25

signal $\frac{\mu V}{40.6} = ^\circ C$

Best fit S = 42.70

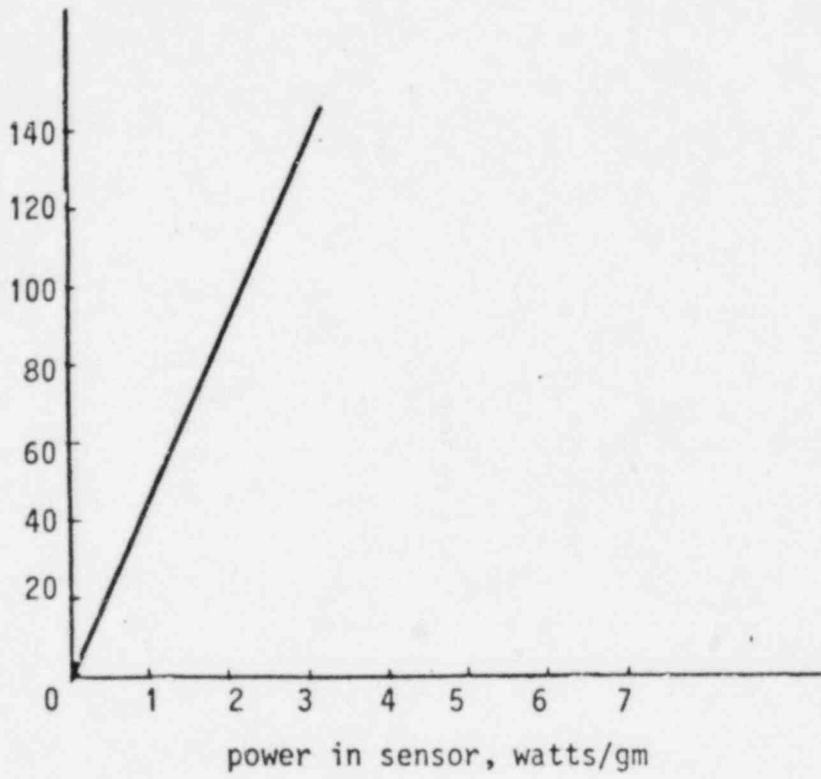


CANNE NO. 4, SENSOR NO. 7

FIGURE 3.1 - 26

signal $\frac{\mu\text{V}}{40.6} = \text{ }^{\circ}\text{C}$

Best fit S = 41.09

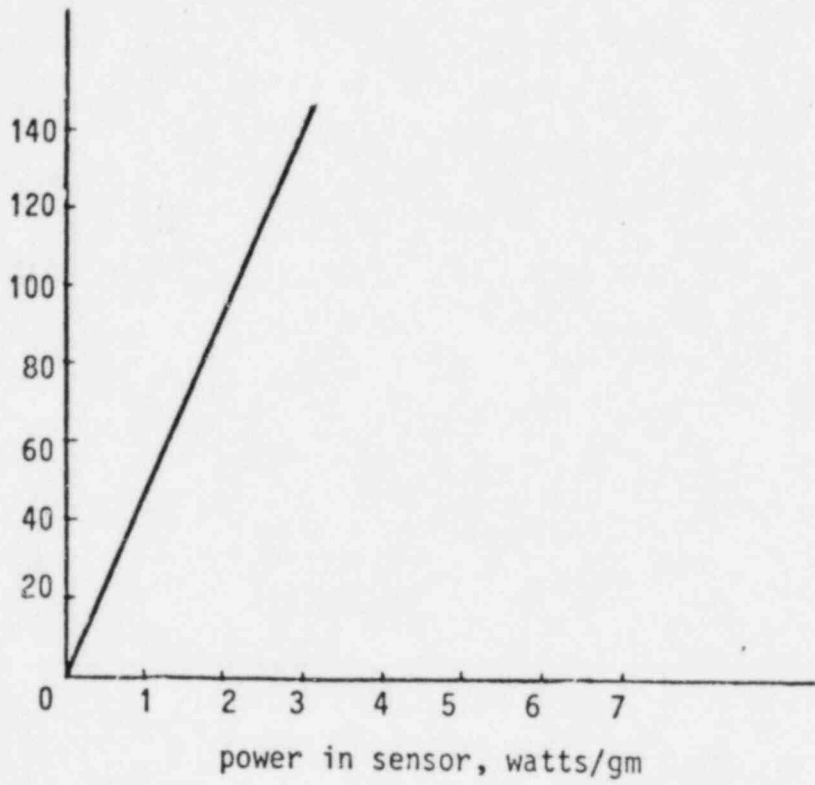


CANNE NO. 4, SENSOR NO. 8

FIGURE 3.1 - 27

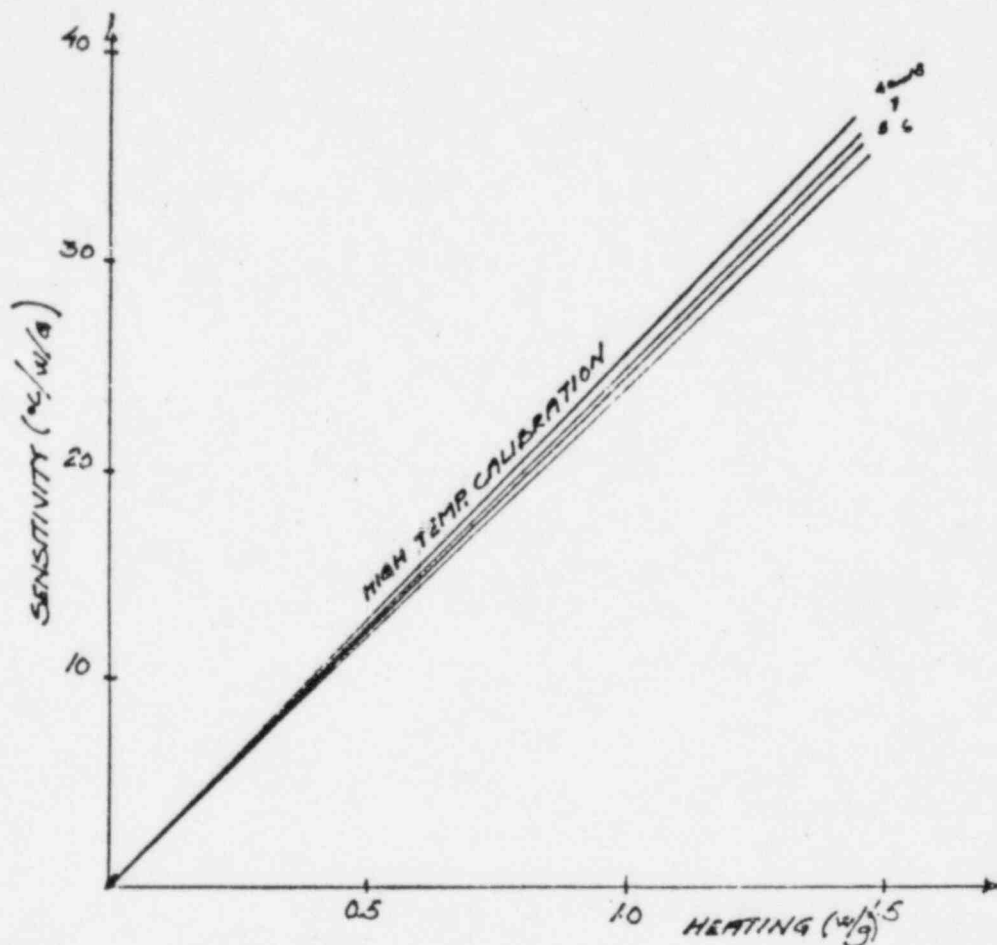
signal $\frac{\mu\text{V}}{40.6} = \text{ }^{\circ}\text{C}$

Best fit S = 44.42



CANNE NO. 4, SENSOR NO. 9

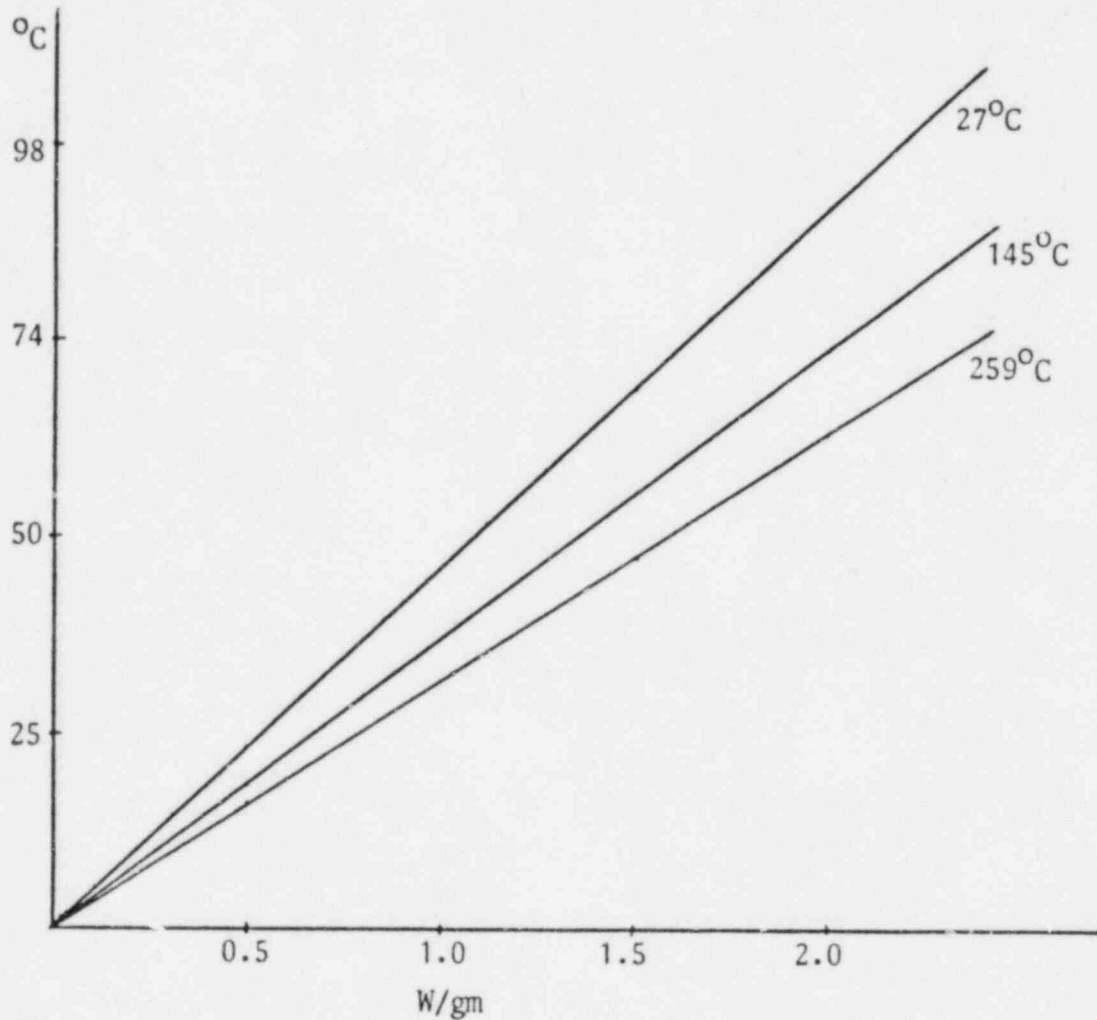
FIGURE 3.1-28: HIGH TEMPERATURE CALIBRATION OF
CANNES NO. 4-8



The figure shows the results of high temperature calibration of Cannes No. 4, 5, 6, 7, 8 - Averages for 9 sensors.

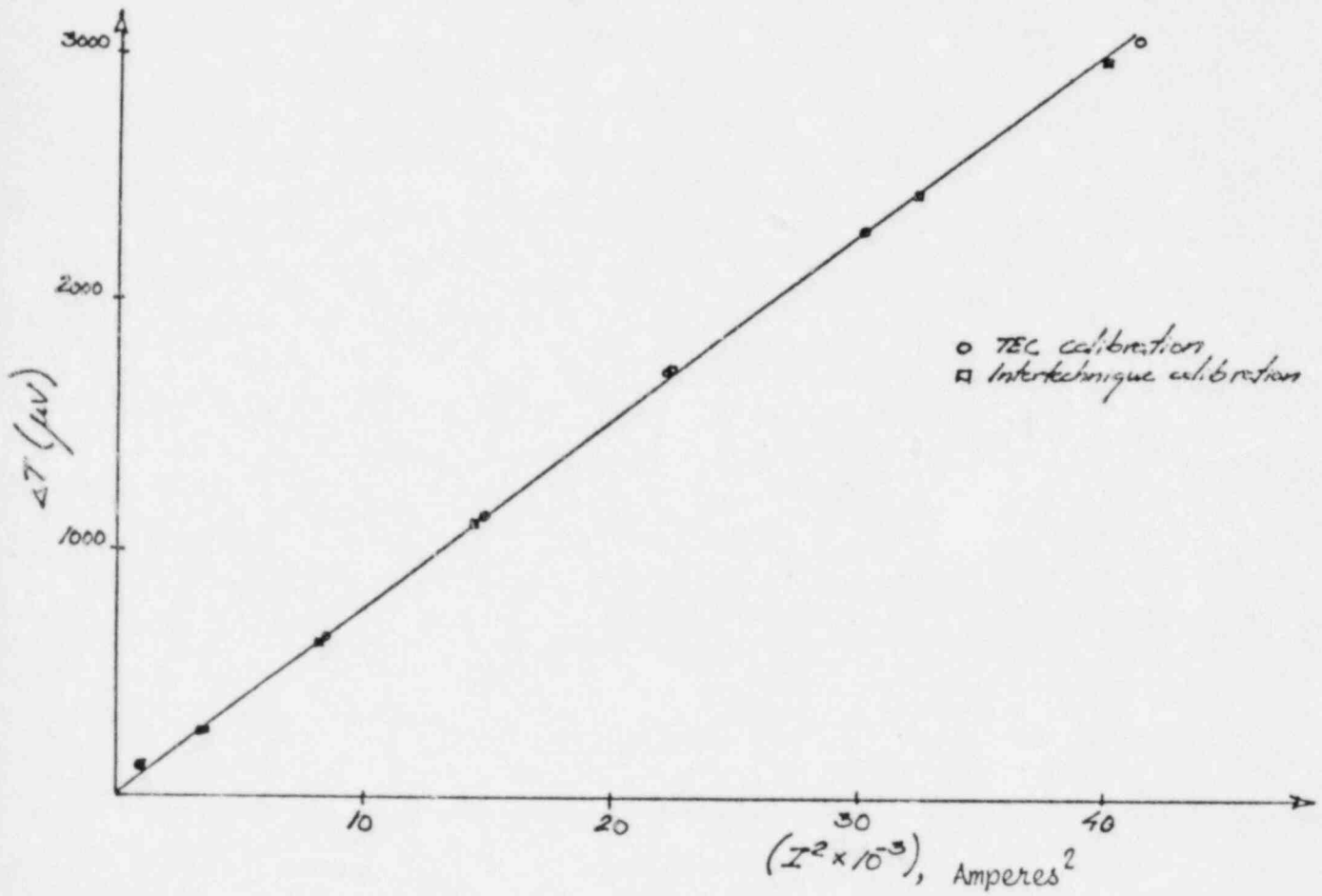
NB! High temperature data are subject to possible systematic revision based on corrections to high temperature resistivities.

FIGURE 3.1-29: EFFECT OF TEMPERATURE ON THE ELECTRICAL CALIBRATION



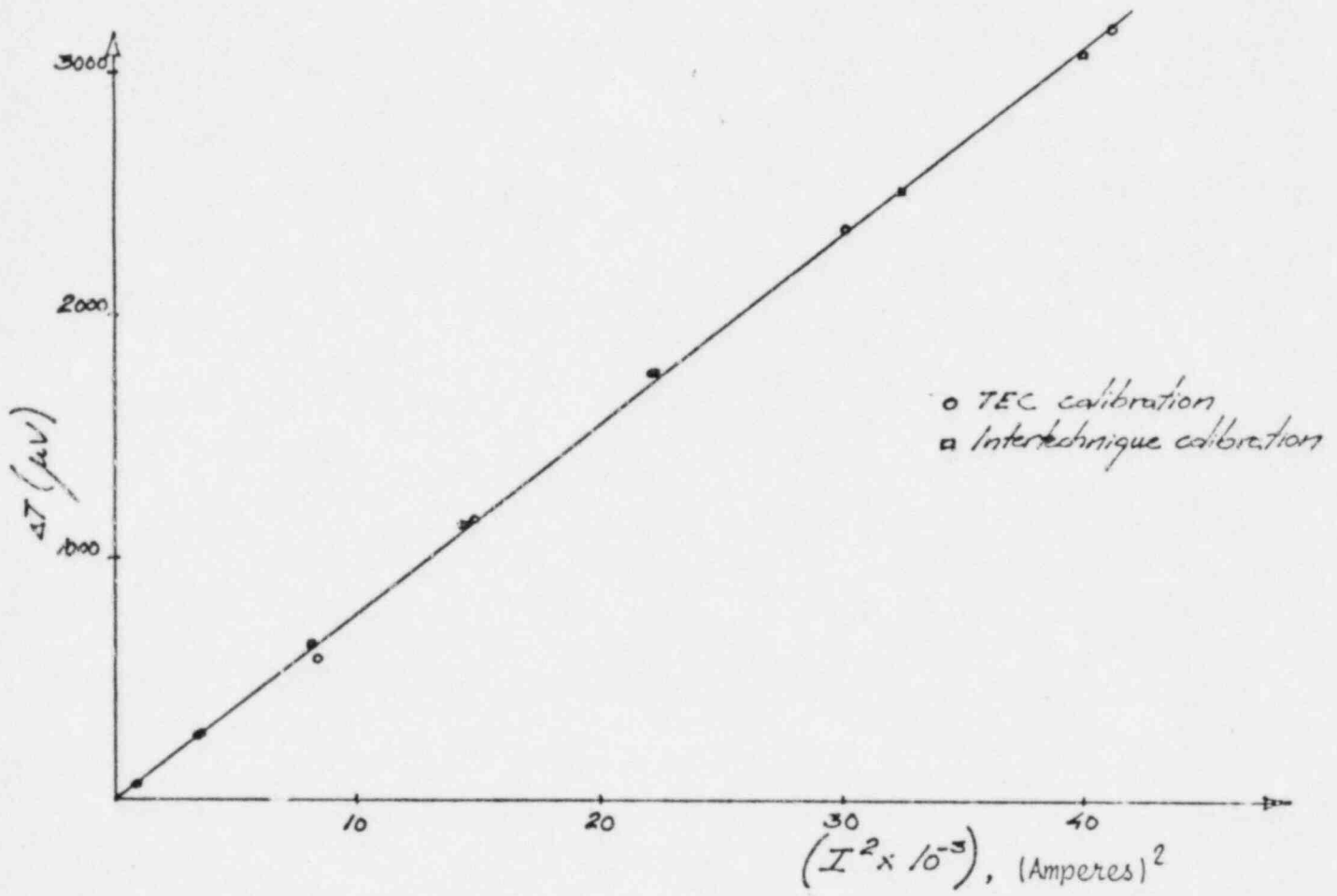
The figure shows the calibration of one of the sensors in Canne 2 at different temperatures. The lower sensitivity at high temperature due to higher thermal conductivity of the materials is clearly indicated, and is predictable by RADCAL/THERMAL. Note that in-reactor coolant temperature variation is quite small compared to this range.

FIGURE 3.1 - 30
INTERLOOP COMPARISON



Intertechnique specimen no. 1, signal DT 11

FIGURE 3.1 - 31
INTERLOOP COMPARISON



Intertechnique specimen no. 1, signal DT 12

FIGURE 3.2-1: USE OF CALIBRATION VALVE AT HALDEN TO MEASURE FUEL POWER DURING GAMMA THERMOMETER CALIBRATION

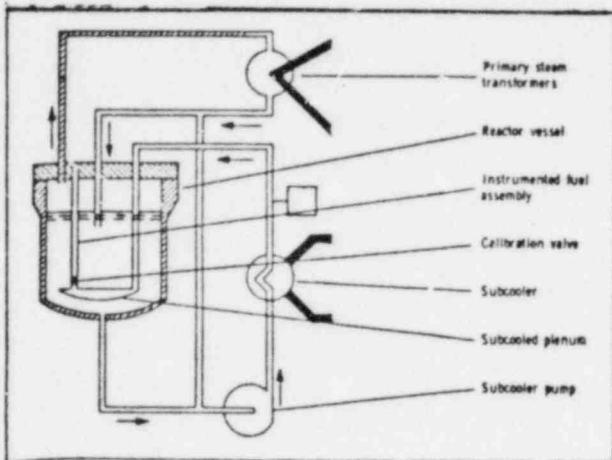


FIG. 1 Simplified HBWR primary circuit diagram, 15 - 20°C subcooled D₂O is available through a plenum chamber below the reactor core.

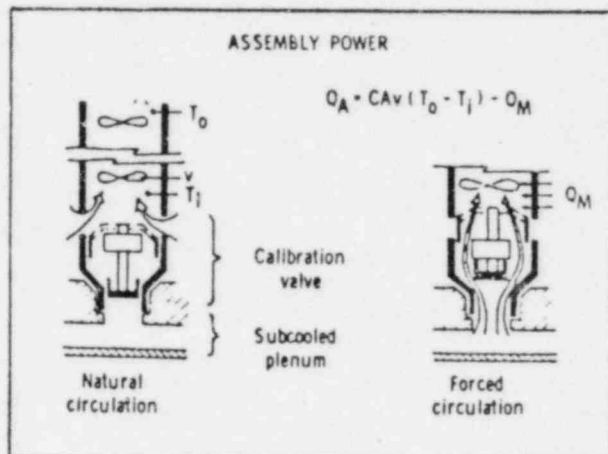


FIG. 2 The calibration valve either permits natural circulation coolant flow or up to 10 tons/hr of forced subcooled flow through a fuel channel.

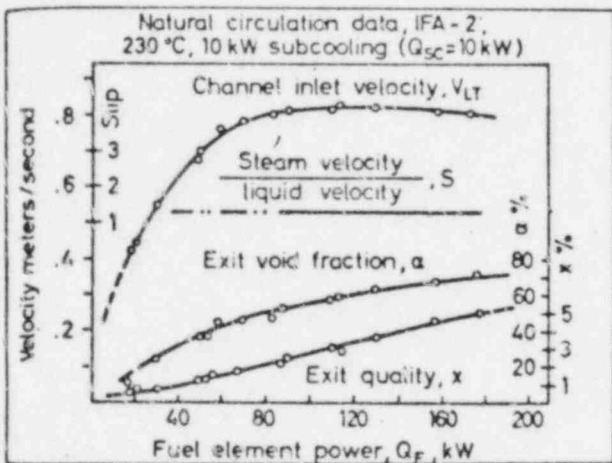


FIG. 3 Measured natural circulation hydraulic data for the instrumented fuel assembly IFA - 2.

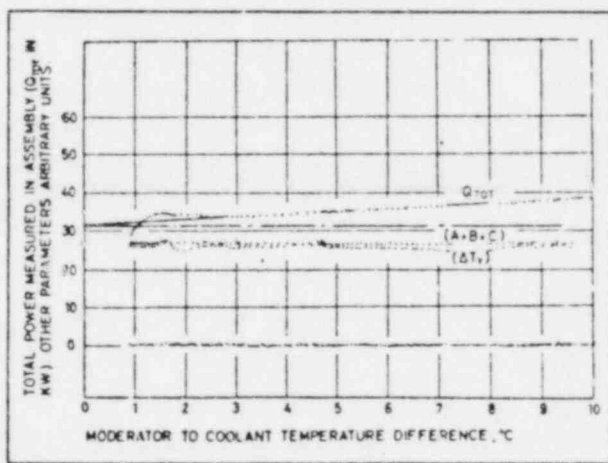


FIG. 4 Experimental determination of heat transfer from the moderator to the instrumented fuel assembly IFA - 4 at 3 MW reactor power and 230°C moderator temperature.

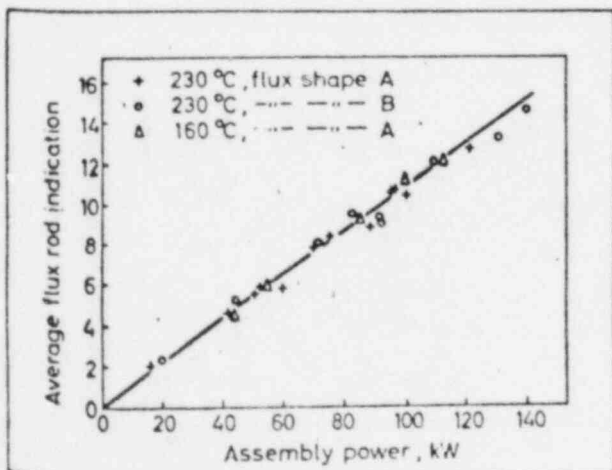


FIG. 5 Flow $\times \Delta T$ measurements in the instrumented fuel assembly IFA - 2, permitted calibration of adjacent flux rod containing three flux chambers against IFA - 2 power.

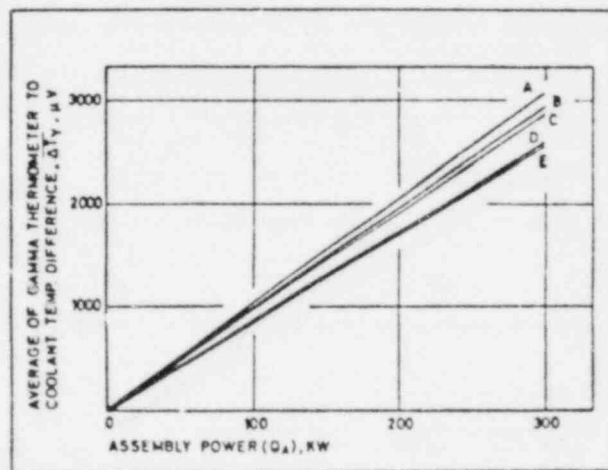


FIG. 6 By means of flow $\times \Delta T$ measurements the gamma thermometers in IFA - 4 was calibrated against power for five different control rod configurations.

FIGURE 3.2-2: DETAILS OF CALIBRATION VALVE

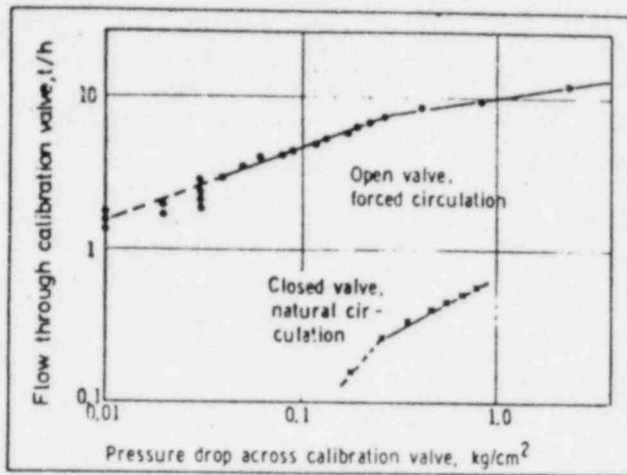


FIG. 7 Flow through fuel channel with open and closed calibration valve as function of pressure difference between subcooled plenum chamber and steam plenum can be used to recheck flow turbine calibration.

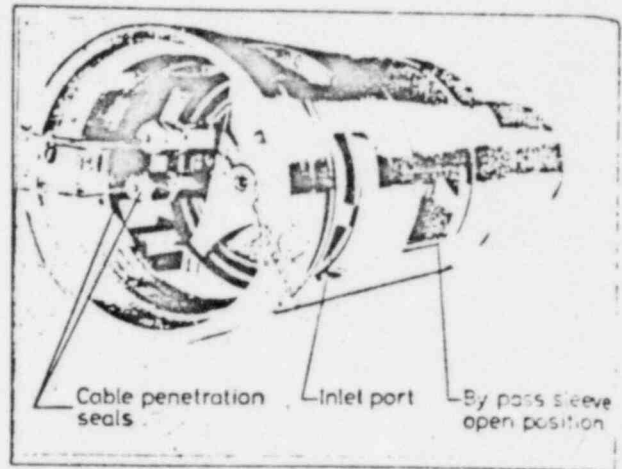


FIG. 9 Photograph showing complete calibration valve assembly ready for mounting at bottom end of instrumented fuel assembly.

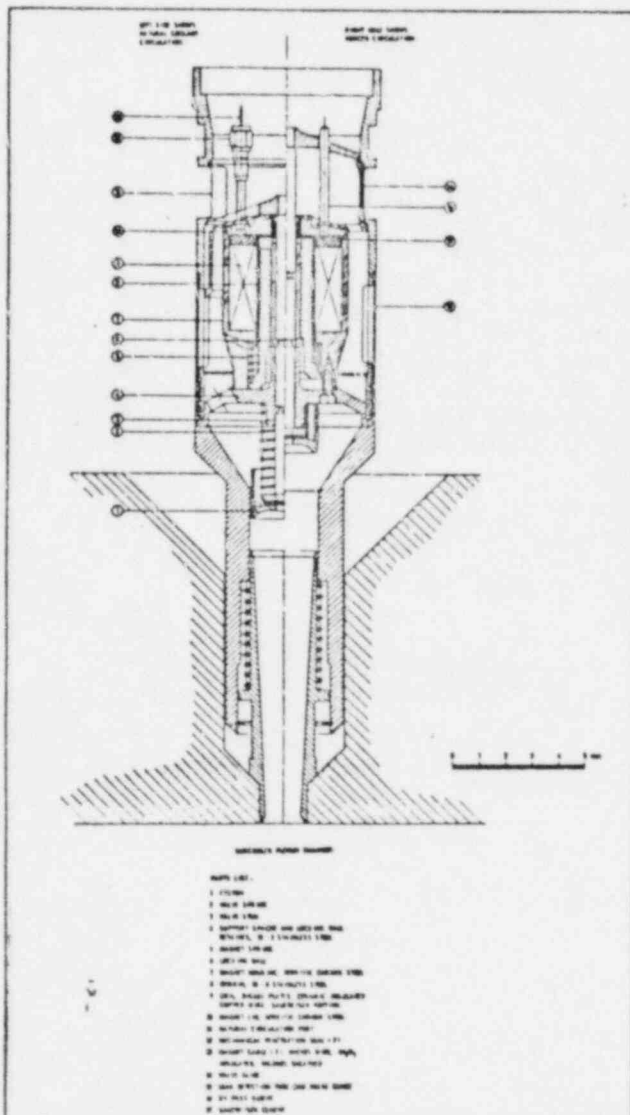


FIG. 8 Technical details of the remotely controlled calibration valve. Two characteristic positions shown.

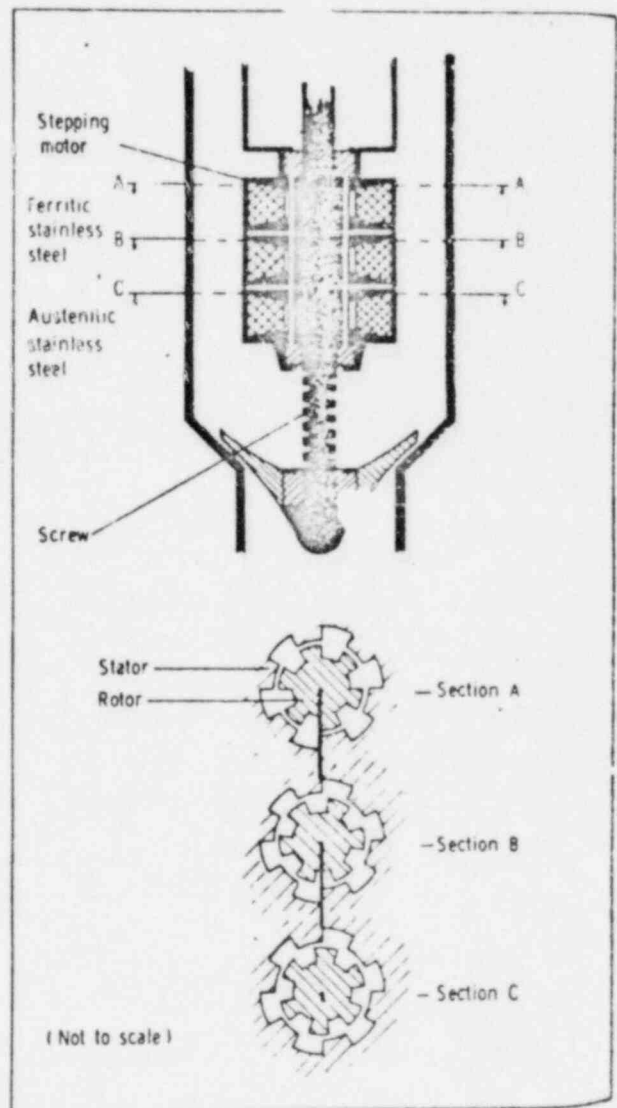
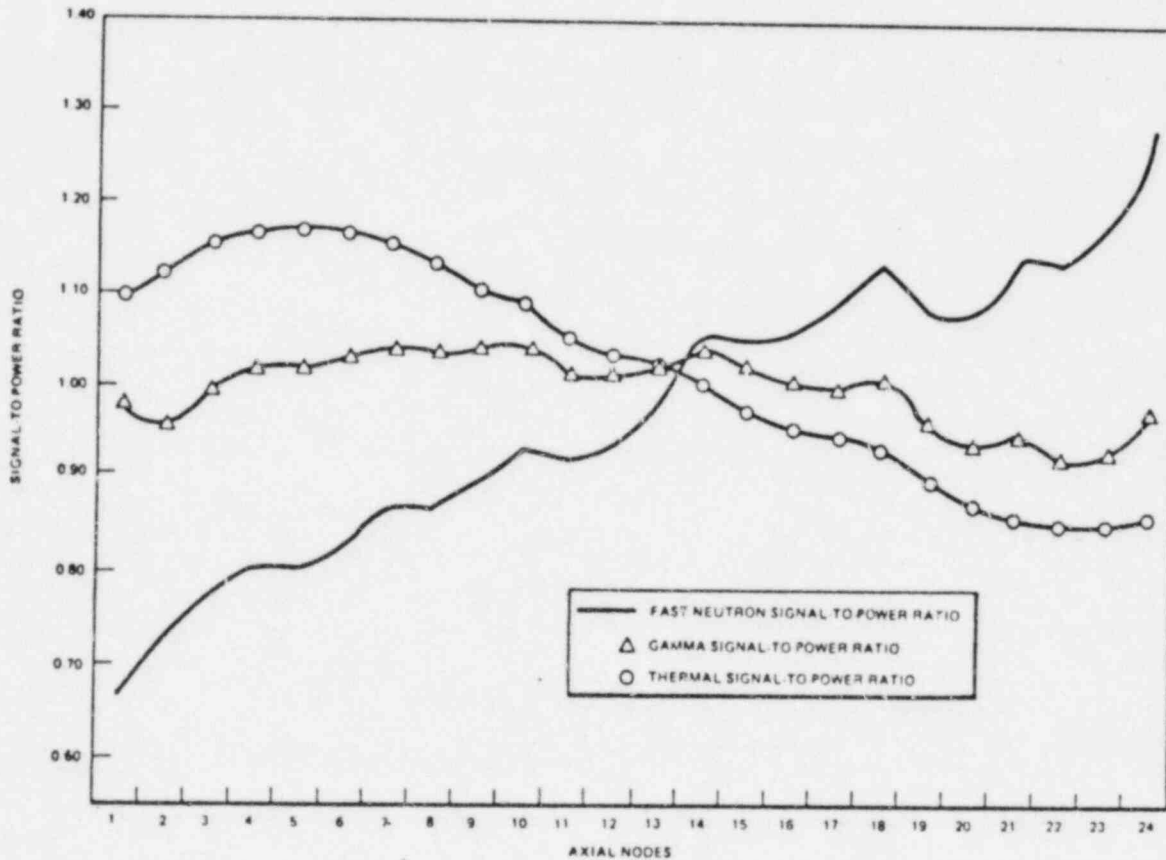


FIG. 10 Proposed design for new calibration valve use lead screw driven by stepping motor.

FIGURE 3.2 - 3

RATIO OF SIGNALS TO POWER
 (Extracted from Hatch 1 Tests)



The ratio of raw signal to ultimate parameter, local fuel power, is a measure of the ultimate "measurement" precision obtainable from the processed signal. In this case the denominator of the ratio is "inexact" because it is the power taken from the neutron TIP signals after processing. The agreement of gamma flux with real local power is even closer.

FIGURE 3.2 - 4

ONE-EIGHTH SECTOR OF 17x 77 FUEL ASSEMBLY
DEFINING PIN ROWS USED IN CEA CALCULATIONS

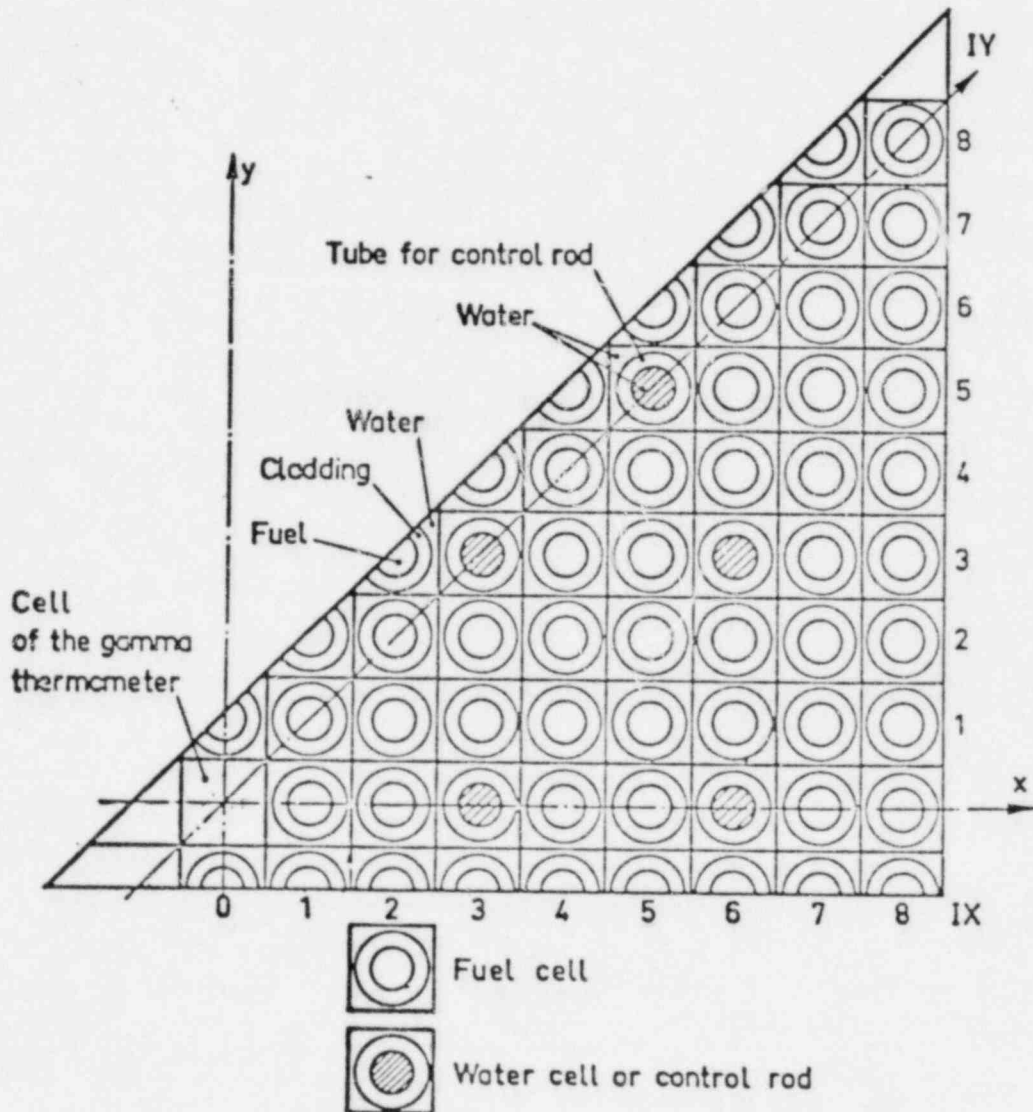
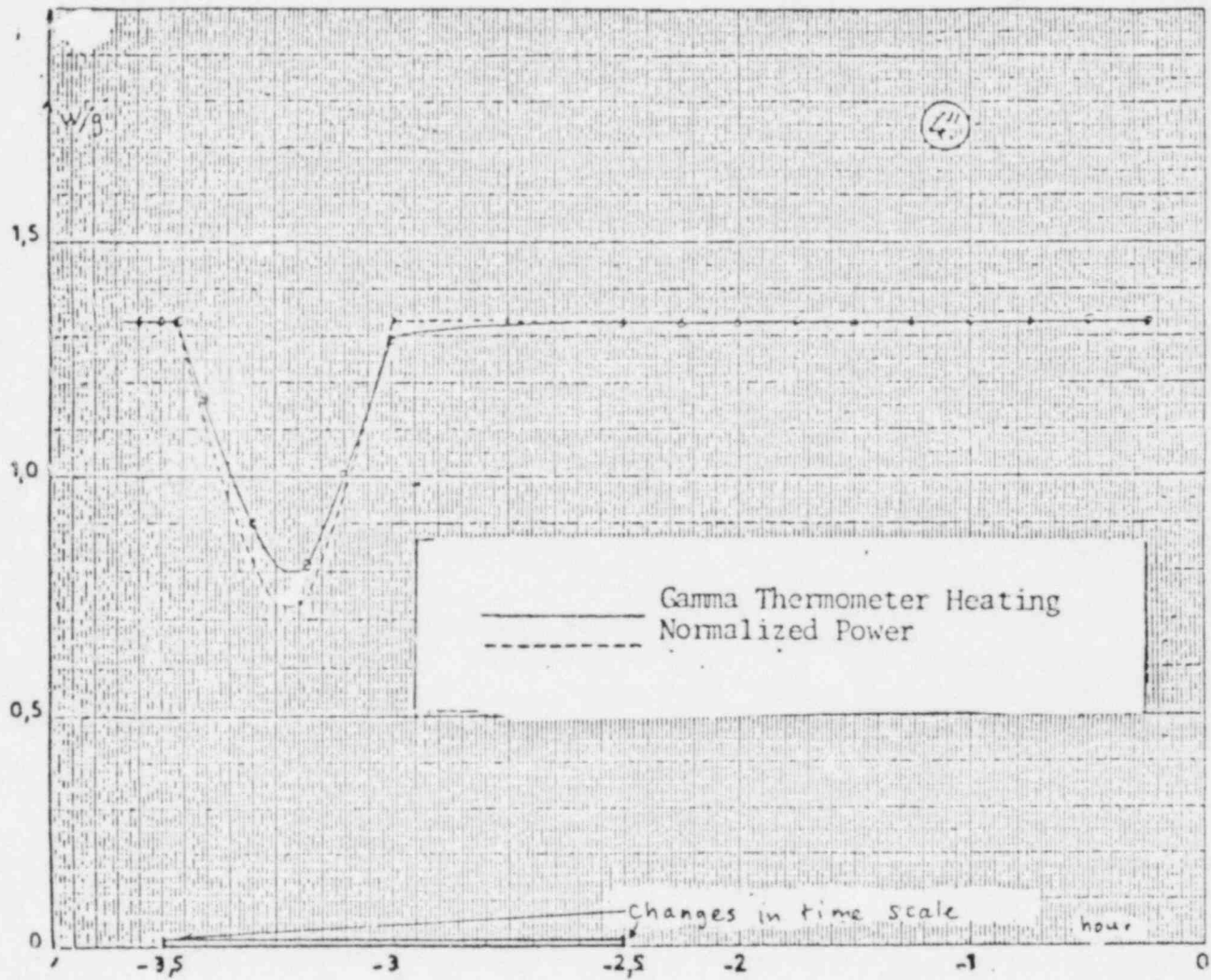


FIGURE 3.2 - 5

INFLUENCE OF A TRANSIENT IN POWER



During the half-hour transient depicted gamma thermometer heating logs actual power giving a 16% excess at the instant of minimum power and a 4% deficiency at the instant of full power restoration. Thirty minutes later heat rate has reached full equilibrium.

FIGURE 3.2 - 6

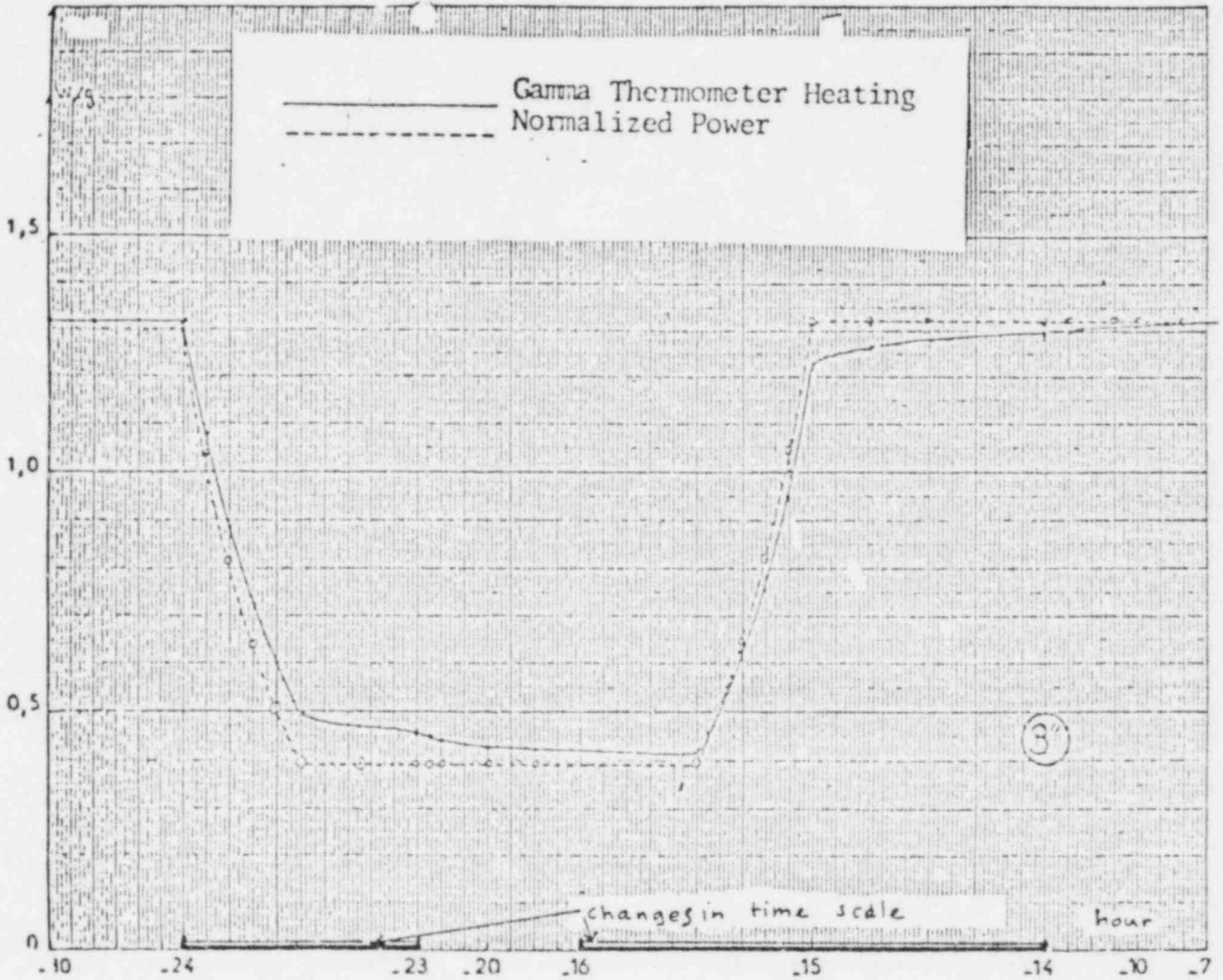
SENSOR HEAT RATE FOLLOWING INSTANT RISE TO FULL POWER



Signal is 72% instantly, 84% in six minutes in this hypothetical case where no fission product contribution is present at time zero and power rise is instantaneous.

FIGURE 3.2 - 7

DYNAMIC RESPONSE OF SENSOR HEATING
TO 8 HOUR LOAD REDUCTION



In this case the low power excess signal is a maximum of 10% and the high power deficit is 7%, dropping to 3.5% 20 minutes after power is restored.

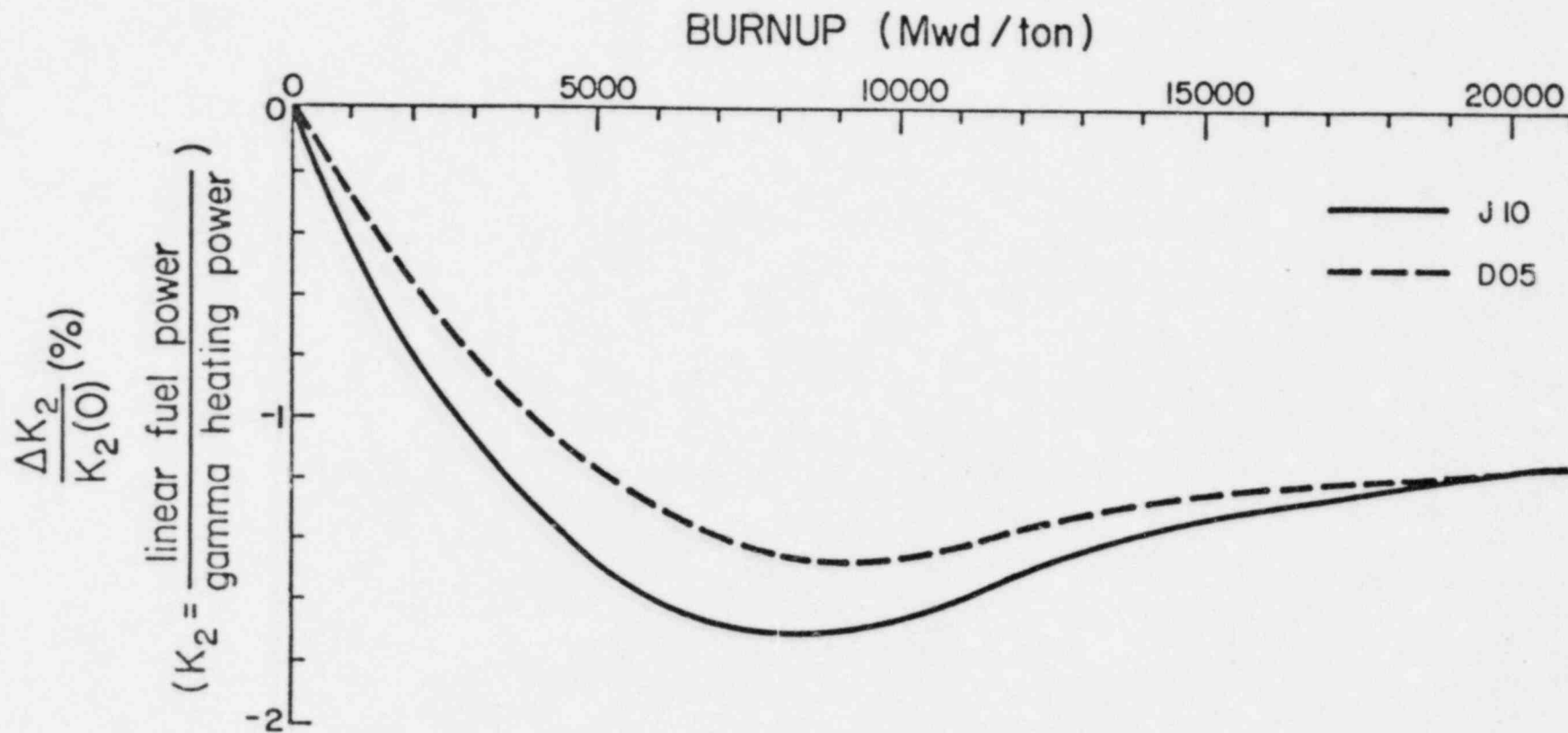
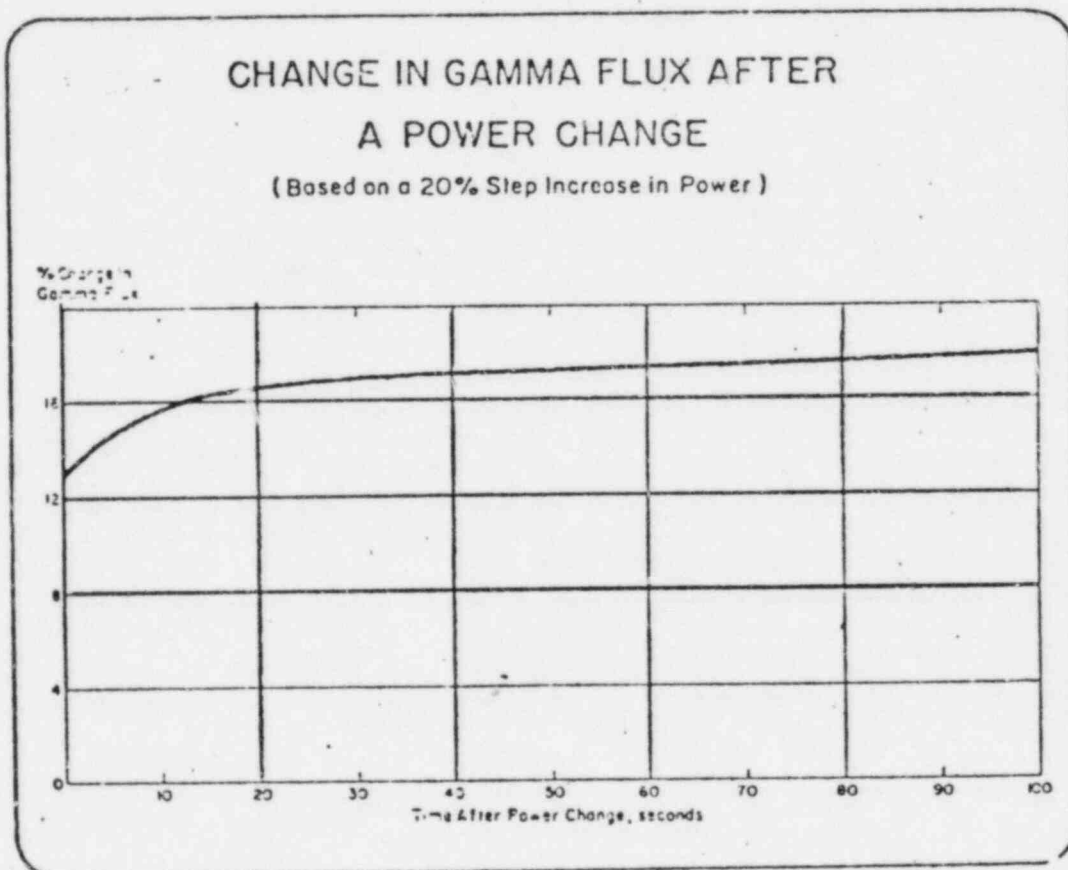


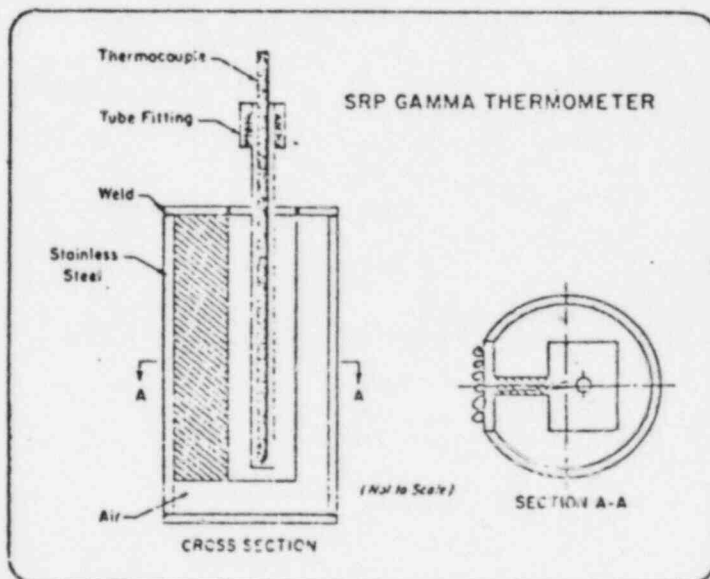
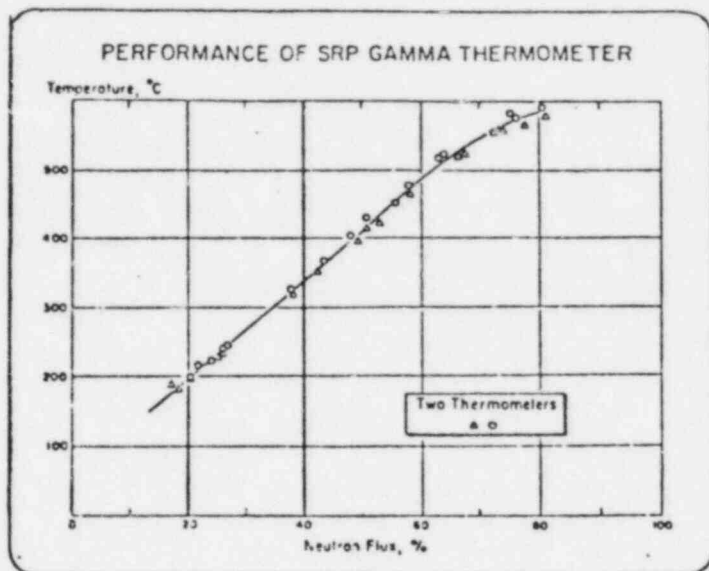
FIGURE 3.2-8: FUEL POWER TO SENSOR HEATING RATIO VERSUS BURNUP AT BUGEY 5
THEORETICAL RESULTS FROM CEA PROGRAM (AGATHE)

FIGURE 3.3 - 1



The observed response to a 20% step change in power at SRP corresponds closely to the response calculated by CEA using APPOLLO-TRIPOLI-MERCUR IV on Westinghouse 17x17 lattice. There is a 10% error after 100 seconds (on the change). This is a 2% signal deficit if the step were from 80 to 100% power. SRP data were normalized to obscure actual fluxes and heat rates in 1961 (Ref. 3-(2))

FIGURE 3.3 - 2

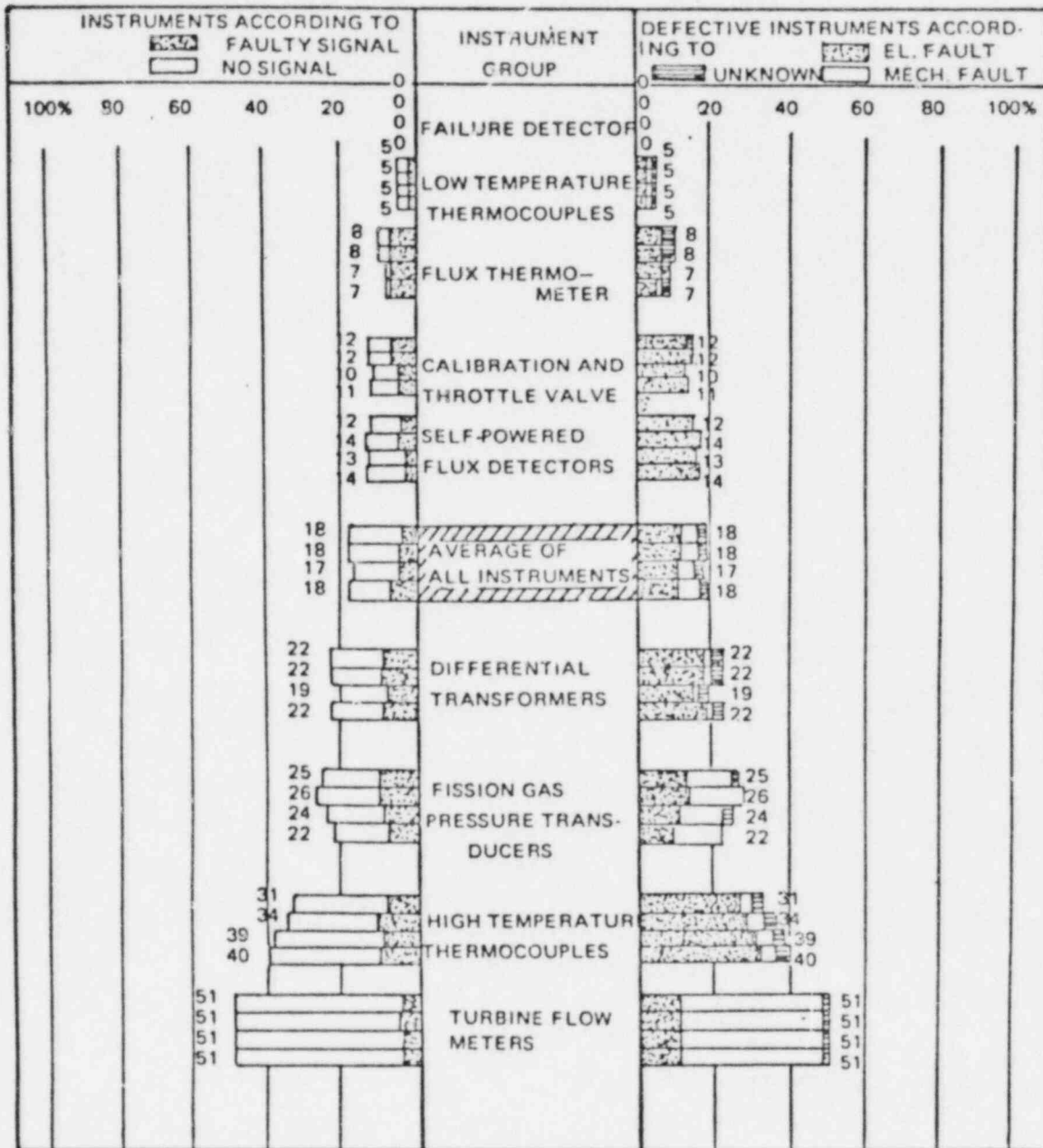


These results are remarkably good when it is considered that:

- No requirements on reproducibility of τ existed at that time (1961)
- Difference thermocouples were not in use
- Signal was extremely high (producing non-linearity)
- No knowledge exists of scatter of the x values of data points (Neutron flux measurement is in itself inexact)

FIGURE 3.3 - 3

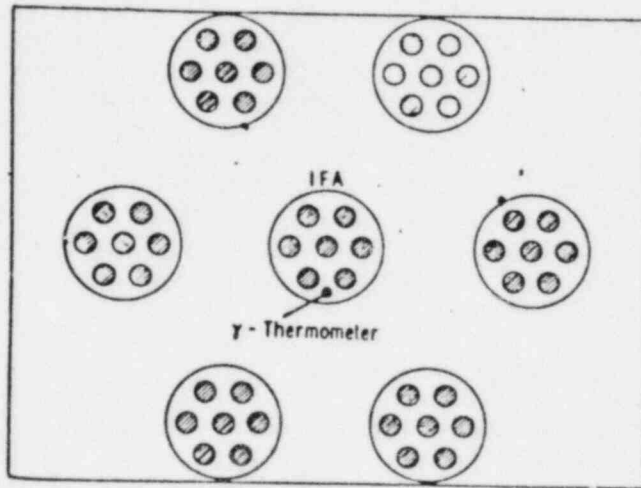
FAILURE FREQUENCY OF INSTRUMENTS IN HBWR



This gives a record of failure frequencies in the HBWR fuel test program which has included 226 gamma thermometers of standard type plus 106 flux thermometers of other types. For standard gamma thermometers the premature failure rate has been about the same as for low temperature thermocouples (~5%). The longest used gamma thermometers were used for seven years without change in calibration. Discounting failures due to water penetration of exposed thermocouple sheaths, premature failure frequency for RGTs is projected to $2\frac{1}{2}\%$. 14% of SPNDs at Halden have failed prematurely, compared to 30-50% in LWRs.

FIGURE 3.3 - 4

SPECIFICITY OF SIGNAL AT HBWR



In core geometrical location of γ -thermometers relative to IFA and adjacent fuel.

IFA 3 1.5 %		Signal specific to: 40 %
IFA 4 6 %		60 %
IFA 6-7-8 10.5 %		90 %
HBWR tubular fuel		> 95 %
31 rod bundle		> 95 %

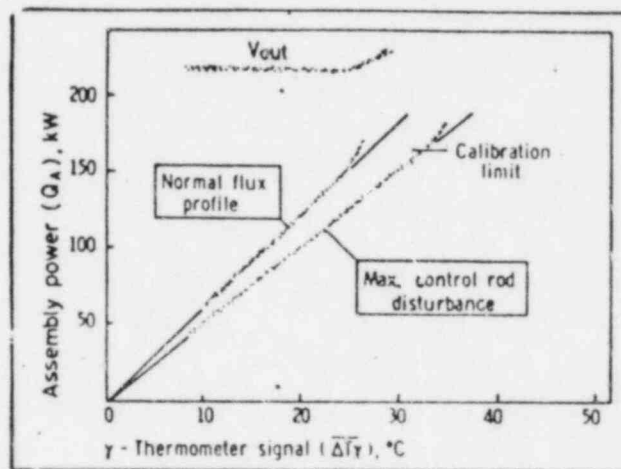
• γ -Thermometer

Specific signal depends on fuel geometry. Percentage figure measured for IFA 4, and calculated for the other arrangements.

The six elements surrounding an IFA (Instrumented Fuel Assembly) at Halden can be of any exposure, design or enrichment, sometimes being only one fuel rod. For structural reasons, the detectors are often eccentrically located (as in IFA-4). Many recent experiments (IFA's) at Halden have used only a single fuel pin because of the space required by travelling profilometers, etc. In this case the signal specificity problem increases from "difficult" to "extremely difficult". The 31-Rod Marviken type bundle (95% specificity) more nearly typifies PWR application.

FIGURE 3.3 - 5

EFFECTS OF NEARBY CONTROL RODS IN HWBR



Calibration of γ -thermometers with assembly power, IFA 4.
Calibration valid till outlet turbine shows void in channel. $\Delta\bar{T}_\gamma$
affected by control rods.

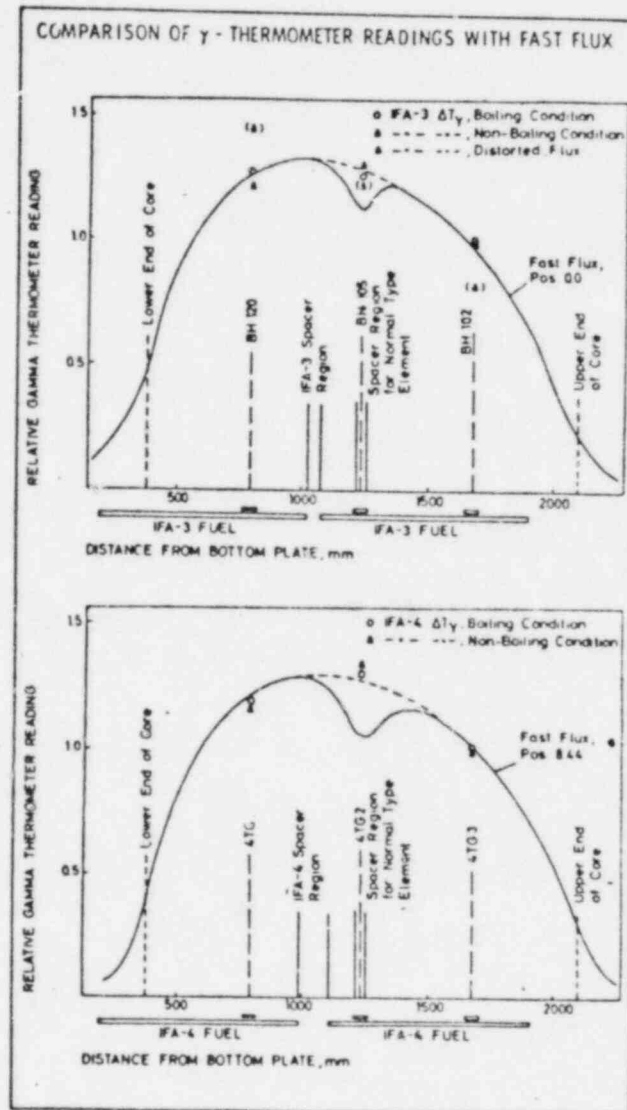
In this plot the sum of three gamma thermometers in IFA-4 are calibrated against calorimetric power of the test fuel assembly. With maximum disturbance of flux shape by an symmetrically placed control rod, the slope changes by about 20%. Such effects are much reduced in PWR's by:

- specificity of signal (local distribution of source γ)
- increased numbers of sensors (7-9 vs 3) in a fuel assembly
- absence of steam bubbles (no void)

In IFA-4 65% of sources of heat producing radiation are within the measured fuel assembly. In a 17x17 PWR assembly, 91%

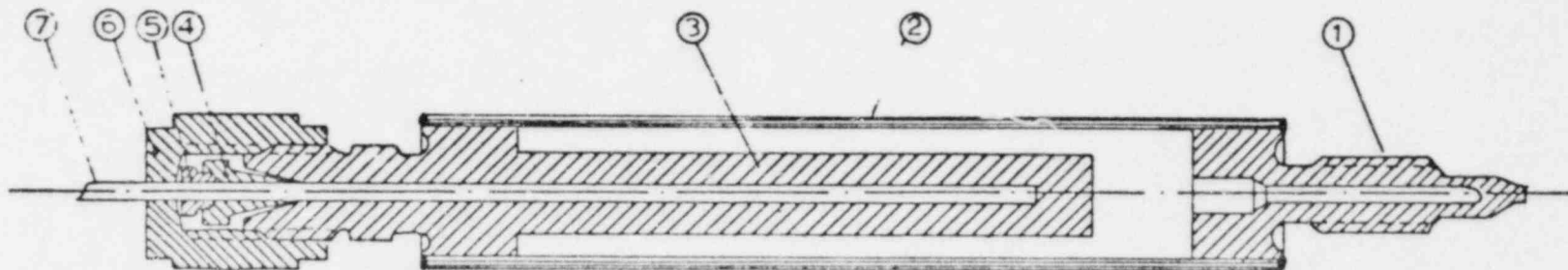
FIGURE 3.3 - 6

COMPARISON OF GAMMA THERMOMETER HEATING
WITH FAST FLUX IN AXIAL POSITIONS AT HBWR



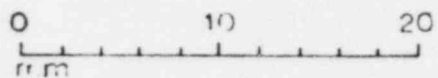
HBWR fuel pieces are separated with about 4 cm of zircaloy between two fuel sectors. The fuel in IFA-4 was deliberately placed off center a little. The post irradiated fast flux traces normally used are shown to be non-representative of fuel power distribution in IFA-3 and IFA 4.

FIGURE 3.3-7: GAMMA THERMOMETER ASSEMBLY, TYPE A



NOTES:

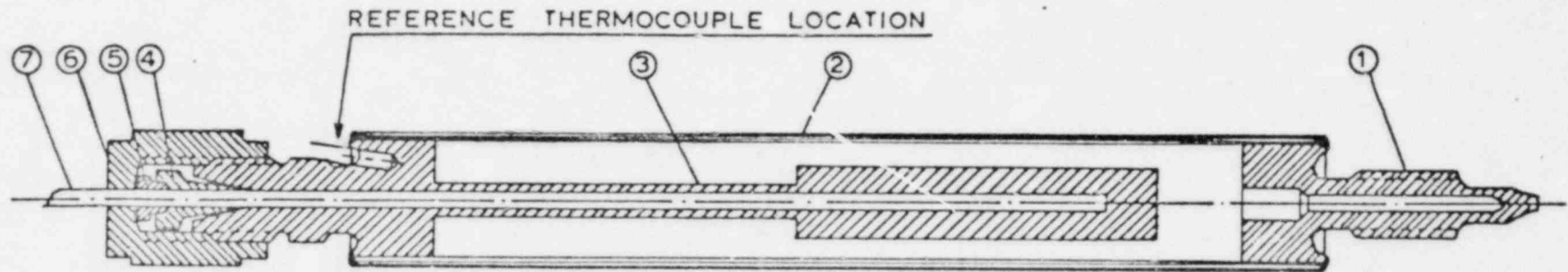
- ARGON ARC WELD
- HELIUM LEAK TEST WELDS
- POLISHED SURFACE TO BE PROTECTED WITH INERT GAS DURING WELDING



- ① BOTTOM PLUG
- ② TUBE
- ③ HEATER
- ④ FRONT FERRULE
- ⑤ BACK FERRULE
- ⑥ NUT
- ⑦ THERMOCOUPLE 2AB I 10

This is the type most used at Halden Reactor.

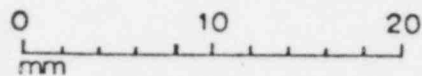
FIGURE 3.3-8: GAMMA THERMOMETER ASSEMBLY, TYPE B



NOTES:

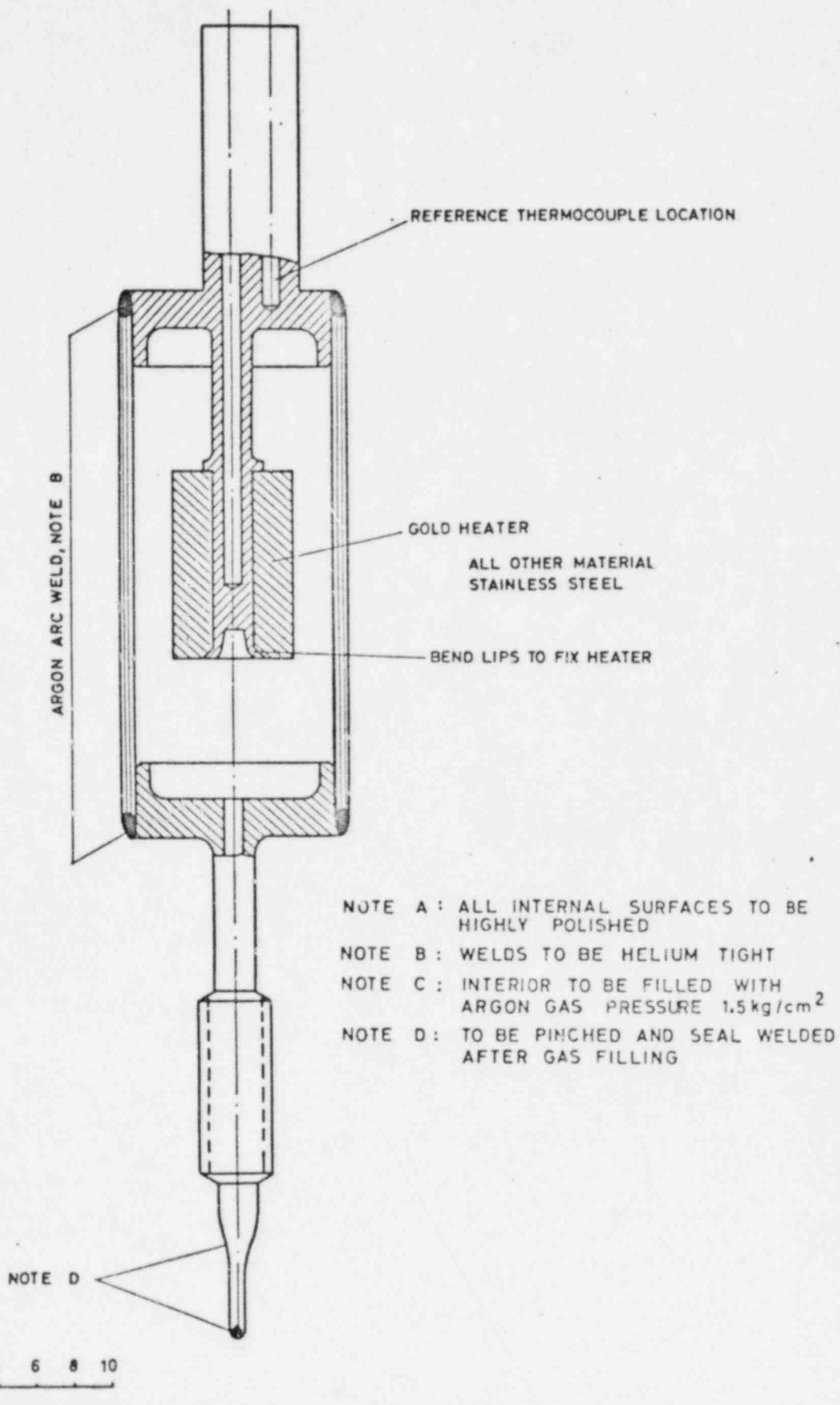
- ARGON ARC WELD
- HELIUM LEAK TEST WELDS
- POLISHED SURFACE TO BE PROTECTED WITH INERT GAS DURING WELDING

- ① BOTTOM PLUG
- ② TUBE
- ③ HEATER
- ④ FRONT FERRULE
- ⑤ BACK FERRULE
- ⑥ NUT
- ⑦ THERMOCOUPLE 2AB I 10



This type was evaluated to produce high signal and incorporates a second thermocouple for reference temperature.

FIGURE 3.3-9: GAMMA THERMOMETER ASSEMBLY, TYPE D



Gold has high density and good conduction. This type tends to give high signal with reasonable τ but is of complex construction.

FIGURE 3.3-10: GAMMA THERMOMETER ASSEMBLY, TYPE E

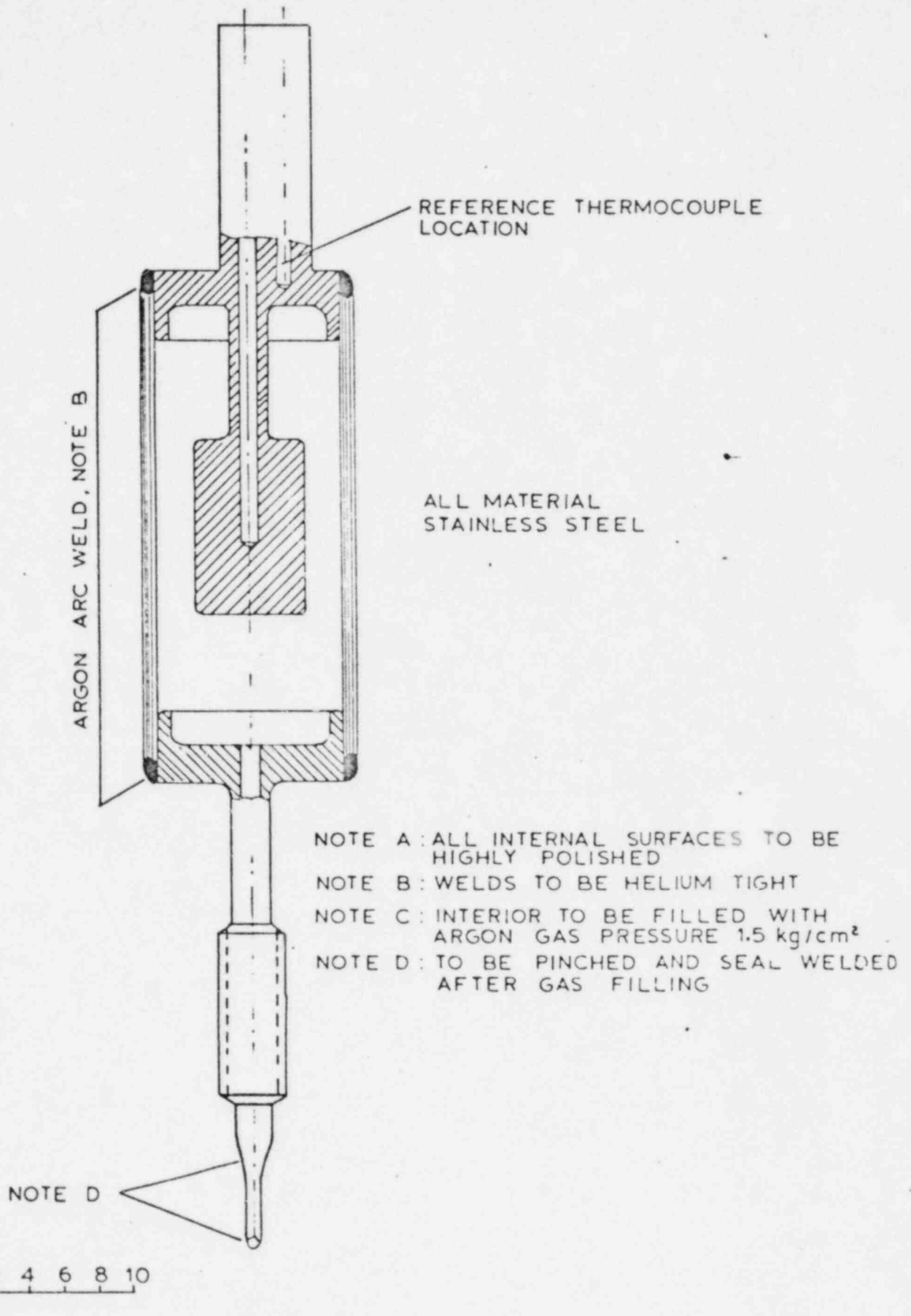
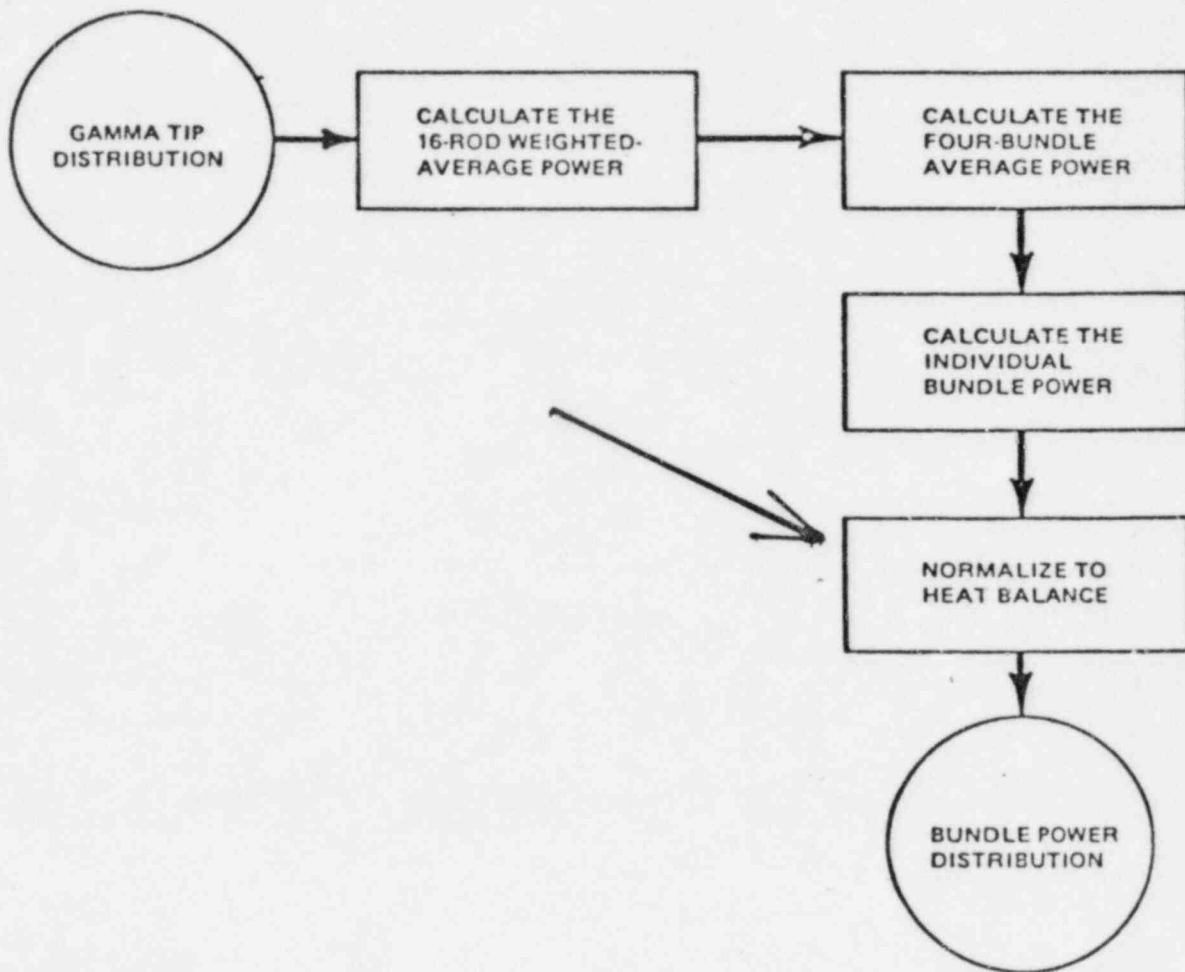
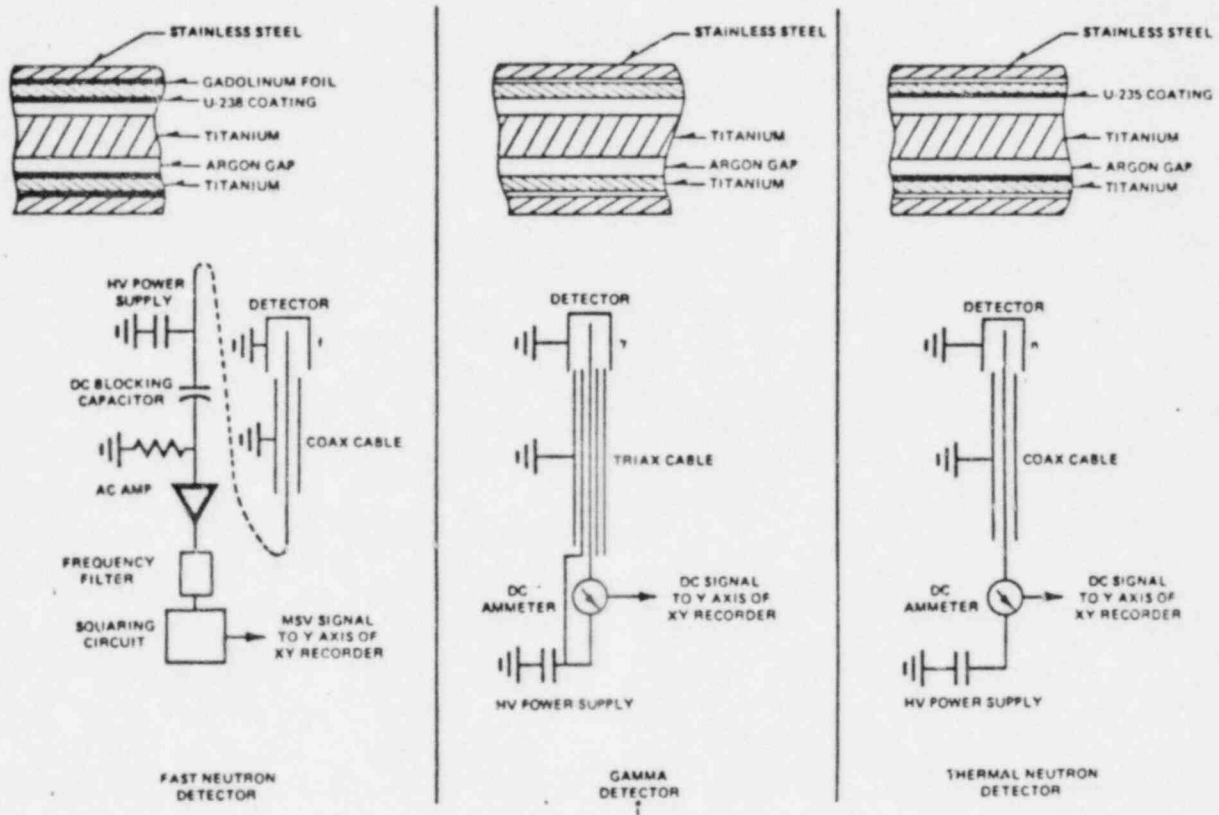


FIGURE 3.3-11: ALL TIP SYSTEMS REQUIRE NORMALIZATION



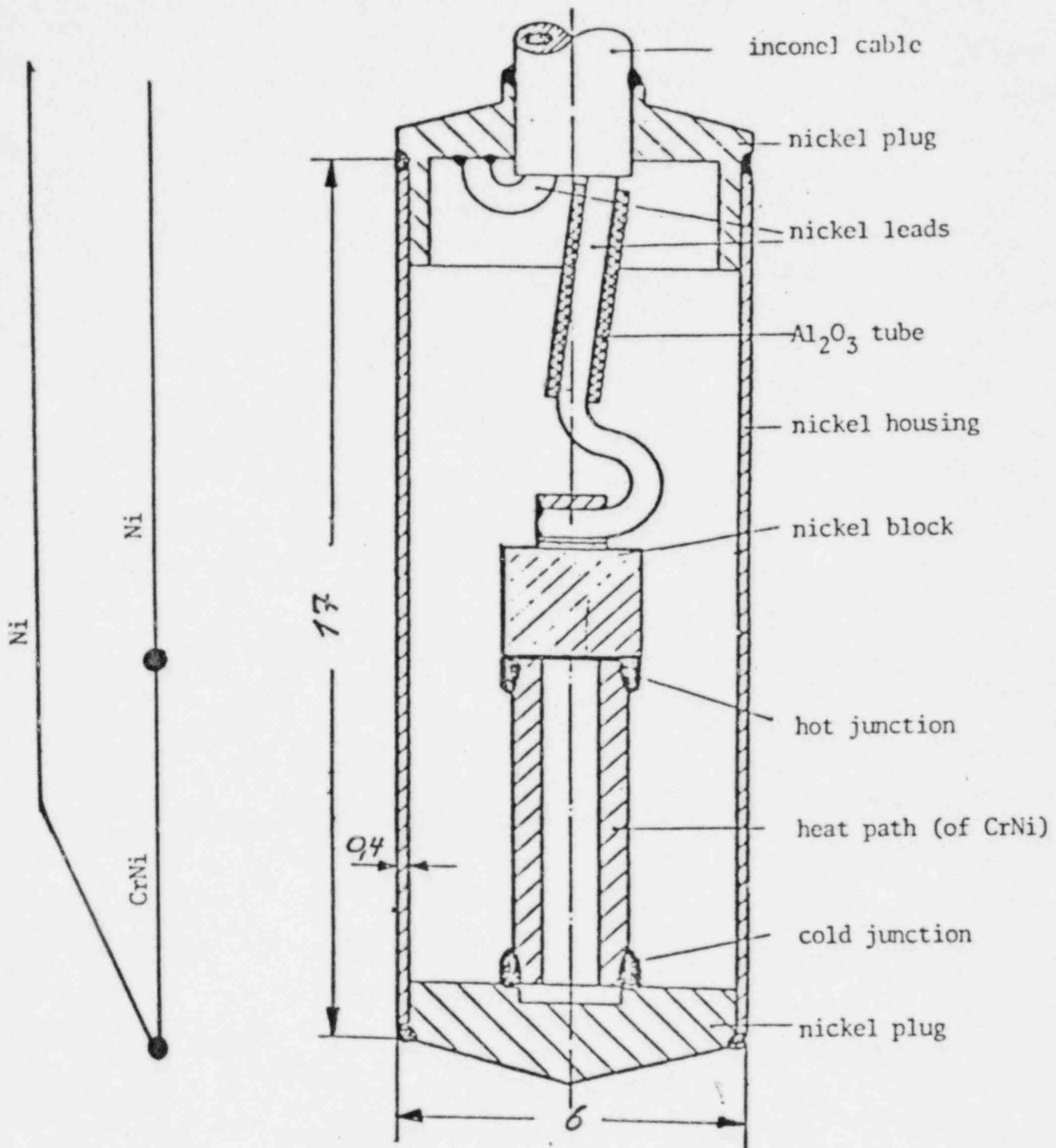
This flow diagram of bundle power calculation with gamma TIP system was extracted from Ref. 1-(6)a. Normalization is required for all travelling probes whose sensitivity is not precisely known. It is also required for SPND systems. The high precision RGT system will give total power generated within 1.5% without normalization.

FIGURE 3.3-12: TIP DEVICES COMPARED AT HATCH I BY GE/EPRI



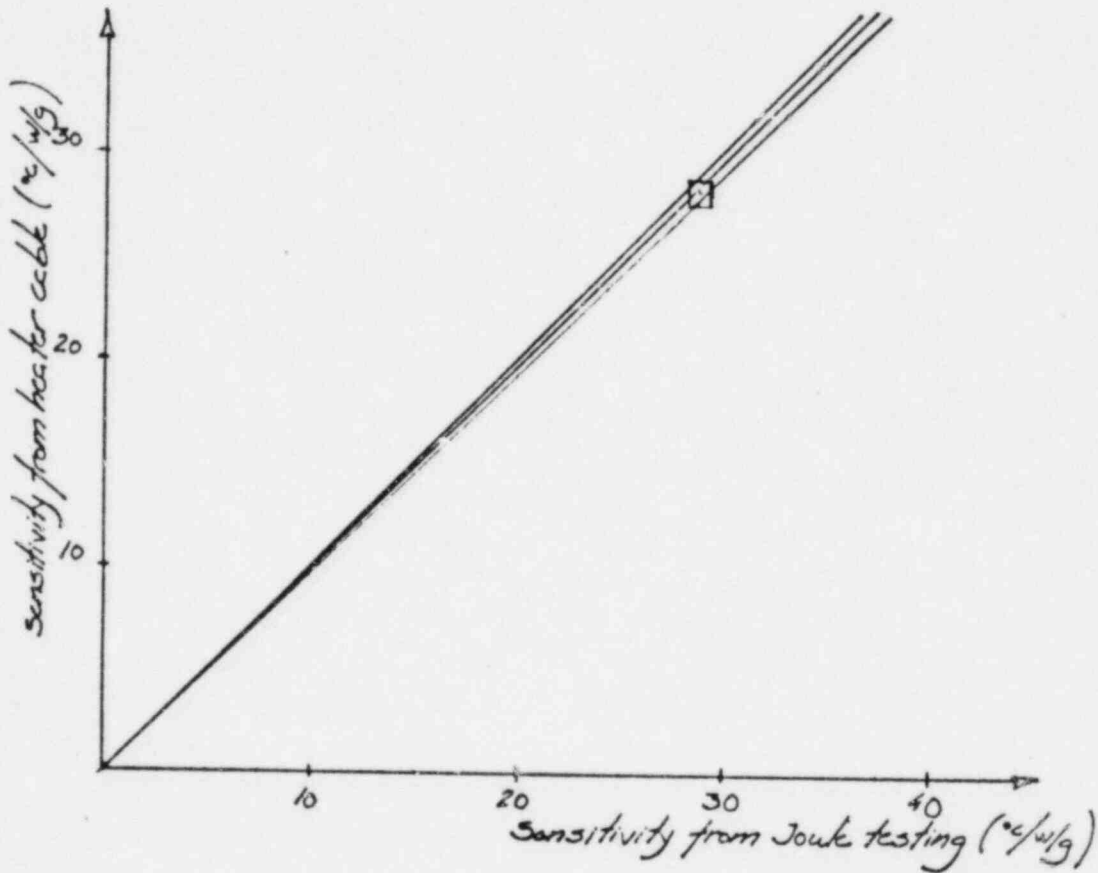
Although the gamma ion chamber proved far superior to the neutron detectors, all devices share the noisy signals, unpredictability of absolute calibration, and difficulties associated with high voltage power applied to cables. The program should have included travelling gamma thermometers.

FIGURE 3.3-13:
AEG GAMMA THERMOMETER



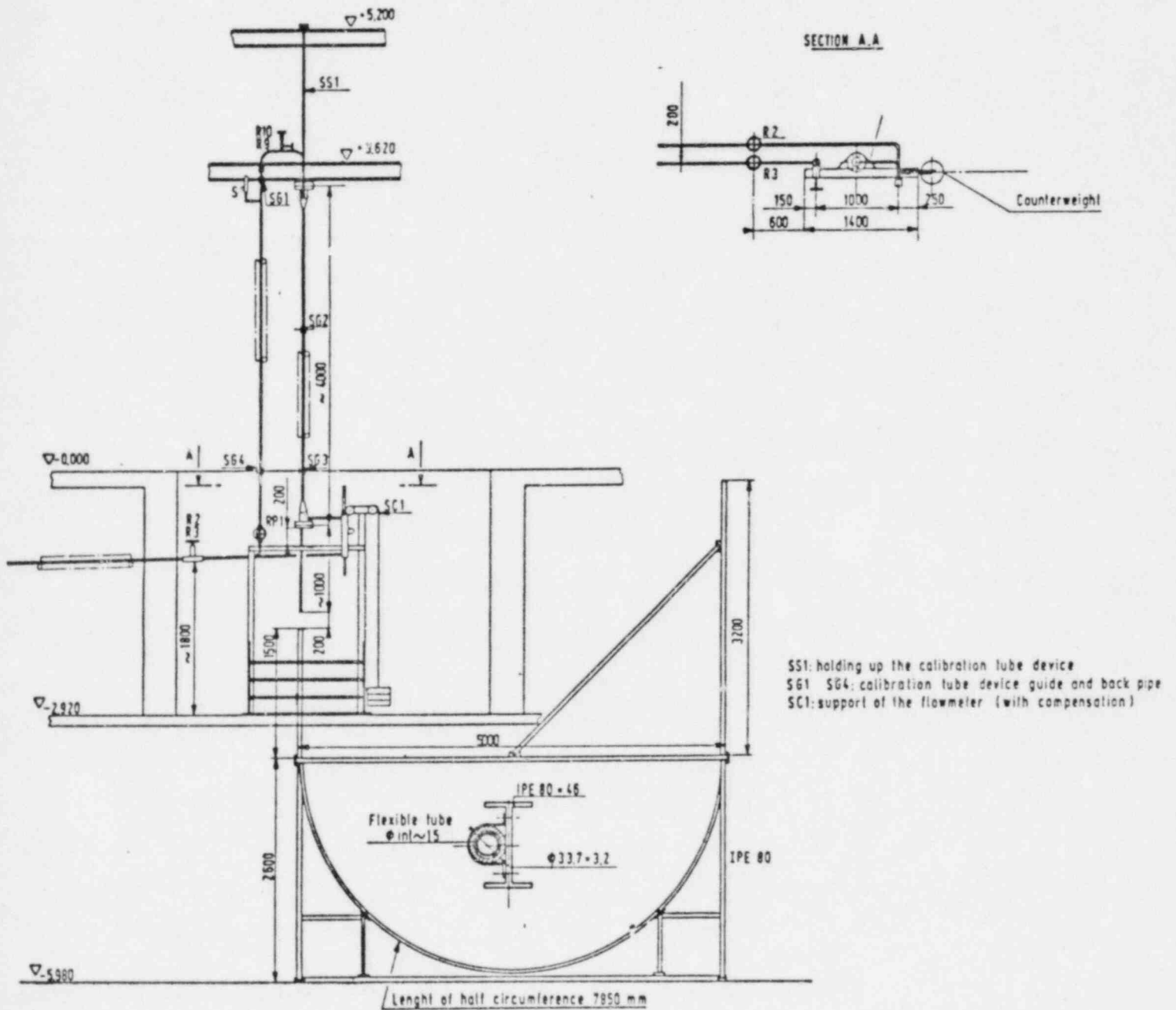
The figure shows the principle design of the AEG gamma thermometer. The sketched difference thermocouple to the left indicates how this measuring technique is integrated into the gamma thermometer design. The whole gamma thermometer is made from nickel to constitute the "nickel leads", while the critical heat path makes up the "CrNi-lead". The gamma thermometer is changed to a neutron sensitive device simply by inserting a U^{235} piece in the nickel block. The measuring technique is not altered.

FIGURE 3.4-1: CALIBRATION COMPARISON



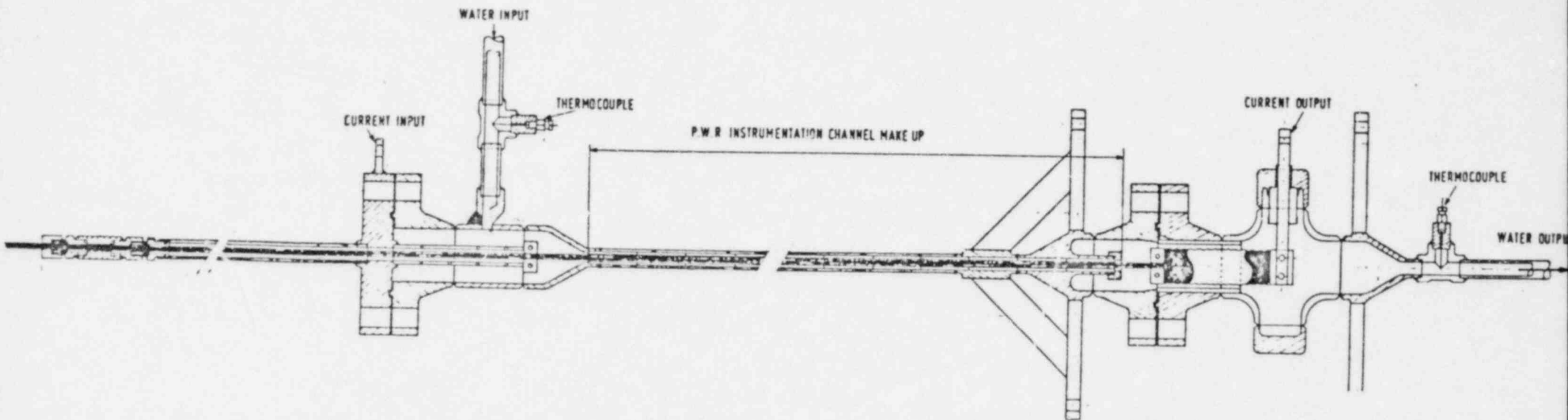
The first tests of the imbedded heater calibration of RGTs vs direct electric, or Joule test, calibrations reveal, as predicted by RADCAL/THERMAL, identity of the two calibrations. Within the 1.9% σ band for joule tests and 3% σ band on heater cable nominal resistivity. In-reactor recalibration of RGTs can eliminate speculation on drift of sensitivity with exposure and provides direct measure, at will, of K_1 and σ_1 to $\pm 1\frac{1}{2}\%$ (attainable).

FIGURE 3.4-2: EDF HIGH PRESSURE TEST LOOP



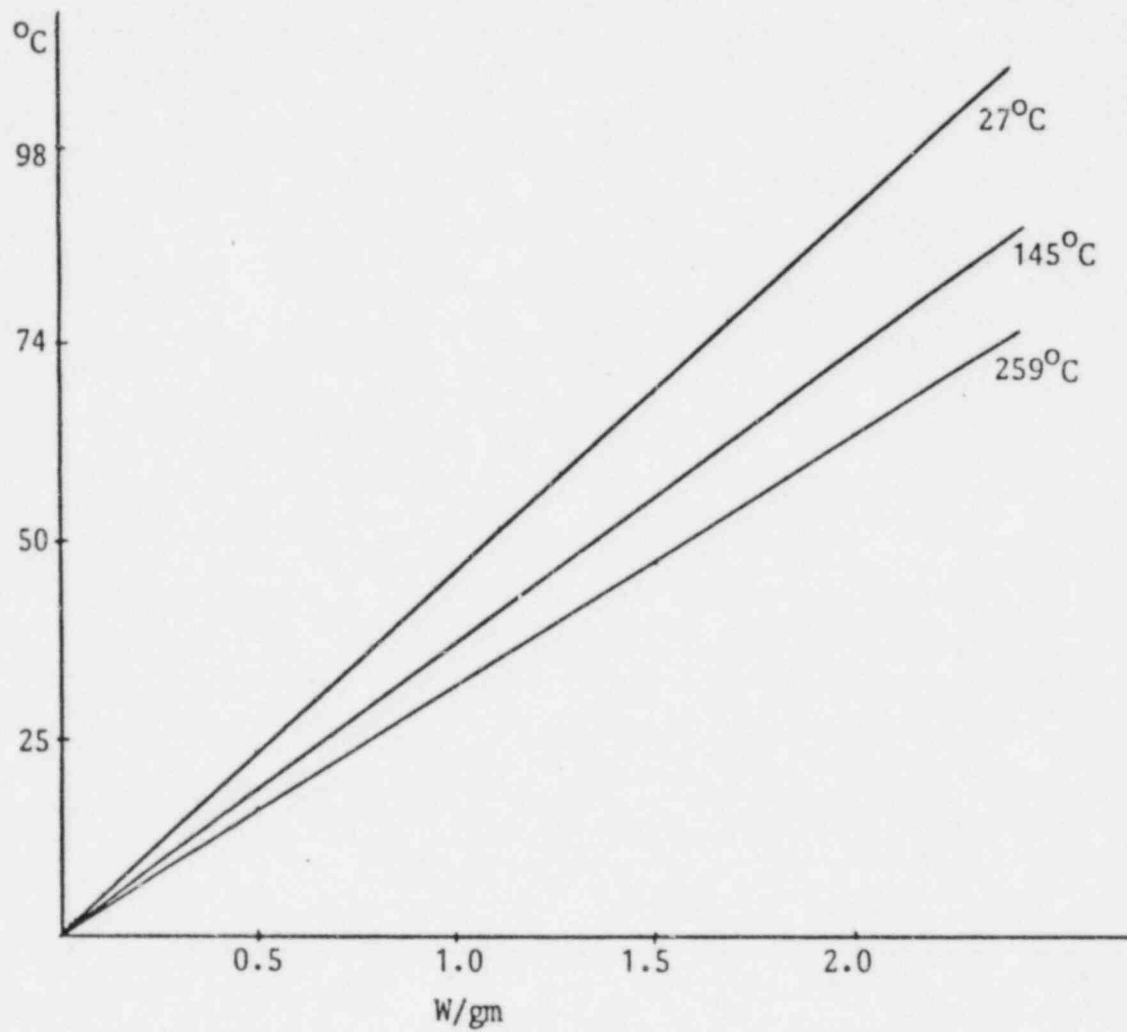
This loop was fabricated by EdF to electrically calibrate RGT assemblies, 10 of which are entering EdF reactors. The loop has been made available by EdF to other utilities installing RGTA prototypes. Temperatures of 350°C and pressures up to 150 bar are attainable.

FIGURE 3.4-3: TEST SECTION IN HIGH PRESSURE TEST LOOP



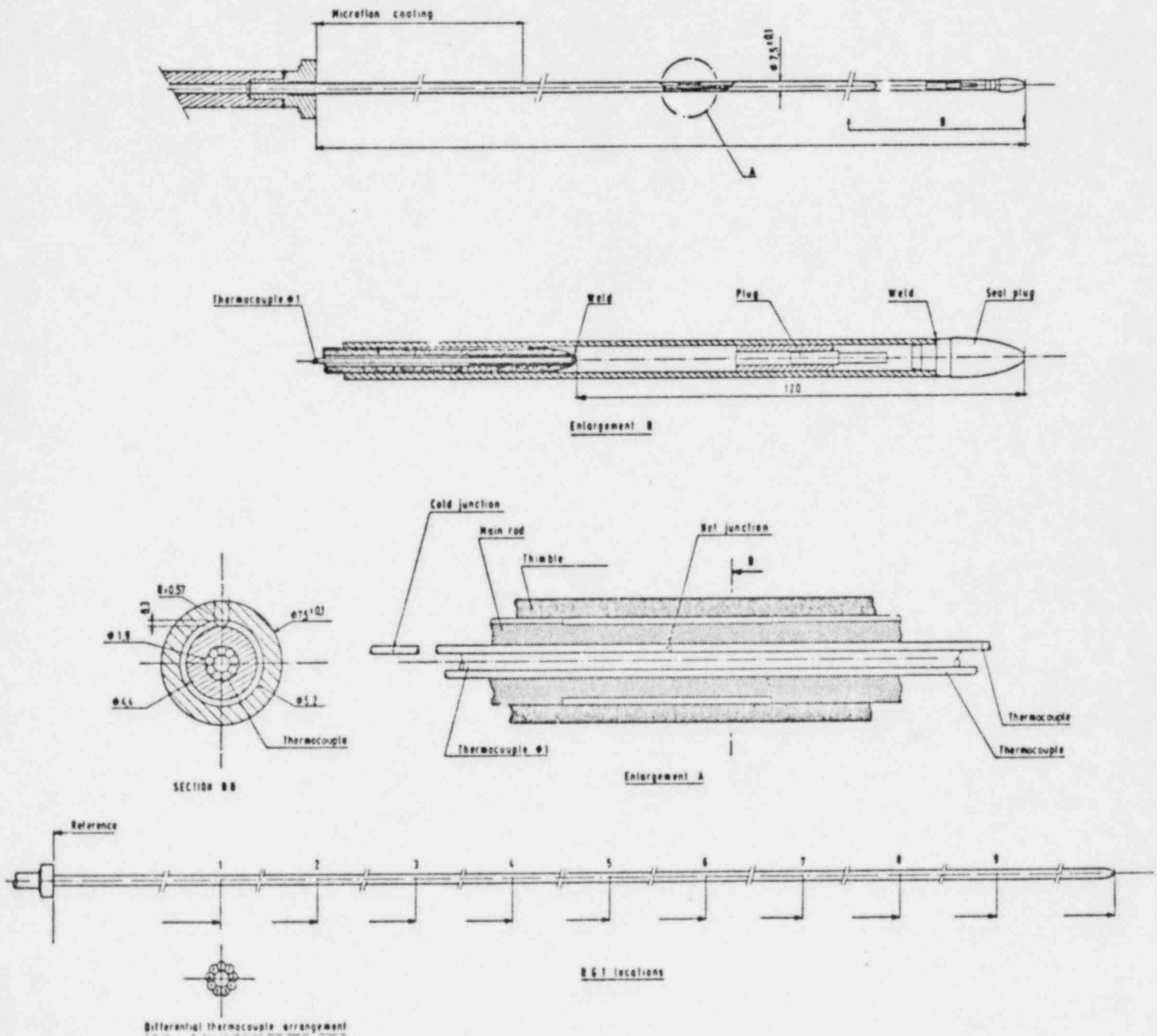
High purity water and precision spacing of RGTAs provide data at 300° in which the 2σ scatter of data points on the best fit line is 0.8%.

FIGURE 3.4-4: COOLANT TEMPERATURE EFFECT ON SENSITIVITY



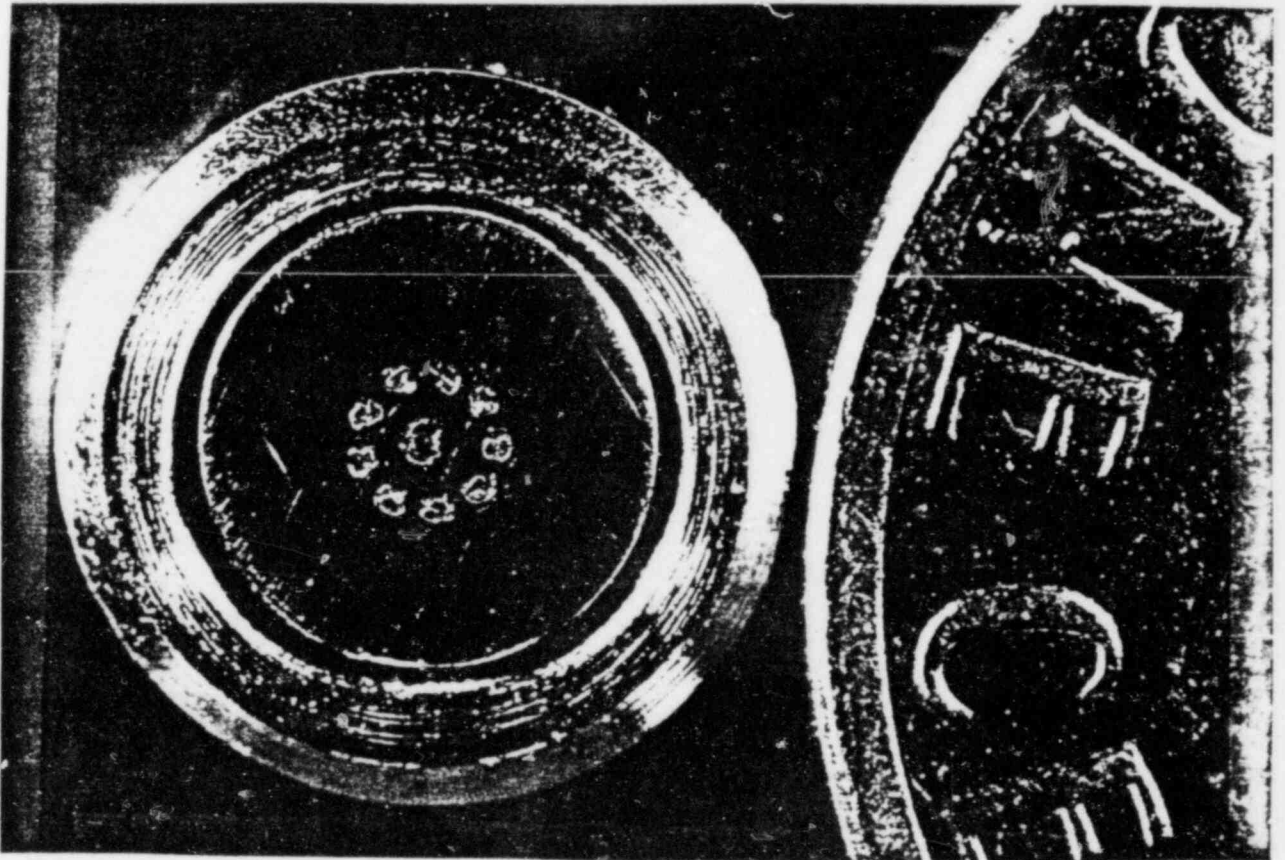
The range of coolant temperatures over which the RGTA is used in a PWR is relatively narrow, 300-340°C on this scale.

FIGURE 3.4-5: EDFY RADCAL ASSEMBLY



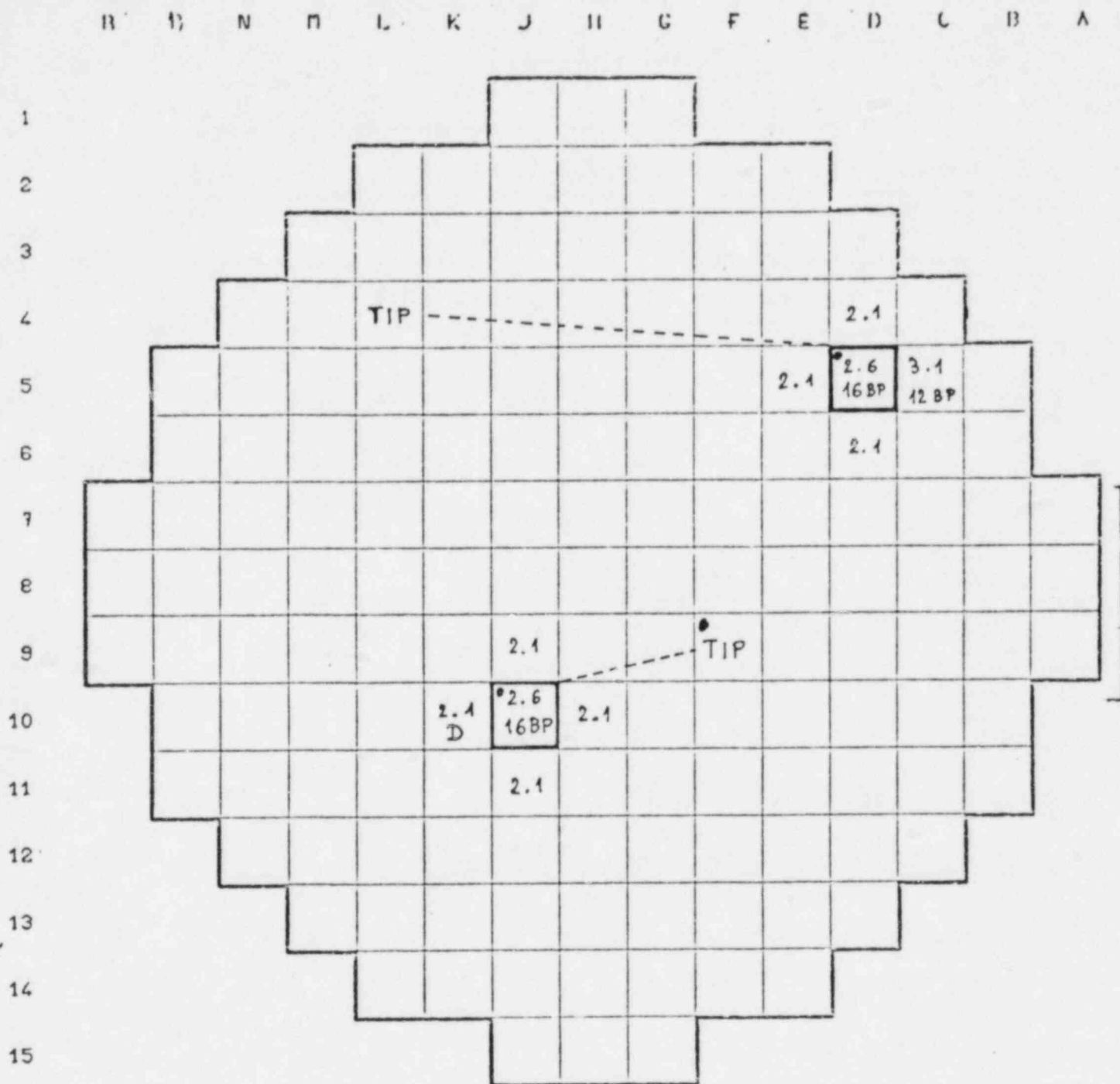
The EdF RGTAs are 20 meters long and identical in outside configuration to the Framatome (Westinghouse) TIP thimbles (droit de gant) which they replace. They contain 9 sensors and a central difference thermocouple which measures coolant ΔT .

FIGURE 3.4-6: PHOTO OF "EXPLODED" PARTS OF EDFYRADCAL

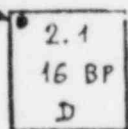


Note that drawing of core tube onto thermocouple pack completely imbeds the thermocouple jackets in stainless steel material of the core rod. The jacket tube draw-down is the next process step.

FIGURE 3.4-7: RGTAS IN BUGEY 5



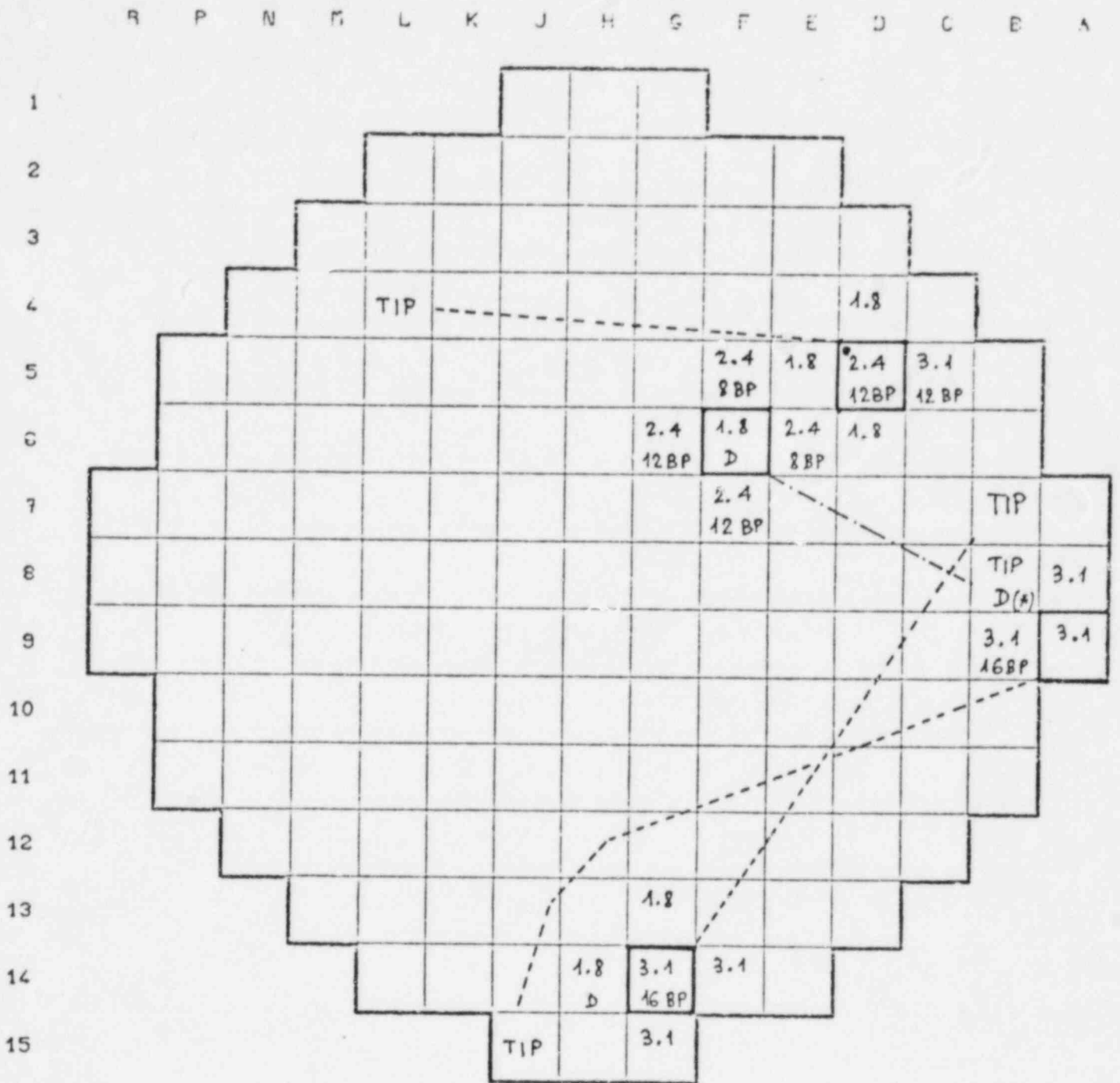
Incore thermocouple



Enrichment in %
Burnable poison rod number
Control rod group

The two RGTAs in Bugey 5 since June, 1979 (Canne no. 3 and 4) contain 18 sensors in positions where readings can be compared by symmetry to TIP traces.

FIGURE 3.4-8: RGTAS IN TRICASTIN 2

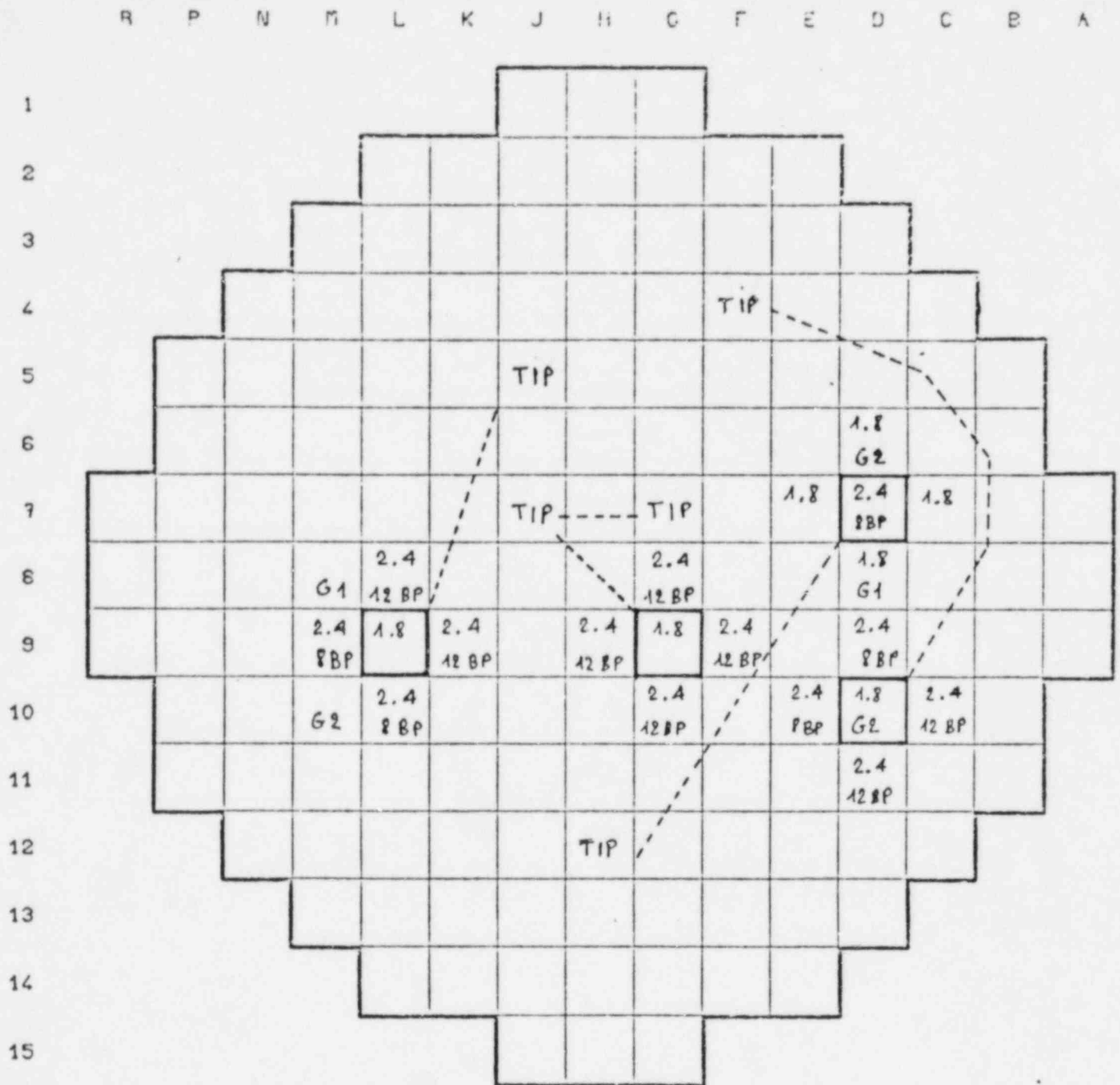


Incore thermocouple

<ul style="list-style-type: none"> 2.1 16 BP D 	Enrichment in % Burnable poison rod number Control rod group
---------------------------------------------------------------------------------	--------------------------------------------------------------------

(*) FG RGTAs has not a TIP symmetrical, but B8 is similar

FIGURE 3.4-9: PLANNED POSITIONS OF RGTAS IN TRICASTIN 3



Incore Thermocouple

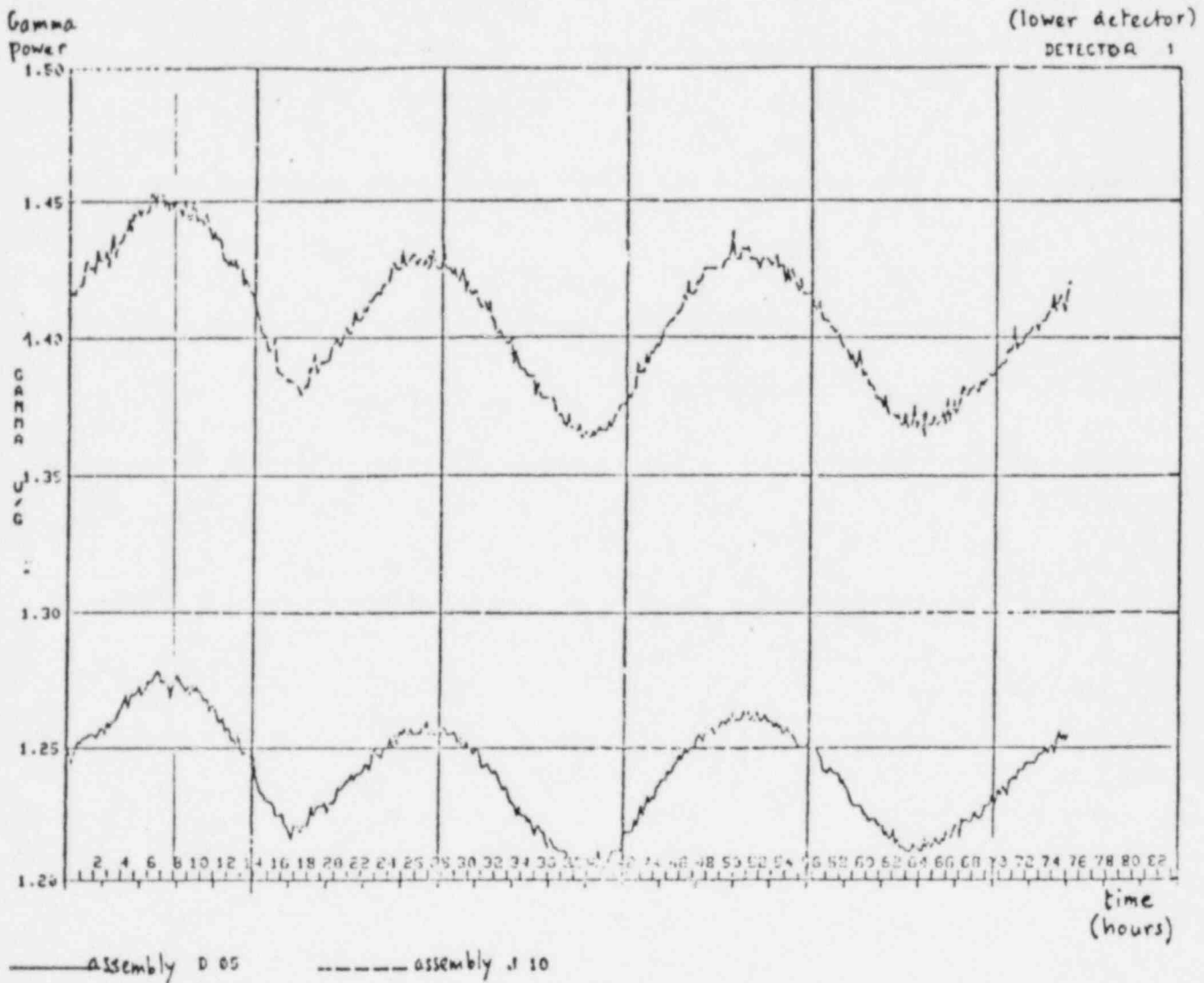


Enrichment in %
Burnable poison rod number
Control rod group

(G is grey rod)

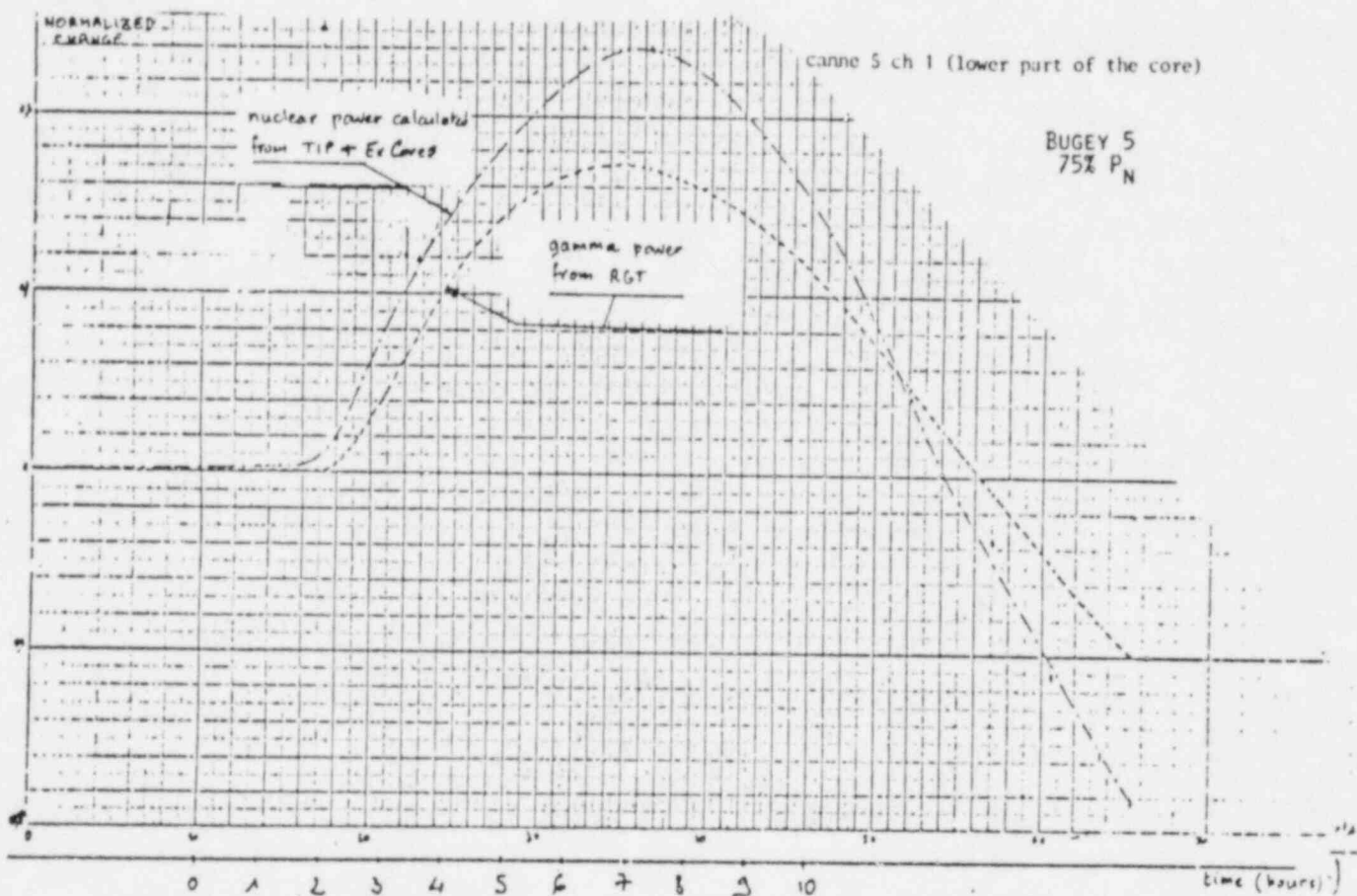
One of the Tricastin 3 RGTAs is symmetrical to 2 TIP positions.

FIGURE 3.4-10: POWER TRACES OF GT SENSORS AT EQUAL CORE ELEVATIONS



Excerpts from paired RGTs at equal elevations in positions D5 and J10 of Bugey 5. For this 100 hour period shown the characteristics of power oscillations are identical.

FIGURE 3.4-11: GT "TRACKED" POWER VS CALCULATED POWER DURING XENON SWING

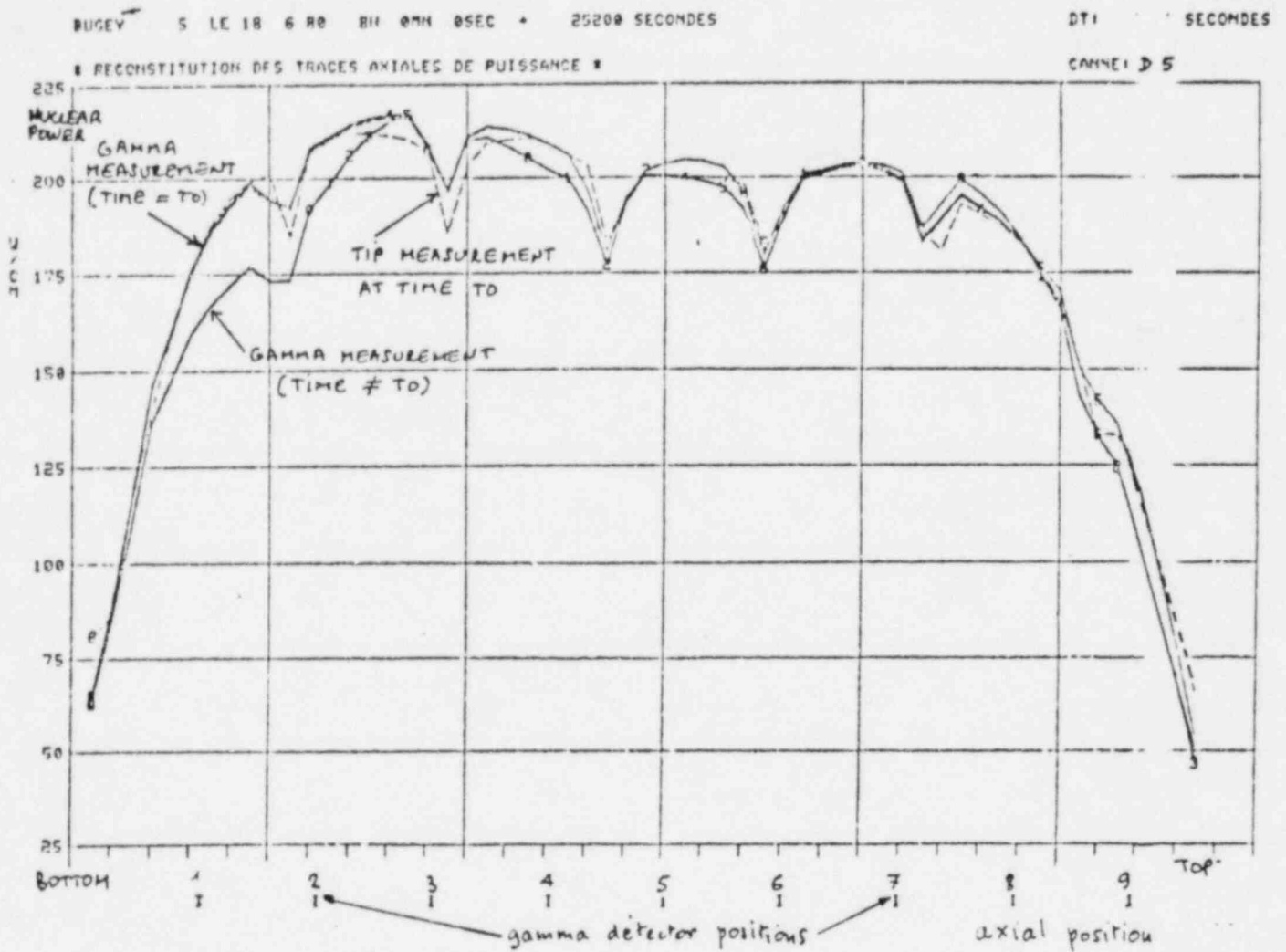


The measurement of vertical and azimuthal power oscillations is a RGT "bonus" for plants having only TIP systems

FIGURE 3.4-12:

AXIAL PROCESSING

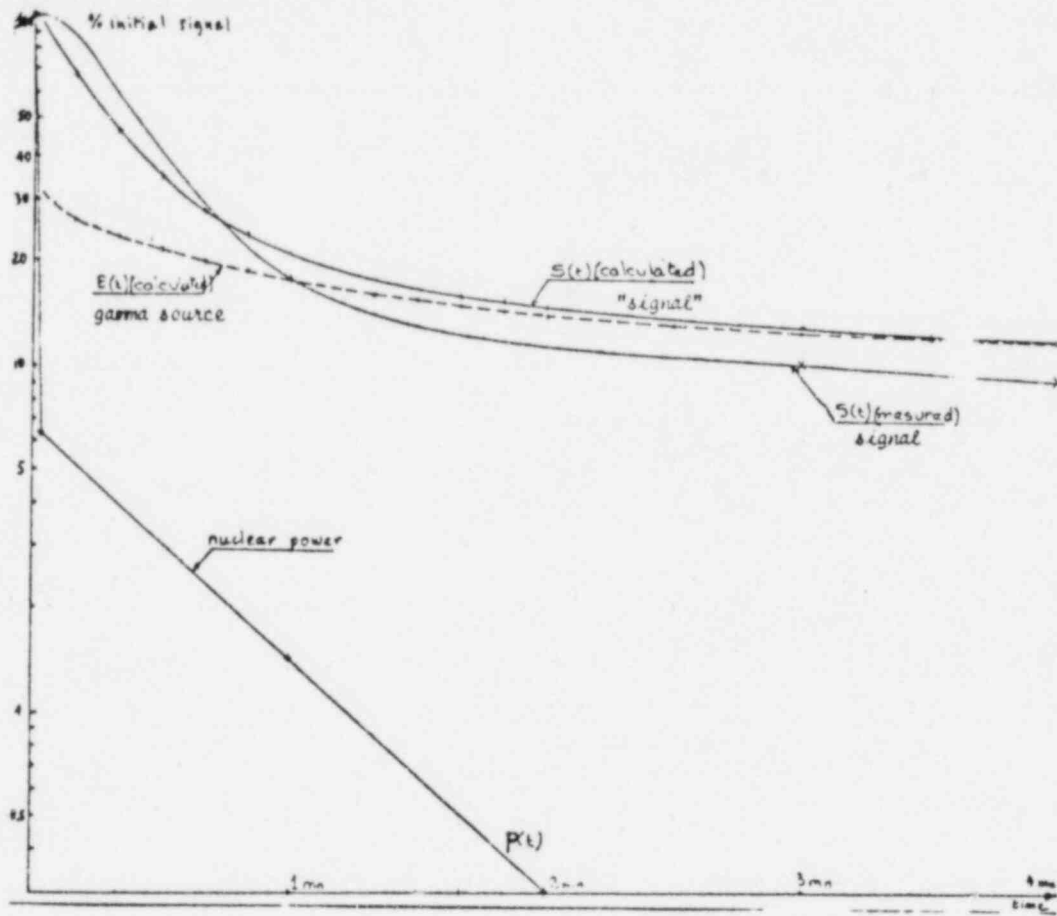
AXIAL SHAPE FROM TIP COMPARED TO AXIAL SHAPE FROM GT



The axial power shape reconstructed from 9 sensors agrees well with the TIP produced shape at time = 0. The power shape obviously changes later without operator awareness (in the absence of a TIP trace at $t \neq 0$).

FIGURE 3.4-13:

GT SIGNAL AFTER SHUTDOWN



Calculations predict an 11% signal from fission products after 4 minutes for this shutdown. Observed signal is 9%.

Figure 3.4-14: Comparison of Gamma Heating and In-core Nuclear Power For canne G9, detector 1, at Tricastin 3.

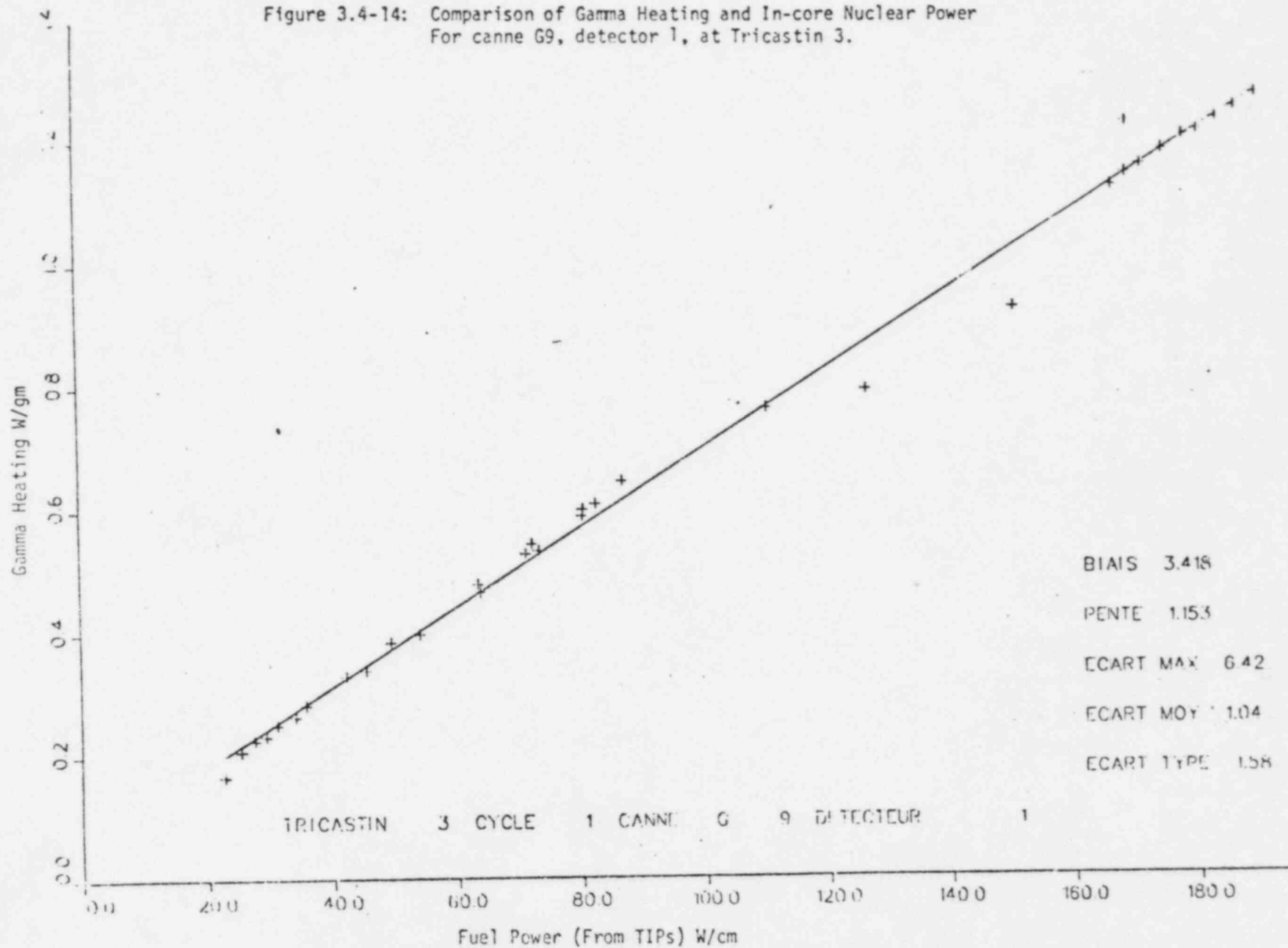


Figure 3.4-15: Comparison of Gamma Heating and In-core Nuclear Power
For canne G9, detector 2, at Tricastin 3.

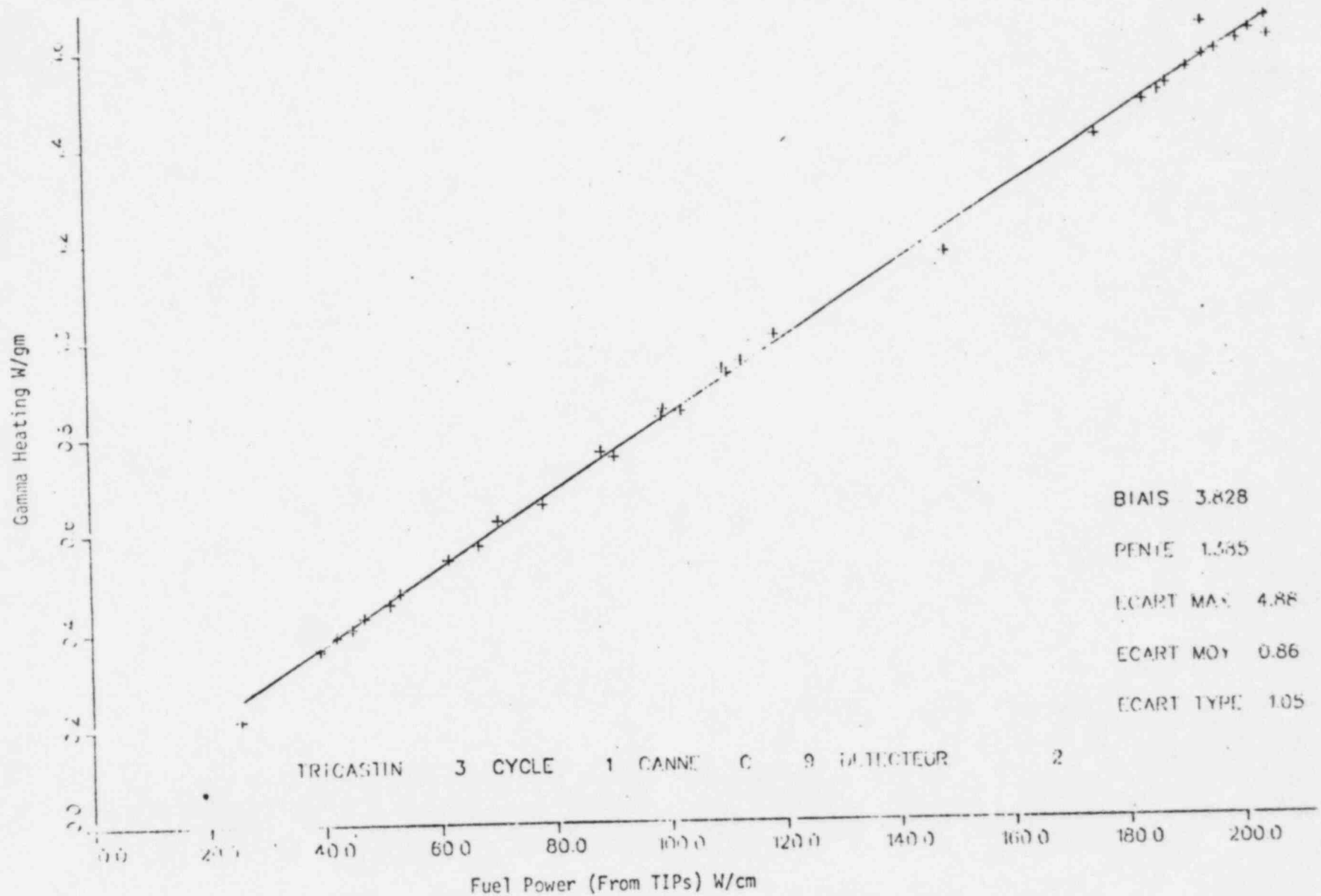


Figure 3.4-16: Comparison of Gamma Heating and In-core Nuclear Power
For canne G9, detector 3, at Tricastin 3.

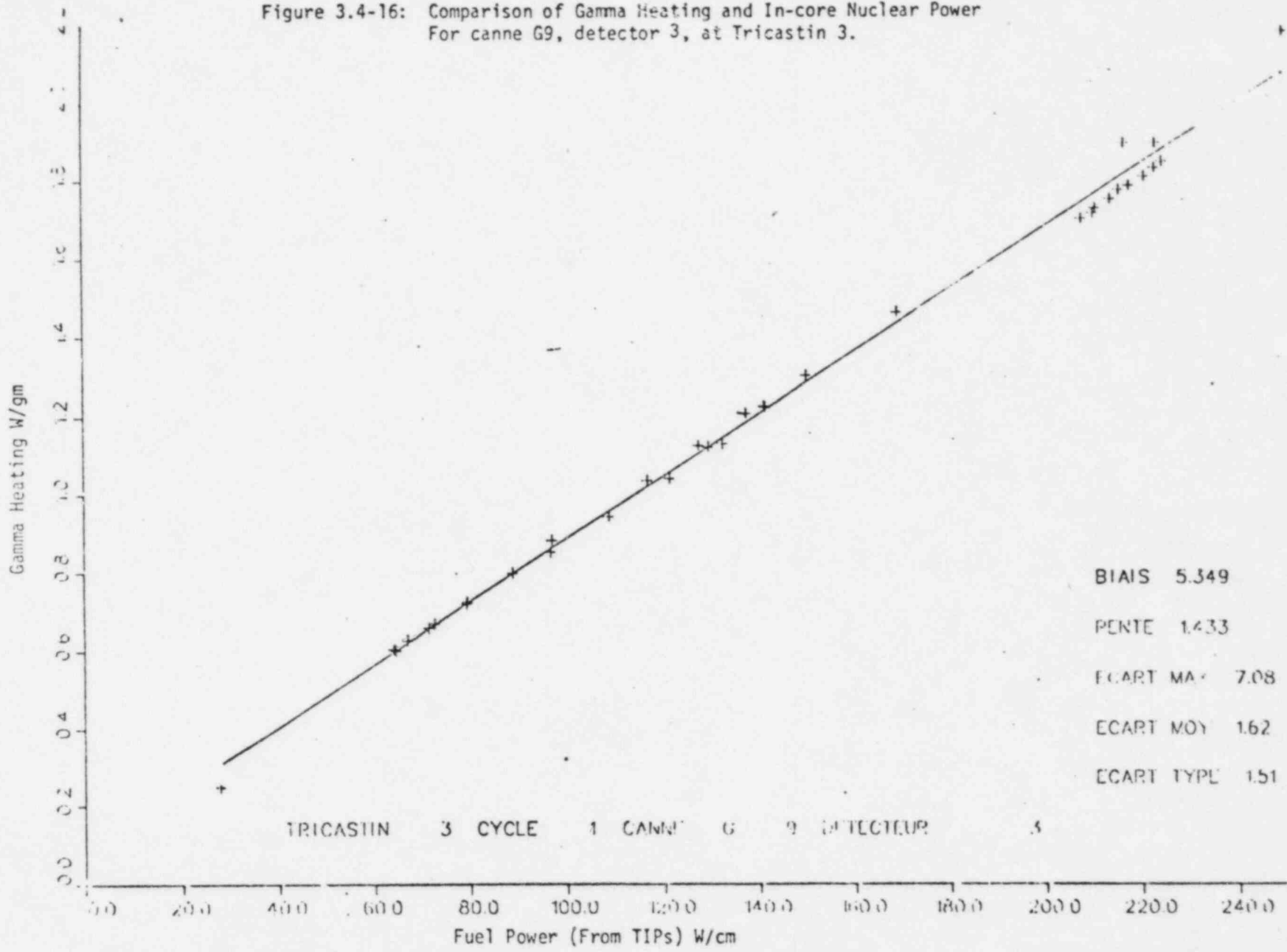


Figure 3.4-17: Comparison of Gamma Heating and In-core Nuclear Power For canne G9, detector 4, at Tricastin 3.

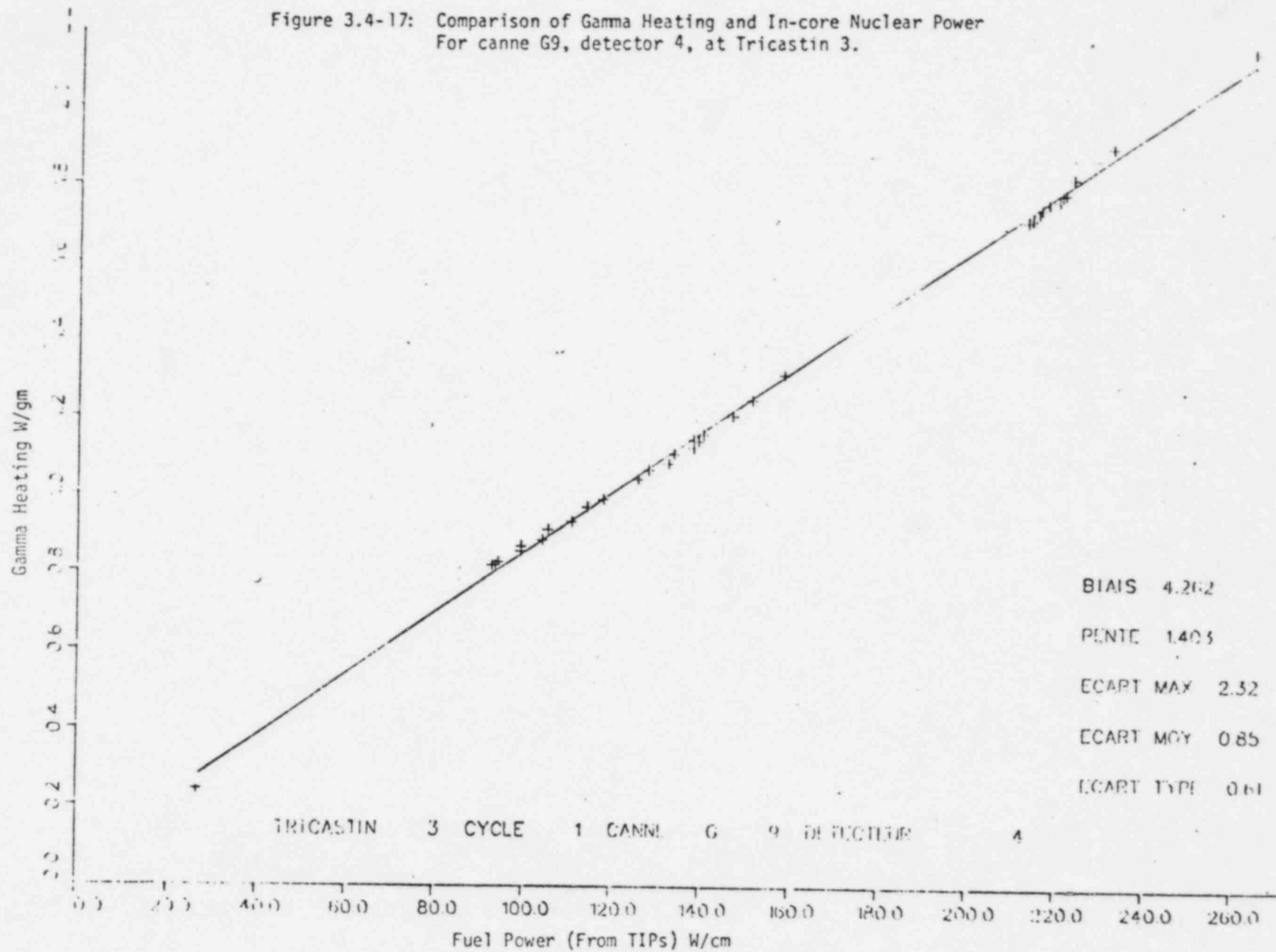


Figure 3.4-18: Comparison of Gamma Heating and In-core Nuclear Power For canne G9, detector 5, at Tricastin 3.

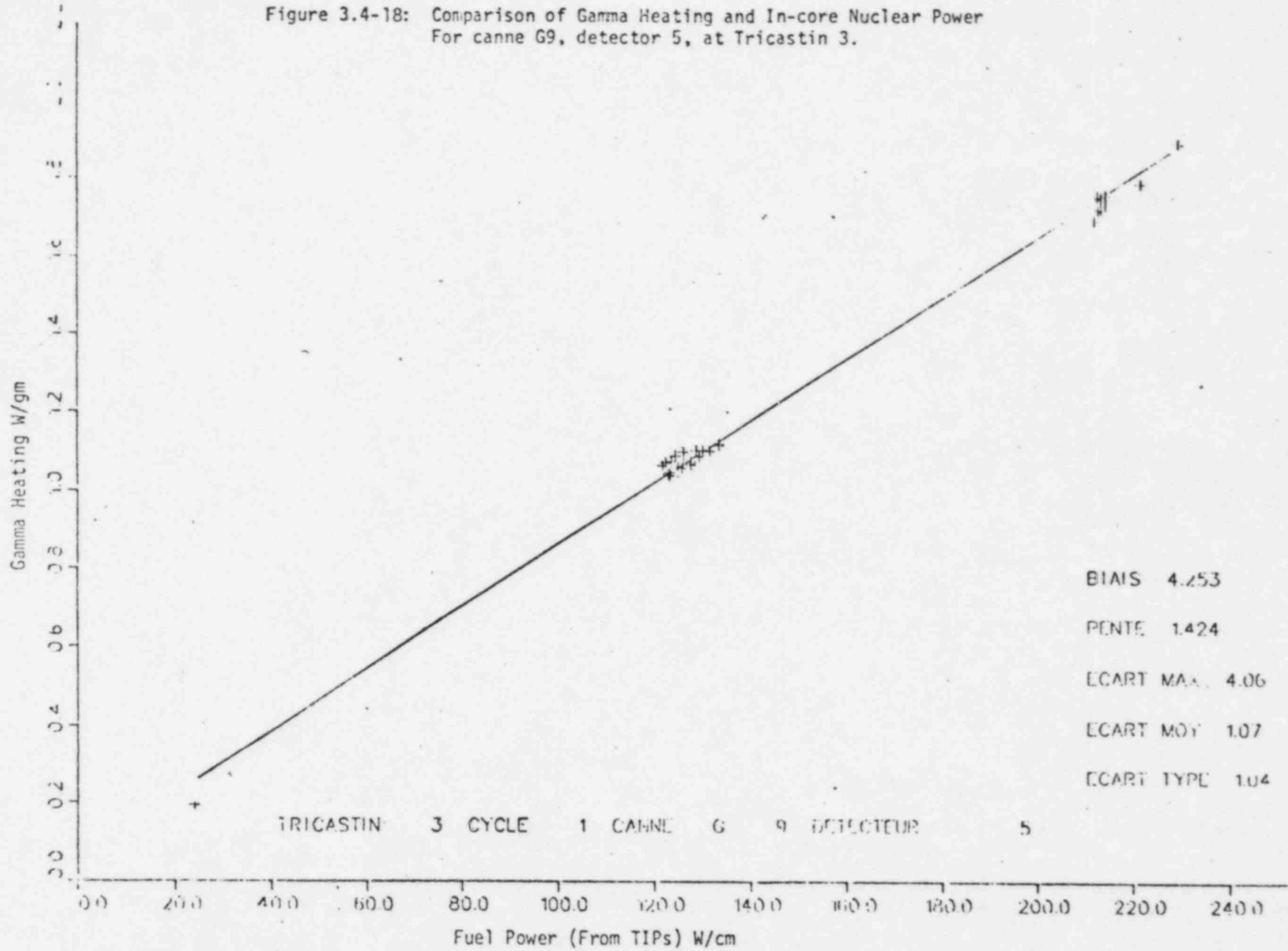


Figure 3.4-19: Comparison of Gamma Heating and In-core Nuclear Power
For canne G9, detector 6, at Tricastin 3.

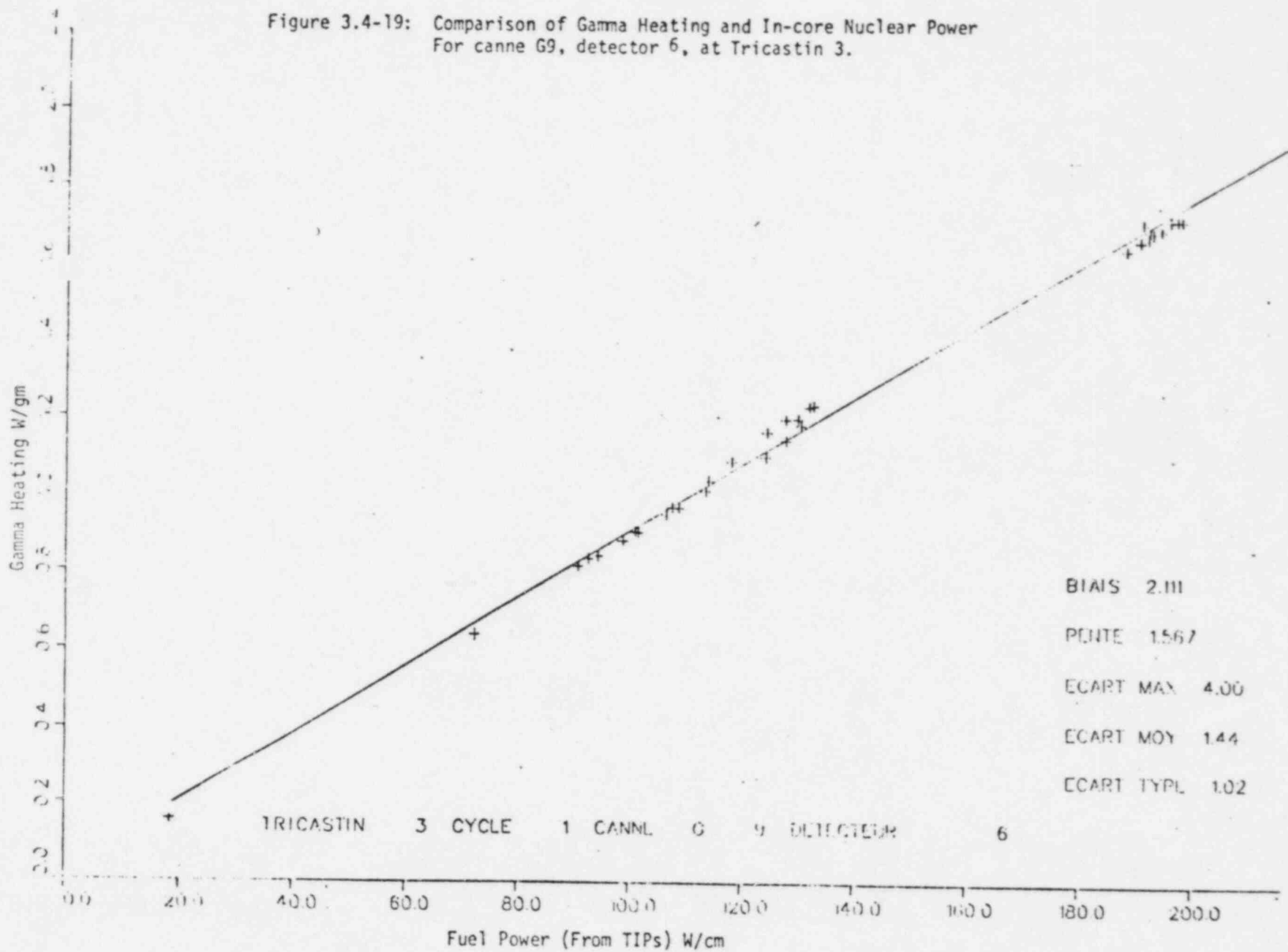


Figure 3.4-20: Comparison of Gamma Heating and In-core Nuclear Power For canne G9, detector 7, at Tricastin 3.

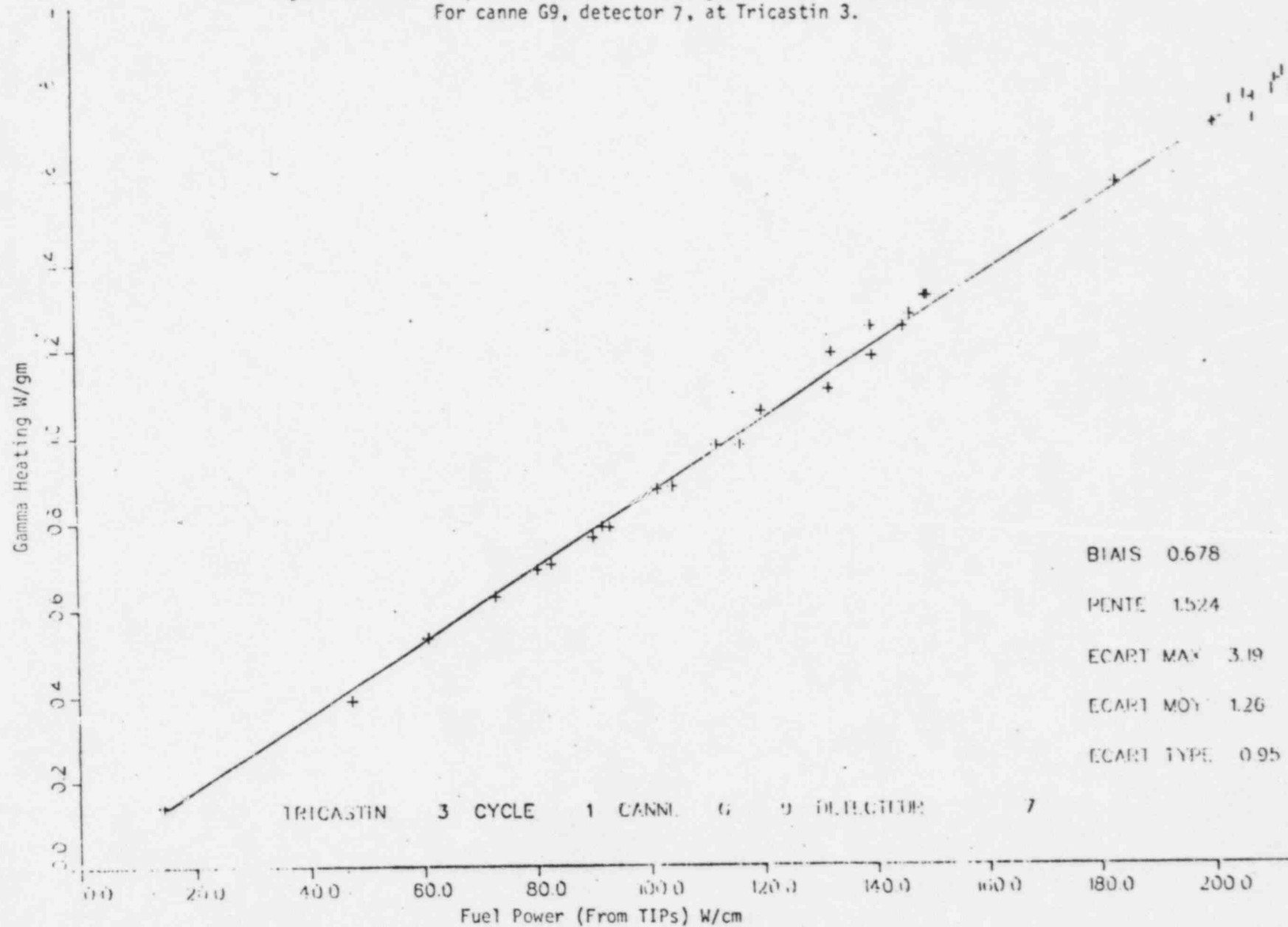


Figure 3.4-21: Comparison of Gamma Heating and In-core Nuclear Power
For canne G9, detector 8, at Tricastin 3.

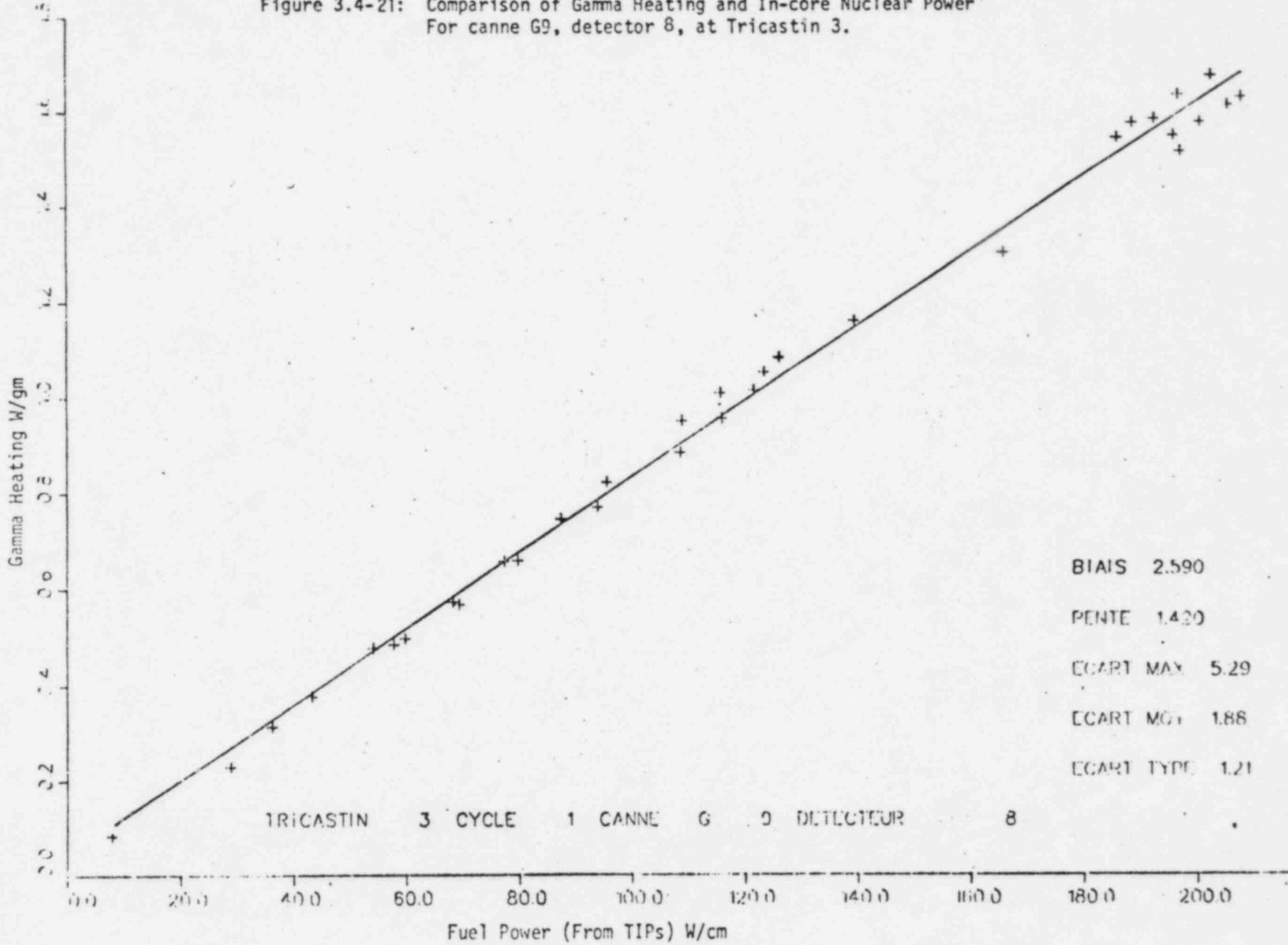
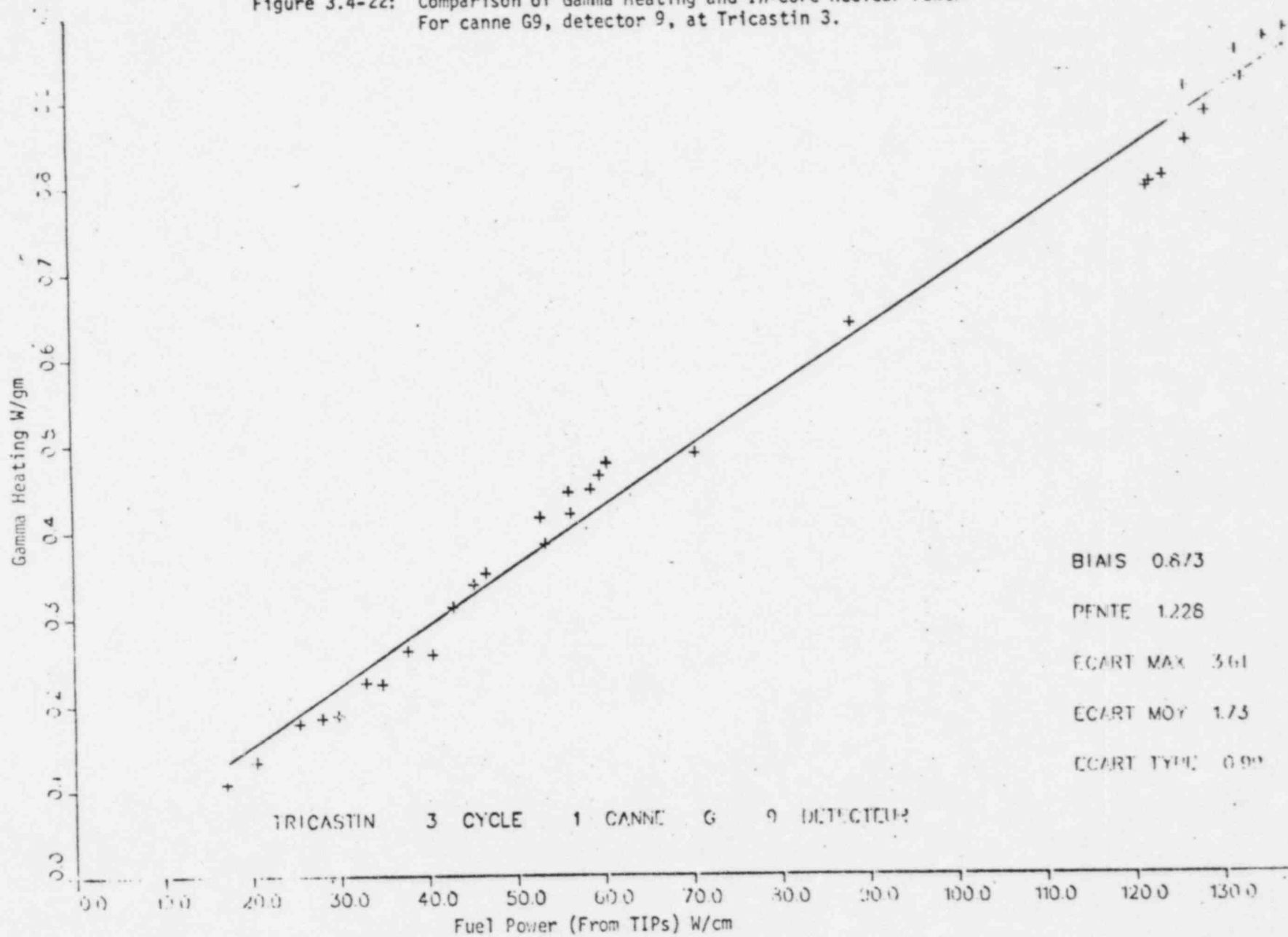


Figure 3.4-22: Comparison of Gamma Heating and In-core Nuclear Power
For canne G9, detector 9, at Tricastin 3.



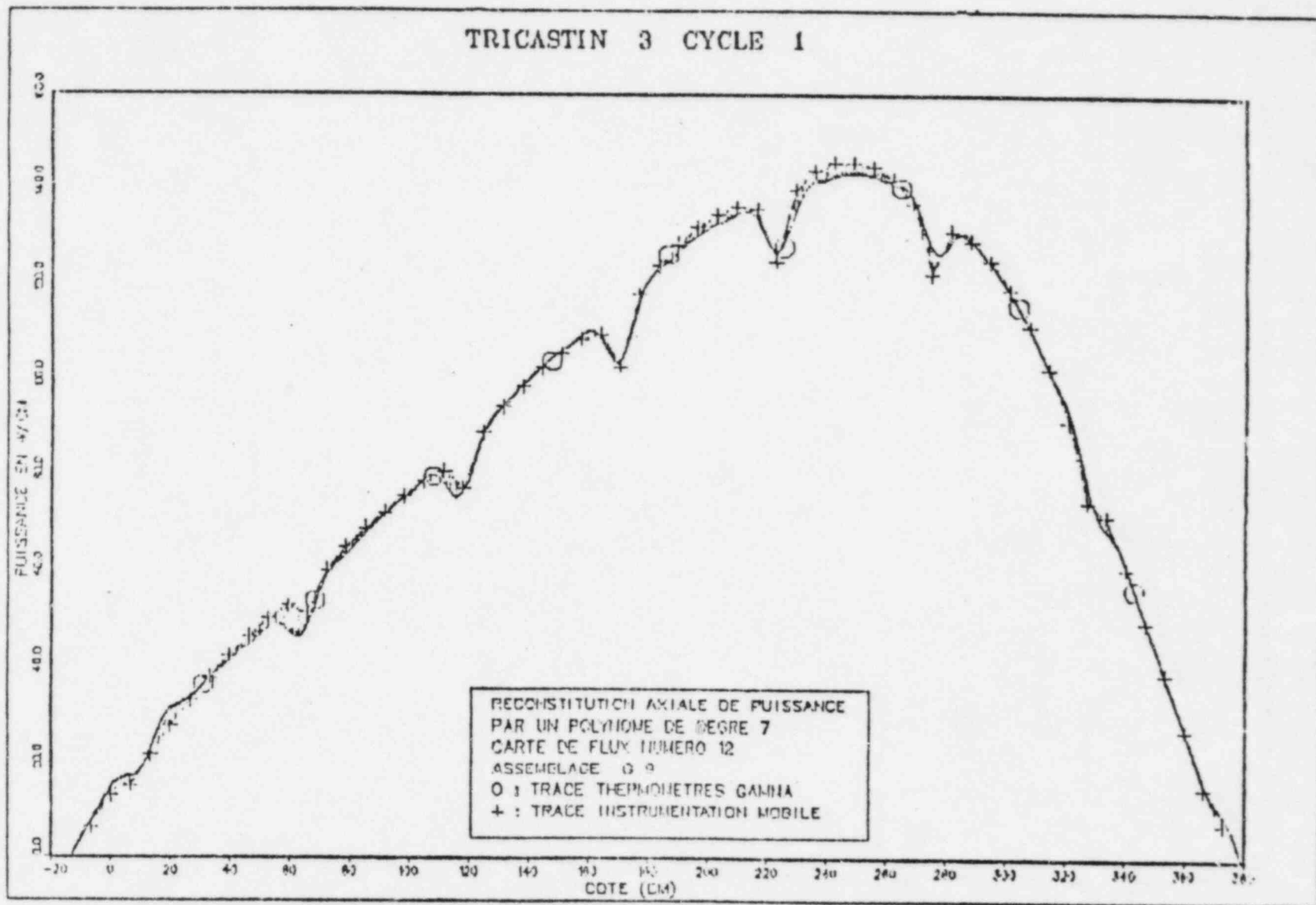


Figure 3.4-23: Comparison of RGT and TIP Measurements for a Xenon Transient - Top Peak

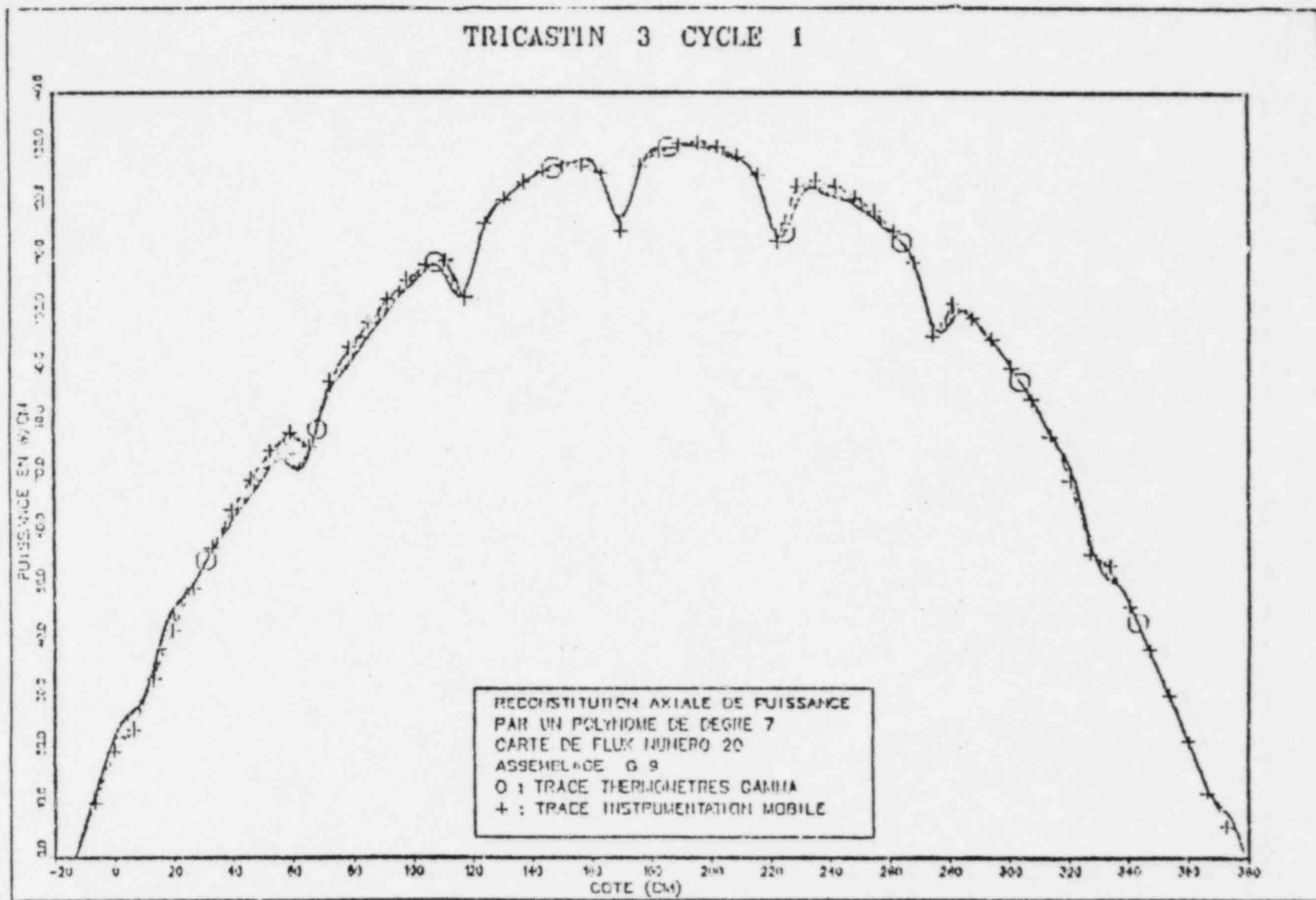


Figure 3.4-24: Comparison of RGT and TIP Measurements for a Xenon Transient - Middle Peak

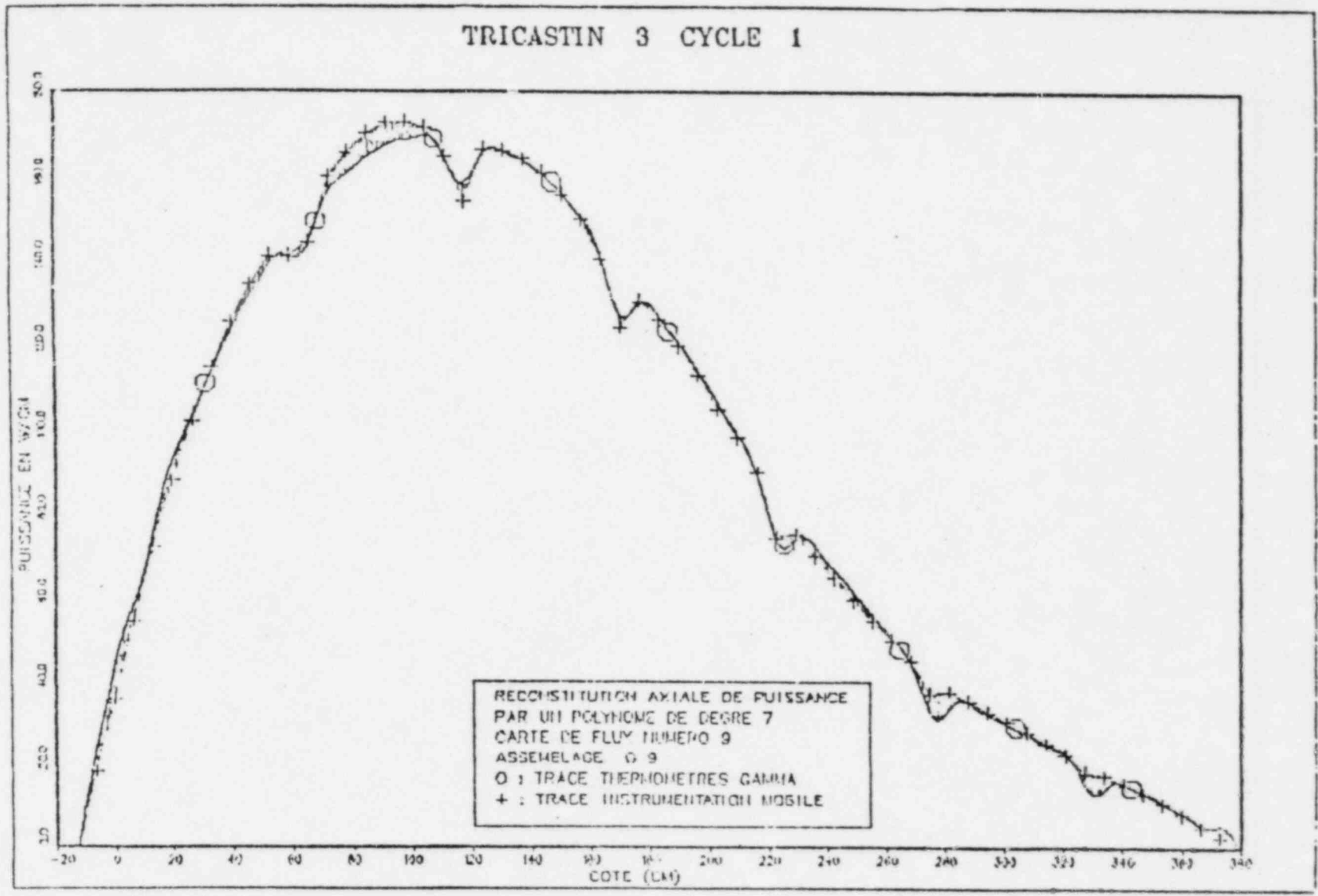


Figure 3.4-25: Comparison of RGT and TIP Measurements for a Xenon Transient - Bottom Peak

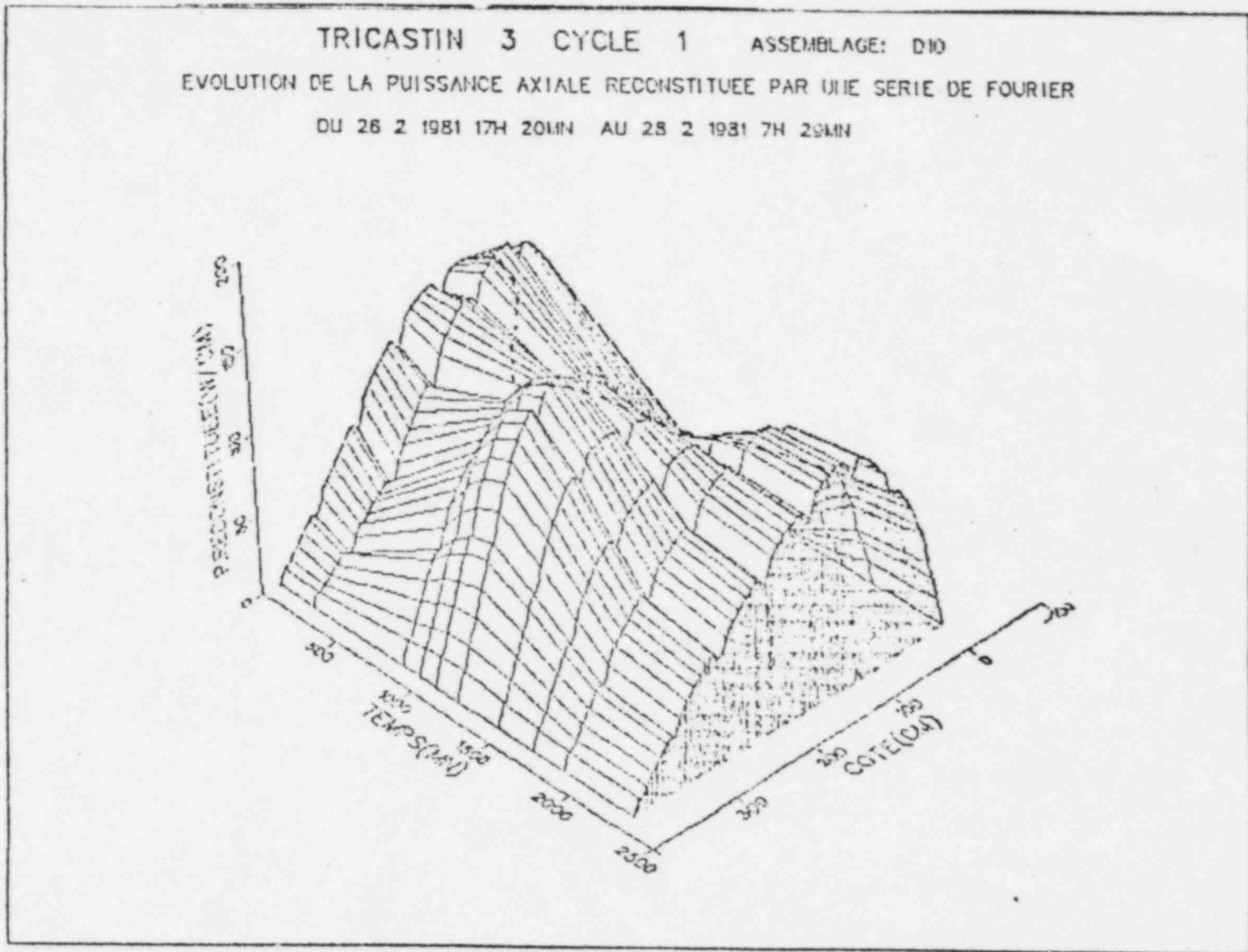


Figure 3.4-26: 3-D Plot of Xenon Transient Using RGT Measurements

TRICASTIN 3 CYCLE 1 ASSEMBLAGE: D10
 EVOLUTION DE LA PUISSANCE AXIALE RECONSTITUEE PAR UNE SERIE DE FOURIER
 DU 26 2 1981 17H 20MIN AU 28 2 1981 7:1 29MIN

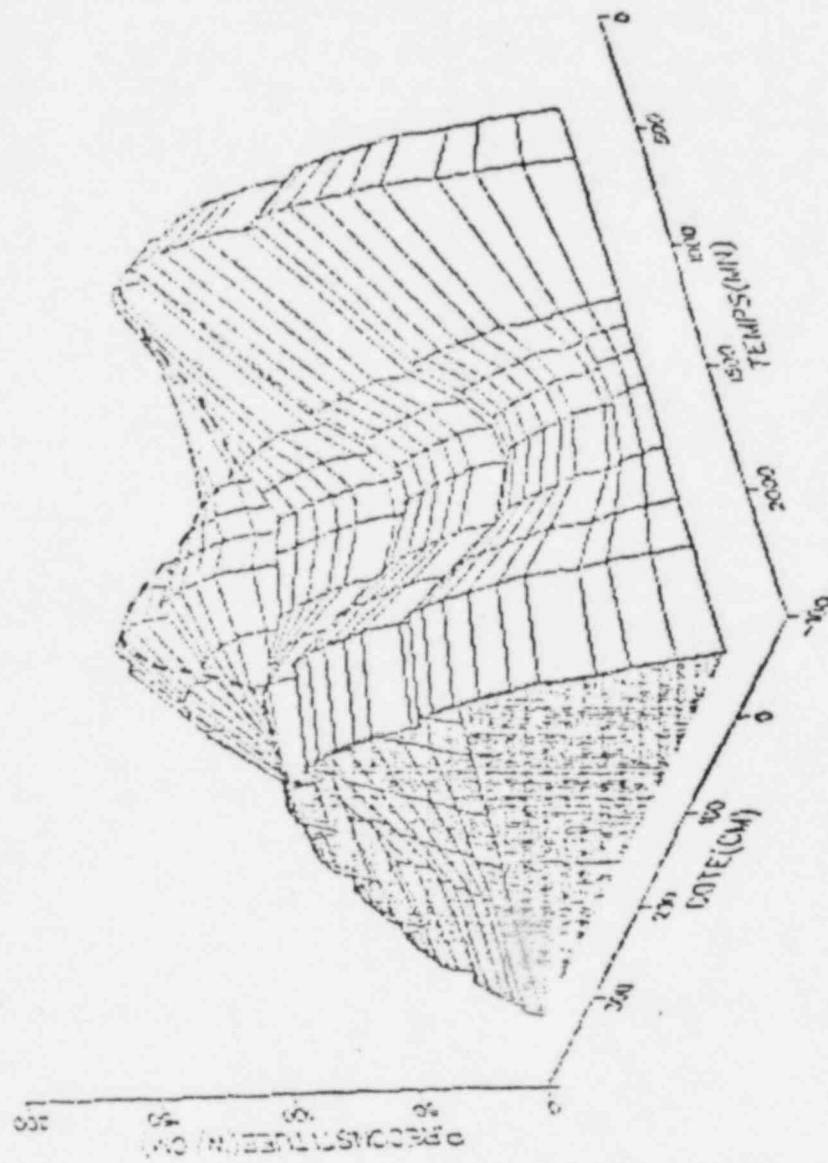
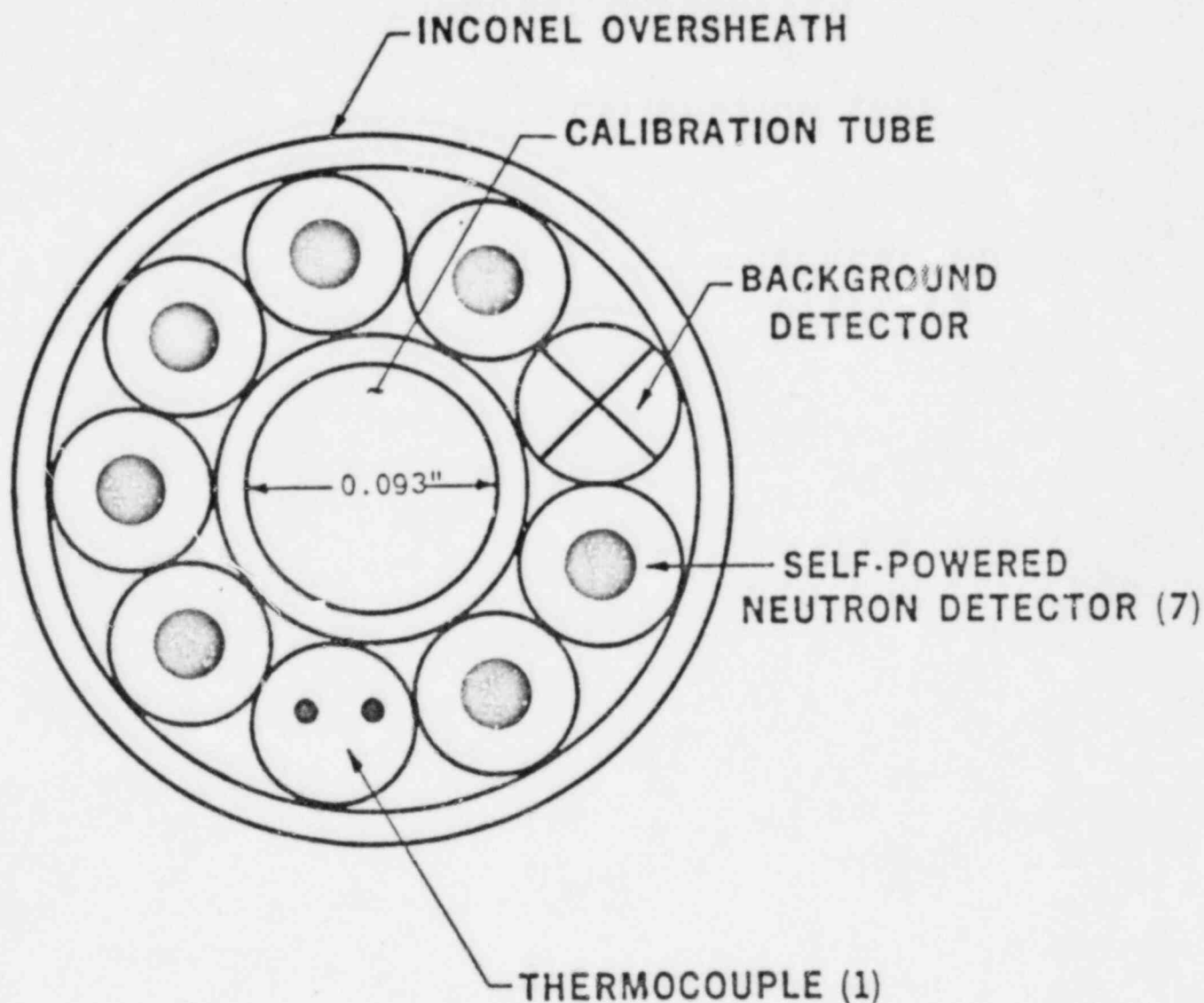


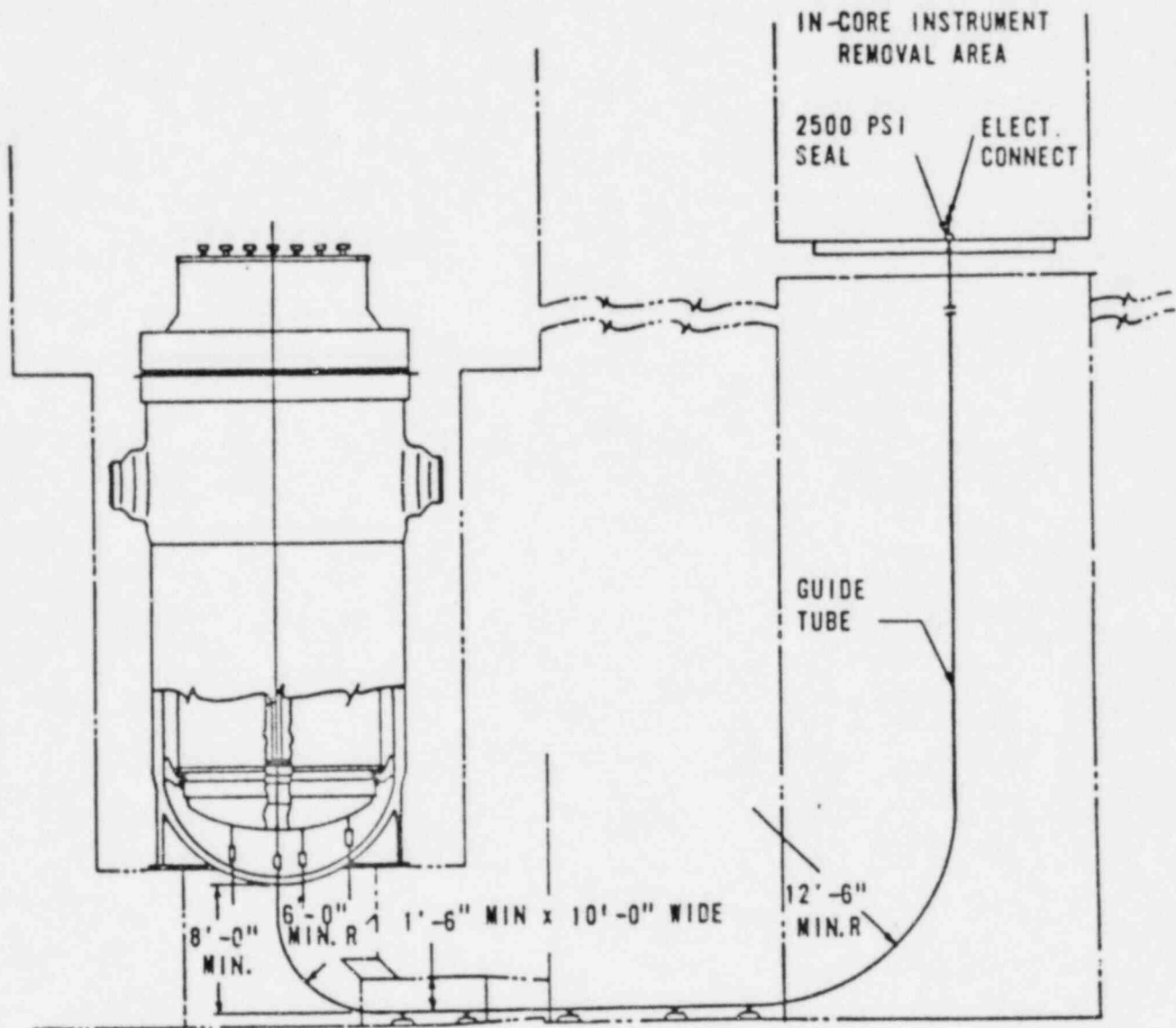
Figure 3.4-27: 3-D Plot of Xenon Transient Using RGT Measurements

FIGURE 3.5-1: CROSS SECTION OF B&W SPND UNIT



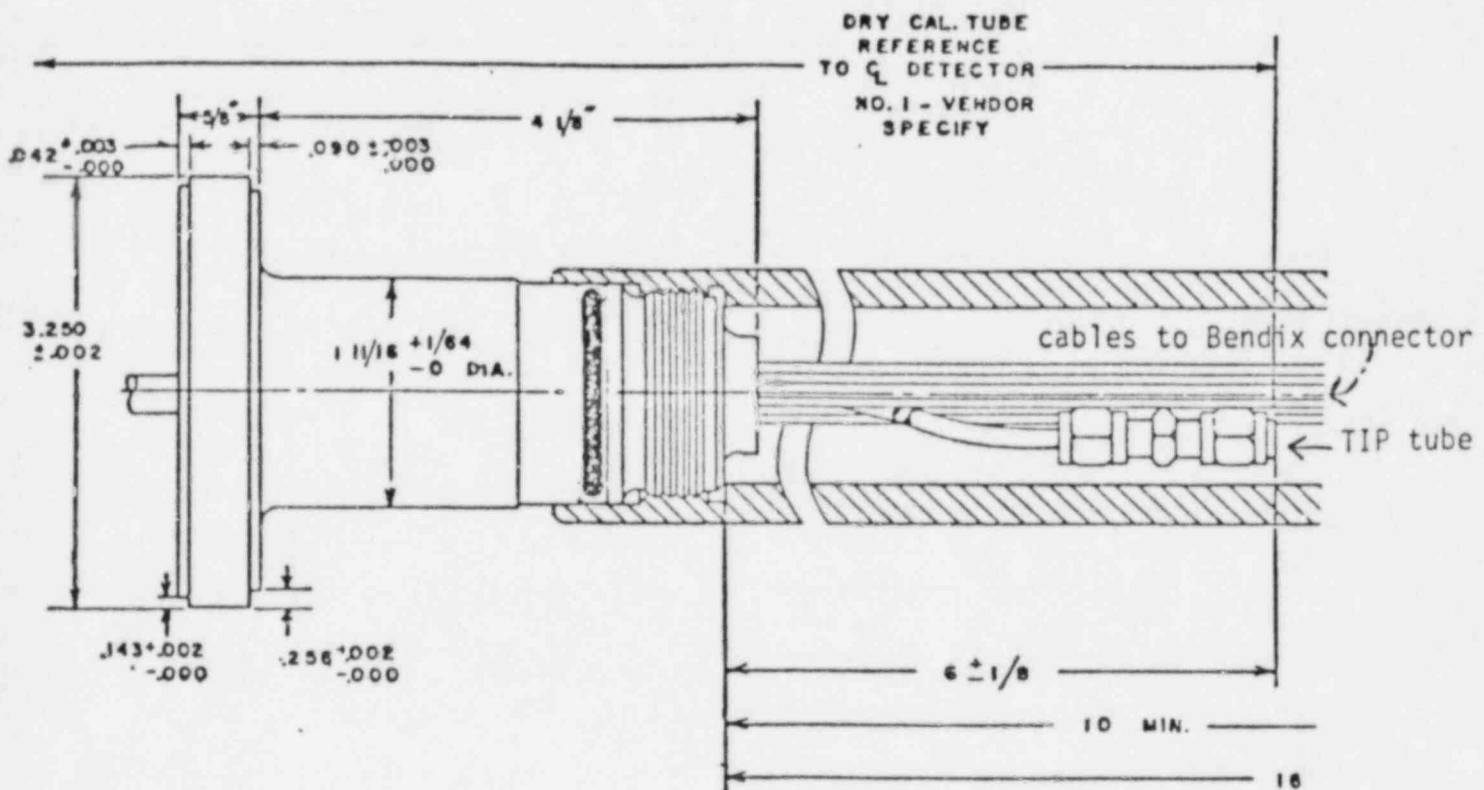
The 0.7 mm thick overshath is exposed to system pressure over its full 30 to 36 meter length. A sheath crack would admit water to the inter-cable space which is continuous to the seal plug in the in-core instrument removal area (pit). The cable space is sealed from the pit by gold braze. The sheath is welded into the seal plug. The dry internal tube extends past the plug and permits access of TIPS with SPND sensors, (MIDs).

FIGURE 3.5-2: DETECTOR ORIENTATION IN A B&W PWR



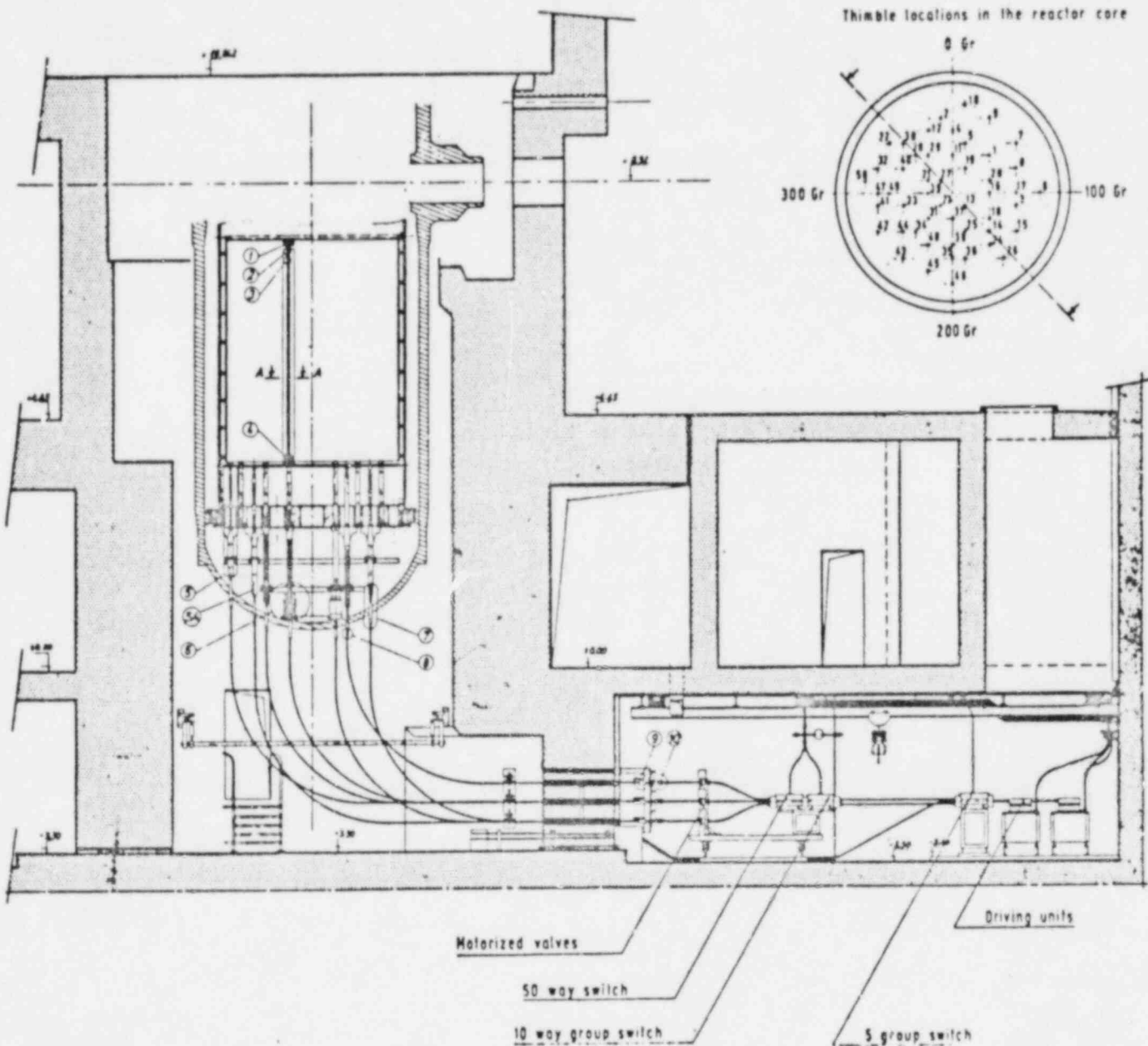
The pipes containing SPNDs (or RGTAs) are from 31 to 36 meters long. The bending radii are such that no permanent strain is induced when the relatively rigid assemblies are first introduced on partly withdrawn and reinserted during fueling. The entire jacket or sheath tube length is exposed to system pressure up to the seal in the pit.

FIGURE 3.5-3: B&W SEAL FLANGE ASSEMBLY



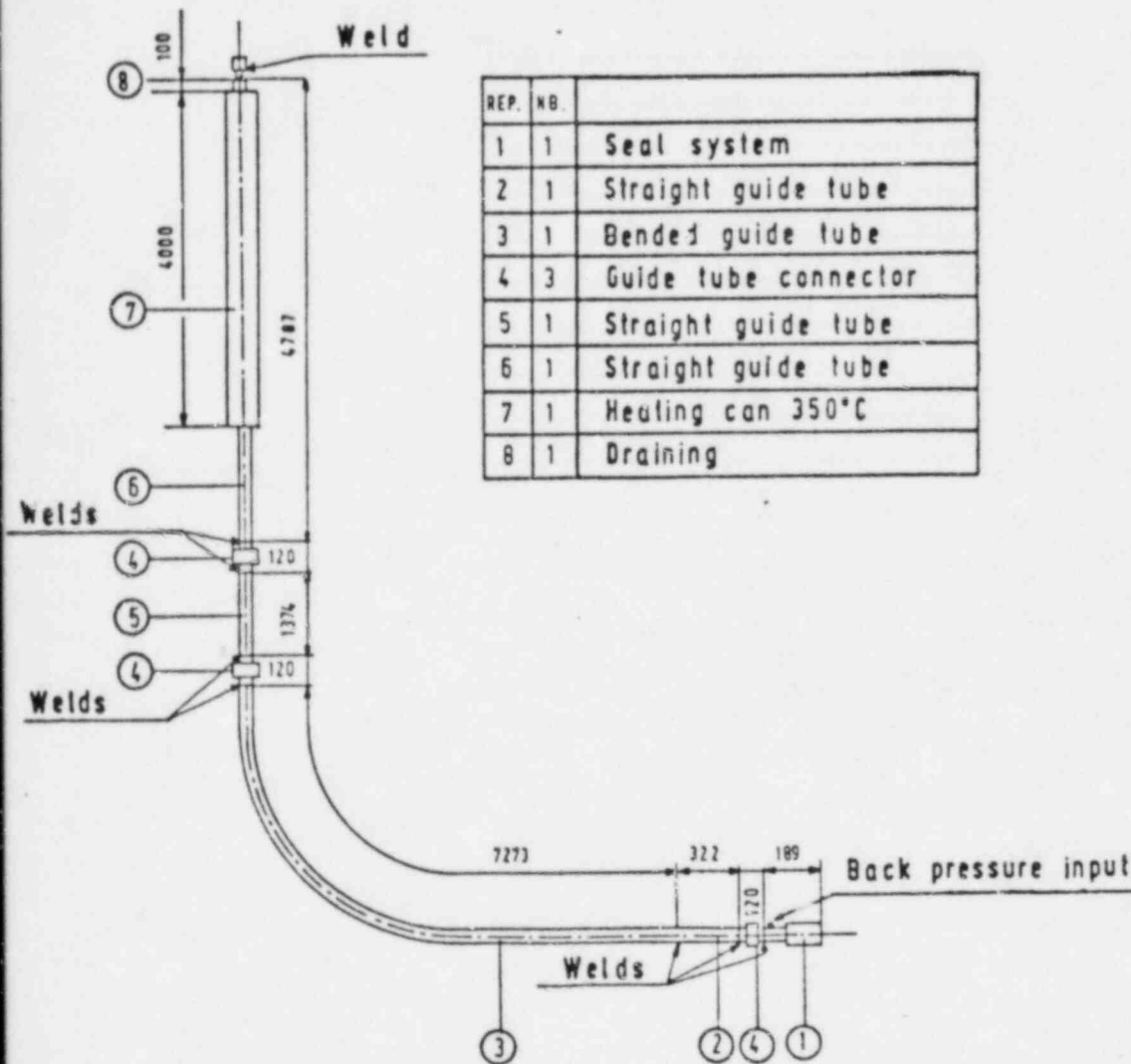
The seal flange is part of the primary pressure barrier and is sealed by a metallic O-ring. A double O-ring construction is used to permit testing of the primary closure by introduction of back pressure between rings. This test must be repeated after each SPND string withdrawal or insertion (installation or refueling). Identical seal flanges are adapted to RGTA prototypes for Ocone.

FIGURE 3.5-4: WESTINGHOUSE (FRAMATOME) ARRANGEMENT OF TIP SYSTEM



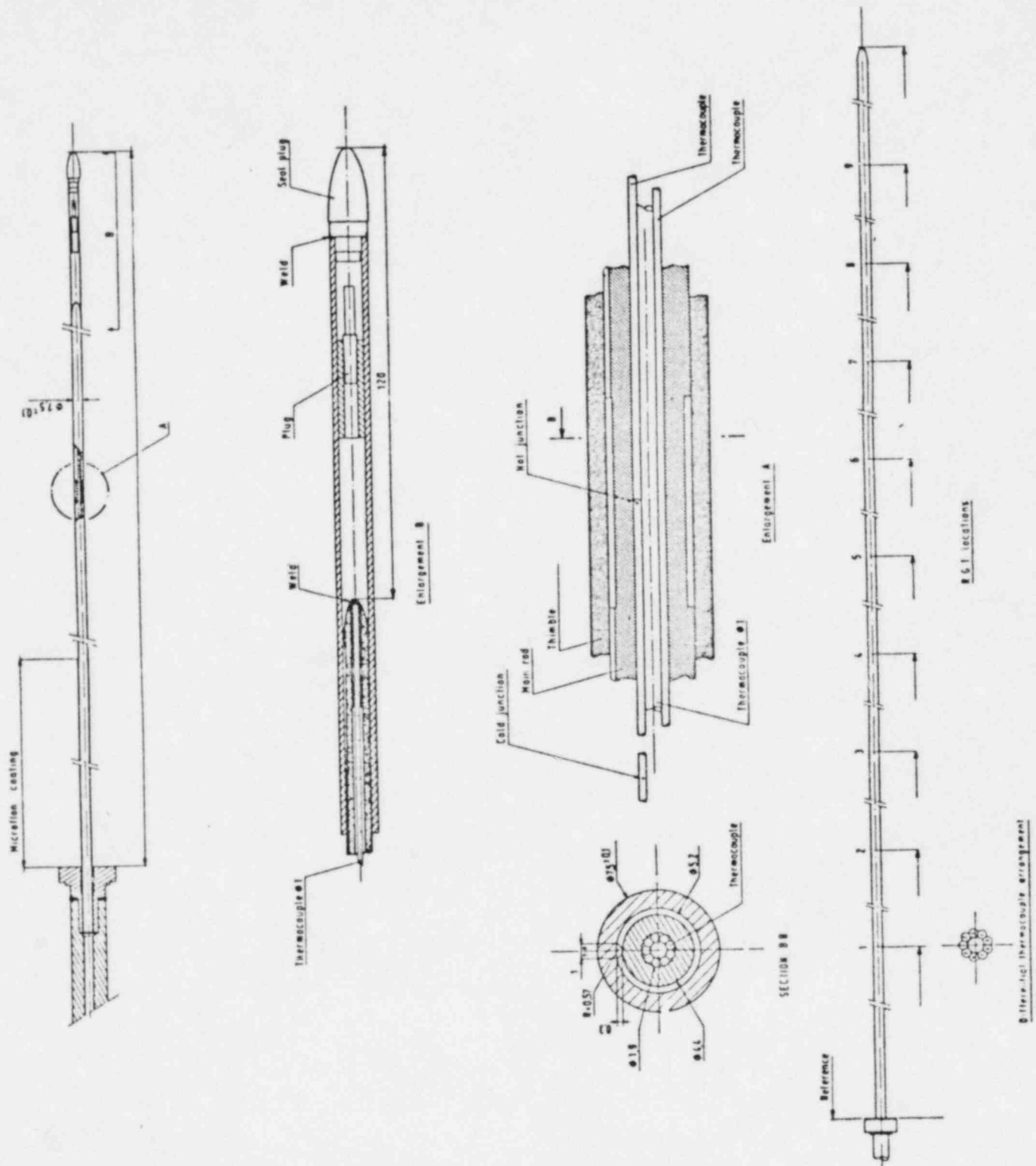
The TIP thimbles are enclosed in high pressure pipes up to the seal flange array. The TIP thimbles are individually part of the primary pressure boundary and explosive driven shear valves have been used to close off a TIP thimble if it leaks while a TIP is inside. Otherwise motorized valves may be used unless the break occurs outside the seal flanges.

FIGURE 3.5-5: FRAMATOME MECHANICAL TEST FACILITY



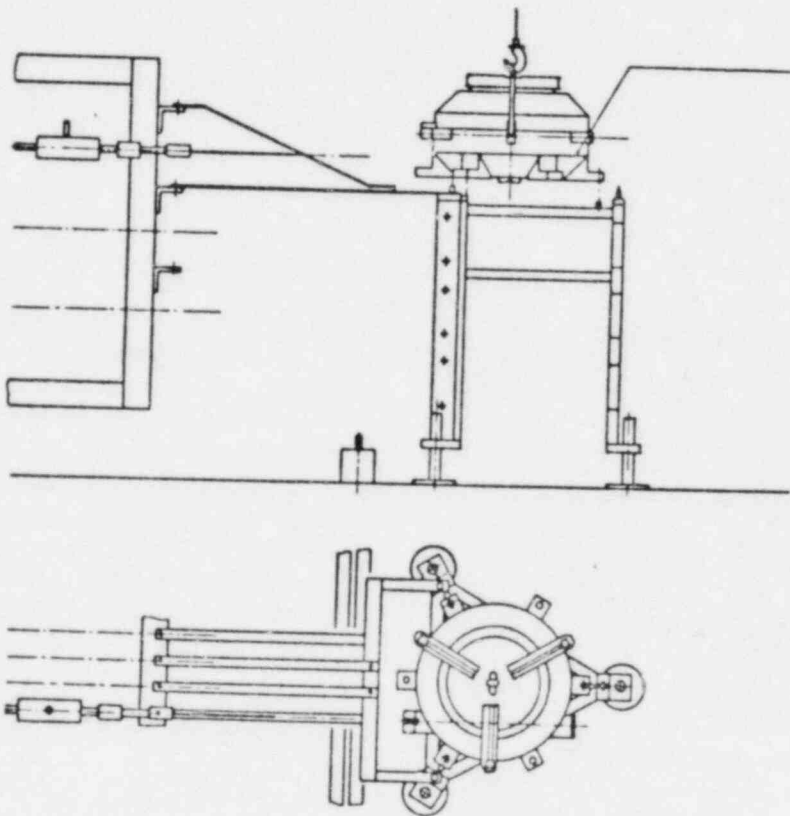
The 14.2 meter long Cannes No. 1 was inserted and removed in this mockup facility more than 40 times. Insertion and removal techniques were checked, effects of insertion on guide tube and RGTA found to be nil. The closure was pressure tested.

FIGURE 3.5-6: EDF RGTA



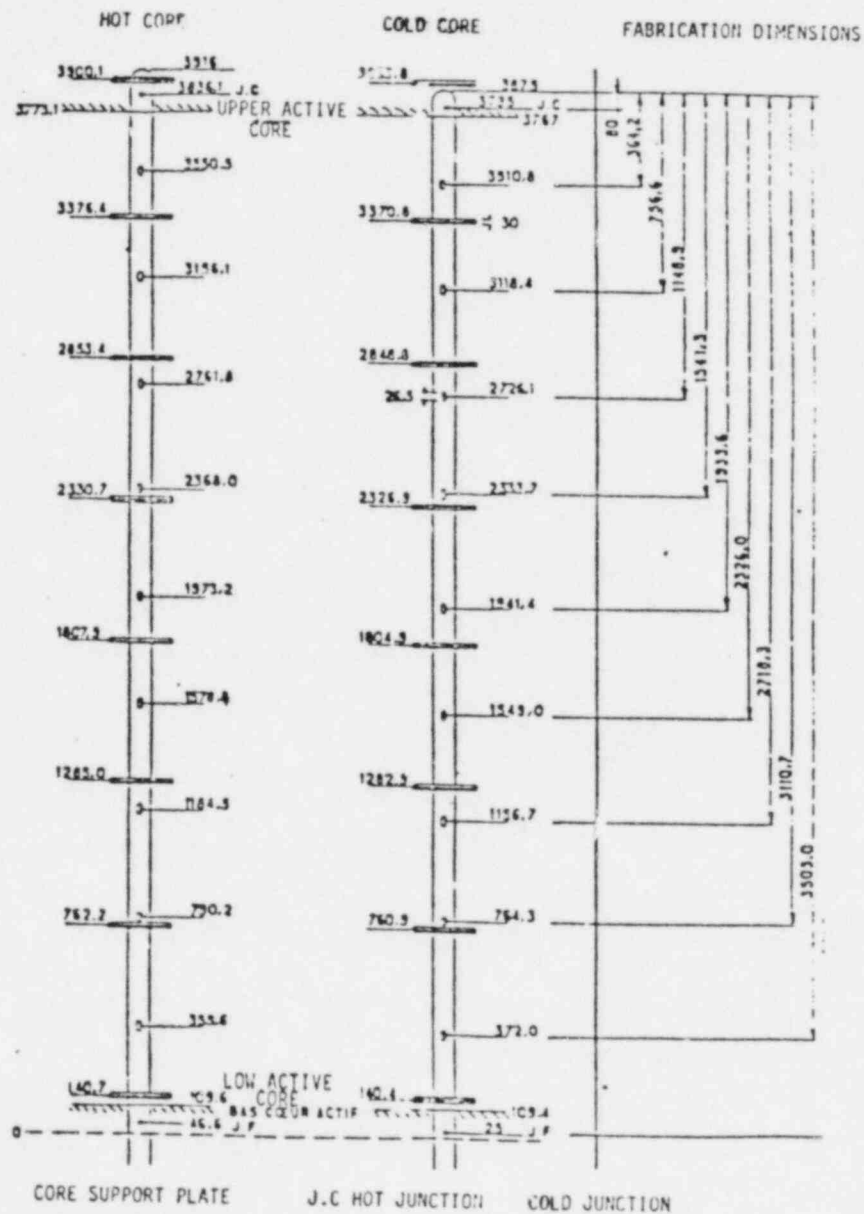
Twelve of these RGTA's containing 108 RGT's have been produced by Intertechnique for EDF. Ten are for in-reactor use.

FIGURE 3.5-7: DISPOSAL OF IRRADIATED TIP TUBES OR RGTA



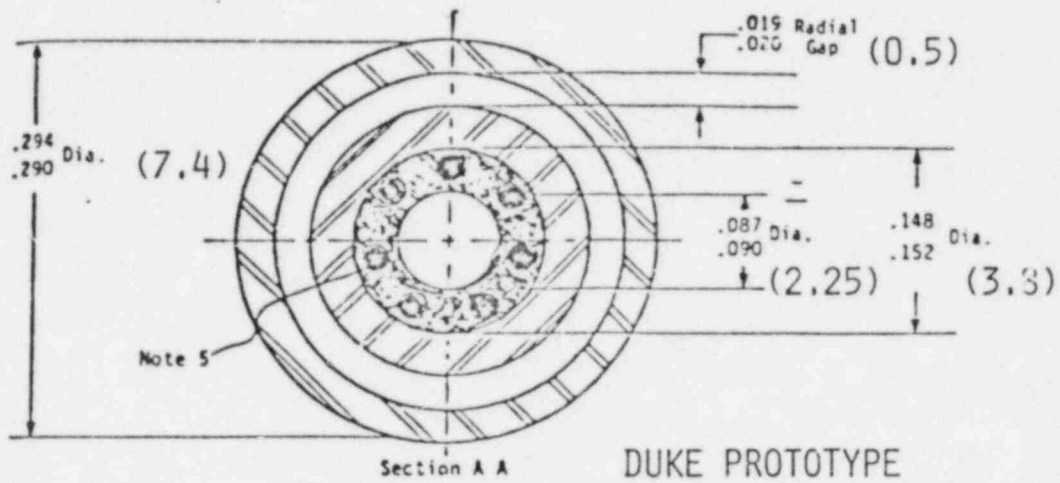
The final test of Canne No. 1 was disposal. The 2/3 meter coiling involved did not damage the thermocouples! Destructive exam showed sensor gaps to be well preserved and no relative motion of jacket tube and core rod had occurred.

FIGURE 3.5-8: CALCULATED HOT AND COLD POSITIONS OF RGTs, BUGEY-3

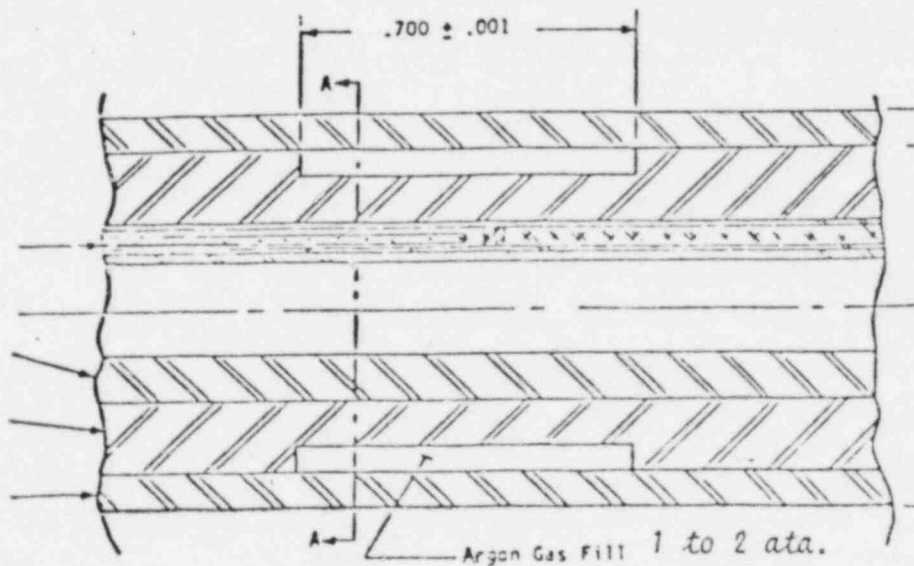


Calculated core positions were confirmed very closely by measurement in Bugey 3.

FIGURE 3.5-9 DETAILS OF DUKE RGTA CONTAINING CALIBRATION TUBE.

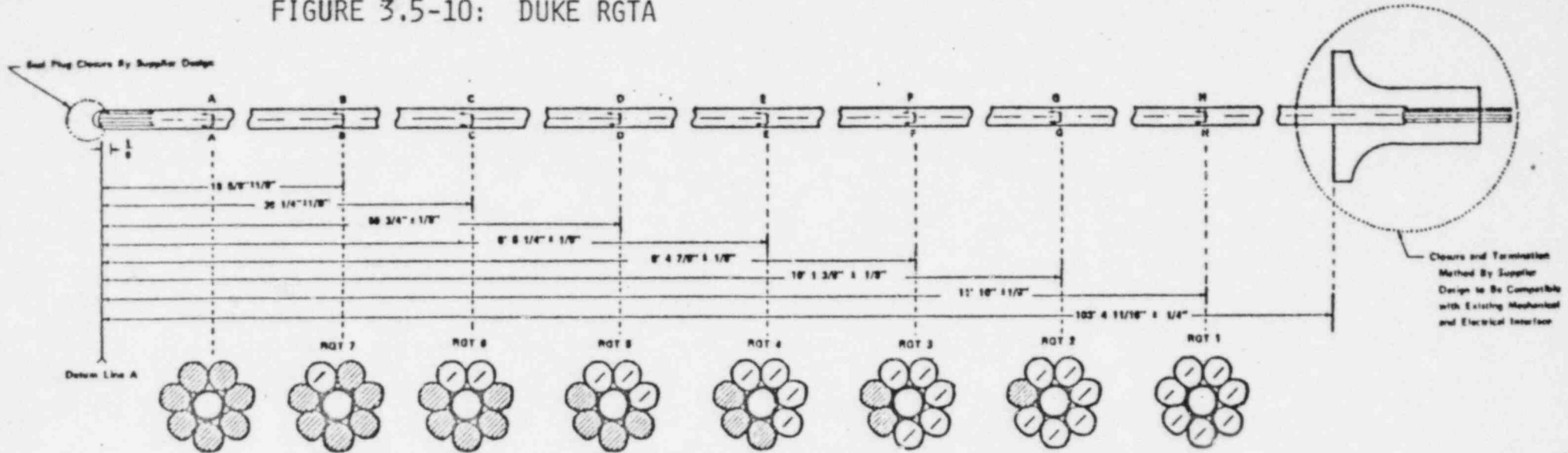


WALL THICKNESS JACKET 0.66 MM
 THERMOCOUPLE OD 0.5 MM
 TO BE TRAVERSED BY SPND OR TRAVCAL ON MIDAS DRIVE
 (SINGLE HOLE SYSTEM)



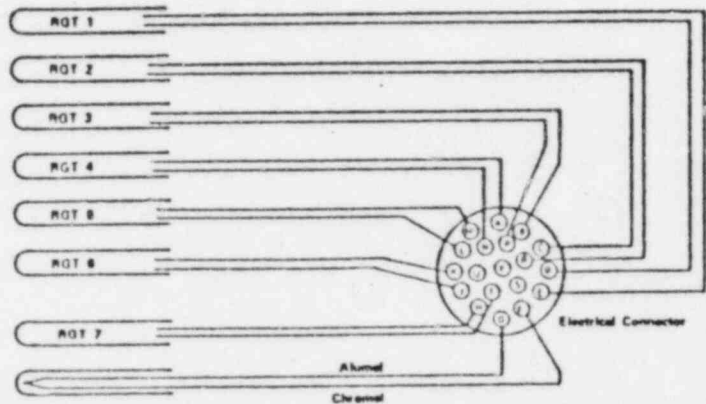
The seven sensor locations correspond to those in present SPNDs and a calibration hole for a TIP is incorporated. Hence the nickname "Cal-Cal" for the Duke RGTAs. Large numbers in () are in mm. Others are inches.

FIGURE 3.5-10: DUKE RGTA



- Calibration tube
- ⊗ DIFFERENTIAL THERMOCOUPLE
- ⊙ FILLER

- NOTES:
1. The RGT Location is measured from Detour Line A to the Midpoint of the RGT Section.
 2. The temperature sensitive tip of the Thermocouple will be located 1/8" from Detour Line A.
 3. Drawing is not to Scale.



DIMENSIONS

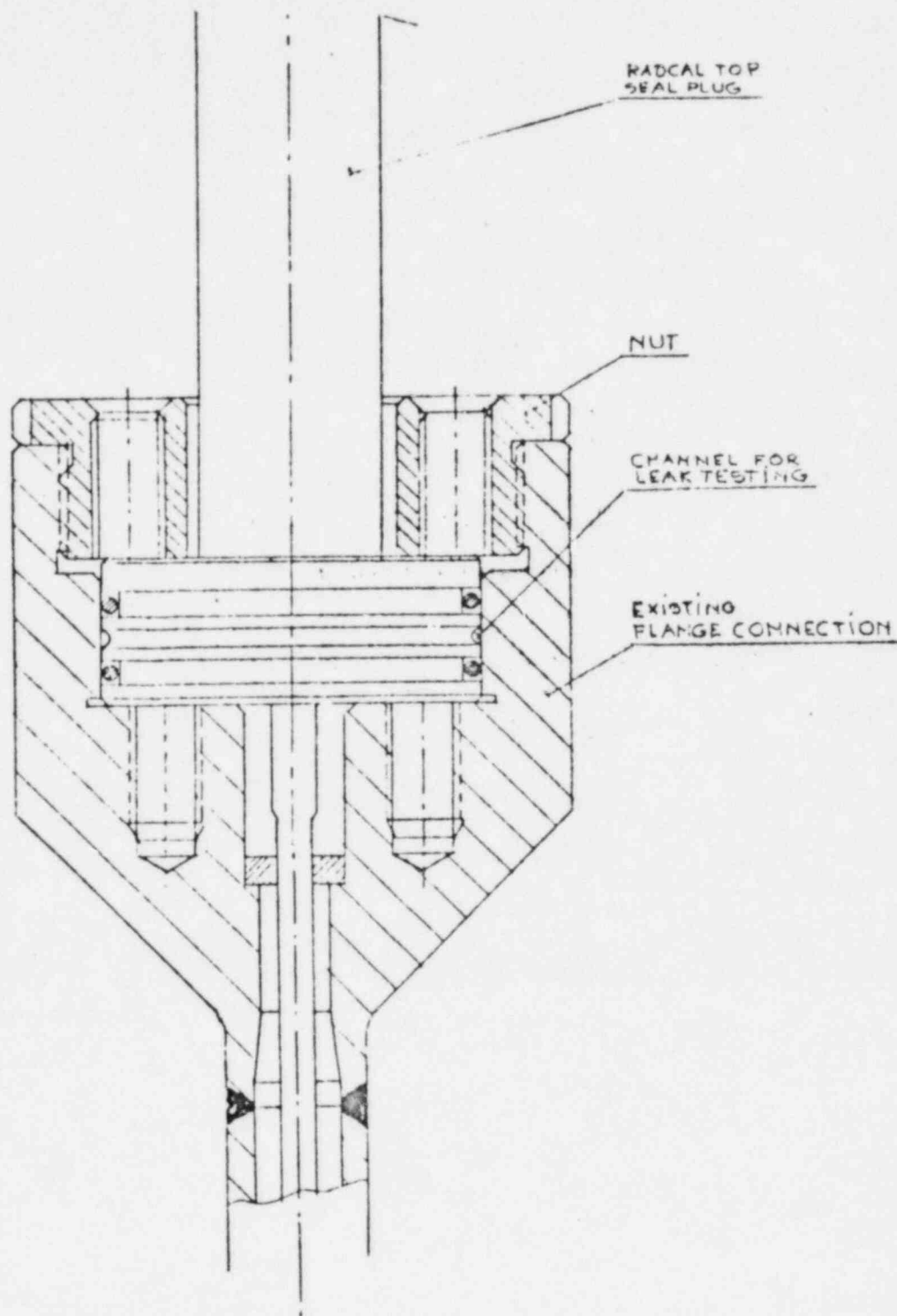
Overheath 292 ± .003 x .826 ± Wall insensd 808

Seal Plug Closure to Extend .145 ± .020 Maximum Beyond Detour Line

At B&W plants even the same cabling and Bendix connectors are used for RGTs as for SPNDs.

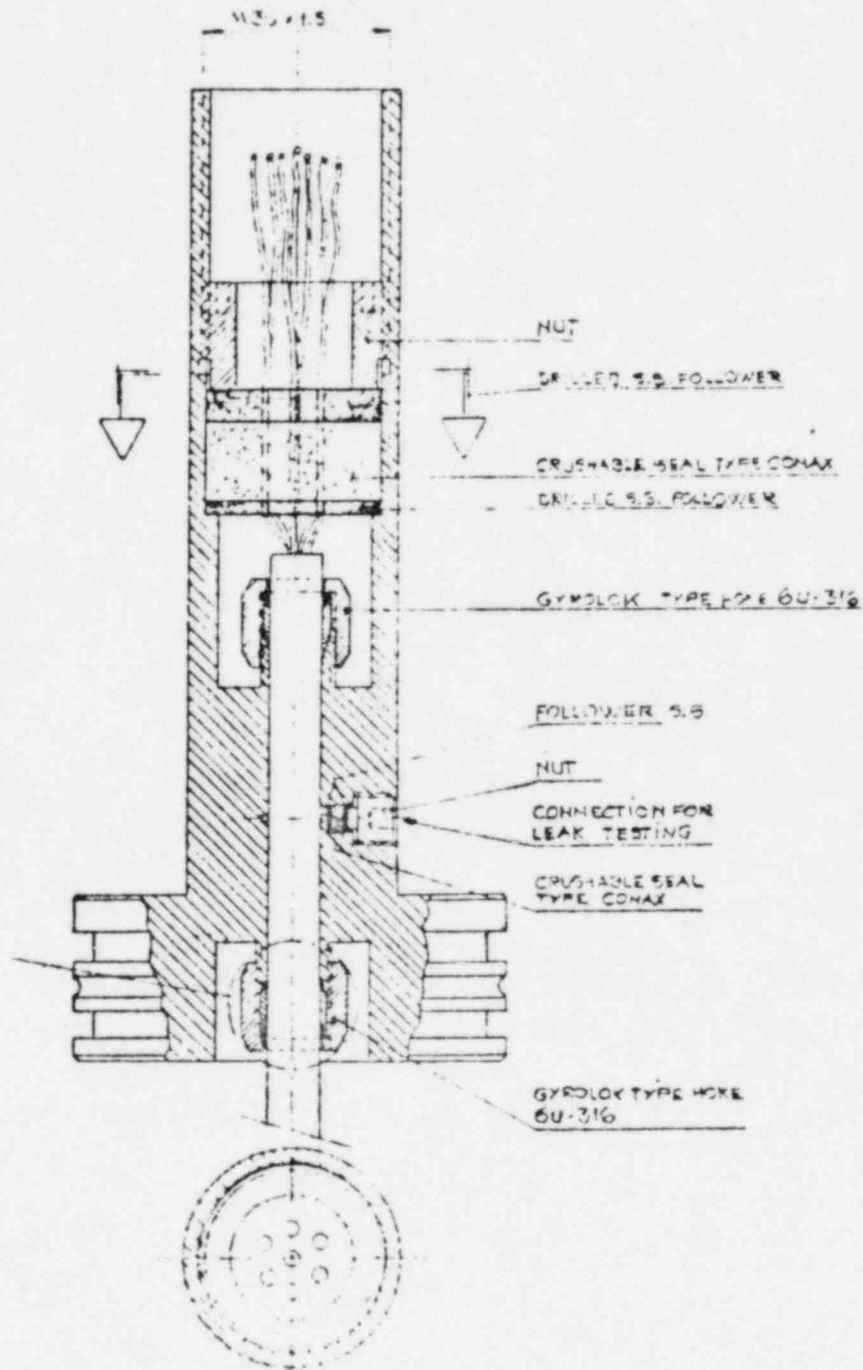
				SCANDPOWER, INC.			
				SCANDPOWER RADCAL GAMMA THERMOMETER			
DWN				CHLD			
INSP				A/FR			
G. ORIGINAL (FIRST DRAFT)							
NO. REVISION				CHKD APPROPRIATE			
				G 77 08 24			

FIGURE 3.5-11: KKMK SEAL FLANGE



This seal flange design improvement is used in recent B&W plants like KKMK. It will be replicated on the four RGTAs being installed by RWE.

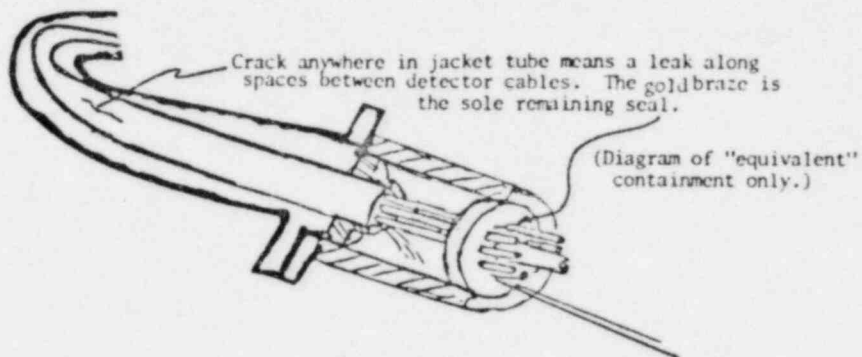
FIGURE 3.5-12: MECHANICAL ALTERNATIVE TO
WELDED SEAL FLANGE FOR KMK



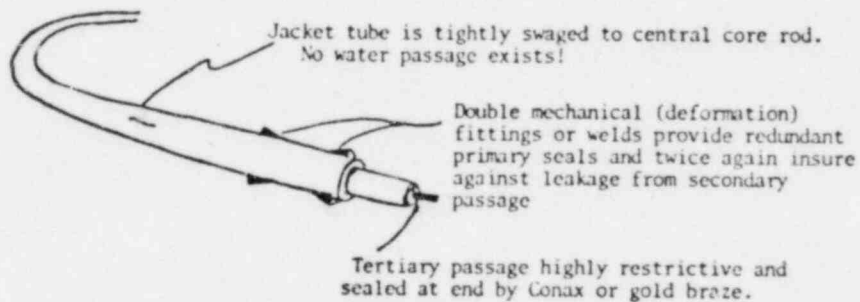
This design uses high pressure mechanical seals to replace welds between jacket tube and seal flange. Once seals have been made up they become permanent and can be back pressure tested at will. KMK qualification program includes complete fracture of RGTA and cable pack without leak.

FIGURE 3.5-13: PRESSURE BARRIER CONSIDERATIONS

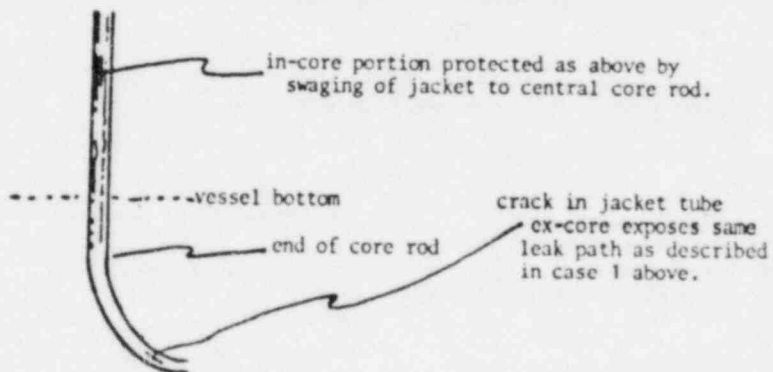
1) BELFAB SPND:



2) RGTA alternative 1 (with full length core rod):



3) RGTA alternative 2 (with partial core rod):



TABLES

TABLE 3.1-1:

EXPERIMENTAL RESULTS FOR EDF CANNE NO. 6

SENSOR LEVEL FROM BOTTOM OF CORE	INDICATED SENSITIVITY, °C/W/G, BEST FIT TO 8 DATA POINTS	STANDARD DEVIATION OF THE RGT DATA POINTS FROM BEST FIT, % OF SI
1	39.73	0.15%
2	41.83	0.17%
3	42.17	0.09%
4	39.56	0.11%
5	41.31	0.11%
6	41.45	0.11%
7	(OPEN CKT)	--
8	39.85	0.21%
(TOP) 9	39.31	0.11%

$$\text{AVG} = 40.65 \text{ } ^\circ\text{C/W/G}$$

STD. DEVIATION OF THE RGT
MEANS = 2.64%

Sensor-to-sensor variation in sensitivity occurs for two main reasons:

- 1) Variation in signal vs temperature of the type K difference thermocouples (est. $\pm 1\%$, 2σ)
- 2) Variation in annular gap width arising from drawing process, est. $2\sigma = 3\%$ on sensitivity

TABLE 3.1-2:

*SUMMARY OF HIGH TEMPERATURE CALIBRATION OF FRENCH
 PROTOTYPES AND SPECIMENS

(P R O V I S I O N A L)

	Si (indicated sensitivity) °C/W/g									Avg/σ%
	sensor no. 1	sensor no. 2	sensor no. 3	sensor no. 4	sensor no. 5	sensor no. 6	sensor no. 7	sensor no. 8	sensor no. 9	
Canne 4	25.13	25.58	25.44	25.71	26.02	25.69	25.90	25.90	27.37	25.86/2.4
Canne 5	27.19	24.66	24.71	24.99	24.34	24.79	24.94	24.99	22.56	24.79/4.7
Canne 6	25.63	24.12	24.17	24.02	24.87	24.74	21.57	24.61	22.97	24.08/4.9
Canne 7	25.90	25.71	26.27	25.80	25.99	25.88	25.82	25.28	22.35	25.11/5.6
Canne 8	25.71	24.99	25.61	25.94	26.65	25.99	25.17	27.40	25.65	25.90/2.8
										25.15/3.0

* The reported sensitivities may later be changed as a result of EdF's attempts to measure electrical resistance at calibration temperatures (300°C). The data above have been evaluated using handbook data for electrical resistance.

TABLE 3.1-4

SCHEDULE OF INSTALLATION OF ACCELERATED IRRADIATION
SPECIMENS IN ORR

Date of Installation	Capsule No. (ORNL No.)	Specimens Contained	Type	Made by
31 July 80	2	1, 2	EdF	INTss
31 July 80	4	3, 10	EdF	INTss/INTzr
21 Aug 80	1	4, 9	DUKE	TEC
23 Sept 80	3	5, 14	RWE	TEC
23 Sept 80	5	6, 7	BWR	IND

Five specimens are withheld from irradiation and serve as standards to determine reproducibility of ORNL plunge tests that are used to calibrate RGT specimens.

TABLE 3.1-5

CRNL TESTS: POST-IRRADIATION RESULTS

<u>PRE-IRRADIATION</u>	<u>SPECIMEN</u> <u>INT-2 (DTC-2)</u>
9 Plunges	
τ_1 (seconds)	1.767
σ_1	3.4%
τ_2	9.79
σ_2	1.3%
S_{pre} ($^{\circ}C$ per W/gm)	14.0
 <u>POST-IRRADIATION</u>	
7 Plunges	
τ_1	2.000
σ_1	7.0%
τ_2	9.500
σ_2	3.0%
S_{post}	15.0

TABLE 3.1-6
FAST NEUTRON EXPOSURE FOR THE ORNL SPECIMENS

<u>Capsule</u>	<u>Specimen</u>	<u>Estimated Fluence $\times 10^{-21}$⁽¹⁾</u>
1	Scp-4 (TEC-5)	6.3 ⁽²⁾
	Scp-9 (TEC-6)	6.3
2	Scp-1 (INT-1)	6.2
	Scp-2 (INT-2)	6.2
3	Scp-14 (TEC-4)	5.2
	Scp-5 (TEC-1)	5.2
4	Scp-10 (INT-5)	6.2
	Scp-3 (INT-3)	6.2
5	Scp-7 (INK-1)	5.2
	Scp-6 (INK-2)	5.2

(1) Neutrons /cm² (nvt) at energies greater than 0.1 MeV.
 (2) All values are $\pm 20\%$.

TABLE 3.2-1: SOURCES OF GAMMA HEATING IN SENSOR

*Fuel Rod Row from which the gamma rays issue	*Number of Fuel Rods in the row	Number of Water Cells in the row	Fraction of gamma heating in sensor, %	Average % contribution from a single rod at this distance
1	8	0	29.9	3.73
2	16	0	22.2	1.39
3	16	8	11.4	.71
4	32	0	10.8	.34
5	36	4	6.6	.18
6	36	12	4.0	.11
7	56	0	3.8	.068
8	64	0	2.8	.044
all others ~			91.5% inside the assembly 8.5	
			<hr/> 100% of gamma heating (exclusive neutron heating) +6.8%	

* See Figure 3.2-4 for row definition

TABLE 3.2-2: DISTRIBUTION OF SOURCE GAMMA CONTRIBUTING
TO SENSOR HEATING

<u>NEAREST FUEL ROD</u>	TRIPOLI	MERCURE IV	$\frac{\text{RATIO}}{\text{MERCURE IV}} \frac{\text{TRIPOLI}}{\text{TRIPOLI}}$
Gamma directly from fission	40.75%	40.70%	0.9988
Gamma fission products	37.91%	37.74%	0.9955
Neutron captures in U ²³⁵	5.69%	5.68%	0.9982
Neutron captures in U ²³⁸	15.65%	15.88%	1.0147
<u>DISTANT FUEL ROD (Row 8)</u>			
Gamma directly from fission	40.31%	40.09%	0.9945
Gamma from fission products	38.84%	38.91%	1.0018
Neutron captures in U ²³⁵	5.62%	5.59%	0.9947
Neutron captures in U ²³⁸	15.23%	15.41%	1.0118

The less complex line-of-sight code Mercur IV gives results very close to those of the full blown 3D Monte-Carlo code Tripoli.

